

INFORMATION TO USERS

This reproduction was made from a copy of a document sent to us for microfilming. While the most advanced technology has been used to photograph and reproduce this document, the quality of the reproduction is heavily dependent upon the quality of the material submitted.

The following explanation of techniques is provided to help clarify markings or notations which may appear on this reproduction.

1. The sign or "target" for pages apparently lacking from the document photographed is "Missing Page(s)". If it was possible to obtain the missing page(s) or section, they are spliced into the film along with adjacent pages. This may have necessitated cutting through an image and duplicating adjacent pages to assure complete continuity.
2. When an image on the film is obliterated with a round black mark, it is an indication of either blurred copy because of movement during exposure, duplicate copy, or copyrighted materials that should not have been filmed. For blurred pages, a good image of the page can be found in the adjacent frame. If copyrighted materials were deleted, a target note will appear listing the pages in the adjacent frame.
3. When a map, drawing or chart, etc., is part of the material being photographed, a definite method of "sectioning" the material has been followed. It is customary to begin filming at the upper left hand corner of a large sheet and to continue from left to right in equal sections with small overlaps. If necessary, sectioning is continued again—beginning below the first row and continuing on until complete.
4. For illustrations that cannot be satisfactorily reproduced by xerographic means, photographic prints can be purchased at additional cost and inserted into your xerographic copy. These prints are available upon request from the Dissertations Customer Services Department.
5. Some pages in any document may have indistinct print. In all cases the best available copy has been filmed.

**University
Microfilms
International**

300 N. Zeeb Road
Ann Arbor, MI 48106

8324115

Kirby, James Thornton, Jr.

PROPAGATION OF WEAKLY-NONLINEAR SURFACE WATER WAVES IN
REGIONS WITH VARYING DEPTH AND CURRENT

University of Delaware

Ph.D. 1983

University
Microfilms
International 300 N. Zeeb Road, Ann Arbor, MI 48106

2

PLEASE NOTE:

In all cases this material has been filmed in the best possible way from the available copy. Problems encountered with this document have been identified here with a check mark .

1. Glossy photographs or pages _____
2. Colored illustrations, paper or print _____
3. Photographs with dark background _____
4. Illustrations are poor copy _____
5. Pages with black marks, not original copy
6. Print shows through as there is text on both sides of page _____
7. Indistinct, broken or small print on several pages
8. Print exceeds margin requirements _____
9. Tightly bound copy with print lost in spine _____
10. Computer printout pages with indistinct print _____
11. Page(s) _____ lacking when material received, and not available from school or author.
12. Page(s) _____ seem to be missing in numbering only as text follows.
13. Two pages numbered _____. Text follows.
14. Curling and wrinkled pages _____
15. Other _____

University
Microfilms
International

PROPAGATION OF WEAKLY-NONLINEAR
SURFACE WATER WAVES IN REGIONS
WITH VARYING DEPTH AND CURRENT

By

James Thornton Kirby, Jr.

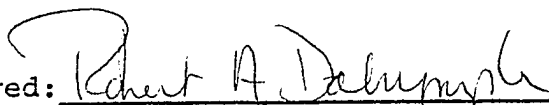
A dissertation submitted to the Faculty of the
University of Delaware in partial fulfillment of the
requirements for the degree of Doctor of Philosophy in
Applied Sciences

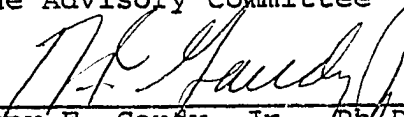
August, 1983


PROPAGATION OF WEAKLY-NONLINEAR
SURFACE WATER WAVES IN REGIONS
WITH VARYING DEPTH AND CURRENT


By

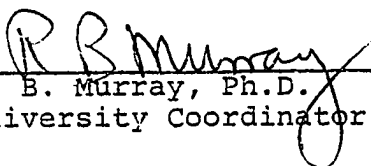
James Thornton Kirby, Jr.

Approved: 
Robert A. Dalrymple, Ph.D.
Professor in charge of dissertation on behalf
of the Advisory Committee

Approved: 
Anthony F. Gaudy, Jr., Ph.D.
Chairman of the Department of Civil Engineering

Approved: 
Jack R. Vinson, Ph.D.
Chairman of the Applied Science Committee

Approved: 
Irwin G. Greenfield, Ph.D.
Dean of the College of Engineering

UMB Approved: 
R. B. Murray, Ph.D.
University Coordinator for Graduate Studies

ACKNOWLEDGEMENTS

This dissertation was written under the supervision of Dr. Robert A. Dalrymple, to whom I am greatly indebted for his continued support and friendship during my years of graduate study. Thanks are also due to Drs. Ib A. Svendsen, Nobuhisa Kobayashi and Michael D. Greenberg, who served on my examining committee, to Dr. Robert G. Dean, who contributed significantly to my education and development, and to Dr. Philip L.-F. Liu, who provided suggestions and further guidance during the development of the dissertation project. I also wish to thank Drs. Osman Borekci and Paul A. Hwang for their support and friendship, and Connie Weber for assistance with typing. Financial support for my studies was provided by the Office of Naval Research through the Coastal Sciences Program, and by the University of Delaware Research Foundation through a fellowship.

This work is dedicated to my parents, James and Pearl, and my wife, Barbara.

TABLE OF CONTENTS

	<u>Page</u>
Acknowledgements	iii
List of Figures	vii
List of Tables	xi
Abstract	xii
Chapter 1. Introduction	1
Chapter 2. Formulation of the Problem	12
2.1. Governing Equations	12
2.2. The Variational Principle and Derivation of the Euler Equations	18
2.3. The Perturbation Scheme and Expansions for ϕ and η	24
Chapter 3. The Lagrangian and Equations Governing Wave Motion	33
3.1. Introduction	33
3.2. The Lagrangian for Stokes Waves	34
3.3. The Governing Equations	38
3.4. The Mild-Slope Approximation and Some Plane Wave Results	46
3.5. The Weakly-Nonlinear Equation for $\tilde{\phi}_1$	50
Chapter 4. Parabolic Approximation and Equations Governing the Complex Amplitude A	59
4.1. Introduction	59

4.2.	Time-Independent Elliptic Models	62
4.3.	Time-Dependent Equations for A	65
4.4.	The Parabolic Approximation	76
Chapter 5.	Comparison of the Mild- and Moderate-Slope Models for Linear Waves	91
5.1.	Introduction	91
5.2.	Linear Edge Waves	94
5.3.	Reflection from Underwater Topography	105
Chapter 6.	Some Examples of Time-Independent Refraction-Diffraction of Initially Plane Linear and Stokes Waves	121
6.1.	Introduction	121
6.2.	Numerical Approximations of the Parabolic Equations	124
6.3.	Treatment of Lateral Boundary Conditions	135
6.4.	A Model for Breaking Waves in the Surf Zone	150
6.5.	Combined Refraction and Diffraction of Waves by a Submerged Shoal	166
6.6.	The Wavefield around a Shore-Attached Breakwater	183
6.7.	Reflection from a Caustic: Topographic Case	197
6.8.	Reflection from a Caustic: Current Case	208
6.9.	Interaction with Rip Currents	218
Chapter 7.	Summary and Suggestions for Further Research	239

References	245
Appendix A. The Stokes Solution to $O(\delta)$ in the Presence of a Current	257
Appendix B. Perturbation Method for the Lagrangian L	268
Appendix C. Derivation of L and the Euler Equation for $\tilde{\phi}_1$	272
C.1. The Lagrangian L	272
C.2. The Linear Equation for $\tilde{\phi}_1$ to $O(\delta^2)$	284
Appendix D. Integrals Appearing in L	293
Appendix E. Conservation Equation for Wave Action	304
Appendix F. The Boundary Integral Method for Normal and Oblique Incidence	308
Appendix G. Relations for the Dissipation Coefficient w based on Various Dissipation Mechanisms	322

LIST OF FIGURES

<u>Figure #</u>	<u>Title</u>	<u>Page</u>
2.1	Definition sketch of fluid domain	13
5.1	Edge wave surface profiles: $n = 0-5$	95
5.2	Dimensionless edge wave wavelength; $n = 0,1,2$	101
5.3	Edge wave wavelength; percent error relative to solution of Ursell (1952)	104
5.4	Generalized topography for section 5.3	106
5.5	BIM domain for reflection from sloping step	115
5.6	Reflection coefficient K_r vs. kh of incident wave. $s = 1/3, \theta = 0^\circ$	116
5.7	Reflection coefficient K_r vs. kh of incident wave. $s = 1/3, \theta = 45^\circ$	117
5.8	Reflection coefficient K_r vs. kh of incident wave. $s = 2/3, \theta = 0^\circ$	118
5.9	Reflection coefficient K_r vs. kh of incident wave. $s = 2/3, \theta = 45^\circ$	119
6.1	Computational grid and labelling of grid points	125
6.2	Relation between grid points, open boundaries and internal reflective boundaries	136
6.3	Reflection coefficient K_R at downwave boundary. Open boundary test, exact value of m	143

6.4	% energy loss at upwave boundary. Open boundary test, exact value of m	144
6.5	Plane wave propagating at $\theta = 45^\circ$ to x-axis. Open boundary conditions, numerical value of m	146
6.6	Interaction of two-component wave field and open boundary conditions; $\theta_1 = 0^\circ$, $\theta_2 = 20^\circ$	148
6.7	Measured waveheights in a laboratory surfzone (from Horikawa and Kuo, 1966)	152
6.8	Surfzone model, plane beach	157
6.9	Waveheight decay in surfzone; $\alpha = 1$, $s = 0.17$	161
6.10	Waveheight decay in surfzone; $\alpha = 3$, $s = 0.0566$	162
6.11	Waveheight decay in surfzone; $\alpha = 10$, $s = 0.017$	163
6.12	Shoaling and wave breaking	164
6.13	Bottom contours and computational domain for experiment of Berkhoff, Booy and Radder (1982)	169
6.14	Computed amplitude contours $ A/A_0 $ for experiment of Berkhoff, Booy and Radder (1982); linear model results	174
6.15	Computed amplitude contours $ A/A_0 $ for experiment of Berkhoff, Booy and Radder (1982); nonlinear model results	175
6.16	Comparison between linear and nonlinear model results and experimental data of Berkhoff, Booy and Radder (1982)	177

6.17	Geometry of shore attached breakwater	184
6.18	Normalized amplitude perpendicular to breakwater; $P_1 = 0$	186
6.19	Normalized amplitude perpendicular to breakwater, $P_1 = 1/4$	187
6.20	Wave field in vicinity of shore-attached breakwater. Test T8	189
6.21	Amplitude contours perpendicular to shore-attached breakwater. Test T8	193
6.22	Amplitude contours perpendicular to shore-attached breakwater. Test T5	194
6.23	Amplitude contours perpendicular to shore-attached breakwater. Test T6	196
6.24	Geometry of wedge-shaped depression	198
6.25	Submerged depression, $\theta = 15^\circ$. Normalized amplitude vs. distance from centerline of depression	200
6.26	Submerged depression, $\theta = 25^\circ$. Normalized amplitude vs. distance from centerline of depression	202
6.27	Instantaneous water surface in vicinity of wedge-shaped depression, linear result, $\theta = 25^\circ$	205
6.28	Instantaneous water surface in vicinity of wedge-shaped depression, nonlinear result, $k_0 A_0 = 0.2$, $\theta = 25^\circ$	206
6.29	Reflection from following current	210
6.30	Reflection of waves from caustic caused by a following current; $\partial U / \partial y = 0.05$, $\theta = 15^\circ$	212
6.31	Reflection of waves from caustic caused by a following current; $\partial U / \partial y = 0.025$, $\theta = 15^\circ$	215

6.32	Pattern of orthogonals and wave crests for waves in presence of rip current (from Arthur, 1950)	220
6.33	Wavefield in presence of rip current; linear results	223
6.34	Amplitude relative to incident wave for waves interacting with rip current; linear results	225
6.35	Error in predicted phase speed relative to results of stream function theory	231
6.36	Wavefield in presence of rip current; nonlinear results	234
6.37	Amplitude relative to incident wave for waves interacting with rip current; nonlinear results	235
F.1	Boundary integral method domain in relation to extent of variable topography	311
F.2	Integration paths for interior points and points on boundary	314
F.3	Geometry for test of BIM	318
F.4	Reflection coefficient: asymmetric trench	320
F.5	Transmission coefficient: symmetric trench	321

LIST OF TABLES

<u>Table #</u>	<u>Title</u>	<u>Page</u>
2.1	Relation between scaling parameters for several wave propagation models	32
5.1	Sample calculated wavenumbers for mode 0, $N = 90$	102
6.1	Test conditions for shore-attached breakwater	191

ABSTRACT

This dissertation represents a study of the equations governing the propagation of weakly nonlinear waves in regions where currents exist and where the depth and current are allowed to vary. After deriving a velocity potential applicable to propagating surface waves according to the Stokes expansion, the Lagrangian governing wave motion in the propagation space is derived. A consistent perturbation scheme then leads to the equations governing the wave and current motion at each order in the Stokes series.

After neglecting time dependence of the wave amplitude, parabolic equations governing the combined refraction and diffraction of Stokes waves of small amplitude are developed and used to calculate the wavefields for several representative cases illustrating the importance of nonlinear effects. The computational models are verified by comparison to laboratory data of wave amplitude for a wavefield focussed by a submerged shoal, and it is found

that the nonlinear model accounts for the major discrepancies found between linear model results and the laboratory data.

CHAPTER 1. INTRODUCTION

One of the central problems in the study of the coastal surface wave environment is the prediction of the transformation of waves as they propagate from the deep ocean towards the shore. During this period of propagation, the waves are subject to many of the physical effects characteristic of general wave problems in many branches of physics. First, the domain of propagation may in general be in motion, due to the effect of tidal or other currents. For the case of currents with scales of variation much larger than the scale of the local wave, which may be characterised by the wavelength, this effect may be quantified locally in terms of a simple Galilean transformation for waves of small amplitude, in which the frequency of the wave oscillation is defined with respect to the moving medium. Secondly, the propagation medium is, in general, inhomogeneous. The inhomogeneity may arise locally due to a smaller scale of variation of the ambient current, and will be apparent over larger distances for any scale of variation. Additionally, after the waves propagate into

water shallow enough so that the phase velocity of the wave becomes a function of the local depth, the pattern of wave propagation will be affected by the spatial variations of depth. Each of these inhomogeneities can cause refractive and diffractive effects, leading to the presence of caustics and related characteristics of the wave field.

In addition to effects related to movement and spatial inhomogeneity of the domain, the wave motion itself is nonlinear, and thus the components of the wave field may interact in both subtle and spectacular ways. The simplest interaction involves the mutual interaction of the components of a single wave, discussed by Phillips (1960), leading to the effect of amplitude dispersion, in which the phase speed of the wave is increased as a function of its local amplitude. In addition, separate wave trains, either propagating colinearly or intersecting obliquely, may exchange energy in a complex manner leading to gradual shifts of the overall characteristics of the wave field. The individual waves of the wave field may respond to the interactions in an unstable manner, leading to amplitude modulations which act over a small spatial scale and which also effect the phase velocity of the individual components.

Wave and current motions are subject both to direct

viscous effects and to small scale turbulence which may be modelled in analogy to viscosity. In general, the presence of viscous effects causes the domain of propagation to be dissipative, so that waves propagating over long distances may lose a significant proportion of their energy content, principally through interaction with the bottom. Viscosity, as well as the rotation of the earth, also leads to rotational current distributions. Finally, the wavefield is subject to the action of applied surface shear stress due to wind, and to spatial fluctuations in the applied atmospheric pressure. The shear stress due to wind is important in the scale of the relatively short surface waves, and leads to surface drift currents as well as growth of the waves as energy is transferred to the water column.

In order for an analytic model of wave propagation to be successfully applicable over all propagation scales, it must begin to address all of the effects listed above. The general problem of water wave propagation is therefore extremely complex, and progress in its study has necessarily been made through the study of subsets of the general problem applicable to problems of a more simplified nature. A major simplification which still allows for a general treatment of a wide range of the mentioned effects is the neglect of viscosity and wind shear effects, leading to the

study of wave states which do not dissipate or increase in energy. This simplification leads to the ability to study a subset of the governing equations applicable to incompressible and inviscid flows. The further assumption of irrotationality allows the entire fluid flow to be described by a velocity potential. It should be noted that the assumption of irrotationality, especially with regard to the large scale current, is strictly invalid in most physical cases, and it would be desirable to obtain an estimate of the error incurred by the neglect of this effect in any given case. In this study, the assumption of irrotationality will be included. The remaining subset of the problem still allows for the study of propagation of nonlinear waves through an inhomogeneous, moving domain, which is the problem investigated here. The governing differential equations and a corresponding variational principle for inviscid and irrotational flow are discussed in Chapter 2, along with the scales of variation to be studied and the small parameter expansion of the independent variables.

In most instances to date, the problems of nonlinear wave-wave interaction and refraction-diffraction have been studied as separate entities. After linearization of the free surface boundary conditions, the sea state may be

characterized as the spectral sum of individual, non-interacting linear components, with the consequence that the propagation characteristics of each component may be calculated separately. As a consequence, much of the work on wave-current interaction and refraction -diffraction has centered on the study of single component wave systems, where the time dependence may be characterised entirely in terms of the absolute wave frequency within a stationary reference frame. Further, the problems of refraction and diffraction have historically been considered separately and have been joined successfully only in the past decade. The first method for studying surface wave refraction in an arbitrarily varying domain was proposed by Obrien and Mason(1940), and is referred to as the ray method. Rays, or orthogonals to the travelling wave crest, are traced independently through the domain and are assumed to be everywhere parallel to the local direction of wave propagation. The local wave amplitude is then calculated based on the assumption that energy does not cross the rays; i.e., that the area between adjacent rays is a tube of constant energy flux. Arthur (1950) extended the ray method to include the effect of wave-current interaction, and calculated the rays by means of Fermat's principle of least time. Skovgaard, Jonsson and Bertelsen (1975) extended the method to include the effect of wave-energy dissipation due

to bottom friction.

Keller(1958) showed that the refraction approximation arises as the first, or geometric optics, approximation in a WKB expansion of the governing equations, after neglecting the effect of wave amplitude gradients normal to the rays. The limitation of the approximation became apparent in the case where one or more rays intersect, leading to singularities in the wave amplitude. These singularities, which arise along curves known as caustics, necessitate the inclusion of diffraction effects, by which energy is allowed to cross the geometric rays, leading to uniform solutions in the neighborhood of the singularity.

The combined effect of refraction and diffraction was first studied in order to provide locally valid solutions in the neighborhood of singularities of the geometric optics approximation. Ludwig (1966) showed that the linear wave field in the neighborhood of a caustic is represented by Airy functions, which are sinusoidal in the illuminated zone upwave of the caustic, decay exponentially in the shadow zone, and are bounded over the entire domain. The wave field in the vicinity of the cusp of a caustic has been studied by Smith (1976a). The problem of

simultaneous refraction and diffraction in a domain with depth inhomogeneities was successfully studied by Berkhoff (1972), who proposed an elliptic equation of the form

$$\nabla_h \cdot (CC_g \nabla_h \hat{\phi}_1) + \omega^2 \frac{C_g}{C} \hat{\phi}_1 = 0 \quad (1.1)$$

which must be solved as a boundary value problem together with appropriate boundary conditions. Here, ω , C , and C_g are the absolute wave frequency, phase speed and group velocity, respectively, and will be defined in Chapter 2. The quantity $\hat{\phi}_1$ is related to the three dimensional potential function ϕ by

$$\phi = \hat{\phi}_1 \frac{\cosh k(h+z)}{\cosh kh} e^{-i\omega t} \quad (1.2)$$

where k and h are the local wave number and water depth. Radder (1979) showed that (1.1) could be transformed to a Helmholtz equation by the scaling

$$\Psi = (CC_g)^{1/2} \hat{\phi}_1 \quad (1.3)$$

and developed a parabolic equation approximation for (1.1) for the case of nearly unidirectional wave propagation. Smith and Sprinks (1975) derived (1.1) by means of Green's identities applied to (1.2), and found several higher order

terms proportional to the square and derivative of the bottom slope; these terms will be discussed in Chapter 3. Booij (1981), using a method based on a variational principle, derived a time-dependent extension of (1.1) including an ambient current; his equation can be written in the slightly altered form

$$\frac{D^2 \tilde{\phi}_1}{Dt^2} + (\nabla_h \cdot \underline{u}) \frac{D \tilde{\phi}_1}{Dt} - \nabla_h \cdot (c c_g \nabla_h \tilde{\phi}_1) + \sigma^2 \left(1 - \frac{c_g}{c}\right) \tilde{\phi}_1 = 0 \quad (1.4)$$

where $\underline{u}(x, y, t)$ is the horizontal ambient current, D/Dt is a total derivation following the current, and $\tilde{\phi}_1$ is related to ϕ by

$$\phi = \frac{\cosh k(h+z)}{\cosh kh} \tilde{\phi}_1 \quad (1.5)$$

The frequency σ is the frequency of oscillation relative to the moving domain. Booij's model is reducible to (1.1) after neglecting the current \underline{u} and assuming purely harmonic motion ($\hat{\phi}_{1,t} = 0$, where subscript t denotes the time derivative). Booij further derived a parabolic equation approximation to (1.4). Equation (1.4) neglects a small term which appears in Booij's equation due to an error in his derivation.

In the conclusion of his dissertation, Booij states

that the principle drawbacks to the model (1.4) include the inability to model the nonlinear effects of amplitude dispersion directly, and the restriction to a monochromatic wave field. The second conclusion is not strictly true, since allowing $\hat{\phi}_1$ to be specified as a time dependent quantity allows for the specification of a wave field with a narrow spectral band width, as long as a carrier wave of frequency ω is identifiable. This allowance is critical to the study of nonlinear waves in the context of the nonlinear Schrodinger equation, as discussed below. The first conclusion is basic to the linearization of the problem. Booij suggested several means for including the effect of nonlinearity based on empirical modifications to the linear dispersion relation suggested by Walker(1976) and Hedges (1976); a similar modification based on the correct nonlinear dispersion relation for Stokes waves will be suggested in Chapter 3. However, the present study emphasises the inclusion of nonlinearity in the problem formulation and model equation from the outset, and such a model equation involving a cubic nonlinearity is proposed in Chapter 3.

The general hyperbolic wave model can be reduced to a first order hyperbolic equation governing the evolution of the amplitude envelope of a wavetrain propagating in a known

(or assumed) direction by substituting the assumed form

$$\tilde{\phi}_1 \sim A(x, y, t) e^{i\psi} \quad (1.6)$$

where ψ is a suitable phase function for plane waves, into the second order model. The resulting evolution equation is shown in Chapter 4 to be consistent with previous results obtained using multiple scale expansions of the governing equations. Equations of this type, based on extended forms of the Schrodinger equation with a cubic nonlinearity, have been shown to be useful in modelling effects in nonlinear wavetrains ranging from predictions of the stability characteristics of various solutions to the description of the evolution of complex wave patterns in the presence of currents and wind. A recent and comprehensive review of this topic has been provided by Yuen and Lake(1982). The correspondence between the first order evolution equations and the second order hyperbolic wave equation described here points out the possibility of modelling complex wave forms with narrow spectral bandwidth, a possibility not fully recognised by Booij.

The general study of waves in a time-dependent, two-space-dimensional approach involves the use of complex numerical schemes such as the ADI method. In this study, we

restrict our attention to steady plane waves. Parabolic approximations for Stokes waves with and without an imposed current field are derived in Chapter 4 and used to investigate a number of examples in Chapter 6. In particular, a comparison between the data set of Berkhoff, Booy and Radder(1982) and predictions of the nonlinear parabolic approximation points out the usefulness of the method in providing estimates of the wave amplitude in regions where ray crossing occurs in the refraction approximation, where both diffraction and nonlinearity become important.

In Chapter 5, the effect of higher order terms involving the bottom slope on the prediction of the wavelength of edge waves on steep bottoms and on the prediction of reflection coefficients for waves passing over an underwater slope are investigated using an elliptic formulation for steady, linear waves.

CHAPTER 2. FORMULATION OF THE PROBLEM

2.1 Governing Equations

In this study, the irrotational motion of an inviscid fluid is considered. The effects of surface tension are also neglected. The fluid domain is bounded below by a rigid, stationary bottom and above by a free surface, and is of infinite lateral extent unless otherwise specified. A definition sketch of the coordinate system and physical domain is given in Figure 2.1. The domain is allowed to have an arbitrary, horizontally varying two-dimensional distribution of ambient, quasi-steady current, with the theoretical restriction that the ambient current must also be irrotational. This restriction is seldom satisfied in practice, although it is known that weak rotationality does not effect the governing equations for the geometric optics approximation, as shown by Mei (1982) and others. The neglect of friction also restricts us to consideration of vertically uniform currents, which may be considered in some cases to represent the depth average of vertically non-uniform currents. It will be demonstrated

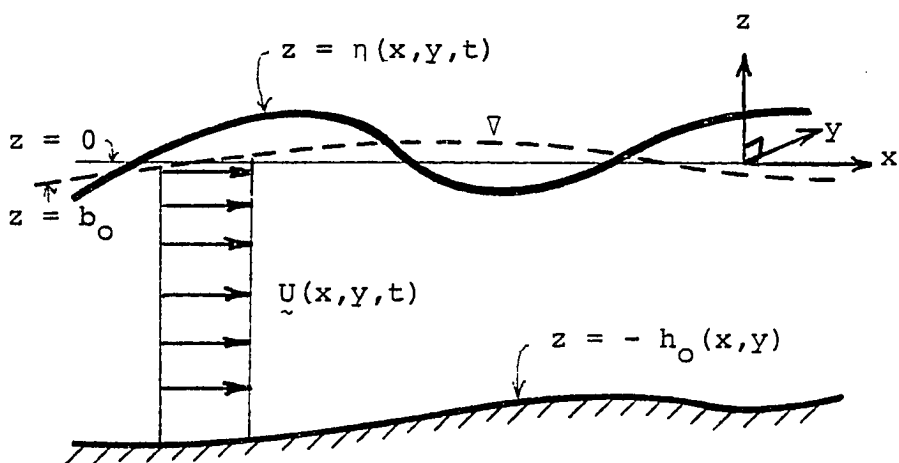


Figure 2.1 Definition sketch of fluid domain

below that the effect of friction may be included in an a posteriori sense; however, it may not be conveniently represented in the context of the present derivation.

The equation of motion appropriate to the given assumptions is Laplace's equation in three dimensions for the velocity potential ϕ :

$$\nabla^2 \phi = \phi_{xx} + \phi_{yy} + \phi_{zz} = 0 \quad ; \quad -h_0 \leq z \leq \eta \quad (2.1.1)$$

Here, x and y are the horizontal coordinates, z is directed vertically upward from the still water surface, η is the instantaneous free surface position, and h_0 is taken to be the water depth in the absence of any motion. Subscripts x , y , z and t will be taken to denote differentiation with respect to the spatial coordinates and time, respectively. Kinematic boundary conditions are prescribed for the bottom and free surface and are given by

$$\nabla_h \phi \cdot \nabla_h h_0 = -\phi_z \quad ; \quad z = -h_0 \quad (2.1.2)$$

and

$$\eta_t + \nabla_h \phi \cdot \nabla_h \eta = \phi_z \quad ; \quad z = \eta \quad (2.1.3)$$

Here, ∇_h is a horizontal gradient operator given by

$$\nabla_h F = F_x \hat{i}_x + F_y \hat{i}_y$$

where \hat{i}_x , \hat{i}_y , and \hat{i}_z are unit vectors in the spatial directions. Fluid velocities are given by

$$\underline{u} = \nabla_h \phi$$

Finally, a dynamic condition is given on the free surface by the choice

$$p(x, y, z, t) = 0 ; z = \eta$$

where p is the fluid pressure. Use of Bernoulli's equation at the free surface then leads to the condition

$$\phi_t + \frac{1}{2}(\nabla\phi)^2 + gz = 0 ; z = \eta \quad (2.1.4)$$

The irrotational motion of an inviscid fluid with uniform density and a free surface and no applied pressure forces or surface tension is completely described by (2.1.1-4) together with appropriate initial and boundary conditions, which will be developed as needed.

The set of equations governing the fluid motion is

nonlinear. In the present study, we will restrict our attention to weakly nonlinear motions, leading to the assumption that the motion can be adequately described by a series expansion in powers of a small parameter, with truncation after a small number of terms. However, rather than expanding the governing equations (2.1.1-4) directly, we proceed instead by using a variational approach involving a Lagrangian for the conservative motion. The Lagrangian can then be shown to lead to the correct set of governing equations after taking the arbitrary variations with respect to the dependent parameters ϕ and η .

The following derivation includes the effect of interaction between the wave motion and the ambient mean current, and it is useful here to define several quantities before proceeding. The ambient current $\underline{U}(x,y,t)$ will be represented by the first term in the expansion for ϕ , and will be presumed to be $O(1)$ with respect to the small expansion parameters. Consideration of the linearised problem for water waves in the presence of a current leads to a leading order solution for the wave potential of the form (see Dean and Dalrymple(1983), sec. 3.4.5).

$$\phi = -i g \frac{A}{\sigma} \frac{\cosh k(h+z)}{\cosh kh} e^{i\psi} \quad (2.1.5)$$

where ψ is the phase function, given by

$$\psi = \int^{\underline{x}} k(\underline{x}) d\underline{x} - \omega t$$

The dispersion relation between the intrinsic, or relative, frequency σ and the vector wavenumber $\underline{k} = \nabla_{\underline{h}} \psi$ is given by

$$\omega = \sigma + \underline{k} \cdot \underline{u} \quad (2.4.6)$$

where ω is the absolute frequency given by $-\psi_t$, and

$$\sigma = (gk \tanh kh)^{1/2}$$

The frequency σ may be interpreted as the wave frequency relative to a frame of reference moving with the local current velocity \underline{u} .

2.2 The Variational Principle and Derivation of Euler Equations

A variational principle equivalent to the boundary value problem given by (2.1.1-4) can be written as

$$\delta \int \int_{\underline{x}, t_1}^{t_2} L(\phi, \phi_t, \nabla_h \phi, \phi_z, \eta) dt d\underline{x} = 0 \quad (2.2.1)$$

where L is the Lagrangian governing the quantities ϕ and η , t_1 and t_2 are two arbitrarily chosen values of time, and \underline{x} , given by

$$\underline{x} = \{x, y\} = x \underline{i}_x + y \underline{i}_y \quad (2.2.2)$$

is the horizontal position in the domain. Here the space $\{\underline{x}, t\}$ may be considered to be the propagation space, and the coordinate z may be considered to be the cross-space, in the terminology of Hayes(1970). The form of L was given by Luke(1967) as

$$L = \int_{-h_0}^{\eta} \left\{ \phi_t + \frac{1}{2} (\nabla \phi)^2 + g z \right\} dz \quad (2.2.3)$$

where the integration over z represents integration over the cross-space, leading to a variational principle governing motion in the coordinates of the propagation space. The

original problem (2.1.1-4) can be recovered by taking variations of (2.2.3) with respect to ϕ and η ; see Whitham(1974), section 13.2 .

Whitham(1967) used the variational principle (2.2.3) to derive the dispersion relation and conservation laws for wave action, momentum and phase for weakly nonlinear Stokes waves with slow amplitude modulation. The Lagrangian was treated in an averaged form given by

$$\mathcal{L}(A, \psi) = \frac{1}{2\pi} \int_0^{2\pi} L d\psi \quad (2.2.4)$$

where A is the amplitude of the wave form. Variation of \mathcal{L} with respect to A yields the dispersion relation

$$G(\sigma, k) + A^2 H(\sigma, k) + O(\epsilon^4) = 0 \quad (2.2.5)$$

where

$$G(\sigma, k) = \left\{ 1 - (\omega - \underline{k} \cdot \underline{u})^2 / \sigma^2 \right\}$$

is the dispersion relation (2.1.6) for the linear problem. Peregrine and Smith(1979) have investigated the effect of the nonlinear contribution $H(\sigma, k)$ on refraction in the vicinity of caustics; this problem will be discussed in

Chapter 6. Conservation laws are obtained from \mathcal{L} through variation of the phase function ψ and use of Noether's theorem.

In the present study, the Lagrangian is utilized in its unaveraged, or primitive, form in order to obtain equations governing the fast varying quantities ϕ and η directly; the resulting equations thus need no assumption about the form of the phase function ψ . This method was applied by Booij(1981) to derive a time-dependent mild-slope model equation for linear waves in the presence of a current. Booij did not make use of a perturbation expansion to order the terms in his Lagrangian; consequently, steady terms appeared in the governing equation for the linearized wave motion and were dropped a posteriori. The present study provides a consistent means for deriving the linearized equation along with the higher order equations to be discussed below. Some use will be made, however, of the properties of Whitham's(1967) approach; in particular, it will be argued that terms which vanish upon integration over the phase do not contribute to the governing equation for the motion, since they can play no role in determining the corresponding conservation laws in the manner employed by Whitham(1967). However, in order to strengthen this argument, it will be shown that the retention of these terms

and proper treatment within the context of the perturbation expansion leads merely to redundant conditions on the dependent variables; this will be demonstrated by example rather than proven conclusively.

The Lagrangian L is manipulated in order to obtain equations governing the instantaneous motion of $\dot{\phi}$ and η , in the form of an Euler equation for $\tilde{\phi}$ and η and a corresponding free surface boundary condition for η . The potential $\tilde{\phi}(\underline{x}, t)$ is the portion of the potential describing motion in the propagation space. After substitution of $\dot{\phi}$ with known cross space structure into L and integration over the depth, L is of the form

$$L = L(\eta, \tilde{\phi}, \tilde{\phi}_t, \nabla_h \tilde{\phi}) \quad (2.2.6)$$

Variation of L with respect to η yields the condition

$$L_\eta(\delta\eta) = 0 \quad (2.2.7)$$

which in turn yields the boundary condition for η after using the arbitrariness of $\delta\eta$. Variation of L with respect to $\tilde{\phi}$ then leads to

$$L_{\tilde{\phi}} (\delta\tilde{\phi}) + L_{\tilde{\phi}_t} \delta(\tilde{\phi}_t) + L_{\nabla_h \tilde{\phi}} \delta(\nabla_h \tilde{\phi}) = 0 \quad (2.2.8)$$

which, after partial integration, leads to the Euler equation

$$L_{\tilde{\phi}} - (L_{\tilde{\phi}_t})_t - \nabla_h \cdot (L_{\nabla_h \tilde{\phi}}) = W \quad (2.2.9)$$

where W may be interpreted as a virtual work term of arbitrary form related to slow spatial and temporal nonperiodicity, and may be used to include the effect of energy dissipation. This step was taken by Booij(1981) to add a term to the mild-slope equation representing the decay of wave energy. Dalrymple, Kirby and Hwang(1983) have related Booij's term to several known results for wave energy dissipation due to friction; in Chapter 6, the formulation will be further extended to include the effect of breaking due to depth limited motion.

Various investigators (see, for example, Jimenez and Whitham (1976) and Ostrovskii and Pelinovskii(1972)) have developed methods for including dissipation effects within the variational scheme in a rigorous manner. The usual

approach is to include a term δW in a generalized Hamilton's principle which may then be written as

$$\delta \int \int_{\underline{x}} L dt d\underline{x} - \int \int_{\underline{x}} \delta W d\underline{x} dt = 0$$

Variations then lead to the inclusion of terms which take on the role of the term W in (2.2.9). These approaches have been summarised recently by Jeffrey and Kawahara(1982). Since the added terms resulting from the rigorous approach are of the same form as the arbitrarily added terms based on the allowable nature of W , we will not go further into these approaches in the present investigation.

2.3 The Perturbation Scheme and Series Expansions for ϕ and η .

Two perturbation scales will be used in the following derivation. The first is given by ϵ and is the usual expansion parameter for the Stokes(1847) wave theory. By nondimensionalising the governing equations with respect to the wavenumber k , it can be shown that ϵ is equal to the wave steepness kA ; here, we will retain dimensional forms and employ ϵ as a formal parameter. The velocity potential and surface displacement are then given by an expansion in powers of ϵ corresponding to the results of Stokes' theory.

A second formal parameter δ is taken to be proportional to the rates of spatial modulation of quantities such as h , k , A , etc. This is equivalent to the use of a multiple scale approach, in which a stretched horizontal coordinate $\underline{x} \sim \delta \underline{x}$ represents the length scale over which variations of the slowly changing quantities are felt. This formalism will enter the derivation through the treatment of horizontal derivatives; for example, the gradient of the depth can be written as

$$\nabla_h h(\delta \underline{x}) \sim \delta h_{\underline{x}} \sim \nabla_H h(\underline{x}) = O(\delta)$$

where the operator ∇_H is then an $O(1)$ quantity in the

stretched coordinate system, while the gradient of a wavelike quantity has both fast and slow variations and can be expanded in the form

$$\nabla_h \begin{Bmatrix} \tilde{\phi} \\ \eta \end{Bmatrix} \sim i\tilde{k} \begin{Bmatrix} \tilde{\phi} \\ \eta \end{Bmatrix} + \nabla_H \begin{Bmatrix} \tilde{\phi} \\ \eta \end{Bmatrix} = O(1) + O(\delta)$$

It is implied that the operator ∇_H operates on the amplitude of the functions $\tilde{\phi}$ and η , while the $O(1)$ derivative is related to the gradient of the phase function ψ .

In the derivation to be presented in Chapter 3, it will be assumed that the spatial variations of the depth h , wavenumber k , ambient current \underline{u} , and relative frequency σ may be characterised by a variation scale δ of $O(\epsilon)$ at the largest. This choice is consistent with the approach of Chu and Mei (1970a,b) who neglected the ambient current \underline{u} (and hence the relative frequency σ). It will be shown that a shift of scaling, with δ taken to be of $O(\epsilon^2)$, then reproduces the mild slope formulation of such authors as Berkhoff (1972) and Booij (1981).

In contrast to the relatively fast spatial variations allowed by the choice of $\delta \sim \epsilon$, we will restrict time variations of the quantities h , k , \underline{u} , and σ to be proportional to $O(\epsilon^3)$; this will have the effect of

excluding time variations of the physical domain from the derivations. This choice is consistent with an assumption that the time dependence of the physical domain is related to tidal variations at the fastest, and corresponds (in a multiple scale approach) to the choice of a stretched coordinate $t_3 = \epsilon^3 t$ for variations other than those of the principle wave. For example, if the incident wave is characterised by a period of 10 seconds and a steepness $\epsilon = 0.1$, then the slow variations in t_3 will occur over a time scale of $O(20 \text{ hours})$.

In the perturbation expansion schemes standardly used for deriving nonlinear evolution equations (see Davey and Stewartson(1974), Chu and Mei(1970b), and Yue(1980) for typical derivations related to Stokes waves in intermediate water depth), the modulation parameter δ is typically related directly to the Stokes expansion parameter ϵ , with disparities in scale maintained by the use of multiple scales in the propagation space. Then, the expansions proceed in powers of the single parameter ϵ . Here, the parameter δ will not be related in size to the parameter ϵ until the point is reached where specific results for certain choices of scale relations are derived. This approach has certain specific advantages over the standard single parameter approach, in that it does not become

necessary to Fourier-expand the boundary value problems at each order, since this need is a direct result of having lumped the expansion parameters in the first place. Thus, terms which are implicitly related to higher order in δ at a given order of ϵ do not become explicitly tied to terms at higher order in ϵ .

In order to obtain the desired results for weakly nonlinear waves, it is necessary to carry the calculation of the Lagrangian L to $O(\epsilon^4)$, based on expansions of ϕ and η to $O(\epsilon^2)$. We will impose the restriction that the smallest terms at each stage of the expansion have exponents of ϵ and δ totalling four; thus terms in L of $O(\epsilon^2)$ must retain terms to $O(\delta^2)$, while terms of $O(\epsilon^4)$ retain no modulation terms. This will have the effect of excluding slow modulations, and thus any consideration of scale, from the nonlinear terms found below. This restriction is consistent with the theories of Chu and Mei(1970b) and subsequent investigators, with the exception of Dysthe(1979), who includes the lowest order modulation effects in the nonlinear contribution.

One drawback of the Lagrangian approach is that it provides no information about the correct form of the expansions of ϕ and η to be used, both in terms of

consistency with the ordering parameters and in terms of the structure of the solution in the cross-space; this has led to several misunderstandings in the past. Whitham(1967) assumed a one-dimensional (in x) expansion of ϕ and η given by

$$\phi = \epsilon f_{10} \tilde{\phi}_1 + \epsilon^2 f_{20} \tilde{\phi}_2 + \beta x - \gamma t \quad (2.3.1a)$$

$$\eta = \epsilon \eta_1 + \epsilon^2 \eta_2 + b \quad (2.3.1b)$$

where

$$f_{10} = \frac{\cosh k(h+z)}{\cosh kh}, \quad f_{20} = \frac{\cosh 2k(h+z)}{\sinh^4 kh} \quad (2.3.2)$$

and where β , γ , and b are $O(\epsilon^2)$. The resulting conservation equations were subsequently found to be inconsistent with multiple scale expansions based on modulations of $O(\delta) \sim O(\epsilon)$, as shown first by Chu and Mei(1970b), and it was surmised that Whitham's theory was basically incomplete. Whitham(1970) showed, by means of a multiple scale expansion, that his results were consistent with the modulation rate $\delta \sim \epsilon^2$. Finally, Yuen and Lake(1975), for the case of deep water, showed that the inclusion in Whitham's approach of the proper forms of $\tilde{\psi}$

and η , consistent with a modulation rate $\delta \sim \epsilon$, produced results consistent with the multiple scale expansions. In the present study, we extend the demonstration of consistency between Whitham's approach and the multiple scale expansions to the case of waves in intermediate water depths, although the treatment of the Lagrangian is altered.

A consequence of the lack of ability to determine the assumed forms of ϕ and η is that appropriate forms must first be obtained by means of an expansion of the governing equations. The solution, including the effect of an $O(1)$ mean current \underline{U} , is derived in Appendix A, following the method outlined by Chu and Mei (1970a). The forms for ϕ and η are given by

$$\begin{aligned} \phi = & \delta^{-1} \phi_0 + \epsilon \left\{ f_{10} - i \delta (\alpha_1 f_{11} + \alpha_2 f_{12} + \alpha_3 f_{13}) \right\} \tilde{\Phi}_1 \\ & + \epsilon^2 f_{20} \tilde{\Phi}_2 + \epsilon^2 \delta^{-1} \phi'_2 - \{ \gamma_0 + \epsilon^2 \gamma_2 \} t + \dots \end{aligned} \quad (2.3.3a)$$

and

$$\eta = b_0 + \epsilon \eta_1 + \epsilon^2 (b_2 + \eta_2) + \dots \quad (2.3.3b)$$

where the steady current potential is given by

$$\phi_0 = \phi_0'(\underline{x}, t) + \delta^2 \phi_0'' \quad (2.3.4a)$$

where

$$\phi_0'' = -\frac{(h_0 + \bar{z})^2}{2} \nabla_h^2 \phi_0' - (h_0 + \bar{z}) \nabla_h h_0 \cdot \nabla_h \phi_0' \quad (2.3.4b)$$

The quantities f_{1i} and α_i are given by

$$f_{11} = k\bar{z} \frac{\cosh k(h+\bar{z})}{\cosh kh}$$

$$f_{12} = k(h+\bar{z}) \frac{\sinh k(h+\bar{z})}{\cosh kh} - kh \tanh kh \frac{\cosh k(h+\bar{z})}{\cosh kh}$$

$$f_{13} = \left\{ k^2(h+\bar{z})^2 - (kh)^2 \right\} \frac{\cosh k(h+\bar{z})}{\cosh kh} \quad (2.3.5)$$

and

$$\alpha_1 = \frac{\underline{k} \cdot \nabla_h h}{k}, \quad \alpha_2 = \frac{\nabla_h \cdot \left\{ \frac{\underline{k}}{k} \left(\frac{A}{\sigma} \right)^2 \right\}}{2k \left(\frac{A}{\sigma} \right)^2}, \quad \alpha_3 = \frac{\underline{k} \cdot \nabla_h k}{2k^3} \quad (2.3.6)$$

where h is the $O(1)$ mean water level given by

$$h = h_0 + b_0 \quad (2.3.7)$$

The forms of the wavelike components of $\hat{\phi}$ and η are essentially similar to those given by Chu and Mei(1970a), with the exception that the absolute frequency ω is replaced everywhere by the relative frequency σ .

Other terms included in (2.3.3) are b_0 and b_2 , which are slowly varying surface terms related to the ambient mean water level and the wave-induced surface fluctuation; ϕ'_2 , which is the potential for the $O(\epsilon^2)$ wave-induced current, and γ_0 and γ_2 , which are Bernoulli constants for the mean flow at each order.

In order to place the present derivation within the context of the implied or explicit scaling assumptions of various studies, a list of the various choices is given in Table 2.1.

Source	Highest order order terms in ϵ	Modulation scale for amplitude A	Modulation scale for h, k, U	Largest mean current related to ϵ
Whitham (1967, 1970)	ϵ^3	$\delta \sim \epsilon^2$	-	ϵ^2
Chu and Mei (1970a,b, 1971) Davey and Stewartson (1974)	ϵ^3	$\delta \sim \epsilon$	$\delta \sim \epsilon$	ϵ^2
Foda and Mei (1981)	ϵ^3	$\delta \sim \epsilon$	$\delta \sim \epsilon$	ϵ
Berkhoff (1972)	ϵ	$\delta \sim \epsilon^2$	$\delta \sim \epsilon^2$	-
Booij (1981)	ϵ	$\delta \sim \epsilon^2$	$\delta \sim \epsilon^2$	1
Present Study	ϵ^3	$\delta \sim \epsilon$	$\delta \sim \epsilon$	1

Table 2.1 Relation between scaling parameters for several wave propagation models

ϵ = Stokes wave steepness, δ = inverse modulation length scale

CHAPTER 3. THE LAGRANGIAN AND EQUATIONS GOVERNING
WAVE MOTION

3.1 Introduction

The Lagrangian L governing the motion of waves with imposed current field $\underline{U}(\underline{x}, t)$ is constructed by substituting the perturbation expansions (in the small parameter ϵ) for ϕ and η , given by (2.3.3), into (2.2.3) and performing the integration over depth. The Lagrangian is then expanded as a series in the small parameter ϵ , yielding the expression

$$L = L_0 + \epsilon L_1 + \epsilon^2 L_2 + \epsilon^3 L_3 + \epsilon^4 L_4 \quad (3.3.1)$$

Then, consistent with the restriction that the exponents of ϵ and δ total no more than four, we may restrict L_2 to $O(\delta^2)$ and L_4 to $O(1)$. L_3 will not contribute any new information, and may be truncated to $O(1)$ in δ for simplicity. Equations governing the various terms in ϕ may then be obtained by varying the term L_{2n} by the member ϕ_n of the perturbation series for ϕ . Since the perturbation method is somewhat unique, an example of its use in a simpler problem is shown in Appendix B.

3.2 The Lagrangian for Stokes Waves

The assumed forms for ϕ and η are given by (2.3.3), based on the derivation for the large current case given in Appendix A. Individual contributions to the Lagrangian are given by gz , ϕ_t and $\nabla\phi$; the subsequent calculations are lengthy and are outlined in Appendix C.1. The results may be written in the expanded form (3.1.1); the individual contributions are given by

$$L_0 = \frac{g b_0^2}{2} - \frac{g h_0^2}{2} + h \left\{ \phi_{0t}' - \gamma_0 + \frac{(\nabla_h \phi_0')^2}{2} \right\} + \frac{h^3}{6} (\nabla_h \phi_0')^2 + \\ + \frac{h}{2} \nabla_h \phi_0' \cdot \nabla_h \left\{ \nabla_h \cdot (h \nabla_h \phi_0') \right\} - \nabla_h \phi_0' \cdot \nabla_h \left\{ \nabla_h \cdot \left(\frac{h^3}{6} \nabla_h \phi_0' \right) \right\} \quad (3.2.1)$$

where $h = h_0 + b_0$ and where ϕ_0 and b_0 are to be expanded in the forms

$$\phi_0 = \phi_0' + \delta^2 \phi_0''$$

and

$$b_0 = b_0' + \delta^2 b_0''$$

and we assume that the time variation of ϕ_0' is $O(\delta^3)$;

$$\begin{aligned}
L_1 = & g b_0 \eta_1 + \eta_1 \left\{ \phi'_{0t} + \frac{(\nabla_h \phi'_0)^2}{2} - \gamma_0 \right\} + (\nabla_h \cdot (h \sigma_h \phi'_0))^2 \frac{\eta_1}{2} \\
& - \nabla_h \phi'_0 \cdot \nabla_h \left\{ \nabla_h \cdot \left(\frac{h^2}{2} \nabla_h \phi'_0 \right) \right\} \eta_1 + J' \tilde{\Phi}_1 \\
& + \left\{ G'_0 - i \sum_{j=1}^3 \alpha_j G'_j \right\} \frac{D' \tilde{\Phi}_1}{Dt} + H' \cdot \nabla_h \tilde{\Phi}_1 \\
& + \left\{ G'_{00} - i \sum_{j=1}^3 \alpha_j G'_{0j} - i \sum_{j=1}^3 \nabla_h \alpha_j G'_j \right\} \cdot \nabla_h \phi'_0 \tilde{\Phi}_1
\end{aligned} \tag{3.2.2}$$

where

$$\frac{D'}{Dt} = \frac{\partial}{\partial t} + \nabla_h \phi'_0 \cdot \nabla_h + \nabla_h \phi''_0 \Big|_0 \cdot \sigma_h$$

and G' , J' , and H' symbolize integrals over the depth which are evaluated where needed in Appendix D;

$$\begin{aligned}
L_2 = & g \frac{\eta_1^2}{2} + g b_0 (\eta_2 + b_2) + G''_0 \eta_1 \frac{D' \tilde{\Phi}_1}{Dt} + h \left\{ \phi'_{2t} + \sigma_h \phi'_0 \cdot \sigma_h \phi'_2 - \gamma_2 \right\} + \\
& + (\eta_2 + b_2) \left\{ \phi'_{0t} + \frac{1}{2} (\nabla_h \phi'_0)^2 - \gamma_0 \right\} + G'_{000} \frac{\tilde{\Phi}_1^2}{2} + H' \frac{D' \tilde{\Phi}_2}{Dt} + \\
& + (G'_{000} \cdot \sigma_h \tilde{\Phi}_1) \tilde{\Phi}_1 + (H'_0 \cdot \sigma_h \phi'_0) \tilde{\Phi}_2 + \\
& + (\eta_2 + b_2) \left\{ \frac{\nabla_h \cdot (h \sigma_h \phi'_0)}{2} \right\}^2 + (\nabla_h^2 \phi'_0) (\nabla_h \cdot (h \sigma_h \phi'_0)) \frac{\eta_1^2}{2} -
\end{aligned}$$

$$\begin{aligned}
& - G_0^{\prime\prime} \nabla_h \cdot (h \nabla_h \phi_0') \eta_1 \tilde{\phi}_1 - (\eta_2 + b_2) (\nabla_h \phi_0' \cdot \nabla_h) (\nabla_h \cdot (\frac{h^2}{2} \nabla_h \phi_0')) + \\
& + \left\{ G_{00}' - 2i \sum_{j=1}^3 \alpha_j G_{0j}' - \sum_{k=1}^3 \sum_{j=1}^3 \alpha_j \alpha_k G_{jk}' \right\} \frac{(\nabla_h \tilde{\phi}_1)^2}{2} + \\
& + \left\{ G_{00}^{\prime\prime} - 2i \sum_{j=1}^3 \alpha_j G_{0j}^{\prime\prime} - \sum_{k=1}^3 \sum_{j=1}^3 \alpha_j \alpha_k G_{jk}^{\prime\prime} \right\} \frac{\tilde{\phi}_1}{2} - \\
& - i \left\{ \nabla_h \left(\sum_{j=1}^3 \alpha_j G_{0j}' \right) + (\nabla_h h) \sum_{j=1}^3 \alpha_j f_{10} f_{1j} \Big|_{-h} \right\} \cdot (\nabla_h \tilde{\phi}_1) \tilde{\phi}_1 \quad (3.2.3)
\end{aligned}$$

where \mathcal{L}' is also an integral expression evaluated in Appendix D;

$$\begin{aligned}
L_3 = & g \eta_1 (\eta_2 + b_2) + \eta_1 \left\{ \phi_{z_t}' + \nabla_h \phi_0' \cdot \nabla_h \phi_2' - \gamma_2 \right\} + \\
& + (\eta_2 + b_2) \frac{D\tilde{\phi}_1}{Dt} + G_0''' \eta_1^2 \frac{D\tilde{\phi}_1}{Dt} + G_{00}'' \eta_1 \frac{(\nabla_h \tilde{\phi}_1)^2}{2} + \\
& + G_{00}^{\prime\prime} \eta_1 \frac{\tilde{\phi}_1^2}{2} + \mathcal{L}'_0 \nabla_h \tilde{\phi}_1 \cdot \nabla_h \tilde{\phi}_2 + \mathcal{L}^{\prime\prime}_0 \tilde{\phi}_1 \tilde{\phi}_2 + \\
& + O(\delta) \quad (3.2.4)
\end{aligned}$$

and

$$\begin{aligned}
L_4 = & (\eta_2 + b_2) \left\{ \phi'_{2t} + \nabla_n \phi'_0 \cdot \nabla_n \phi'_2 - \gamma_2 \right\} + \frac{h}{2} (\nabla_n \phi'_2)^2 + \\
& + g \frac{(\eta_2 + b_2)^2}{2} + \left\{ 2\eta_1 (\eta_2 + b_2) G_0''' + \eta_1^3 G_0'' \right\} \frac{D\tilde{\phi}_1}{Dt} + \\
& + \left\{ \mathcal{G}'' (\eta_2 + b_2) + \mathcal{G}''' \eta_1^2 \right\} \frac{D\tilde{\phi}_2}{Dt} + \eta_1 \nabla_n \tilde{\phi}_1 \cdot \nabla_n \phi'_2 + \\
& + \left\{ G_{00}'' (\eta_2 + b_2) + G_{00}''' \eta_1^2 \right\} \frac{(\nabla_n \tilde{\phi}_1)^2}{2} + \mathcal{G}_0'' \eta_1 \nabla_n \tilde{\phi}_1 \cdot \nabla_n \tilde{\phi}_2 + \\
& + \left\{ G_{00}^{\tilde{z}''} (\eta_2 + b_2) + G_{00}^{\tilde{z}'''} \eta_1^2 \right\} \frac{\tilde{\phi}_1^2}{2} + \mathcal{G}_0^{\tilde{z}''} \eta_1 \tilde{\phi}_1 \tilde{\phi}_2 + \\
& + \mathcal{G}' \nabla_n \phi'_2 \cdot \nabla_n \tilde{\phi}_2 + \mathcal{G}^{2'} \frac{(\nabla_n \tilde{\phi}_2)^2}{2} + \mathcal{G}^{2\tilde{z}'} \frac{\tilde{\phi}_2^2}{2} \quad (3.2.5)
\end{aligned}$$

The expressions for $L_0 - L_4$ form the basis for the perturbation method outlined in Appendix B.

3.3 The Governing Equations

We proceed by determining the Euler equations for each order in ϵ , following the method outlined in Appendix B. First, by varying L_0 with respect to b_0 , we obtain the expression

$$gb'_0 + \phi'_{0,t} + \frac{(\nabla_h \phi'_0)^2}{2} - \gamma_0 = 0 + O(\delta^2) \quad (3.3.1)$$

By requiring that b_0 vanish in the absence of a current, we set $\gamma_0 = 0$. Then, varying L_0 with respect to ϕ_0 and performing the partial integration over the propagation space, we obtain the continuity equation

$$b'_{0,t} + \nabla_h \cdot \{ h \nabla_h \phi'_0 \} = 0 + O(\delta^3) \quad (3.3.2)$$

By taking the horizontal gradient of (3.3.1), we obtain a momentum equation for the $O(1)$ mean flow:

$$\underline{u}_t + (\underline{u} \cdot \nabla_h) \underline{u} + g \nabla_h b'_0 = 0 \quad (3.3.3)$$

where $\underline{u} = \nabla_h \phi'_0$. Recalling from (3.2.1) that b_0 and ϕ_0 are to be expanded in orders of δ , and that $\frac{\partial}{\partial t} \sim O(\delta^3)$ for the zeroth order flow, we find that

$$\nabla_h \cdot \{ (h_0 + b'_0) \nabla_h \phi'_0 \} = 0 + O(\delta^3) \quad (3.3.4)$$

and

$$gb_0' = -\frac{1}{2}(\nabla_h \phi_0')^2 + O(\delta^2) \quad (3.3.5)$$

to leading order. All contributions to L_1 and L_2 involving $\nabla_h(h\nabla_h \phi_0')$ may therefore be dropped. The contribution of ϕ_0'' in L_2 is thus reduced to a small correction to the operator D/Dt and the $O(1)$ mean water level h , and enters the overall equation in tandem with ϕ_0' . It should be noted that in L_4 , which is expanded only to $O(\delta^0)$, the contribution from b_0'' and ϕ_0'' in h and D'/Dt should be dropped; however, retaining them introduces only a small error. It is apparent from (3.3.4-5) that the current is effectively steady to leading order, and the smallness of b_{0x}' justifies the neglect of time derivatives of the f functions in ϕ .

Moving to $O(\epsilon)$, we note that the average of L_1 over the phase for any choice of temporally periodic function for ϕ vanishes; i.e.,

$$\bar{L}_1 = \frac{1}{2\pi} \int_0^{2\pi} L_1 d\psi = 0$$

Thus L_1 does not contribute in any significant way to the governing and conservation equations, following the results of Whitham(1967). As a test of this hypothesis, we need to show that variations of L_1 produce only redundant conditions on b_0 and ϕ_0 . At $O(\epsilon)$, our lowest order

unknowns are η_1 and $\tilde{\phi}_1$, since we can assume that b_0 and ϕ_0' are specified by (3.3.1-2). Varying L_1 with respect to η_1 gives (3.3.1) again. Varying L_1 with respect to $\tilde{\phi}_1$ after dropping the $O(\delta^3)$ contribution of H' and J' leads to the condition

$$\left\{ G_0' - i \sum_{j=1}^3 \alpha_j G_j' \right\}_t = 0 \quad (3.3.6)$$

which is accurate due to our assumptions about the time scale of variation of the current.

Moving to $O(\epsilon^2)$, we take variations of L_2 with respect to the still unknown quantities η_1 and $\tilde{\phi}_1$. The η_1 variation leads to the well known surface boundary condition:

$$g \eta_1 + G_0'' \frac{D\tilde{\phi}_1}{Dt} = 0 \quad (3.3.7)$$

where $G_0'' = 1$. The variation with respect to $\tilde{\phi}_1$ and the subsequent partial integration are tedious and are presented in Appendix C.2. The resulting second order wave equation for $\tilde{\phi}_1$ is given by

$$\begin{aligned} \frac{D^2 \tilde{\phi}_1}{Dt^2} + (\nabla_h \cdot \mathcal{U}) \frac{D\tilde{\phi}_1}{Dt} - \nabla_h \cdot \{ g G_{00}' \nabla_h \tilde{\phi}_1 \} + g G_{00}'' \tilde{\phi}_1 \\ + g (\alpha + F) \tilde{\phi}_1 = W_1 \end{aligned} \quad (3.3.8)$$

where F is a complicated coefficient given below and derived in Appendix C.2. The term

$$\alpha = G'_{\nabla_0 \nabla_0} - \nabla_h \cdot G'_{0 \nabla_0} \quad (3.3.9)$$

is identical to the higher order terms found by Smith and Sprinks (1975); however it is not the only correction at $O(\delta^2)$ involving the bottom slope. The term F is given, for the general case of currents and depth varying at $O(\delta)$, by

$$\begin{aligned} F = & -\bar{z}_1 \beta_1 + (\bar{z}_2 - \bar{z}_3) \beta_2 - \bar{z}_2 (\beta_3 - \beta_4 + \beta_5) \\ & - \gamma_1 \alpha_1^2 + \gamma_2 \alpha_1 \alpha_3 + \gamma_3 \alpha_3^2 - 2 \bar{z}_{03} \alpha_1 \beta_6 \\ & + \gamma_4 (2\alpha_1 \beta_7 - \alpha_1 \beta_8) + \gamma_5 \alpha_3 \beta_6 + \gamma_6 (2\alpha_3 \beta_7 - \alpha_3 \beta_8) \\ & - \bar{z}_2 (\beta_7 \beta_8 - \beta_8^2/4) \end{aligned} \quad (3.3.10)$$

where

$$\begin{aligned} \beta_1 &= \frac{\underline{k} \cdot \nabla_h (k \alpha_1)}{k^3} & \beta_2 &= \frac{\underline{k} \cdot \nabla_h (2k^3 \alpha_3)}{k^3} \\ \beta_3 &= \frac{\underline{k} \cdot \nabla_h (k^2 A \beta_6)}{k^4 A} & \beta_4 &= \frac{\underline{k} \cdot \nabla_h (k^2 \sigma \beta_7)}{k^4 \sigma} \\ \beta_5 &= \underline{k} \cdot \nabla_h (k^2 \beta_8) / 2k^4 \end{aligned} \quad (3.3.11)$$

are $O(\delta^2)$ quantities, and

$$\beta_6 = \frac{\underline{k} \cdot \nabla_h A}{k^2 A} \quad \beta_7 = \frac{\underline{k} \cdot \nabla_h \sigma}{k^2 \sigma}$$

$$\beta_8 = \frac{\nabla_h \cdot \underline{k}}{k^2} \quad (3.3.12)$$

are $O(\delta)$ quantities appearing in products. The quantities $\gamma_1 - \gamma_6$ and $\tilde{\sigma}$ arise from integrals of the normal mode structure; explicit values are given in Appendix D. The term α can be expanded explicitly as

$$\alpha = \delta_1 \nabla_h^2 h^2 + \delta_2 \nabla_h h \cdot \nabla_h k + \delta_3 \nabla_h k^2 - \nabla_h \cdot \{ \delta_4 \nabla_h h + \delta_5 \nabla_h k \} \quad (3.3.13)$$

and $\delta_1 - \delta_5$ are also given in Appendix D.

Equation (3.3.8) is an equation for linear waves in a domain with depth and currents which vary at $O(\delta)$; as such, it serves as the first higher order correction to Booij's (1981) model, which is essentially similar to (3.3.8) after neglecting F and α .

Moving to L_3 , variation with respect to the unknown second order free surface ($b_2 + \eta_2$) yields (3.3.7) as a redundant condition. Varying L_3 with respect to $\tilde{\phi}_2$ yields a second governing equation similar to (3.3.8); this equation

can be shown to be satisfied at lowest order by waves governed by the linear dispersion relationship (2.1.6), and is therefore also a redundant condition.

Variation of L_4 with respect to $(\eta_2 + b_2)$ yields the free surface condition,

$$g(\eta_2 + b_2) + \phi_2'_{,t} + \nabla_h \phi_0' \cdot \nabla_h \phi_2' - \gamma_2 + 2G_0''' \eta_1 \frac{D\tilde{\phi}}{Dt} + g'' \frac{D\tilde{\phi}_2}{Dt} + \frac{G_0''}{2} (\nabla_h \tilde{\phi}_1)^2 + \frac{G_0''}{2} \tilde{\phi}_1^2 = 0 \quad (3.3.14)$$

which specifies the complete second order free surface. The mean surface b_2 can be extracted from this expression by taking the mean over a wave period. After substituting (3.3.7), this operation results in

$$g b_2 + \frac{D\phi_2'}{Dt} - \gamma_2 = \frac{2G_0'''}{g} \left(\frac{D\tilde{\phi}_1}{Dt} \right)^2 - \frac{G_0''}{2} (\nabla_h \tilde{\phi}_1)^2 - \frac{G_0''}{2} \tilde{\phi}_1^2 \quad (3.3.15)$$

Again, by requiring that b_2 vanish in the absence of waves, we set $\gamma_2 = 0$. Then, varying L_4 with respect to ϕ_2' leads to the expression

$$-(\eta_2 + b_2)_{,t} - \nabla_h \cdot \{ (\eta_2 + b_2) \nabla_h \phi_0' \} - \nabla_h \cdot \{ h \nabla_h \phi_2' \} - \nabla_h \cdot \{ \eta_1 \nabla_h \tilde{\phi}_1 \} - \nabla_h \cdot \{ g' \nabla_h \tilde{\phi}_2 \} = 0 \quad (3.3.16)$$

Taking the mean over a wave period, (3.3.16) reduces to

$$\frac{D b_2}{D t} + (\nabla_h \cdot \underline{u}) b_2 + \nabla_h \cdot (h \nabla_h \phi_2') = - \nabla_h \cdot \overline{\{\eta_1 \nabla_h \tilde{\phi}_1\}} \quad (3.3.17)$$

This is the continuity equation for the second order wave-induced current $\nabla_h \phi_2'$. Writing the R.H.S. of (3.3.15) as \mathcal{B} and eliminating b_2 from (3.3.15-17) leads to a forced wave equation for the second order mean flow, given by

$$\frac{D^2 \phi_2'}{D t^2} + (\nabla_h \cdot \underline{u}) \frac{D \phi_2'}{D t} - g \nabla_h \cdot (h \nabla_h \phi_2') = \frac{D \mathcal{B}}{D t} + (\nabla_h \cdot \underline{u}) \mathcal{B} + g \nabla_h \cdot \overline{\{\eta_1 \nabla_h \tilde{\phi}_1\}} \quad (3.3.18)$$

This equation is equivalent in spirit to the forced wave equation given by Davey and Stewartson (1974) after including the effect of $O(1)$ currents; the connection will be seen more clearly after substituting for \mathcal{B} and $\nabla_h \cdot \overline{\{\eta_1 \nabla_h \tilde{\phi}_1\}}$ based on plane wave approximations.

Variation of L_4 with respect to $\tilde{\phi}_2$ leads to the governing equation

$$\begin{aligned} & - \frac{D}{D t} \{ (\eta_2 + b_2) \mathcal{A}'' + \eta_1^2 \mathcal{A}''' \} - \nabla_h^2 \phi_0' \cdot \{ (\eta_2 + b_2) \mathcal{A}'' + \eta_1^2 \mathcal{A}''' \} \\ & - \nabla_h \cdot \{ \mathcal{A}_0'' \eta_1 \nabla_h \tilde{\phi}_1 \} + \mathcal{A}_0''' \eta_1 \tilde{\phi}_1 - \nabla_h \cdot \{ \mathcal{A}' \nabla_h \phi_2' \} - \nabla_h \cdot \{ \mathcal{A}^2 \nabla_h \tilde{\phi}_2 \} \\ & + \mathcal{A}^{22'} \tilde{\phi}_2 = 0 \end{aligned} \quad (3.3.19)$$

(3.3.16) and (3.3.19) may be combined by eliminating

$(\eta_2 + b_2)$; the resulting equation governs the second order potential $\tilde{\phi}_2$. Equations (3.3.2), (3.3.7-8), (3.3.18) and (3.3.19) represent the complete set of governing equations for the Stokes wave train to $O(\epsilon^2)$, with modulation rates of $O(\delta \sim \epsilon)$ allowed for all quantities with the exception of time-variations of ϕ_0 .

3.4 The Mild Slope Approximation and Some Plane Wave Results

Reduction of the previously derived models to the case of very slowly varying ($O(\delta^2)$) currents and depth can be obtained by truncating the equations to $O(\delta)$. This removes the effects of the α_i and ϕ_0'' from ϕ , and leads to the neglect of the coefficients F and α in (3.3.8). (It is noted that, in some instances, it may be desirable to retain the fast modulation rate for the wave amplitude, contained in the coefficients β_3 and β_6 , due to the influence of nonlinear effects.) The first order wave equation becomes, after substituting for the coefficients from Appendix D

$$\frac{D^2 \tilde{\phi}_1}{Dt^2} + (\nabla_h \cdot \mathcal{U}) \frac{D \tilde{\phi}_1}{Dt} - \nabla_h \cdot \{CC_g \nabla_h \tilde{\phi}_1\} + \sigma^2(1-\kappa) \tilde{\phi}_1 = W_1 \quad (3.4.1)$$

which is equivalent to Booij's model after neglecting an $O(\delta^2)$ term which appears due to an error in Booij's free surface boundary condition. The terms at $O(\delta^2)$ are unaltered, since modulations were not considered at that order.

Several expressions from section (3.3) may be cast in more familiar form by introducing plane wave

approximations for the terms η_1 and $\tilde{\phi}_1$, obtained from Appendix A. The term $\nabla_h \cdot \overline{\eta_1 \nabla_h \tilde{\phi}_1}$ may be reduced to the usual expression for the wave-induced mass flux

$$\nabla_h \cdot \overline{\eta_1 \nabla_h \tilde{\phi}_1} = \nabla_h \cdot \left(\frac{E}{\sigma} \underline{k} \right) \quad (3.4.2)$$

where

$$E = \frac{1}{2} g |A|^2$$

In the absence of a mean current \underline{u} , (3.3.17) becomes the familiar continuity equation

$$b_{2,t} + \nabla_h \cdot \left\{ h_0 \nabla_h \phi_2' + \frac{E}{\omega} \underline{k} \right\} = 0 \quad (3.4.3)$$

found originally by Whitham(1962) and Longuet-Higgins and Stewart(1962). The extension to the case including a current is given by

$$\frac{\partial b_2}{\partial t} + \nabla_h \cdot \left\{ b_2 \underline{u} + h \nabla_h \phi_2' + \frac{E}{\sigma} \underline{k} \right\} = 0 \quad (3.4.4)$$

which reflects the interaction between the mass flux of the $O(1)$ current and the small correction to the total depth given by b_2 .

In (3.3.18), the quantity \tilde{S} may be estimated by the plane wave approximation

$$B = \frac{-gk}{2 \sinh 2kh} |A|^2 \quad (3.4.5)$$

In a quasi-steady wave field with small spatial variations, b_2 is therefore given by

$$b_2 = b_{2s} = \frac{-k|A|^2}{2 \sinh 2kh} \quad (3.4.6)$$

which is recognisable as the steady $O(\epsilon^2)$ wave-induced setdown, given by Longuet-Higgins and Stewart (1964). The extension to the unsteady case with current is given by

$$gb_2 = gb_{2s} - \frac{D\phi_2'}{Dt} \quad (3.4.7)$$

where b_{2s} is given by (3.4.6). The forced wave equation (3.3.18) may then be simplified by the use of (3.4.2) and (3.4.5) to give

$$\begin{aligned} \frac{D^2 \phi_2'}{Dt^2} + (\nabla_h \cdot \underline{u}) \frac{D\phi_2'}{Dt} - g \nabla_h \cdot (h \nabla_h \phi_2') &= \frac{-gk}{2 \sinh 2kh} |A|^2_t + \\ + \frac{g^2}{2} \nabla_h \cdot \left\{ k \frac{|A|^2}{\sigma} \right\} + g \nabla_h \cdot \left\{ b_{2s} \nabla_h \phi_0' \right\} &= 0 \end{aligned} \quad (3.4.8)$$

A form of this equation applicable to water of constant depth in the absence of an $O(1)$ current is given by

$$\phi'_{2tt} - gh \nabla_h^2 \phi'_2 = \frac{g^2}{2b} \underline{k} \cdot \nabla_h |A|^2 - \frac{gk}{2 \sinh 2kh} |A|^2_t \quad (3.4.9)$$

which, after specifying that the principle wave $\tilde{\phi}_1$ travel in the x direction

$$\underline{k} = \{k, 0\}$$

and using the lowest order energy equation (Appendix E)

$$|A|^2_t = -C_g |A|^2_x$$

yields

$$\phi'_{2tt} - gh \nabla_h^2 \phi'_2 = \frac{\omega^2}{2} \left\{ \frac{1}{k \tanh^2 kh} + \frac{C_g}{2 \sinh^2 kh} \right\} |A|^2_x \quad (3.4.10)$$

given by Yue(1980) and in slightly different form by Davey and Stewartson(1974).

3.5 The Weakly-nonlinear Equation for $\tilde{\phi}_1$

In the preceding sections, a method has been described by which linear equations governing the evolution of the first two terms in the Stokes expansion for ϕ , given by $\tilde{\phi}_1$ and $\tilde{\phi}_2$, are obtained. This method could be carried to higher orders after allowing perturbation of the wavenumber k to account for secular terms arising at $O(\epsilon^3)$; however, the algebra involved becomes exceedingly tedious for the general theory being developed here. The results described so far allow for the calculation of the $O(\epsilon)$ linear wave field, with subsequent calculation of the $O(\epsilon^2)$ forced harmonic following based on the result for the linear fundamental. Truncation at this level provides results consistent with the Stokes solution to second order, with the waveform characterised by short crests and broad troughs due to the second order correction. However, the results do not include the effect of amplitude dispersion on the phase velocity; this result would arise at $O(\epsilon^3)$ through the choice of the first perturbation correction to the wavenumber k .

One method of correcting this deficiency could proceed by calculating k based on a nonlinear form of the dispersion relation (2.1.6). Booij(1981) suggested two

empirical modifications to the linear dispersion relation based on suggestions by Walker (1976) and Hedges(1976); however, it is simple enough to use the dispersion relation from nonlinear theory directly, thus dispensing with the empirical approximations. By averaging a Lagrangian similar to (3.3.1-5), neglecting the $O(\xi^2)$ terms, Whitham obtained a dispersion relation given by (including the current \underline{u})

$$(\omega - (\underline{u} + \nabla_h \phi_2') \cdot \underline{k})^2 = gk \tanh kh (1 + (k|A|)^2 D) \quad (3.5.1)$$

where

$$D = \frac{\cosh 4kh + 8 - 2 \tanh^2 kh}{8 \sinh^4 kh} \quad (3.5.2)$$

The relation (3.5.1) then provides a means by which the value of k may be determined based on local values of the amplitude A . Inclusion of this effect in the linear model (3.3.8) requires an iteration in order to obtain the initial guess for the updated local value of A , after which the corrected value of k is determined. This method was suggested by Booij as a means for incorporating the empirical nonlinear dispersion relations of Hedges(1976) or Walker(1976) in the linear model; and will be employed in section 6.9 where Stokes theory is not appropriate to the description of the problem.

In the recent literature on nonlinear water waves,

the most successful approach to including the effect of low order nonlinearity in the basic governing equation, and to producing tractable computational models, has been to include the nonlinear effects in the form of nonlinear terms added to the linear governing equation. The added terms, proportional to the third power of the local amplitude, account for the effect of amplitude dispersion provided by the nonlinear dispersion relation (3.5.1) or its fast-modulation counterpart.

We proceed by deriving the third order correction terms to be included in the linear governing equation. This development leads to the correct inclusion of amplitude dispersion in the linear wave equation, which was only suggested on approximate grounds by Booij(1981). In addition the second-order hyperbolic form of the governing equation allows for the study of reflections in an arbitrary domain, which has been investigated only occasionally in the context of the nonlinear Schrodinger equation approach (see for example Smith (1976b) and Newell (1978)).

It is sufficient to consider a reduced form of L given by

$$L = L_2(O(\epsilon^2, \delta^0)) + L_4 \quad (3.5.3)$$

Here, we have dropped terms of $O(\delta^2)$ from L_2 for the sake of computational simplicity; these terms are unaltered by the derivation and may be replaced subsequently. Also, we drop L_3 entirely on the grounds that its average over the phase is zero, implying that it has no effect on the conservation equations; alternatively, we can argue that variation of L_3 with respect to $\tilde{\phi}_1$ in the following derivation leads to terms which are steady or proportional to $e^{-2i\omega t}$, and are asynchronous with the linear wave component; they therefore do not contribute to the motion of the fundamental wave. However, L_4 , when varied with respect to $\tilde{\phi}_1$ and η_1 , produces terms proportional to $e^{-i\omega t}$ and $e^{-3i\omega t}$; the first set of terms is then retained as the principle nonlinear correction to the governing equation for $\tilde{\phi}_1$.

First, the reduced Lagrangian (3.5.3) is varied with respect to $\tilde{\phi}_1$, and the resulting expression is partially integrated to give the nonlinear counterpart of (C.2.1):

$$\begin{aligned}
& -\frac{D\eta_1}{Dt} - (\nabla_h \cdot \underline{u})\eta_1 - \nabla_h \cdot (G'_{00} \nabla_h \tilde{\phi}_1) + G^{\bar{z}'}_{00} \tilde{\phi}_1 - G^{\bar{z}}_0 \frac{D}{Dt} (\eta_1^3) \\
& - 2G'''_0 \left\{ b_2 \frac{D\eta_1}{Dt} + \frac{D}{Dt} (\eta_1 \eta_2) \right\} - b_2 \left\{ G''_{00} \nabla_h^2 \tilde{\phi}_1 - G^{\bar{z}''}_{00} \tilde{\phi}_1 \right\} \\
& - G'''_{00} \nabla_h \cdot \{ \eta_1^2 \nabla_h \tilde{\phi}_1 \} + G^{\bar{z}''}_{00} \eta_2 \tilde{\phi}_1 + G^{\bar{z}'''}_{00} \eta_1^2 \tilde{\phi}_1 + G^{\bar{z}''}_{00} \eta_1 \tilde{\phi}_2 \\
& - G''_0 \nabla_h \cdot \{ \eta_1 \nabla_h \tilde{\phi}_2 \} - \nabla_h \cdot \{ \eta_2 \nabla_h \tilde{\phi}_1 \} - \nabla_h \phi'_2 \cdot \nabla_h \eta_1 = 0 \quad (3.5.4)
\end{aligned}$$

Varying L with respect to η_1 and dividing by g leads to the nonlinear free surface boundary condition:

$$\begin{aligned} & \eta_1 + \frac{1}{g} \frac{D\tilde{\phi}_1}{Dt} + 2G_0''' \frac{b_2}{g} \frac{D\tilde{\phi}_1}{Dt} + 3G_0^{\text{IV}} \frac{\eta_1^2}{g} \frac{D\tilde{\phi}_1}{Dt} + G_{00}''' \eta_1 (\nabla_h \tilde{\phi}_1)^2 \\ & + 2\mathcal{G}''' \eta_1 \frac{D\tilde{\phi}_2}{Dt} + \mathcal{G}_0'' \nabla_h \tilde{\phi}_1 \cdot \nabla_h \tilde{\phi}_2 + G_{00}^{\text{z}'''} \eta_1 (\tilde{\phi}_1)^2 + \mathcal{G}_0^{\text{z}''} \tilde{\phi}_1 \tilde{\phi}_2 \\ & + \nabla_h \phi_2' \cdot \nabla_h \tilde{\phi}_1 = 0 \end{aligned} \quad (3.5.5)$$

In the equations (3.5.4-5), b_2 is given by (3.4.7). Differentiating (3.5.5) and substituting in (3.5.4), we obtain a nonlinear governing equation for $\tilde{\phi}_1$, with nonlinear terms including the first and second order fluctuating surfaces η_1 and η_2 :

$$\begin{aligned} & \frac{1}{g} \frac{D^2 \tilde{\phi}_1}{Dt^2} + \frac{(\nabla_h \cdot \underline{u})}{g} \frac{D\tilde{\phi}_1}{Dt} - \nabla_h \cdot (G_{00}' \nabla_h \tilde{\phi}_1) + G_{00}^{\text{z}'} \tilde{\phi}_1 + G_{00}^{\text{z}''} \eta_2 \tilde{\phi}_1 + \\ & + b_2 \left\{ G_{00}^{\text{z}''} \tilde{\phi}_1 - \nabla_h^2 \tilde{\phi}_1 - 2G_0''' \frac{D\eta_1}{Dt} + 2G_0''' \frac{D^2 \tilde{\phi}_1}{Dt^2} \right\} + \frac{2}{g} \mathcal{G}''' \frac{D}{Dt} \left(\eta_1 \frac{D\tilde{\phi}_2}{Dt} \right) + \\ & + \nabla_h \phi_2' \cdot \left\{ \frac{1}{g} \frac{D}{Dt} (\nabla_h \tilde{\phi}_1) - \nabla_h \eta_1 \right\} + 2G_0''' \left\{ \frac{1}{g} \frac{D}{Dt} \left(\eta_2 \frac{D\tilde{\phi}_1}{Dt} \right) - \frac{D}{Dt} (\eta_1 \eta_2) \right\} + \\ & + G_0^{\text{IV}} \left\{ \frac{3}{g} \frac{D}{Dt} \left(\eta_1^2 \frac{D\tilde{\phi}_1}{Dt} \right) - \frac{D}{Dt} (\eta_1^3) \right\} + G_{00}''' \left\{ \frac{1}{g} \frac{D}{Dt} \left(\eta_1 (\nabla_h \tilde{\phi}_1)^2 - \nabla_h (\eta_1^2 \nabla_h \tilde{\phi}_1) \right) \right\} + \end{aligned}$$

$$\begin{aligned}
& + G_0'' \left\{ \frac{1}{g} \frac{D}{Dt} (\nabla_h \tilde{\Phi}_1 \cdot \nabla_h \tilde{\Phi}_2) - \nabla_h (\eta_1 \nabla_h \tilde{\Phi}_2) \right\} - \nabla_h (\eta_2 \nabla_h \tilde{\Phi}_1) + \\
& + G_0''' \left\{ \frac{1}{g} \frac{D}{Dt} (\eta_1 \tilde{\Phi}_1^2) + \eta_1^2 \tilde{\Phi}_1 \right\} + \\
& + G_0'''' \left\{ \eta_1 \tilde{\Phi}_2 + \frac{1}{g} \frac{D}{Dt} (\tilde{\Phi}_1 \tilde{\Phi}_2) \right\} = 0 \quad (3.5.6)
\end{aligned}$$

Here, nonlinear terms involving $(\nabla_h \cdot \underline{U})$ have been dropped due to the assumptions about modulation scales. Equation (3.5.6) may be written entirely in terms of the potential $\tilde{\Phi}_1$ by the laborious substitution of the governing equations for η_1 , η_2 , and $\tilde{\Phi}_2$; use of approximate forms of these equations based on the local neglect of modulations does not alter the level of accuracy of the nonlinear terms in (3.5.7). We will proceed, instead, to a much reduced form of the nonlinear equation by substituting the plane wave results of Appendix A in the nonlinear terms of (3.5.6). This approximation would lead to errors of $O(\epsilon^3)$ in the direct calculation of nonlinear standing waves, where the amplitude modulation cannot be considered to be small; however, many of the examples below are for quasi-unidirectional wave propagation, and the substitution made here is entirely

acceptable. We also neglect derivatives of the amplitude A during the substitution, which would lead to the inclusion of inconsistently small terms of $O(\epsilon^3, \delta)$. Substituting (3.4.7) and the plane wave approximations into (3.5.6) leads to the equation

$$\begin{aligned} \frac{1}{g} \frac{D^2 \tilde{\phi}_1}{Dt^2} + \frac{(\nabla_h \cdot \underline{u})}{g} \frac{D \tilde{\phi}_1}{Dt} - \nabla_h \cdot (C g \nabla_h \tilde{\phi}_1) + G_{00}^{\tilde{z}'} \tilde{\phi}_1 + 2 \frac{\sigma}{g} \omega_2 \tilde{\phi}_1 + \\ + 2 \frac{\sigma}{g} \left\{ \underline{k} \cdot \nabla_h \phi_2' - \frac{k^2}{2\sigma \cosh^2 kh} \frac{D \phi_2'}{Dt} \right\} \tilde{\phi}_1 = W_1 + \text{Asynchronous terms} \end{aligned} \quad (3.5.7)$$

where

$$\omega_2 = \sigma \frac{k^2}{2} D |A|^2 \quad (3.5.8)$$

and D is defined in (3.5.2). Substituting for the integrals $G_{00}^{\tilde{z}'}$ and $G_{00}^{\tilde{z}''}$, dropping the asynchronous terms proportional to $e^{-3i\omega t}$ and rearranging, we arrive at

$$\begin{aligned} \frac{D^2 \tilde{\phi}_1}{Dt^2} + \frac{(\nabla_h \cdot \underline{u})}{g} \frac{D \tilde{\phi}_1}{Dt} - \nabla_h \cdot (C g \nabla_h \tilde{\phi}_1) + \sigma^2 (1 - \kappa) \tilde{\phi}_1 + \sigma^2 k^2 D |A|^2 \tilde{\phi}_1 \\ + 2 \sigma \left\{ \underline{k} \cdot \nabla_h \phi_2' - \frac{k^2}{2\sigma \cosh^2 kh} \frac{D \phi_2'}{Dt} \right\} \tilde{\phi}_1 = W_1 \end{aligned} \quad (3.5.9)$$

This represents the mild-slope equation for $\tilde{\phi}_1$, in the presence of a slowly varying ambient current \underline{u} , correct to $O(\epsilon^3)$. The added terms, proportional to $|A|^2$ and ϕ_2' ,

represent the direct effect of amplitude dispersion and the interaction with the wave induced current $\nabla_h \phi_2'$, respectively. Note that ϕ_2' must also be solved for in the general case, using the results of section 3.4.

The fast modulation corrections to the third order model equation (3.5.9) may be obtained by including the $O(\epsilon, \delta^2)$ terms from (3.3.8), to give

$$\begin{aligned} \frac{D^2 \tilde{\phi}_1}{Dt^2} + (\nabla_h \cdot \underline{u}) \frac{D \tilde{\phi}_1}{Dt} - \nabla_h \cdot (c c_2 \nabla_h \tilde{\phi}_1) + \sigma^2 (1 - \kappa) \tilde{\phi}_1 + g(\alpha + F) \tilde{\phi}_1 \\ + \sigma^2 k^2 D|A|^2 \tilde{\phi}_1 + 2\sigma \left\{ k \cdot \nabla_h \phi_2' - \frac{k^2}{2\sigma \cosh^2 kh} \frac{D \phi_2'}{Dt} \right\} \tilde{\phi}_1 = W_1 \end{aligned} \quad (3.5.10)$$

Equation (3.5.10) is a principle result of this investigation.

In order to deliniate the connection between (3.5.10) and the results of previous investigators, we remark that

$$\omega_2 = \omega_2^S + \omega_2^D$$

where ω_2^S and ω_2^D are given by Chu and Mei (1970), and correspond to the second order frequency corrections due to amplitude dispersion and change in mean water level, respectively. In addition, $\underline{k} \cdot \nabla_n \phi_2'$ is equivalent to Chu and Mei's ω_2^{12} , while the remainder of (3.5.10) corresponds to their ω_2^X and ω_2^T , after accounting for the inclusion of the fast wavelike motion.

CHAPTER 4. EQUATIONS GOVERNING THE AMPLITUDE A IN
QUASI ONE-DIMENSIONAL PROPAGATION

4.1 Introduction

The second order hyperbolic models (any of (3.3.8), (3.4.1), (3.5.9) or (3.5.10)) represent a very general approach to the solution of wave propagation in a domain with correctly posed initial and boundary conditions; however, the existing numerical solution methods for this type of problem in an arbitrary domain (in particular, finite element or finite difference methods) are costly and, in the case of finite element programs, require a nontrivial programming effort. In several applications, one or both of two simplifying assumptions may be appropriately utilized. First, the wave amplitude may be assumed to be steady in time; thus the only contribution of terms like $\partial \tilde{\phi}_1 / \partial t$ is the $O(1)$ phase contribution $-\lambda \omega \tilde{\phi}_1$. This approximation may be used in most applications of the linear wave equations unless it is desirable to study time variations of the wave field due to unsteady incident wave amplitude, representing the effect of wave groups or transient disturbances. For

nonlinear applications, use of this simplifying assumption implies the tacit assumption that nonlinear interactions between waves in a multicomponent system will not lead to the onset of significant amplitude modulations, such as Benjamin-Feir instabilities, over the length and time scales being modelled; this assumption is problematic and has not been fully investigated for the case of an initially unmodulated plane wave. Equations based on the use of this assumption in order to reduce the second order hyperbolic system to an elliptic system will be given in section 4.2.

An independent assumption of quasi-one-dimensional wave propagation can be made a priori, with the resulting restriction that the reflection of waves counter to the principle direction of propagation cannot be considered in the same computational step. In this case, the choice of x as the principle propagation direction, with the concurrent choice

$$\underline{k} = \{k, 0\}$$

leads to a general set of equations in $\{x, t\}$ where the dependence in y is related to oblique modulations of the amplitude. In cases where refraction, and resulting bending of wave rays, is important, the y dependence is used to take up errors resulting from k not being truly aligned with x .

Time dependent equations based on this approximation are given in section 4.3, and we study the connection between the general fast modulation model studied here and previously derived models based on the nonlinear Schrodinger equation, which are related to subsets of the general problem.

Finally, in section 4.4, an approximation method analogous to the splitting matrix approach (see, for example, Coronas (1975), McDaniel(1975), and Radder(1979)) is used to obtain the parabolic approximation to steady, quasi-one-dimensional propagation, based on the elliptic models of section 4.2. We also demonstrate the connection between the parabolic equations and the scaling assumptions necessary for the recovery of these approximations from the initially time dependent models of section 4.3. The coupling between forward and back-scattered wave components will be neglected.

4.2 Time-independent Elliptic Models

Before proceeding with the reduction of the hyperbolic model to an elliptic form, we choose a form for the wave energy dissipation function W_1 :

$$W_1 = -w \frac{D\tilde{\phi}_1}{Dt} \quad (4.2.1)$$

which is slightly different than the form assumed by Booij(1981) and reduces to the more carefully derived form found by Jimenez and Whitham(1976), among others. A method for relating w to several known dissipation mechanisms is given in Appendix G. Substituting (4.2.1) into the full nonlinear model (3.5.10) and making the assumption

$$\tilde{\phi}_{1,t} = -i\omega \tilde{\phi}_1 \quad (4.2.2)$$

reduces (3.5.10) to the elliptic form

$$\begin{aligned} & -2i\omega \underline{u} \cdot \nabla_h \tilde{\phi}_1 + \underline{u} \cdot \nabla_h (\underline{u} \cdot \nabla_h \tilde{\phi}_1) + (\nabla_h \cdot \underline{u}) (\underline{u} \cdot \nabla_h \tilde{\phi}_1) - \nabla_h \cdot (c c_g \nabla_h \tilde{\phi}_1) \\ & + (\sigma^2 - \omega^2 - n\sigma^2 - i\omega (\nabla_h \cdot \underline{u})) \tilde{\phi}_1 + g(\alpha + F) \tilde{\phi}_1 + \sigma^2 k^2 D|A|^2 \tilde{\phi}_1 \\ & + 2\sigma (\underline{k} \cdot \nabla_h \phi_2') \tilde{\phi}_1 = i\sigma w \tilde{\phi}_1 \end{aligned} \quad (4.2.3)$$

where we have used the fact that $\phi'_{2,t} = 0$ in a steady wave field. The corresponding mild-slope approximation for linear waves is given by

$$\begin{aligned}
 & -2i\omega \underline{u} \cdot \nabla_h \tilde{\phi}_1 + \underline{u} \cdot \nabla_h (\underline{u} \cdot \nabla_h \tilde{\phi}_1) + (\nabla_h \cdot \underline{u})(\underline{u} \cdot \nabla_h \tilde{\phi}_1) - \nabla_h \cdot (CC_g \nabla_h \tilde{\phi}_1) \\
 & + (\sigma^2 - \omega^2 - \kappa\sigma^2 - i\omega(\sigma_h \cdot \underline{u})) \tilde{\phi}_1 = i\sigma_w \tilde{\phi}_1 \quad (4.2.4)
 \end{aligned}$$

which is similar to equation (3.23) in Booij(1981). Neglecting the $O(1)$ current \underline{u} reduces (4.2.4) to the form

$$\nabla_h \cdot (CC_g \nabla_h \tilde{\phi}_1) + (\kappa\omega^2 + i\omega w) \tilde{\phi}_1 = 0 \quad (4.2.5)$$

which is the mild slope model of Berkhoff(1972,1976) extended to include wave energy dissipation.

The time independence applied to the second order results of section 3.4 leads to

$$\nabla_h \cdot \left\{ h \nabla_h \phi'_2 + b_2 \underline{u} + \frac{E}{\sigma} \underline{k} \right\} = 0 \quad (4.2.6)$$

and

$$b_2 = b_{2s}(\underline{x}) \quad (4.2.7)$$

where (4.2.6) is a statement that the total second order component of the mean volume flux is nondivergent.

Equations (4.2.4) and (4.2.6) must be solved as a coupled pair in the general case.

4.3 Time-Dependent Equations for A

In this section, we use the assumed form for $\tilde{\phi}_1$:

$$\tilde{\phi}_1 = -i \frac{g_1}{\sigma} A e^{i\psi} \quad (4.3.1)$$

to derive a time dependent governing equation for A. The resulting equation for one-directional wave propagation is in the form of a modified cubic nonlinear Schrödinger equation, and subsets of the general equation can be directly related to the governing equations arising in previous studies of the dynamics of nonlinear waves.

The most general form of the governing equation is given by (3.5.10), and is rewritten here for convenience.

$$\begin{aligned} & \frac{D^2 \tilde{\phi}_1}{Dt^2} + (\nabla_h \cdot \underline{u}) \frac{D \tilde{\phi}_1}{Dt} - \nabla_h \cdot (CC_g \nabla_h \tilde{\phi}_1) + \sigma^2 (1 - \kappa) \tilde{\phi}_1 \\ & + g_1 (\alpha + F) \tilde{\phi}_1 + \sigma^2 k^2 D |A|^2 \tilde{\phi}_1 + 2\sigma \left\{ \underline{k} \cdot \nabla_h \phi_2' - \right. \\ & \left. - \frac{k^2}{2\sigma \cosh^2 kh} \frac{D \phi_2'}{Dt} \right\} \tilde{\phi}_1 - i\sigma w \tilde{\phi}_1 = 0 \end{aligned} \quad (4.3.2)$$

The term $(\alpha + F)$ is given in section (3.3). The equation also

contains a dissipation term. In addition to the wave equation, we will also need the lowest order energy equation, derived from the results of Appendix E:

$$A_t + (\underline{C}_g + \underline{u}) \cdot \nabla_h A + \frac{1}{2} \left\{ \sigma \nabla_h \cdot \left(\frac{\underline{C}_g + \underline{u}}{\sigma} \right) - \frac{1}{\sigma} \sigma_t \right\} A = 0 \quad (4.3.3)$$

The reduction to the cubic nonlinear Schrödinger equation (NLS) is made by substituting (4.3.1) into (4.3.2) and cancelling the factor $e^{i\psi}$. The $O(1)$ current \underline{u} may be written in its x and y components as

$$\underline{u} = \{u, v\} \quad (4.3.4)$$

The resulting equation for A is given by

$$\begin{aligned} & i(A_t + \underline{C}_{g_a} \cdot \nabla_h A) + \frac{i}{2} \left\{ \nabla_h \cdot \left(\frac{\underline{C}_{g_a}}{\sigma} \right) \sigma - \frac{1}{\sigma} \sigma_t \right\} A \\ & + \frac{1}{2} \left\{ \frac{(\nabla_h \cdot \underline{u})}{\sigma^2} \frac{D\sigma}{Dt} + \frac{D}{Dt} \left(\frac{1}{\sigma^2} \frac{D\sigma}{Dt} \right) - \nabla_h \cdot \left(\frac{C_{g_a} \nabla_h \sigma}{\sigma^2} \right) \right\} A + \frac{1}{\sigma^2} \frac{D\sigma}{Dt} \frac{DA}{Dt} \\ & - \frac{C_{g_a}}{\sigma^2} \nabla_h \sigma \cdot \nabla_h A - \frac{1}{2\sigma} A_{ttt} - \frac{1}{\sigma} \underline{u} \cdot \nabla_h (A_t) - \frac{1}{2\sigma} \underline{u} \cdot \nabla_h (\underline{u} \cdot \nabla_h A) \\ & - \frac{1}{2\sigma} (\nabla_h \cdot \underline{u}) \frac{DA}{Dt} + \frac{1}{2\sigma} \nabla_h \cdot (C_{g_a} \nabla_h A) - \frac{g}{2\sigma} (\alpha + F) A + i \frac{W}{2} A \\ & - \frac{\sigma k^2}{2} D|A|^2 A - \left\{ \underline{k} \cdot \nabla_h \phi_2' - \frac{k^2}{2\sigma \cosh^2 kh} \frac{D\phi_2'}{Dt} \right\} A = 0 \end{aligned} \quad (4.3.5)$$

Here, $\underline{\zeta}g_a$ is the absolute group velocity in a stationary reference frame, given by

$$\underline{\zeta}g_a = \underline{\zeta}g + \underline{U} \quad (4.3.6)$$

At this stage, no assumption has been made concerning the orientation of \underline{k} or \underline{U} with respect to stationary Cartesian axes x and y . The terms (I) have been given previously in the present form (but for one space dimension) by Turpin(1981), Benmoussa(1983) and Turpin, Benmoussa and Mei(1983), who have studied the effect of following and adverse currents on the shoaling of Stokes wave packets (in the form of solitons) in one dimension. The steady-state, current-free counterpart of the term (I) is directly related to the spatially varying shoaling term in the parabolic approximation, as will be seen below. The terms (II), involving derivatives of σ , represent further corrections of $O(\delta^2)$ due to the presence of a varying current. The presence of the second unknown $\dot{\phi}_2'$ requires a second equation for closure; this is given by the forced wave equation (3.3.18) for $\dot{\phi}_2'$.

$$\frac{D^2 \phi_2'}{Dt^2} + (\underline{\sigma}_h \cdot \underline{U}) \frac{D \phi_2'}{Dt} - g \nabla_h \cdot (h \nabla_h \phi_2') = \frac{D B}{Dt} + (\underline{\sigma}_h \cdot \underline{U}) B + g \nabla_h \cdot (\eta_1 \nabla_h \hat{\phi}_1)$$

(4.3.7)

A number of virtually independent simplifying assumptions may be applied to the pair of coupled equations (4.3.5) and (4.3.7), and we illustrate several choices here in order to relate the results of the present study to those of other investigators. The first thorough study of Stokes waves in a domain with "fast" modulations ($\epsilon \sim O(\epsilon)$) was made by Chu and Mei (1970a,b), who investigated essentially the same problem as studied here but neglected the presence of a large current. Dropping the terms involving the $O(1)$ mean current \underline{U} from (4.3.5) and (4.3.7) leads to the simplified set

$$\begin{aligned}
 & i(A_t + c_g \nabla_h A) + \frac{i}{2}(\nabla_h \cdot c_g)A + \frac{1}{2\omega} \nabla_h \cdot (c c_g \nabla_h A) - \frac{A_{tt}}{2\omega} \\
 & - \frac{g}{2\omega} (\alpha + F') - \omega \frac{k^2}{2} D|A|^2 A - \left\{ \underline{k} \cdot \nabla_h \phi'_2 - \frac{k^2}{2\omega \cosh^2 kh} \phi'_{2t} \right\} A \\
 & + i \frac{U}{2} A = 0
 \end{aligned} \tag{4.3.8}$$

and

$$\phi'_{2tt} - g \nabla_h \cdot (h \nabla_h \phi'_2) = \frac{-gk}{2 \sinh 2kh} |A|^2_t + \frac{g}{2\omega} \nabla_h \cdot (k |A|^2) \tag{4.3.9}$$

where F' is a simplified form of F obtained by setting β_4 and $\beta_7=0$. Equations(4.3.8-9) contain the same information as the results of Chu and Mei, who left their equations in the form of a set of conservation equations.

A mild slope ($\bar{\sigma} \cdot \epsilon^2$) form of the current-free model may be constructed by neglecting terms of $O(\epsilon)$ and higher in (4.3.8-9) after the shift in scaling. We remark that the modulations of A must be left at $O(\epsilon)$, since nonlinear instabilities such as the Benjamin-Feir instability may lead to fast amplitude modulation in an otherwise slowly varying domain (see Benjamin, 1967, and Benjamin and Feir, 1967). The coupled equations then further reduce to

$$i(A_t + c_g \cdot \nabla_h A) + \frac{i}{2}(\nabla_h \cdot c_g)A - \frac{A_{tt}}{2\omega} + \frac{1}{2\omega} \nabla_h \cdot (c c_g \nabla_h A) - \omega \frac{k^2}{2} D|A|^2 A +$$

$$+ g \mathcal{F}_2 \left\{ \frac{k \cdot \nabla_h (k \cdot \nabla_h A)}{2\omega k^4} \right\} - \left\{ k \cdot \nabla_h \phi_2' - \frac{k^2}{2\omega \cosh^2 kh} \phi_2' \right\} + i \frac{\omega}{2} A = 0$$
(4.3.10)

with (4.3.9) altered to

$$\phi_2'_{tt} - gh \nabla_h^2 \phi_2' = \frac{-gk}{2 \sinh 2kh} |A|^2_t + \frac{g^2}{2\omega} k \cdot \nabla_h |A|^2 \quad (4.3.11)$$

The three models mentioned so far may in principle be solved as an initial boundary value problem in an

arbitrary domain; however, the determination of the direction of \underline{k} at a local point in the domain is problematic since the phase surface $\psi(\underline{x}, t)$ is not being determined. For problems in domains where a principle direction of propagation may be defined, it is convenient at this stage of the derivation to specify that the phase surface is one dimensional in space. Choosing x as the principle direction of propagation and defining

$$\psi = \int^x k(x') dx' - \omega t \quad (4.3.12)$$

leads to the simplifications

$$\underline{c}_g = c_g \underline{i}_x, \quad \underline{k} = k \underline{i}_x \quad (4.3.13)$$

The amplitude is then allowed to vary in the y -direction to account for modulations and small deviations from the principle propagation direction. The ability to model the deviation in travel direction will be crucial to the results of Chapter 6. Inserting the simplifications (4.3.12-13) into (4.3.10-11), and noting that

$$\nabla^2 = \frac{\omega^2}{g} \frac{kh}{\sinh 2kh} (1 - kh \tanh kh) - \frac{\omega^2}{2g} \left(1 + \frac{(kh)^2}{\cosh^2 kh} \right) \quad (4.3.14)$$

in the absence of a current, reduces the mild slope formulation to

$$\begin{aligned}
& i(A_t + C_g A_x) + \frac{i}{2} C_g A - \frac{A_{tt}}{2\omega} + \frac{1}{2\omega} \left\{ \frac{2\omega^2}{k^2} \frac{kh}{\sinh 2kh} (1 - kh \tanh kh) \right\} A_{xx} \\
& + \frac{1}{2\omega} (CC_g A_y)_y - \omega \frac{k^2}{2} D|A|^2 A - \left\{ k \phi'_x - \frac{k^2}{2\omega \cosh^2 kh} \phi'_{z_t} \right\} A \\
& + i \frac{W}{2} A = 0 \tag{4.3.15}
\end{aligned}$$

$$\phi'_{z_{tt}} - gh \nabla_h^2 \phi'_z = \frac{-gk}{2 \sinh 2kh} |A|^2_t + \frac{g^2 k}{2\omega} |A|^2_x \tag{4.3.16}$$

which is the extension of the equation of Djordjevic and Redekopp (1978) to two space dimensions. Note that the term $(CC_g A_y)_y$ in (4.3.15) can be expanded as

$$(CC_g A_y)_y = CC_g A_{yy} + (CC_g)_y A_y$$

The second term is formally of $O(\epsilon^4)$ in the mild slope approximation, and could be dropped. However, we will retain it for the sake of consistency with previously derived models, as will be demonstrated in section 4.4. Finally, for water of constant depth, (4.3.15-16) take the following form after substituting for time derivatives of A using (4.3.3):

$$i(A_t + C_g A_x) + \frac{CC_g}{2\omega} A_{yy} - \frac{C_g^2}{2\omega} \left\{ 1 - \frac{gh}{C_g^2} \frac{(1 - kh \tanh kh)}{\cosh^2 kh} \right\} A_{xx} -$$

$$-\omega \frac{k^2}{2} D |A|^2 A - \left(R \phi_2' \right)_x - \frac{k^2}{2\omega \cosh^2 kh} \phi_2' \phi_2' A + i \frac{\omega}{2} A = 0 \quad (4.3.17)$$

$$\phi_2' \phi_2' \phi_2' - gh \nabla_h^2 \phi_2' = \frac{g^2 k}{2\omega} \left(1 + \frac{k C_a}{2\omega \cosh^2 kh} \right) |A|^2_x \quad (4.3.18)$$

Equations (4.3.17-4.3.18) are equivalent to the coupled equations derived by Davey and Stewartson (1974) and Yue (1980). It is generally impossible to eliminate ϕ_2' between (4.3.17) and (4.3.18), and so ϕ_2' must be solved for in addition to A. The exception to this rule is in the case of a strictly one dimensional envelope A oriented colinearly or at some angle to the propagation direction x. The colinear case corresponds to the strictly one-dimensional problem described originally by Hasimoto and Ono (1972). In the case of the envelope function A making an oblique angle with the direction of wave propagation, solutions in the form of oblique envelope solitons and groups have been found by Saffman and Yuen (1978) and Hui and Hamilton (1979), for the case of deep water, and by Kirby and Dalrymple (1983c) for the case of intermediate water depth.

For cases where the $O(1)$ current is retained, the same series of gradual reductions may be applied. We

present here, in order to show consistency with previous investigators' results, the equations resulting from the assumption of a mild slope and propagation in one spatial direction, including the effect of a following or opposing current.

Dropping higher order terms (II) and the y-dependence from (4.3.5) leads to the one-dimension evolution equation

$$\begin{aligned}
 & i(A_t + C_{ga} A_x) + \frac{i}{2} \left\{ \sigma \left(\frac{C_{ga}}{\sigma} \right)_x - \frac{1}{\sigma} \sigma_t \right\} A - \frac{1}{2\sigma} A_{tt} - \frac{1}{\sigma} U A_{xt} - \\
 & - \frac{1}{2\sigma} U^2 A_{xx} + \frac{1}{2\sigma} \left\{ \frac{2\sigma^2}{k^2} \left(\frac{kh}{\sinh 2kh} \right) (1 - kh \tanh kh) \right\} A_{xx} - \sigma \frac{k^2}{2} D|A|^2 A - \\
 & - \left\{ k \phi_2' \right\}_x - \frac{k^2}{2\sigma \cosh^2 kh} \frac{D\phi_2'}{Dt} \Big\} A = 0 \quad (4.3.19)
 \end{aligned}$$

where we have used the definition (4.3.14) for $\frac{1}{\sigma^2}$ after replacing ω by σ , and have neglected dissipation. The second derivative terms may be combined using the lowest order energy equation. Restricting attention to a slowly varying (in time) current field then reduces (4.3.19) to

$$\begin{aligned}
 & i(A_t + C_{ga} A_x) + \frac{i\sigma}{2} \left(\frac{C_{ga}}{\sigma} \right)_x A - \frac{C_g^2}{2\sigma} \left\{ 1 - \frac{gh}{C_g^2} \frac{(1 - kh \tanh kh)}{\cosh^2 kh} \right\} A_{xx} \\
 & - \sigma \frac{k^2}{2} D|A|^2 A - \left\{ k \phi_2' \right\}_x - \frac{k^2}{2\sigma \cosh^2 kh} \frac{D\phi_2'}{Dt} \Big\} A = 0 \quad (4.3.20)
 \end{aligned}$$

The corresponding forced wave equation for ϕ_2' is given by

$$\begin{aligned} \phi_2'_{tt} + 2U\phi_2'_{xt} + U_x\phi_2'_t + (U^2\phi_2'_x)_x - g(h\phi_2'_x)_x &= \\ &= -\frac{gk}{2\sinh 2kh} |A|^2_t - \frac{g}{2} \left(\frac{Uk|A|^2}{\sinh 2kh} \right)_x + \frac{g^2}{2\omega} (k|A|^2)_x \end{aligned} \quad (4.3.21)$$

Equations (4.3.20-21) contain the same information as the evolution equation of Turpin, Benmoussa and Mei (1983), who derived a single equation in A directly. Defining the moving coordinate

$$\tau = \epsilon \left\{ \int \frac{dx}{C_{ga}} - t \right\}$$

and the slow coordinate

$$X_2 = \epsilon^2 X$$

(4.3.20-21) may be combined to give

$$\begin{aligned} A_{X_2} + \frac{\sigma}{2C_{ga}} \left(\frac{C_{ga}}{\sigma} \right)_{X_2} A + \frac{1}{2\sigma C_{ga}} \left(\frac{C_{ga}}{C_g} \right)^2 \left\{ 1 - \frac{gh}{C_g^2} \frac{(1 - kh \tanh kh)}{\cosh^2 kh} \right\} A_{\tau\tau} + \\ + \frac{i}{C_{ga}} \frac{\sigma k^2}{2} \left\{ D - \frac{\sigma^2}{(gh - C_g^2)} \left(\frac{kC_g}{2\sigma \cosh^2 kh} + 1 \right)^2 \frac{1}{k^2 \tanh^2 kh} \right\} |A|^2 A + \\ + iQA = 0 \end{aligned} \quad (4.3.22)$$

where Q is a real function involving the integration

constant of $\dot{\phi}_2^*$. In the case of an isolated wave packet, where $\dot{\phi}_2^* \rightarrow 0$ for $x \rightarrow \pm\infty$, Q may be set equal to zero. Equation (4.3.21) is equivalent to the result of Turpin, Benmoussa and Mei (1983).

4.4. Parabolic Equations

Under a restrictive set of assumptions, the elliptic model of section 4.2 and the hyperbolic models of section 4.3 may each be reduced to parabolic, initial boundary value problems for waves propagating in or close to a pre-specified direction. The first assumption, already applied in section 4.2, is that the wave field is purely harmonic in time. The resulting neglect of the time dependence of the amplitude \bar{A} bars the consideration of wave fields which are groupy in nature as well as precluding the study of the onset of instabilities. The parabolic equations which follow are thus applicable only to the study of plane waves.

The second major assumption involves the specification of one-directional propagation. This assumption has already been made with regard to the equations of section 4.3, and the parabolic equation then follows directly from these results after neglecting time dependence and introducing a shift in scaling. The application of a splitting matrix to the elliptic model in section 4.2 leads to a set of coupled equations for the forward and back-scattered components of \tilde{r}_1 , as in the derivation of Radder (1979). In this section, we will use

the method employed by Booij(1981) to obtain a single equation in the forward scattered component $\hat{\phi}_1^+$ which neglects the coupling with the back-scattered component $\hat{\phi}_1^-$. The result will be to extend the parabolic approximation of Booij to include the effect of nonlinearity.

As a first example, the derivation of a parabolic equation from the mild-slope, time-dependent equation (4.3.15) is illustrated. A shift in scaling is introduced by specifying that the x-derivative of A be $O(\epsilon^3)$, consistent with the assumption that the variation of the phase ϕ accounts for all the fast variation in the direction of propagation. In contrast, the y-derivative of A will remain at $O(\epsilon^2)$, on the assumption that waves turned at a small angle to the x-direction will exhibit slow phase-like variation in the y direction. The term $(CC_g A_y)_y$ will be kept in its entirety; this choice leads to the retention of the formally small component $(CC_g)_y A_y$, but we note that, for waves turned at large angles to the principle propagation direction, A_y should approach $O(\epsilon)$, in which case $(CC_g)_y A_y$ is comparable in order to the remaining terms. We also note that $\hat{\phi}_{1,x}$ is formally of $O(\epsilon^3)$ in this approximation. These scaling assumptions and the neglect of time dependence reduce (4.3.15) to the parabolic equation

$$iC_g A_x + \frac{i}{2}(C_g)_x A + \frac{1}{2\omega}(CC_g A_y)_y - \omega \frac{k^2}{2} D |A|^2 A + i \frac{W}{2} A = 0 \quad (4.4.1)$$

It is helpful in applications of parabolic equations to define the amplitude with reference to a fixed wavenumber k_0 based on some characteristic of the physical domain of interest (usually the initial conditions). The introduction of k_0 facilitates the reconstruction of the instantaneous water surface η_i since all phase information not contained in $k_0 x$ is then absorbed by the amplitude function A . We therefore let

$$A = A' e^{i(k_0 x - \int^x k dx)} \quad (4.4.2)$$

A' is then the amplitude of a wave $\tilde{\phi}_i$ given by

$$\tilde{\phi}_i = -i \frac{g}{\omega} A'(x, y) e^{i(k_0 x - \omega t)} \quad (4.4.3)$$

Substituting (4.4.2) into (4.4.1) leads to the revised equation

$$iC_g A'_x + (k - k_0)C_g A' + \frac{i}{2}C_{g_x} A' + \frac{1}{2\omega}(CC_g A'_y)_y - \omega \frac{k^2}{2} D |A'|^2 A' + i \frac{W}{2} A' = 0 \quad (4.4.4)$$

After dropping the dissipation term, (4.4.1) and (4.4.4) are

equivalent to equations (2.18) and (2.22) of Kirby and Dalrymple(1983b), which were derived using a multiple scale perturbation technique. Each model may be further reduced to an equation for pure diffraction by setting $k=k_0$ =constant and $C, C_g =$ constant. Noting that $A'=A$ in this case, (4.4.1) and (4.4.4) both reduce to

$$2ik_0 A_x + A_{yy} - \frac{\omega k_0^3}{C_g} D|A|^2 A + \frac{ik_0}{C_g} \omega A = 0 \quad (4.4.5)$$

which is equivalent to the diffraction equation of Yue and Mei(1980) after neglecting the dissipation term.

Kirby and Dalrymple (1983b) have shown that the linearized form of (4.4.1) or (4.4.4) is consistent with the parabolic equation of Radder(1979) for the forward scattered wave $\tilde{\phi}_1^+$ after neglecting dissipation. This consistency will be demonstrated again subsequent to the application of a splitting method to the elliptic model (4.2.3). The equivalence of the results of the splitting method to the time-independent form of the nonlinear Schrodinger equation after introducing the slower scaling in x allows us to draw an important conclusion before proceeding to the derivation of a general model including currents. If we neglect the mean current \underline{U} and the time dependency in the wave-action equation (4.3.3), and assume that $\underline{C}_g = C_g \hat{z}_x$, (4.3.3) reduces

to

$$C_g A_x + \frac{1}{2} C_{gx} A = 0 \quad (4.4.6)$$

which is equivalent to the leading two terms in (4.4.1). It is apparent that a requirement for a correct parabolic approximation is that the governing equation must contain the correct form of the relation for wave action conservation. To further illustrate this point, we drop the higher order terms (II), introduce the slow scaling in x , and neglect time dependence in the general nonlinear Schrödinger equation (4.3.5) to arrive at the form

$$\begin{aligned} & i \left\{ (C_g + u) A_x + V A_y + \frac{\sigma}{2} \left[\left(\frac{C_g + u}{\sigma} \right)_x + \left(\frac{V}{\sigma} \right)_y \right] A + \frac{W}{2} A \right\} + \\ & + \frac{1}{2\sigma} (C C_g A_y)_y - \frac{1}{2\sigma} \underline{u} \cdot \nabla_h (\underline{u} \cdot \nabla_h A) - \frac{1}{2\sigma} (\nabla_h \cdot \underline{u}) (\underline{u} \cdot \nabla_h A) - \\ & - \sigma \frac{k^2}{2} D |A|^2 A - \left\{ k \phi'_2 x - \frac{k^2}{2\sigma \cosh^2 kh} \underline{u} \cdot \nabla_h \phi'_2 \right\} A = 0 \end{aligned} \quad (4.4.7)$$

It is apparent that the bracketed term is the equation for wave action conservation including energy dissipation, and contains the essential features of (4.3.3). We may require that the results of a splitting method applied to the

elliptic model (4.2.3) should reproduce this information in as close to the exact form as possible.

Booij(1981) presented a splitting method and resulting parabolic equation for the velocity potential $\tilde{\phi}_1^+$ based on the mild-slope, linearized equation (4.2.4). A quick inspection of Booij's resulting parabolic equation shows that it cannot reproduce the terms $(UA_x + VA_y)$ and $[(U/\sigma)_x + (V/\sigma)_y]$ which are important components of the wave action conservation equation. We use instead a modified form of Booij's derivation which leads to a more nearly correct form of the wave action conservation equation.

Booij showed that the second order elliptic equation

$$\frac{\partial}{\partial x} \left(\frac{1}{\gamma} \frac{\partial \phi_m}{\partial x} \right) + \gamma \phi_m = 0 \quad (4.4.8)$$

can be split exactly into equations governing forward and backward moving (with respect to x) disturbances ϕ_m^+ and ϕ_m^- , which are given by

$$\frac{\partial \phi_m^+}{\partial x} = i \gamma \phi_m^+ \quad (4.4.9a)$$

$$\frac{\partial \phi_m^-}{\partial x} = -i \gamma \phi_m^- \quad (4.4.9b)$$

Since the split is exact, the equation governing ϕ_m^- is then discarded since there is no coupling between the two potentials. The assumed exactness of the split of the elliptic model and the subsequent neglect of certain derivative terms removes the option of calculating the reflected wave by an iterative procedure, as employed by Liu and Tsay (1983) to calculate reflection from isolated submerged obstacles in the absence of a current. The remainder of the problem centers on determining γ and the relation between ϕ_m and the wave potential $\tilde{\phi}_1$. Booij chose the relation

$$\phi_m = \xi \tilde{\phi}_1 \quad (4.4.10)$$

where $\tilde{\xi}$ is an as yet unknown operator on $\tilde{\phi}_1$. Substituting (4.4.10) into (4.4.8), expanding and neglecting derivatives of $\tilde{\xi}$ alone then leads to the result

$$\tilde{\phi}_1_{xx} + \left(\frac{\xi \gamma^2}{\delta}\right)^{-1} \left(\frac{\xi \gamma^2}{\delta}\right)_x \tilde{\phi}_1_x + \gamma^2 \tilde{\phi}_1 = 0 \quad (4.4.11)$$

The elliptic model (4.2.3) must now be put into the form (4.4.11) as closely as possible. Letting $p = CC_q$ and expanding some terms in their spatial components allows (4.2.3) to be written as

$$\begin{aligned}
& (\rho \tilde{\phi}_{1,x})_x + (\rho \tilde{\phi}_{1,y})_y + k^2 \rho \tilde{\phi}_1 + (\omega^2 - \sigma^2 + i\omega(\nabla_h \cdot \underline{u}) - \sigma^2 k^2 D/|A|^2) \tilde{\phi}_1 \\
& + i\sigma\omega \tilde{\phi}_1 - (u^2 \tilde{\phi}_{1,x})_x - (v^2 \tilde{\phi}_{1,y})_y - (uv \tilde{\phi}_{1,x})_y - (uv \tilde{\phi}_{1,y})_x \\
& + 2i\omega \underline{u} \cdot \nabla_h \tilde{\phi}_1 = 0 \tag{4.4.12}
\end{aligned}$$

In the following, we will neglect the interaction with $\nabla_h \dot{\phi}_2'$ and b_2 . Booij chose to drop terms involving squares of the mean current components based on the assumption that they are likely to be arithmetically smaller than terms involving p except in the vicinity of stopping points. This choice leads directly to Booij's inability to derive the correct wave action equation and also would lead to difficulties in the derivation to follow. Booij then arranged (4.4.12) in the form

$$\tilde{\phi}_{1,xx} + \rho^{-1} (\rho_x + 2i\omega u) \tilde{\phi}_{1,x} + k^2 \left(1 + \frac{M}{k^2 \rho}\right) \tilde{\phi}_1 = 0 \tag{4.4.13}$$

where $M \tilde{\phi}_1$ is given by

$$\begin{aligned}
M \tilde{\phi}_1 &= (\omega^2 - \sigma^2 + i\omega(\nabla_h \cdot \underline{u}) - \sigma^2 k^2 D/|A|^2 + i\sigma\omega) \tilde{\phi}_1 + \\
&+ 2i\omega v \tilde{\phi}_{1,y} + (\rho \tilde{\phi}_{1,y})_y \tag{4.4.14}
\end{aligned}$$

(Here, Booij's derivation is extended to include the

nonlinear term). (4.4.13) is then compared to (4.4.11) to complete the splitting process. We note that the inclusion of the term $2i\omega U \tilde{\phi}_{1,x}$ in the splitting procedure leads to the neglect of the term $U A_x$ in the final parabolic equation, since $U A_x$ is already contained in the term $2i\omega U \tilde{\phi}_{1,x}$. We thus follow an alternate approach. Assuming that waves are oriented in the +x direction (phase given by $e^{i \int k dx}$), the dispersion relation may be written as

$$\sigma = \omega - kU \quad (4.4.15)$$

leading to the result

$$\omega^2 - \sigma^2 = 2\omega kU - (kU)^2 \quad (4.4.16)$$

Equation (4.4.12) may then be written as

$$\left\{ (\rho - U^2) \tilde{\phi}_{1,x} \right\}_x + k^2 (\rho - U^2) \tilde{\phi}_1 + M \tilde{\phi}_1 = 0 \quad (4.4.17)$$

where $M \tilde{\phi}_1$ is given by

$$\begin{aligned} M \tilde{\phi}_1 = & \left\{ 2\omega kU + i\omega (\nabla_n \cdot \underline{u}) - \sigma^2 k^2 D |A|^2 + i\sigma \omega \right\} \tilde{\phi}_1 \\ & - (UV \tilde{\phi}_{1,y})_x - (UV \tilde{\phi}_{1,x})_y + \left\{ (\rho - V^2) \tilde{\phi}_{1,y} \right\}_y + 2i\omega \underline{u} \cdot \nabla_n \tilde{\phi}_1 \end{aligned} \quad (4.4.18)$$

We have thus imbedded the term $U \tilde{\Phi}_{1,x}$, which we don't want to reduce in order, in $M \tilde{\Phi}_1$. (4.4.17) may then be written in the form of (4.4.11);

$$\tilde{\Phi}_{1,xx} + (\rho - u^2)^{-1} (\rho - u^2)_x \tilde{\Phi}_{1,x} + k^2 \left(1 + \frac{M}{k^2(\rho - u^2)} \right) \tilde{\Phi}_1 = 0 \quad (4.4.19)$$

Comparison with (4.4.11) leads immediately to the results

$$\gamma^2 = k^2 \left(1 + \frac{M}{k^2(\rho - u^2)} \right) \tilde{\Phi}_1 \quad (4.4.20)$$

$$\xi^2/\gamma = (\rho - u^2) \quad (4.4.21)$$

or

$$\gamma = k \left(1 + \frac{M}{k^2(\rho - u^2)} \right)^{1/2} \quad (4.4.22)$$

$$\xi = k^{1/2} (\rho - u^2)^{1/2} \left(1 + \frac{M}{k^2(\rho - u^2)} \right)^{1/4} \quad (4.4.23)$$

Booij points out that Radder's (1979) approximation is equivalent to the immediate choice

$$\gamma_R = k \left(1 + \frac{M}{2k^2(\rho - u^2)} \right) \quad (4.4.24)$$

$$\xi_R = k^{1/2} (\rho - u^2)^{1/2} \quad (4.4.25)$$

while Booij's approximation retains the full expression and then approximates the resulting parabolic equation

$$\begin{aligned} \frac{\partial}{\partial x} \left\{ k^{1/2} (p-u^2)^{1/2} \left(1 + \frac{M}{k^2(p-u^2)} \right)^{1/4} \tilde{\phi}_1^+ \right\} = \\ = ik k^{1/2} (p-u^2)^{1/2} \left(1 + \frac{M}{k^2(p-u^2)} \right)^{3/4} \tilde{\phi}_1^+ \end{aligned} \quad (4.4.26)$$

by expanding the pseudo-operators in the form

$$\left(1 + \frac{M}{k^2(p-u^2)} \right)^{1/4} \tilde{\phi}_1^+ \cong \left(1 + \frac{M}{4k^2(p-u^2)} \right) \tilde{\phi}_1^+ \quad (4.4.27)$$

$$\left(1 + \frac{M}{k^2(p-u^2)} \right)^{3/4} \tilde{\phi}_1^+ \cong \left(1 + \frac{3}{4} \frac{M}{k^2(p-u^2)} \right) \tilde{\phi}_1^+ \quad (4.4.28)$$

The results of both expansions may be summarized in the general equation

$$\begin{aligned} \frac{\partial}{\partial x} \left\{ k^{1/2} (p-u^2)^{1/2} \left(1 + \frac{P_1 M}{k^2(p-u^2)} \right) \tilde{\phi}_1^+ \right\} = \\ = ik k^{1/2} (p-u^2)^{1/2} \left(1 + \frac{P_2 M}{k^2(p-u^2)} \right) \tilde{\phi}_1^+ \end{aligned} \quad (4.4.29)$$

where

.

$$P_1 = \begin{cases} 0 & \text{Radder} \\ 1/4 & \text{Booij} \end{cases} \quad (4.4.30)$$

and where $P_2 - P_1 = 1/2$ for both approximations. The approximation with $P_1 = 0$ then should correspond to the information contained in the nonlinear Schrödinger equation. Equation (4.4.29) may be expanded to yield the expression

$$\begin{aligned} k(p-u^2) \tilde{\phi}_1^+ + \frac{1}{2} \{k(p-u^2)\}_x \tilde{\phi}_1^+ &= \\ &= ik^2(p-u^2) \tilde{\phi}_1^+ + \frac{i}{2} M \tilde{\phi}_1^+ \end{aligned} \quad (4.4.31)$$

Then, an equation for the complex amplitude is obtained by expanding $M \tilde{\phi}_1^+$ and making the substitution

$$\tilde{\phi}_1^+ = -ig \left(\frac{A}{\sigma} \right) e^{i \int k dx} \quad (4.4.32)$$

which results in the equation

$$\begin{aligned} (C_g + u) A_x + \left(\frac{\omega}{\sigma} \right) V A_y + \frac{\sigma}{2} \left(\frac{C_g + u}{\sigma} \right)_x A + \left(\frac{\omega}{2} V_y - \frac{\omega}{\sigma} V \sigma_y \right) A - \\ - \frac{i}{2\sigma} (C_g A_y)_y + \frac{\omega}{2} A + i\sigma \frac{k^2}{2} D |A|^2 A = 0 \end{aligned} \quad (4.4.33)$$

where terms containing products of components of the ambient current have been dropped. This equation may then be

compared with (4.4.7), and we note that errors have been introduced through the factor (ω/σ) multiplying VA'_y and the appearance of ω rather than $\tilde{\omega}$ in the y derivative term for V and \tilde{J} . A complicated procedure involving a double splitting of the equation in x and y shows that the errors appearing in (4.4.33) result from the choice of $\underline{k} = k \hat{x}$ and the effect of this choice on the assumed dispersion relation (4.4.15). However, the resulting approximation is more complete than the approximation obtained by Booij due to the inclusion of the term UA'_x and the correct form of the derivative of $(C_g + U)/J'$. Errors resulting from the use of (4.4.33) rather than the more strictly correct form (4.4.7) will be investigated in section 6.9. The approximate equation (4.4.34) is further modified by the shift to a reference phase function $e^{i.k.x}$, resulting in the equation

$$\begin{aligned}
 & (C_g + U)A'_x + i(k_0 - k)(C_g + U)A' + \left(\frac{\omega}{\sigma}\right)VA'_y + \frac{\sigma}{2}\left(\frac{C_g + U}{\sigma}\right)_x A' + \\
 & + \left\{ \frac{1}{2}\omega V_y - \left(\frac{\omega}{\sigma}\right)V\sigma_y \right\}A' - \frac{i}{2\sigma}\{CC_g A'_y\}_y + \frac{W}{2}A' + \\
 & + i\sigma\frac{k^2}{2}D|A'|^2A' = 0 \qquad (4.4.34)
 \end{aligned}$$

where A' is related to $\tilde{\Phi}_1$ by (4.4.2). In the absence of a current \underline{U} , (4.4.34) reduces identically to (4.4.4).

The equations (4.4.4) and (4.4.34) form the basis for the computational schemes used in most of the examples presented in Chapter 6. In several examples where currents are neglected, use is also made of the more accurate approximation with $P_1=1/4$, $P_2=3/4$. The derivation of the equation governing the complex amplitude A' for this case follows along similar lines; however several simplifications are introduced. In particular, the approximation

$$\frac{\partial}{\partial x} \left\{ \frac{D|A|^2 \tilde{\Phi}_1^+}{CC_g} \right\} \sim \frac{i k D |A|^2 \tilde{\Phi}_1^+}{CC_g} \quad (4.4.35)$$

is made, consistent with the neglect of amplitude modulations in the nonlinear term. Further, we introduce

$$\frac{\partial}{\partial x} \left\{ i \sigma w \tilde{\Phi}_1^+ \right\} \sim - \sigma k w \tilde{\Phi}_1^+ \quad (4.4.36)$$

consistent with the assumption of a small coefficient for the damping term. Substituting (4.4.32), (4.4.35) and (4.4.36) into (4.4.30) with $P_1=1/4$ and $P_2=3/4$ and neglecting currents leads to the governing equation

$$\begin{aligned} & i C_g A'_x + (k - k_0) C_g A' + \frac{i}{2} C_{gx} A' + \frac{P_2}{\omega} (C C_g A'_y)_y + \\ & + \frac{i P_1}{\omega k} (C C_g A'_y)_{yx} - \frac{P_1}{\omega k} \left\{ k_0 + i \frac{k_x}{k} + \frac{i (k C C_g)_x}{2 k^2 C C_g} \right\} (C C_g A'_y)_y \end{aligned}$$

$$-\omega \frac{k^2}{2} D |A'|^2 A' + i \frac{W}{2} A' = 0 \quad (4.4.37)$$

where we have also neglected some small derivative terms multiplying the nonlinear and damping terms. Equation (4.4.4) is recovered from (4.4.37) by setting $P_1 = 0$ and $P_2 = 1/2$, consistent with Radder's splitting scheme. The numerical schemes used to solve (4.4.4), (4.4.34) and (4.4.37) are discussed in section 6.2.

CHAPTER 5. COMPARISON OF THE MILD AND MODERATE
SLOPE APPROXIMATIONS FOR LINEAR WAVES

5.1. Introduction

For most applications to water wave propagation problems, the mild-slope form of the models derived in Chapter 3 should be adequate for a reasonably accurate representation of the wave field. In particular, ocean bottoms consisting of loose material typically have bottom slopes on the order of 0.001- 0.01, and retention of terms in $(\nabla_h h)^2$ and $\nabla_h^2 h$ is clearly unnecessary. Tidal currents interacting with these smooth topographies would also be expected to be very slowly varying in the horizontal directions, thus alleviating the need to retain terms to $O(\delta^2)$ covering variations of σ and k . The mild-slope approximation, given in linear form by Booij (1981) and by (3.4.1) and in nonlinear form by (3.5.9), should then be adequate for the modelling of waves in most physically realistic domains. The principle exception to this conclusion is that the term involving $\tilde{\tau}_3$ in $F\tilde{\phi}_1$ is required for the study of unsteady nonlinear waves in order

to avoid the types of singularities in amplitude observed by Lighthill (1965,1967) in his study of Whitham's conservation laws; see also Chu and Mei (1970a,1971). This requirement is consistent with the fact that the amplitude may become a fast varying quantity even in a very slowly varying or homogeneous domain as wave instabilities develop and wave groups form. The connection of the term in \hat{r}_1 to the higher order dispersive terms in the NLS was discussed in Chapter 4.

Exceptions to the assumptions of a globally slowly-varying domain can arise in several situations. Relatively large bottom slopes may exist over short physical expanses on rocky bottoms or in the vicinity of naturally or artificially maintained channels, and tidal currents interacting with these relatively rapidly varying bottoms will themselves exhibit the same rapid variations provided that the changes in depth occupy a significant proportion of the total depth. In addition, ambient currents in an otherwise slowly varying domain may exhibit fast variation due to specialized circumstances, such as the flow fields characteristic of tidal ebb currents from inlets and rivers, rip currents, and discharge plumes from outfall structures. Such concentrated flows, which often assume the form of turbulent entraining jets, violate the assumptions of the

present theory in two important ways. First, the small and intermediate scale turbulence of the ambient flow field violates the assumption of irrotationality on a local scale of the order of a wavelength or smaller. Savitsky(1970) studied the refraction of waves in the presence of a turbulent flow with mean current gradient, and concluded that the effect of the turbulence was small in comparison to the interaction with the mean characteristics of the flow. This result is encouraging; however, the mean flows themselves are generally rotational over a large scale. It is known (see, for example, Mei(1982), section (3.6)) that, for current variations of $O(\epsilon^2)$, the refraction approximation for waves in the presence of rotational currents is unaltered from the strictly irrotational case. No such results are currently available for the faster variations implied in this study.

In this chapter, we study several cases involving relatively steep bottoms with the intent of determining the range of significance, if any, of the $O(\epsilon^2)$ terms added to the mild slope form in Chapter 3.

5.2. Linear Edge Waves

As a first example, we investigate the effect of the steep bottom terms on numerical predictions of the longshore wavelength of edge waves. We consider the topography

$$h(x) = mx \quad (5.2.1)$$

where m is the beach slope and x is directed offshore. Edgewaves are trapped modes which propagate alongshore in the $+$ or $-$ y direction (or both, in the case of standing waves) and are trapped between the shoreline and an offshore turning point by refraction. For water of intermediate depth, Ursell (1952) has provided an exact solution for the discrete spectrum of the linearized solution; the dispersion relation is given by

$$\frac{\omega^2}{g\lambda} = \sin \left\{ (2n+1) \tan^{-1} m \right\} \quad (5.2.2)$$

in the absence of currents, where λ is the longshore wavenumber of the edge wave and n is the mode number. A family of normalized surface profiles for $n=0-5$ is shown in Figure 5.1. The trapping mechanism requires that the longshore wavelength be shorter than the deepwater wavelength for a wave of the same frequency, or

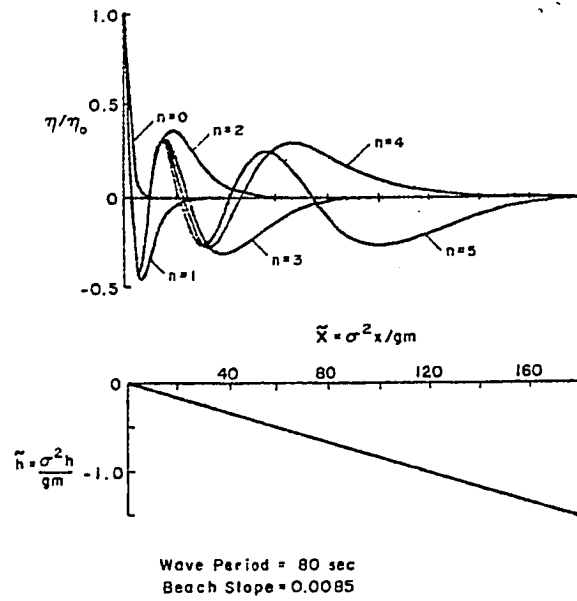


Figure 5.1 Edge wave surface profiles:
 $n = 0 - 5$

$$\lambda > \frac{\omega^2}{g} = k_0 \quad (5.2.3)$$

where k_0 is the deepwater wavenumber. For each given mode number n , (5.2.3) then requires that

$$\sin \left\{ (2n+1) \tan^{-1} m \right\} < 1 \quad (5.2.4)$$

or

$$m < \tan \left\{ \frac{\pi}{2(2n+1)} \right\} \quad (5.2.5)$$

Condition (5.2.5) must be met for a mode n wave to exist on a given beach. Interestingly, (5.2.5) is satisfied for all finite values of m when $n=0$.

In the present application, we study the prediction of λ by reducing the linear wave equation to an ordinary differential equation on the domain $0 \leq x \leq x$; λ is then related to the eigenvalues of the reduced system. After neglecting currents and dissipation, and assuming purely harmonic motion, (3.3.8) reduces to

$$\nabla_h \cdot \{ c c_g \nabla_h \tilde{\phi}_1 \} + k^2 c c_g \tilde{\phi}_1 - g(\alpha + F) \tilde{\phi}_1 = 0 \quad (5.2.6)$$

The coefficient F involves the expression $\underline{k} \cdot \nabla_h(\)$ in each term. If we interpret \underline{k} to be oriented in the direction of λ alongshore, it is apparent that each term in F is zero, and (5.2.6) reduces further to the form

$$\nabla_h \cdot \{ CC_g \nabla_h \tilde{\phi}_1 \} + (k^2 CC_g - g\alpha) \tilde{\phi}_1 = 0 \quad (5.2.7)$$

The mild slope equation is recovered by dropping α . Smith and Sprinks (1975) used the mild slope equation to calculate λ on a plane slope, and Kirby, Dalrymple and Liu (1981) have used the mild slope equation in a finite difference form to study edge waves on arbitrary bottom profiles. In the present case, we will use (5.2.7) to determine the effect of the term α on the prediction of values of λ , using a numerical method similar to that of Kirby, Dalrymple and Liu.

First, the wave $\tilde{\phi}_1$ is assumed to be of the form

$$\tilde{\phi}_1(x, y) = \phi_1(x) e^{\pm i\lambda y} \quad (5.2.8)$$

Substituting (5.2.8) into (5.2.7) yields an eigenvalue problem

$$(CC_g \phi_{1,x})_x + (k^2 CC_g - g\alpha) \phi_1 = \lambda^2 CC_g \phi_1 \quad (5.2.9)$$

for λ^2 and ϕ_1 . Boundary conditions on ϕ_1 are given by

$$\phi_1 = \begin{cases} \text{bounded AS } x \rightarrow 0 \\ \rightarrow 0 \quad \text{AS } x \rightarrow \infty \end{cases} \quad (5.2.10)$$

The shoreline boundary condition is computationally awkward, and we introduce a new dependent variable

$$\xi = x \tilde{\phi}_1$$

such that (5.2.9) and (5.2.10) become

$$\begin{aligned} & c c_g x^2 \xi_{xx} + \left\{ x^2 (c c_g)_x - 2 c c_g x \right\} \xi_x + \\ & + \left\{ 2 c c_g - x (c c_g)_x + x^2 (k^2 c c_g - g \alpha) \right\} \xi = \lambda^2 x^2 c c_g \xi \end{aligned} \quad (5.2.11)$$

$$\xi = 0 \quad ; \quad x=0, \quad x \rightarrow \infty \quad (5.2.12)$$

Nondimensional variables are introduced according to

$$(h, x, 1/\lambda, 1/k) = \frac{g}{\omega^2} (\tilde{h}, \tilde{x}, 1/\tilde{\lambda}, 1/\tilde{k})$$

$$(c, c_g) = \frac{g}{\omega} (\tilde{c}, \tilde{c}_g)$$

$$\bar{\eta} = \frac{g^3}{\omega^3} \tilde{\eta}$$

$$\alpha = \frac{\omega^2}{g} \tilde{\alpha}$$

where $\tilde{}$ denotes dimensionless quantities. Dropping $\tilde{}$'s and defining $p = CC_g$ reduces (5.2.11) to

$$\begin{aligned} p x^2 \bar{\xi}_{xx} + \{x^2 p_x - 2xp\} \bar{\xi}_x + \{2p - xp_x + x^2(\kappa - \alpha)\} \bar{\xi} = \\ = \lambda^2 x^2 p \bar{\xi} \end{aligned} \quad (5.2.13)$$

The dependent variable x is then stretched according to

$$x = e^{\gamma z} - 1 \quad (5.2.14)$$

in order to provide greater detail near the shoreline, yielding the final equation

$$\begin{aligned} p (e^{\gamma z} - 1)^2 \bar{\xi}_{zz} + \{ (e^{\gamma z} - 1)^2 p_z - \gamma [(e^{\gamma z} - 1)^2 + 2e^{\gamma z} \cdot \\ \cdot (e^{\gamma z} - 1)] p \} \bar{\xi}_z + \{ 2\gamma^2 e^{2\gamma z} p - \gamma e^{\gamma z} (e^{\gamma z} - 1) p_z + \\ + \gamma^2 e^{2\gamma z} (e^{\gamma z} - 1)^2 (\kappa - \alpha) \} \bar{\xi} = \\ = \lambda^2 \gamma^2 e^{2\gamma z} (e^{\gamma z} - 1)^2 p \bar{\xi} \end{aligned} \quad (5.2.15)$$

Equation (5.2.15) is solved on a truncated domain $0 \leq z \leq z_{\max}$, where z_{\max} is chosen such that the wave profile for the highest desired edge wave mode may decay in an unconstrained fashion, with $\zeta(z_{\max})=0$. The numerical scheme employs central differences on evenly spaced points z_i .

Results for the dimensionless inverse wavenumber $\omega^2/g\lambda$ as a function of beach slope m are plotted for modes 0, 1, and 2 in Figure 5.2. Results for both the mild-slope (neglecting α) and the moderate slope cases are virtually indistinguishable from the exact solution for modes 1 and 2. For the mode 0 wave, results were calculated up to a beach slope $m=2.0$. Both the moderate and mild slope results are seen to diverge from the exact solution with increasing slope, with the mild-slope model overpredicting the wavenumber and the moderate slope model underpredicting it. The moderate slope results are seen to diverge from the exact solution earlier and faster than the mild slope results. Table 5.1 presents a comparison of calculated values of $\omega^2/g\lambda$ from each model with the exact results.

A possible explanation for the faster divergence of the moderate slope results from the exact solution in the range $m > .5$ is that the large slope values invalidate the expansion procedure used to obtain the term α , in which the

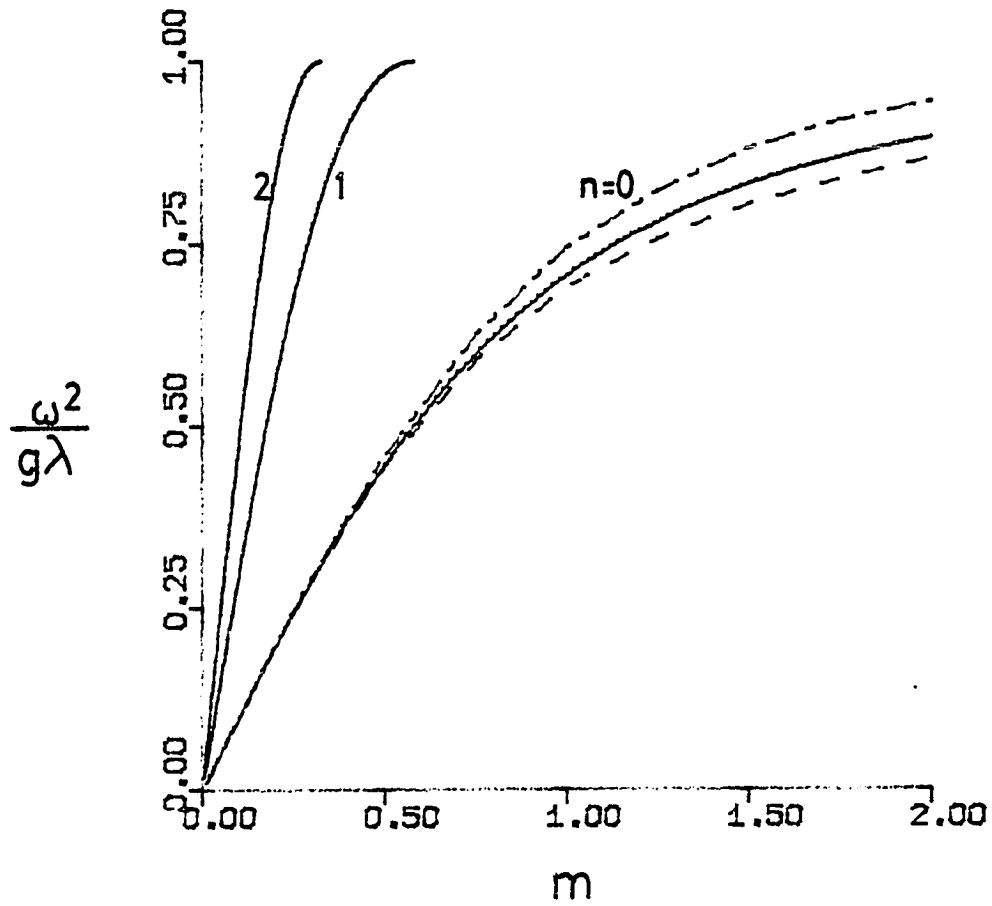


Figure 5.2 Dimensionless edge wave wavelength;
 $n = 0, 1, 2$.
 — Ursell (1952);
 - - - mild slope, $n = 0$;
 - · - · moderate slope, $n = 0$

slope m	$\omega^2/g\lambda$ Ursell (1952)	$\omega^2/g\lambda$ mild slope	% Error mild slope	$\omega^2/g\lambda$ moderate slope	% Error moderate slope
.01	.01000	.01023	2.31	.01023	2.31
0.05	.04994	.05078	1.69	.05080	1.72
0.1	.09950	.10070	1.21	.10084	1.34
0.2	.19612	.19739	0.65	.19849	1.21
0.5	.4472	.44583	-0.31	.45977	2.81
0.75	.6000	.59217	-1.30	.62668	4.45
1.00	.7071	.69061	-2.33	.74499	5.36
1.25	.7809	.75717	-3.04	.82196	5.26
1.50	.8321	.80418	-3.36	.88036	5.80
1.75	.8682	.83872	-3.40	.91760	5.69
2.00	.8944	.86490	-3.30	.94400	5.52

Table 5.1 Sample calculated wavenumbers for mode 0, N = 90

slope is assumed to be a small parameter. Both models exhibit moderately large errors for small slope values; this result is probably due to numerical discretization errors. The error relative to the exact solution of Ursell(1952) is shown in Figure 5.3 for the choices of $N=50$ and 90 and $z_{MAX}=1$. Further increase in N reduced the error for small values of bottom slope only slightly, indicating slow convergence of the numerical solution.

The numerically calculated values of λ differ slightly in the range $0.03 < m < 0.2$. For higher values of m , the two solutions diverge rapidly. Due to the presence of the numerical error at small values of m , it was impossible to determine which model (mild or moderate slope) exhibits more accurate behavior for intermediate values of the bottom slope.

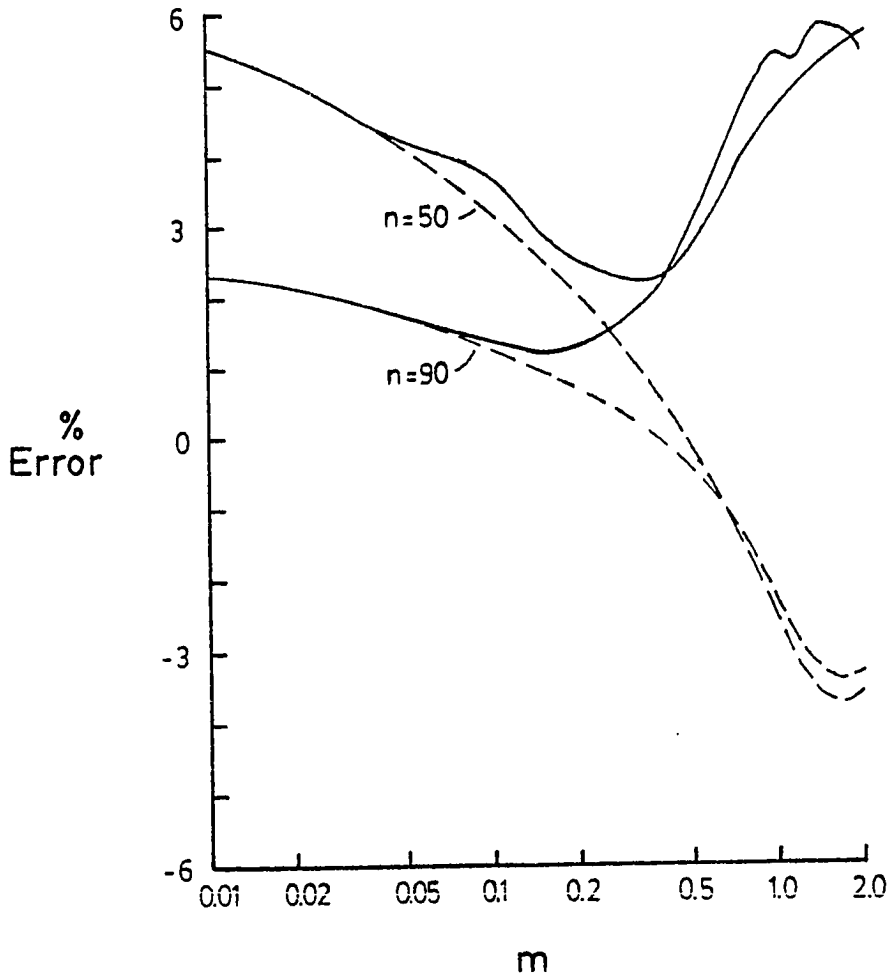
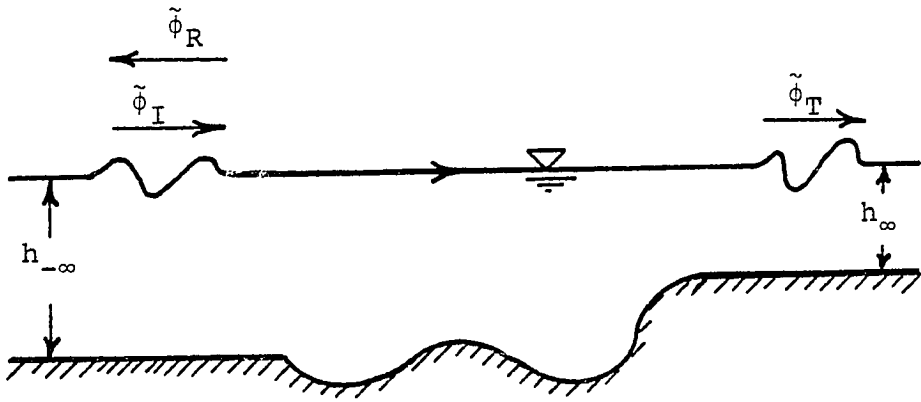


Figure 5.3 Edge wave wavelength; percent error relative to solution of Ursell (1952).
 ---- mild slope (neglecting α)
 ——— moderate slope (with α)

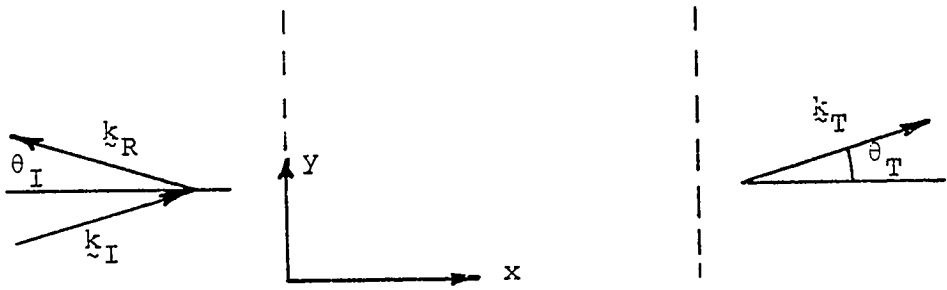
5.3. Reflection from Underwater Topography

In this section, we study the reflection and transmission characteristics for one case of plane waves incident on one-dimensional bottom variations. The topography will be taken to vary in the x -direction, and is assumed to be uniform in the y -direction. Plane waves are incident from $x = -\infty$ at an angle θ to the x axis. The variations of the topography are considered to be of bounded extent horizontally; however, the depths at $\pm\infty$ are allowed to differ. The physical domain is described schematically in Figure 5.4. In the limit of topographic variations characterized by vertical walls separating regions of constant depth, the general case of differing depths at $\pm\infty$ has been studied by Lassiter (1972) for normal wave incidence ($\theta = 0$) and by Kirby and Dalrymple (1983a) for arbitrary angles of incidence, using methods based on the matching of eigenfunction expansions along the vertical boundaries of subdomains of the fluid region. Kirby and Dalrymple also included results obtained using the boundary integral method (BIM) of Raichlen and Lee (1978) as a test of the principle results, and extended the method to include oblique wave incidence.

A wave propagation method based on the mild slope



a) elevation



b) plan

Figure 5.4 Generalized topography for section 5.3

equation (3.4.1) has been applied by Booij (1981) to study the reflection and transmission characteristics for waves in regions characterised by gentle slopes. In particular, Booij studied the reflection of waves normally incident on an underwater slope joining two regions of constant depth (with waves propagating from deep to shallow water and being partially reflected), and also studied oblique incidence on a submerged trench. Of particular interest in this connection is the case where a caustic forms on the upwave trench boundary. If the trench width is narrow enough to allow the exponentially decaying wave amplitude in the geometric shadow to reach the second caustic line on the downwave boundary, then significant wave energy may be transmitted past the finite-width shadow boundary.

We wish to determine the importance (or the ability to improve results) of the higher order terms in δ added to the mild slope formulation in Chapter 3. The present formulation allows for unambiguous specification of the term α , which depends only on the bottom slope and wave frequency. However, the $O(\delta^2)$ term F depends on the specification of a wavenumber vector \underline{k} and the gradient of the amplitude A , and these quantities are not well defined in a partial standing wave system. The assumptions used in evaluating F are discussed below. We neglect dissipation

and restrict our attention to linear plane waves with steady amplitude in the absence of currents. For this case, the linear model (3.3.8) can be written as (after assuming harmonic motion)

$$\nabla_h \cdot (CC_g \nabla_h \tilde{\phi}_1) + k^2 CC_g \tilde{\phi}_1 - g(\alpha + F) \tilde{\phi}_1 = 0 \quad (5.3.1)$$

The restriction to one-dimensional topography allows for some major simplifications to the general governing equation. The definition of the wavenumber vector \underline{k} leads to the result that

$$\nabla_h \times \nabla_h \psi = \nabla_h \times \underline{k} = 0 \quad (5.3.2)$$

Then, writing \underline{k} in its components $\underline{k} = \{k \cos \theta, k \sin \theta\}$ leads to the result

$$(k \sin \theta)_x = 0$$

or

$$k(x) \sin \theta(x) = m = \text{CONSTANT} \quad (5.3.3)$$

which is a statement of Snell's law. Thus, for a given

distribution of depth, the local wave angle $\theta(x)$ is uniquely determined. The wavenumber component ℓ in the x-direction can then be determined according to

$$\ell(x) = (k^2(x) - m^2)^{1/2} \quad (5.3.4)$$

For waves propagating from shallow to deep water, it is possible for m to be $> k(x)$; according to (5.3.4), ℓ then takes on imaginary values, and no physical significance can be attached to the local value of $\cos \theta(x)$. The point $\ell = 0$ is a turning point of the differential equation and represents a caustic line extending in the y-direction through the point. Waves in the region of ℓ imaginary are constrained to travel parallel to the caustic, with the wave profile decaying exponentially away from the turning point.

From our one dimensional assumption,

$$\tilde{\phi}_{1,y} = im \tilde{\phi}_1 \quad (5.3.5)$$

and the elliptic model is reduced to the O.D.E. :

$$(CC_g \tilde{\phi}_{1,x})_x + \ell^2 CC_g \tilde{\phi}_1 - g(\alpha + F) \tilde{\phi}_1 = 0 \quad (5.3.6)$$

The term α may be written as

$$\alpha = \delta_1 h_x^2 + \delta_2 h_x k_x + \delta_3 k_x^2 - (\delta_4 h_x + \delta_5 k_x)_x \quad (5.3.7)$$

The term F is evaluated by assuming only the presence of the incident wave propagating in the $+x$ direction. This assumption will lead to errors which increase in magnitude with increasing reflection. In the absence of a current, F may be written as

$$\begin{aligned} F = & -\mathcal{F}_1 \beta_1 + (\mathcal{F}_2 - \mathcal{F}_3) \beta_2 - \mathcal{F}_2 (\beta_3 + \beta_5) \\ & - \gamma_1 \alpha_1^2 + \gamma_2 \alpha_1 \alpha_3 + \gamma_3 \alpha_3^2 - 2\mathcal{F}_{03} \alpha_1 \beta_6 \\ & + \gamma_5 \alpha_3 \beta_6 - \gamma_4 \alpha_1 \beta_8 - \gamma_6 \alpha_3 \beta_8 - \frac{\mathcal{F}_{22}}{4} \beta_8^2 \end{aligned} \quad (5.3.8)$$

The terms α_1, α_3 and β_i may be written as

$$\alpha_1 = \ell h_x / k \quad ; \quad \alpha_3 = \ell k_x / 2k^3 \quad ; \quad \beta_6 = \ell A_x / k^2 A$$

$$\beta_8 = k_x / k^2 \quad ;$$

$$\beta_1 = \ell (\ell h_x)_x / k^3 \quad ; \quad \beta_2 = \ell (\ell k_x)_x / k^3$$

$$\beta_3 = l(lA_x)_x / k^4 A \quad ; \quad \beta_5 = l(k_x)_x / 2k^4 \quad (5.3.9)$$

The gradient of A may be further evaluated using the energy conservation equation

$$\nabla_h \cdot (E \underline{c}_g) = 0$$

yielding

$$(c_g l A^2 / k)_x = 0 \quad (5.3.10)$$

or

$$A_x = \frac{-(c_g l / k)_x}{2c_g l / k} A \quad (5.3.11)$$

and thus A may be eliminated from the evaluation of F.

Solutions of (5.3.6) are obtained by rewriting (5.3.6) in the form

$$\tilde{\phi}_{1,xx} + \frac{(cc_g)_x}{cc_g} \tilde{\phi}_{1,x} + \left(l^2 - g \frac{(\alpha + F)}{cc_g} \right) \tilde{\phi}_1 = 0 \quad (5.3.12)$$

and then writing (5.3.12) in central difference form. Boundary conditions are specified at x positions outside the

region of varying depth. In this case, we may specify the wavefield on the incident wave (-x) side as

$$\tilde{\phi}_i = \tilde{\phi}_I + \tilde{\phi}_r \quad (5.3.13)$$

where $\tilde{\phi}_I$ is the incident wave of unit amplitude and $\tilde{\phi}_r$ is a reflected wave with amplitude K_r . K_r is then the reflection coefficient. The transmitted wave at x downwave of the bottom variation is given by

$$\tilde{\phi}_t = \tilde{\phi}_T \quad (5.3.14)$$

Application of radiation conditions at the x boundaries then leads to

$$\tilde{\phi}_{i,x} = \begin{cases} i l_1 (2 \tilde{\phi}_I - \tilde{\phi}_i) & x \rightarrow \infty \\ i l_2 \tilde{\phi}_i & x \rightarrow -\infty \end{cases} \quad (5.3.15)$$

where l_1 and l_2 refer to values of l at $h=h_1(x \rightarrow -\infty)$ and $h=h_2(x \rightarrow +\infty)$ respectively. Equations (5.3.12) and (5.3.15) yield a tridiagonal system which is solved by a standard double elimination method.

As an example of reflection from an isolated depth variation, we choose a bottom consisting of a smooth transition from a depth h_1 ($x \leq 0$) to a depth h_2 ($x \geq L$), with the bottom profile in the region $0 < x < L$ given by

$$h(x) = \frac{h_1 + h_2}{2} - \frac{(h_1 - h_2)}{2} \cos\left(\frac{s\pi x}{h_1 - h_2}\right)$$

where $s = (h_1 - h_2)/L$. For both cases studied, we take $h_2/h_1 = 0.2$, with waves incident from the depth h_1 . The maximum bottom slope occurs at $x = L/2$ and has the value $\pi s/2$. Results were calculated for values of $s = 1/3$ and $2/3$ and for angles of incidence of $\theta = 0^\circ$ and 45° . Reflection coefficients for each of the four cases are calculated by four methods; mild slope equation (5.3.12) neglecting α and F , moderate slope equation (5.3.12) retaining only the unambiguous term α , moderate slope equation (5.3.12) using α and F , and the boundary integral method (BIM) described in Appendix F. The boundary integral method provides the theoretically correct answer and may be used as the basis for comparison between the wave propagation methods based on (5.3.12), although the method described in Appendix F neglects local curvature of the bottom boundary and therefore may introduce some error. The discretised

boundary for the BIM for the case of $s=2/3$ is shown in Figure 5.5.

Results for the reflection coefficient K_r as a function of kh , for the incident wave are shown in Figures 5.6-5.9 for the four cases mentioned above. For the case of $s=1/3$ (Figures 5.6 and 5.7), the mild slope equation provides the best agreement with results of the BIM for the 45° angle of incidence, while, for normal incidence, the full formulation with α and F agrees more closely except in the range of $kh' < 0.75$, where K_r is large and errors associated with the specification of F become important. In this range, the moderate slope equation retaining only α agrees more closely with the BIM results.

For the case of $s=2/3$, the mild slope equation provides the best estimate of the reflection coefficient for normal wave incidence, while for $\theta=45^\circ$ the moderate slope equation with F neglected provides the best agreement over the range of kh values tested. Agreement between BIM and the moderate slope equation with α and F is poor for both angles of incidence in this case.

The results of the cases studied here indicate that none of the approximate methods are accurate in terms of



Figure 5.5 Boundary integral method domain for reflection from sloping step.
Case of $s = 2/3$

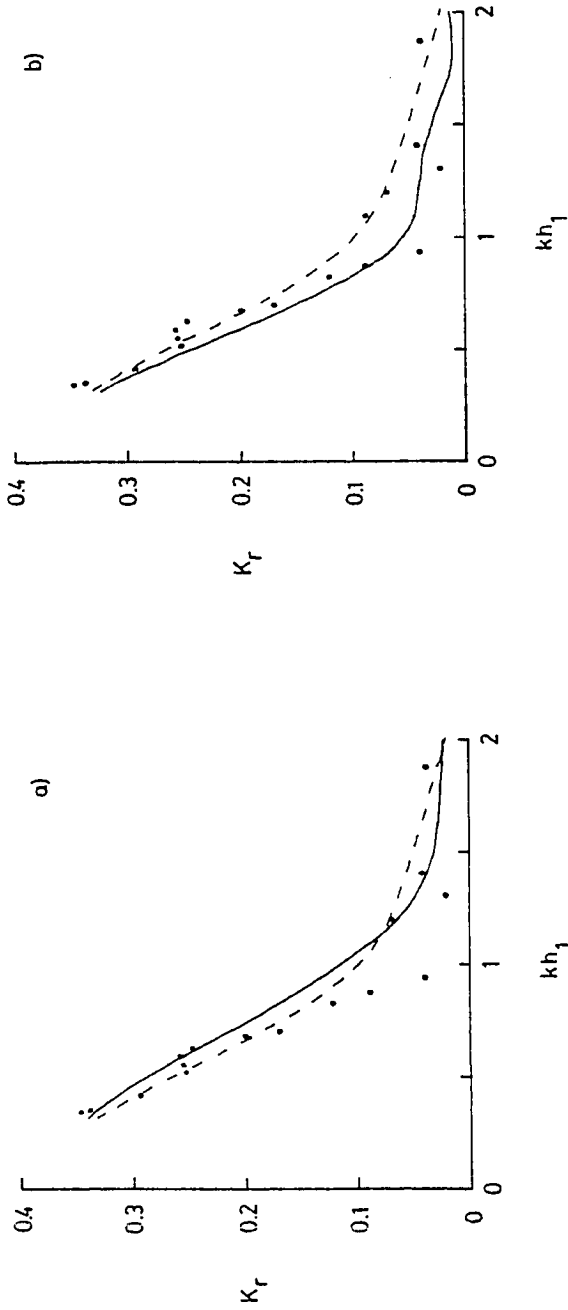


Figure 5.6 Reflection coefficient K_r vs. kh of incident wave.

$s = 1/3, \theta = 0^\circ$.

a) α only b) $\alpha + F$

• BIM solution; --- mild-slope; — moderate slope.

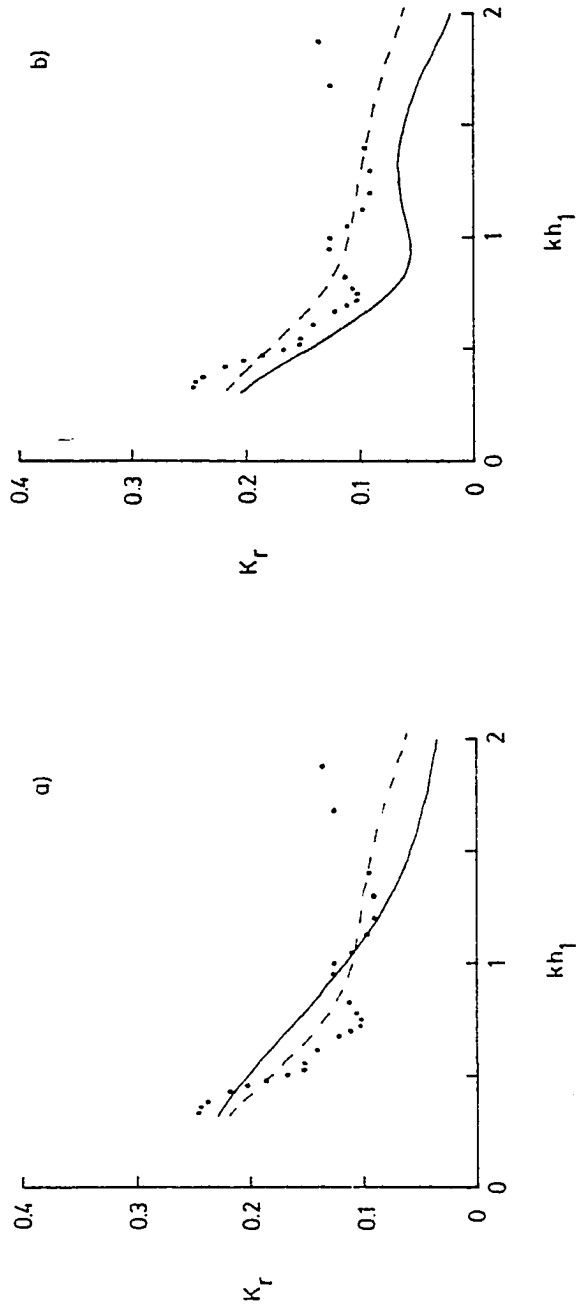


Figure 5.7 Reflection coefficient K_r vs. kh of incident wave.
 $s = 1/3$, $\theta = 45^\circ$
 a) α only, b) $\alpha + F$
 . BIM solution; --- mild-slope; — moderate slope

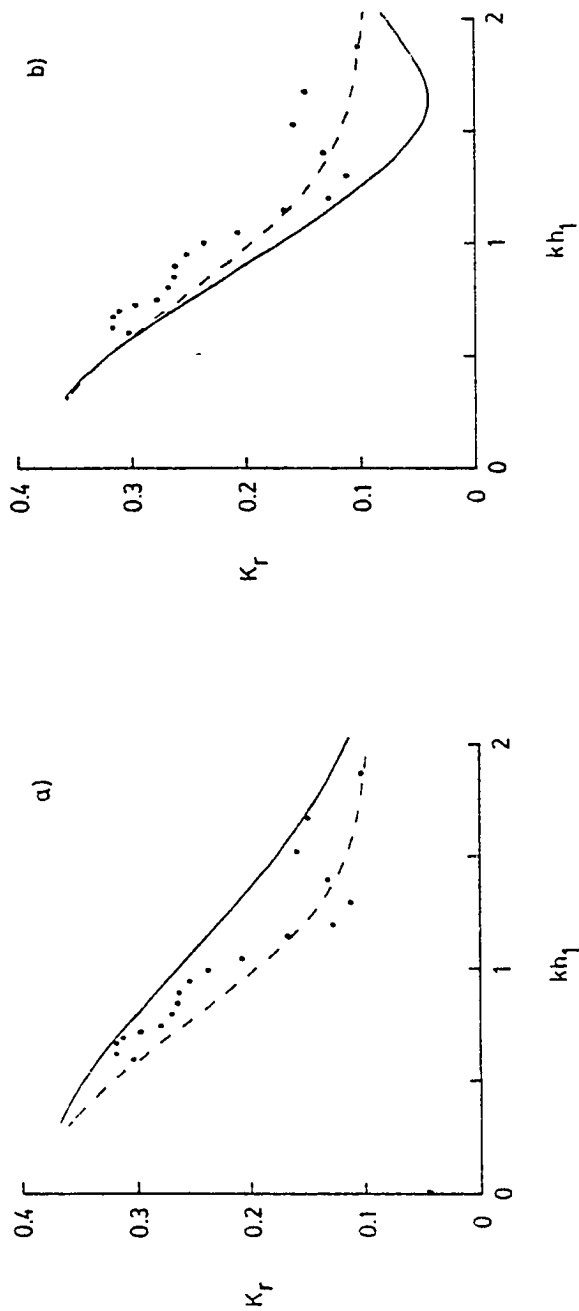


Figure 5.8 Reflection coefficient K_r vs. kh_1 of incident wave
 $s = 2/3$, $\theta = 0^\circ$.
 a) α only, b) $\alpha + F$
 . BIM solution; --- mild slope; — moderate slope

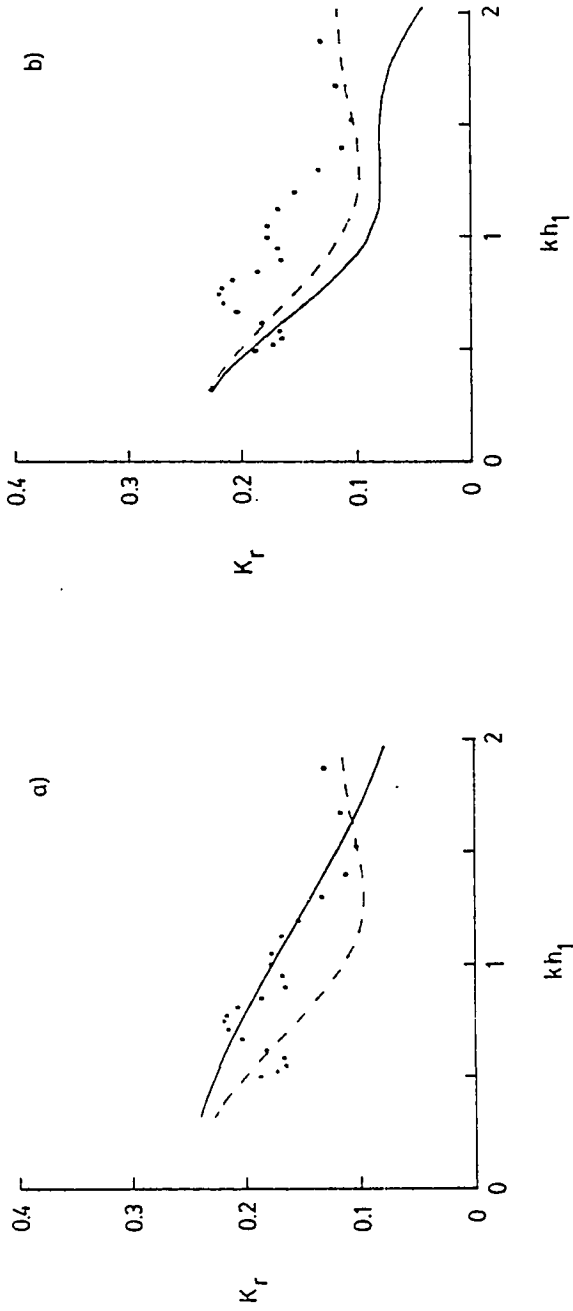


Figure 5.9 Reflection coefficient K_r vs. kh_1 of incident wave
 $s = 2/3$, $\theta = 45^\circ$
 a) α only, b) $\alpha + F$
 • BIM solution; ---- mild-slope; — moderate slope

predicting the magnitude or variations of the reflection coefficient with changing incident wavelength, although all of the methods produce qualitatively similar results approaching the limit of small kh , where accurate results may be obtained simply by matching surface elevation and mass flux across a discontinuity in depth between $h=h_1$ and h_2 . Of the models described above, it would be expected that the moderate slope model with F retained would yield the more accurate results in comparison to the BIM, although a rational scheme for specifying F , based either on a formulation for standing waves or an iterative scheme linking the incident and reflected waves, remains to be developed.

CHAPTER 6. SOME EXAMPLES OF THE COMBINED REFRACTION-
DIFFRACTION OF LINEAR AND STOKES WAVES

6.1. Introduction

In this chapter, we use the time-independent parabolic models of section 4.4 to study several examples of the combined refraction and diffraction of linear and Stokes waves by variable depth and currents. Examples include a study of wave focussing by a submerged shoal and diffraction of waves by a shore-attached breakwater, for which data are available for comparison.

Yue and Mei(1980) have shown that the reflection of a wave at glancing angle of incidence on a vertical wall produces an effect known as the "Mach" stem, where the linear result of an incident plane wave and scattered reflected wave, leading to a short-crested pattern in the far field, is replaced by a region of plane waves of uniform amplitude propagating along the wall. Peregrine(1983) analysed Yue and Mei's parabolic approximation for diffraction of Stokes waves and found that the equation is

analogous to the nonlinear equation governing the development of an undular bore. The incident wave and the wave in the stem region can thus be interpreted as being conjugate wave states divided by a jump. Peregrine hypothesised that similar effects could be expected in situations where refraction leads to ray-crossing and overlapping of segments of the incident wave. Kirby and Dalrymple(1983b) have demonstrated this effect in the case of waves focussed by a submerged shoal. The development of a conjugate state also has implications for the evolution of wavefields in the vicinity of straight or curved caustics, where the development of a jump may preclude the evolution of steady state solutions for the wave field in the vicinity of the caustic. These steady state solutions can be found in terms of the second Painleve transcendent (see, for example, Miles 1978), and would be qualitatively similar to the linear solution in terms of Airy functions. With this in mind, we study the development of the wavefield from the leading edge of a pair of straight caustics caused by increasing water depth in section 6.7, and also look at the situation of waves reflected by a distribution of following current in section 6.8.

Finally, in section 6.9, we study the combined refraction and diffraction of an incident wave field by the

rip current velocity distribution given by Artnur (1950). Here, the nonlinearity occurs at too large an Ursell number for Stokes theory to be valid, and we employ instead a dispersion relation based on the empirical findings of Walker(1976), as mentioned in section 3.5.

6.2. Numerical Approximation of the Parabolic Equation

The parabolic equations of section 4.4 are nonlinear and in general have variable coefficients due to inhomogeneity of the physical domain (in terms of depth and current variations). Consequently, a numerical treatment is required in order to obtain solutions to any but the simplest problems. The parabolic nature of the equations leads to the choice of a solution technique based on the implicit, forward-stepping scheme of Crank and Nicolson, detailed below. In analogy to heat transfer and diffusion problems which are also parabolic in nature, we choose the x coordinate as the forward-marching, time-like dimension, while the y -coordinate then serves as the physical spatial coordinate. For all examples studied in this chapter, we will restrict our attention to a rectilinear coordinate system as shown in Figure 6.1. The solution scheme also requires the specification of lateral boundary conditions on the y -coordinate, which will be discussed in section 6.3.

For waves in the absence of currents, we will consider both the lowest order approximation (4.4.4), referred to hereafter as the "Radder" approximation, and the higher order approximation (4.4.38), referred to as the "Booij" approximation. For waves in the presence of

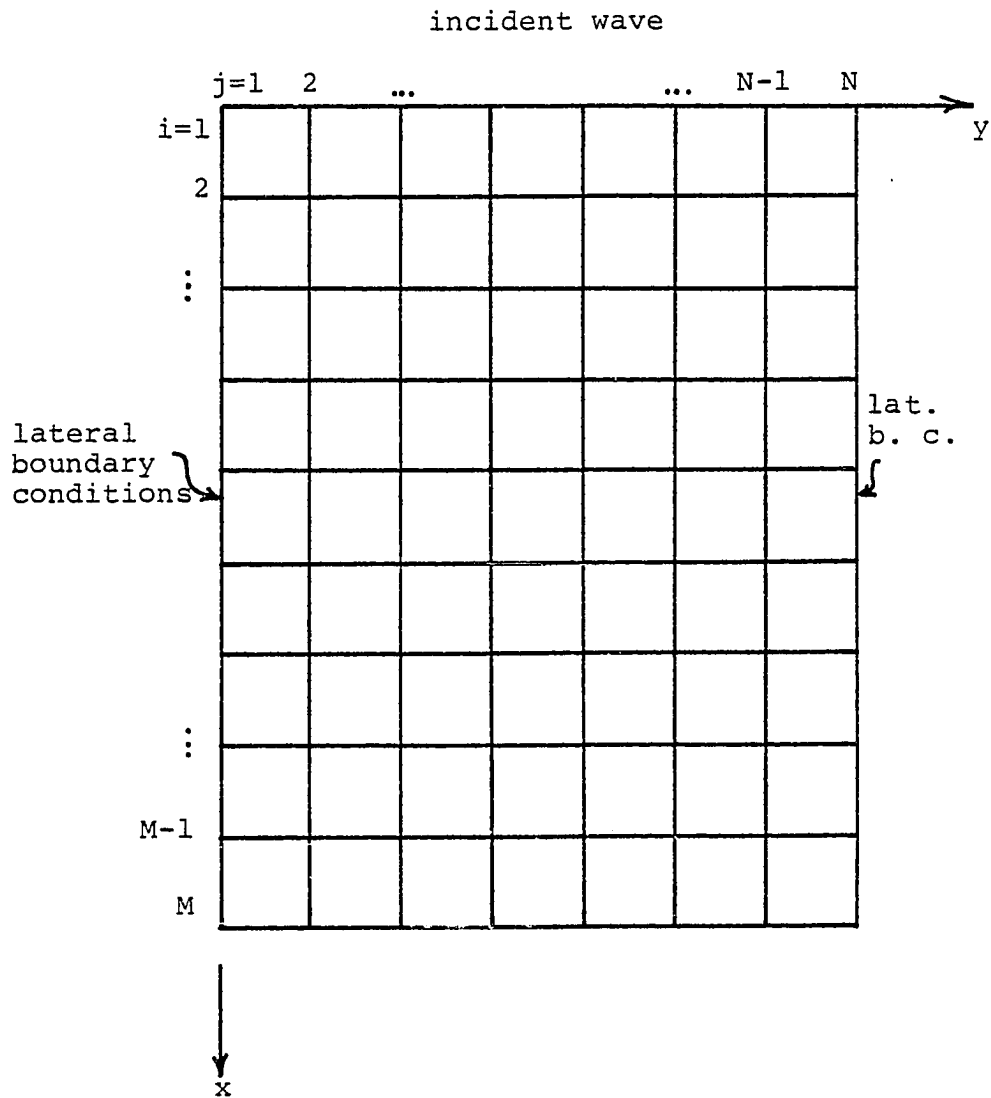


Figure 6.1 Computational grid and labelling of grid points

currents, the higher order approximation is quite complex and its use does not produce significantly different results than the model equation (4.4.35) in the examples studied in sections 6.8 and 6.9. Consequently, we will restrict our attention to the simpler model (4.4.35). The current-free equations (4.4.4) and (4.4.38) will be treated separately from the wave-current model (4.4.35), due to slight differences in finite-difference approximations of the coefficients.

Both approximations (4.4.4) and (4.4.38) may be represented by the general equation

$$A_x + i(k_0 - k)A + \frac{1}{2kp}(kp)_x A - \frac{iP_2}{kp}(pA_y)_y + \frac{P_1}{k^2p}(pA_y)_{yx} + \frac{iP_1}{k^2p}\beta(pA_y)_y + \frac{i}{2}K'|A|^2A + \frac{\omega W}{2kp}A = 0 \quad (6.2.1)$$

where

$$p = CC_y \quad (6.2.2)$$

$$K' = k^3 D/n \quad (6.2.3)$$

$$\beta = k_0 + i \left\{ \frac{k_x}{R} + \frac{(kp)_x}{2kp} \right\} \quad (6.2.4)$$

and where primes (') have been dropped from the amplitude A for convenience. Note that the reference phase function ϕ' is still given by ik_0x . The Radder approximation is recovered by the choice $P_1=0$, $P_2=1/2$, while the choice $P_1=1/4$, $P_2=3/4$ gives the Booij approximation.

A rectangular grid with uniform spacing in the x and y directions is established as shown in Figure 6.1. We define

$$X_i = (i-1)\Delta x + x_r \quad ; \quad 1 \leq i \leq M \quad (6.2.5)$$

For all examples studied, the depth will be taken as being uniform on $i=1$, and the wavenumber on the first grid row will be chosen as k_0 . Values of y_j are defined according to

$$y_j = (j-1)\Delta y + y_r \quad ; \quad 1 \leq j \leq N \quad (6.2.6)$$

In (6.2.5-6), x_r and y_r are arbitrarily chosen to allow a shift in origin.

The parabolic model (6.2.1) is written in finite difference form using the implicit Crank-Nicolson scheme.

The coefficient β_j^i is written as

$$\beta_j^i = k_0 + \frac{2i}{\Delta x} \frac{(k_j^{i+1} - k_j^i)}{(k_j^{i+1} + k_j^i)} + \frac{i}{\Delta x} \frac{[(kp)_j^{i+1} - (kp)_j^i]}{[(kp)_j^{i+1} + (kp)_j^i]} \quad (6.2.7)$$

where the i row contains known values of A and the $i+1$ row is the row to be determined by the implicit step. The second derivative term $(pA_y)_y$ is approximated according to

$$(pA_y)_y^i = \frac{(p_{j+1}^i + p_j^i)(A_{j+1}^i - A_j^i) - (p_j^i + p_{j-1}^i)(A_j^i - A_{j-1}^i)}{2(\Delta y)^2} \quad (6.2.8)$$

Using (6.2.7-8), the parabolic model is approximated by the finite-difference equation:

$$\begin{aligned} & \frac{A_j^{i+1} - A_j^i}{\Delta x} + \frac{i}{2} \left\{ (k_0 - k_j^{i+1}) A_j^{i+1} + (k_0 - k_j^i) A_j^i \right\} + \\ & + \left[\frac{(kp)_j^{i+1} - (kp)_j^i}{(kp)_j^{i+1} + (kp)_j^i} \right] \frac{(A_j^{i+1} + A_j^i)}{2\Delta x} - \frac{i}{2} \left\{ \frac{P_2}{(kp)_j^{i+1}} - \frac{P_1 \beta_j^i}{(k^2 p)_j^{i+1}} \right\} (pA_y)_y^i \\ & - \frac{i}{2} \left\{ \frac{P_2}{(kp)_j^i} - \frac{P_1 \beta_j^i}{(k^2 p)_j^i} \right\} (pA_y)_y^i + \frac{P_1}{2} \left\{ \frac{1}{(k^2 p)_j^{i+1}} + \frac{1}{(k^2 p)_j^i} \right\} \frac{[(pA_y)_y^{i+1} - (pA_y)_y^i]}{\Delta x} + \end{aligned}$$

$$\begin{aligned}
& + \frac{i}{4} \left\{ K'_j{}^{i+1} |\tilde{A}_j{}^{i+1}|^2 A_j{}^{i+1} + K'_j{}^i |A_j{}^i|^2 A_j{}^i \right\} + \\
& + \frac{i\omega}{4} \left\{ \frac{W_j{}^{i+1}}{(kp)_j{}^{i+1}} A_j{}^{i+1} + \frac{W_j{}^i}{(kp)_j{}^i} A_j{}^i \right\} = 0 \quad (6.2.9)
\end{aligned}$$

Equation (6.2.9) may be arranged so as to solve for the $A_j{}^{i+1}$ based on the known values of $A_j{}^i$. Using the two-point lateral boundary conditions discussed in section 6.3 leads to a tridiagonal system of N equations in the N unknown $A_j{}^{i+1}$, and solutions are obtained rapidly using the double-elimination scheme described by Carnahan, Luther and Wilkes (1969), with their numerical algorithm modified to handle complex arithmetic. Previous to this step, however, an estimate must be obtained for the unknown value $\tilde{A}_j{}^{i+1}$ in the nonlinear term at row $(i+1)$. This value is provided by an intermediate explicit step given by

$$\begin{aligned}
& \frac{\tilde{A}_j{}^{i+1} - A_j{}^i}{\Delta x} + i(k_0 - k_j{}^i) A_j{}^i + \left\{ \frac{(kp)_j{}^{i+1} - (kp)_j{}^i}{(kp)_j{}^{i+1} + (kp)_j{}^i} \right\} \frac{A_j{}^i}{\Delta x} - \\
& - i \left\{ \frac{P_2}{(kp)_j{}^i} - \frac{P_1 \beta_j{}^i}{(kp^2)_j{}^i} \right\} (p A_y)_y j^i + \\
& + \frac{i}{2} K'_j{}^i |A_j{}^i|^2 A_j{}^i + \frac{\omega W_j{}^i}{2(kp)_j{}^i} A_j{}^i = 0 \quad (6.2.10)
\end{aligned}$$

Note that in the intermediate step the derivative $(kp)_x$ and the term \dot{A}_j^2 are off-center with respect to the value of A , while the term $(pA_y)_{yx}$ is neglected.

The implicit scheme (6.2.9) has truncation errors of $O((\Delta x)^2, (\Delta y)^2)$. While it is generally difficult to assess the stability of nonlinear difference equations with variable coefficients, it is known that the linear, constant coefficient counterpart of (6.2.9) is unconditionally stable with respect to choices of Δx and Δy . Further, the scheme in the linear, constant coefficient case preserves mean square quantities (here related to the wave energy $|A|^2$) identically, subject to the accuracy of the lateral boundary conditions.

The explicit-implicit scheme described by (6.2.9-10) was found to be stable in all experiments for all values of kh , with the explicit value $|\tilde{A}_j^{i+1}|$ generally falling within 10% of the final value $|A_j^{i+1}|$. A somewhat different scheme involving a two-step implicit iteration, as used by Kirby and Dalrymple (1983b), was found to develop an unstable

divergence in alternate iterations for the value of \tilde{A}_j^{i+1} for values of kh less than 0.15 in general. Both schemes exhibit stable behavior for ranges of parameters where Stokes' theory is valid.

The finite-difference scheme for the wave-current interaction model (4.4.35) is given by

$$\begin{aligned}
& \frac{A_j^{i+1} - A_j^i}{\Delta x} + \frac{i}{2} \left\{ (k_0 - k_j^{i+1}) A_j^{i+1} + (k_0 - k_j^i) A_j^i \right\} \\
& + \frac{1}{2} \left\{ \left(\frac{\omega}{\sigma_j^{i+1}} \right) \left(\frac{V_j^{i+1}}{C_{gj}^{i+1} + u_j^{i+1}} \right) \frac{[A_{j+1}^{i+1} - A_{j-1}^{i+1}]}{2\Delta y} + \left(\frac{\omega}{\sigma_j^i} \right) \left(\frac{V_j^i}{C_{gj}^i + u_j^i} \right) \frac{[A_{j+1}^i - A_{j-1}^i]}{2\Delta y} \right\} + \\
& + \frac{1}{2\Delta x} \left\{ \frac{(C_{gj}^{i+1} + u_j^{i+1})/\sigma_j^{i+1} - (C_{gj}^i + u_j^i)/\sigma_j^i}{(C_{gj}^{i+1} + u_j^{i+1})/\sigma_j^{i+1} + (C_{gj}^i + u_j^i)/\sigma_j^i} \right\} (A_j^{i+1} + A_j^i) + \\
& + \frac{1}{2} \left\{ \left(\frac{\omega}{\sigma_j^{i+1}} \right) \left[\frac{V_{j+1}^{i+1} - V_{j-1}^{i+1}}{4\Delta y} + \frac{V_j^{i+1} (\sigma_{j+1}^{i+1} - \sigma_{j-1}^{i+1})}{2\sigma_j^{i+1} \Delta y} \right] \frac{A_j^{i+1}}{(C_{gj}^{i+1} + u_j^{i+1})} + \right. \\
& \left. + \left(\frac{\omega}{\sigma_j^i} \right) \left[\frac{V_{j+1}^i - V_{j-1}^i}{4\Delta y} + \frac{V_j^i (\sigma_{j+1}^i - \sigma_{j-1}^i)}{2\sigma_j^i \Delta y} \right] \frac{A_j^i}{(C_{gj}^i + u_j^i)} \right\} \\
& - \frac{i}{4} \left\{ \frac{(PA_y)_{y_j}^{i+1}}{\sigma_j^{i+1} (C_{gj}^{i+1} + u_j^{i+1})} + \frac{(PA_y)_{y_j}^i}{\sigma_j^i (C_{gj}^i + u_j^i)} \right\} +
\end{aligned}$$

$$\begin{aligned}
& + \frac{i}{4} \left\{ \frac{C_{g_j}^{i+1}}{C_{g_j}^{i+1} + u_j^{i+1}} K_j^{i+1} |\tilde{A}_j^{i+1}|^2 A_j^{i+1} + \right. \\
& \quad \left. + \frac{C_{g_j}^i}{C_{g_j}^i + u_j^i} K_j^i |A_j^i|^2 A_j^i \right\} + \\
& + \frac{1}{4} \left\{ \frac{W_j^{i+1} A_j^{i+1}}{C_{g_j}^{i+1} + u_j^{i+1}} + \frac{W_j^i A_j^i}{C_{g_j}^i + u_j^i} \right\} = 0 \quad (6.2.11)
\end{aligned}$$

The intermediate value \tilde{A}_j^{i+1} is provided by the explicit step

$$\begin{aligned}
& \frac{\tilde{A}_j^{i+1} - A_j^i}{\Delta x} + i(k_0 - k_j^i) A_j^i + \left(\frac{\omega}{\sigma_j^i} \right) \left(\frac{V_j^i}{C_{g_j}^i + u_j^i} \right) \frac{(A_{j+1}^i - A_{j-1}^i)}{2\Delta y} + \\
& + \frac{1}{\Delta x} \left\{ \frac{(C_{g_j}^{i+1} + u_j^{i+1})/\sigma_j^{i+1} - (C_{g_j}^i + u_j^i)/\sigma_j^i}{(C_{g_j}^{i+1} + u_j^{i+1})/\sigma_j^{i+1} + (C_{g_j}^i + u_j^i)/\sigma_j^i} \right\} A_j^i \\
& + \left(\frac{\omega}{\sigma_j^i} \right) \frac{1}{(C_{g_j}^i + u_j^i)} \left\{ \frac{V_{j+1}^i - V_{j-1}^i}{4\Delta y} + \left(\frac{V_j^i}{\sigma_j^i} \right) \frac{(\sigma_{j+1}^i - \sigma_{j-1}^i)}{2\Delta y} \right\} A_j^i + \\
& + i \left(\frac{C_{g_j}^i}{C_{g_j}^i + u_j^i} \right) \frac{K_j^i |A_j^i|^2 A_j^i}{2} + \frac{W_j^i A_j^i}{2(C_{g_j}^i + u_j^i)} -
\end{aligned}$$

$$-\frac{i}{2\sigma_j^2(c_{gj}^2 + \kappa_j^2)} (\rho A_y)_{y_j}^i = 0 \quad (6.2.12)$$

This scheme is used in the examples of sections 6.8 and 6.9. For each scheme, linear results may be obtained by neglecting the cubic nonlinear terms and eliminating the explicit steps except in the case where waves are breaking, where the explicit step is used to obtain the forward value \tilde{A}_j^{i+1} used in estimating the dissipation coefficient w . This procedure is discussed in section 6.4.

The numerical procedure requires the specification of A_j^i , $1 < j < N$ on the first grid row. In the cases studied below, we will restrict our attention to monochromatic waves, in which case A^i may be specified simply by

$$A_j^i = A_0 e^{i k_0 \sin \theta y_j} \quad ; \quad 1 \leq j \leq N$$

where A_0 is the initial amplitude and θ is the angle of incidence of the wave with respect to the x-direction. In principle, the method may be used for a directional spectra of incident waves which may be specified by

$$A_j^i = \sum_{l=1}^n A_l e^{i(k_0 \sin \theta_l y_j - \omega_l t)} \quad ; \quad 1 \leq j \leq N$$

where n is the number of components each having amplitude A_ℓ , direction $\hat{\mathbf{e}}_\ell$ and phase shift $\hat{\phi}_\ell$, with the restriction that each component be a plane wave with absolute frequency ω .

6.3. Treatment of the Lateral Boundary Conditions

The solution of the numerical problem presented in section 6.2 requires the specification of lateral boundary conditions on the y-boundaries of the computational grid. In the examples studied in this chapter, two types of simple boundaries are included; completely reflective, and completely transmitting. The completely reflective barrier, representative of a vertical wall, is considered first. For a plane wall oriented in the x-direction, the condition of no velocity component normal to the wall leads to the condition

$$A_y \Big|_{y=y_w} = 0 \quad (6.3.1)$$

where y_w is the position of the wall. For all cases considered below, the wall will be centered midway between two adjacent grid rows, as shown in Figure 6.2a. The finite difference form of (6.3.1) centered on the wall is given by

$$A_{j+1} = A_j \quad (6.3.2)$$

where the wall is located at $y_w = (j+1/2)\Delta y$. Taylor series expansion of (6.3.2) about y_w leads to the result

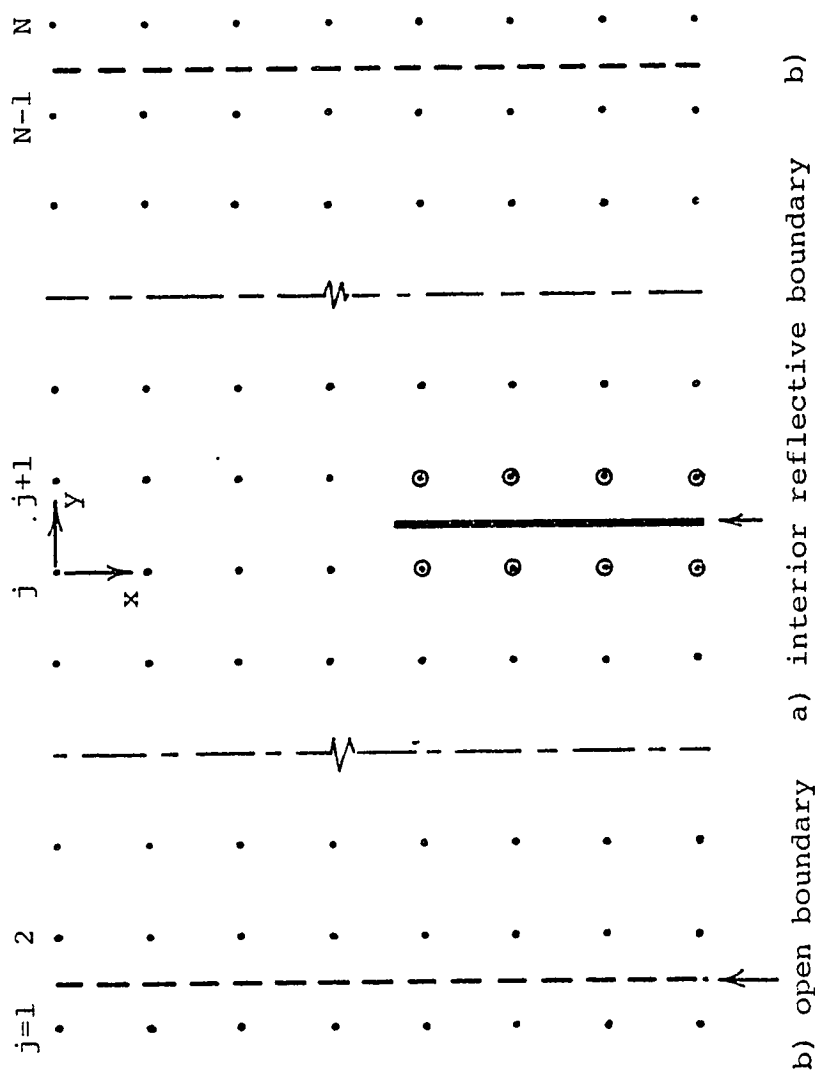


Figure 6.2 Relation between grid points, open boundaries and internal reflective boundaries

\cdot grid points \odot overlapped grid points in numerical scheme

$$A_y = \frac{-1}{24} A_{yyy} (\Delta y)^2 = O + O(\Delta y)^2 \quad (6.3.3)$$

indicating second order (in Δy) accuracy for the boundary condition. The centering of the wall between two adjacent grid rows is accomodated in the schemes of section 6.2 by generating auxiliary grid rows to handle the required overlapping of wave data on the two rows adjacent to the wall.

Open, transmitting boundaries may occur on either the up- or downwave side of the computational grid. For the downwave boundary, the boundary condition must allow waves to radiate freely from the numerical grid with as little reflection as possible, while, for the upwave boundary, the condition must allow the entry of a wave to replace the waves propagating away from the boundary into the grid interior, thus avoiding the creation of a shadow adjacent to the grid boundary.

The application of an upwave boundary is in general fraught with difficulty, since no definite information beyond pure assumption exists to indicate the exact nature of waves approaching the boundary from the exterior of the grid. For the application to the study of a shore attached breakwater on a plane beach in section 6.6, the lateral

boundaries are placed far from the obstacle, and we may assume as a first step that the wave field consists entirely of the shoaling and refracting incident wave and the wave scattered from the breakwater. The incident wave has the characteristics of uniform amplitude in the y -direction and a longshore wavenumber component m which is constant as a result of Snell's law. If we presume that the boundaries are far enough from the breakwater such that no scattered wave reaches the boundary, then both the up- and downwave boundary conditions can be specified exactly by

$$A_y = im A \quad ; \quad y = y_1, y_N \quad (6.3.4)$$

Once again, assuming that the physical grid boundary is centered between adjacent grid rows, as in Figure 6.2b, (6.3.4) may be rewritten in finite difference form as

$$\frac{A_{j+1}^i - A_j^i}{\Delta y} = im \left(A_{j+1}^i - A_j^i \right) \quad (6.3.5)$$

where m is presumed to be known precisely. (6.3.5) is rearranged to read

$$A_{j+1}^i \left(1 - im \left(\frac{\Delta y}{2} \right) \right) = A_j^i \left(1 + im \left(\frac{\Delta y}{2} \right) \right) \quad (6.3.6)$$

Introducing Taylor expansions of A centered at $y = (j+1/2)\Delta y$

leads to the result

$$A_y = imA + i\frac{m}{8} A_{yy} (\Delta y)^2 - \frac{A_{yyy}}{24} (\Delta y)^2 = imA + O(\Delta y)^2 \quad (6.3.7)$$

The errors involved in (6.3.5) are thus seen to be comparable in order to the error encountered in (6.3.2); however, the larger coefficient and lower order derivative in (6.3.7) as compared to (6.3.2) indicated that larger numerical errors are likely to be associated with the approximate radiation condition (6.3.5).

For cases where the value of m cannot be determined based on Snell's law, or where the scattered wave represents a significant contribution to the total wave field, the value of m must be estimated on a numerical basis. For the case of a wavefield consisting of more than one component, we assume that the wave may be estimated locally at the boundary as a plane wave of unknown direction and slowly varying amplitude A in the y -direction. Then (6.3.4) may be used again. Assuming that the wave field changes slowly in the x and y directions, m at grid row $x=i\Delta x$ may be estimated by the results at grid row $x=(i-1)\Delta x$ by

$$m_N^i = -i A_{yy}^{i-1} / A^{i-1} \quad (6.3.8)$$

Then, applying the centered finite difference scheme at $x=(i-1)\Delta x$, $y=(j+1/2)\Delta y$ yields the estimate for the numerical value m

$$m_N^i = -\frac{2i}{\Delta y} \left(\frac{A_{j+1}^{i-1} - A_j^{i-1}}{A_{j+1}^{i-1} + A_j^{i-1}} \right) \quad (6.3.9)$$

This estimate introduces a further numerical error which may be estimated by inspecting the case where m is known and $|A|$ is uniform in the x and y directions. Employing Taylor series expansions about the center point $y=(j+1/2)\Delta y$ leads to the result

$$m_N^i = \frac{-i \left(A_y/A + (A_{yyy}/A)(\Delta y)^2/24 \right)}{\left(1 + \frac{(\Delta y)^2}{8} A_{yy} \right)} \quad (6.3.10)$$

Then, assuming that the relation (6.3.4) is exact, (6.3.10) reduces to

$$m_N^i \cong m \left(1 + m^2 \frac{(\Delta y)^2}{12} \right) \quad (6.3.11)$$

which again has an $O(\Delta y^2)$ error due to the differencing scheme. Substituting (6.3.10) into the error estimate for the boundary condition (6.3.7) leads to the revised formula

$$A_y = imA + im(\Delta y)^2 \left\{ \frac{m^2}{12} A + \frac{1}{12} A_{yy} \right\} \quad (6.3.12)$$

indicating that the approximation is actually self-correcting at $O(\Delta y^2)$. Retention of higher powers in Δy in each expansion shows that the discretization errors actually cancel to any order in Δy , rendering the boundary condition exact in regions where Snell's law holds and amplitude is uniform in the y direction. However errors may be expected to occur in short crested wave fields, where A may have large variations over several grid spacings.

Results of several numerical experiments are presented here in order to indicate the errors associated with the application of the radiating boundary condition to both up- and downwave open boundaries. Tests were conducted using a single wavelength and period for waves propagating over a flat bottom. Water depth, wavelength and period were given by

$$h = 10\text{m.}$$

$$L = 100\text{m. ; } k = 0.0628\text{m}^{-1}$$

$$T = 10.726\text{s.}$$

The formulation (6.3.6) was tested using both the exact value $m = k \sin \zeta$ and the numerical value m_N^i , given by

(6.3.9), for angles $\hat{c} = 10, 20, 30, \text{ and } 40^\circ$, where \hat{S} is the angle between the direction of wave propagation and the x-axis, and for grid spacings $(\Delta x, \Delta y)/L = 0.1, 0.2, 0.3, 0.4, \text{ and } 0.5$. Typical errors associated with the discretization of the spatial domain occur in the form of partial reflection of the incident wave at the downwave boundary, and decay of wave energy at the upwave boundary, again due to reflection of waves trying to enter the domain. For tests using the exact value of m and the monochromatic wavefield, the reflection coefficient at the downwave boundary and the loss of energy at the upwave boundary are plotted as functions of wave angle and grid spacing in figures 6.3 and 6.4, respectively. The loss of energy is represented as a percent error between the minimum energy occurring within ten wavelengths of the starting grid row and the starting value. Calculations were performed using the difference scheme (6.2.9) in linearised form with $P_1=0$. Results indicate that the numerical errors are relatively small for all angles of incidence using small grid spacing, and increase rapidly with the loss of detail in representation of the wave at higher grid spacings.

Results using the numerically exact condition employing the calculated value of m verified the condition as being an exact representation of the boundary conditions

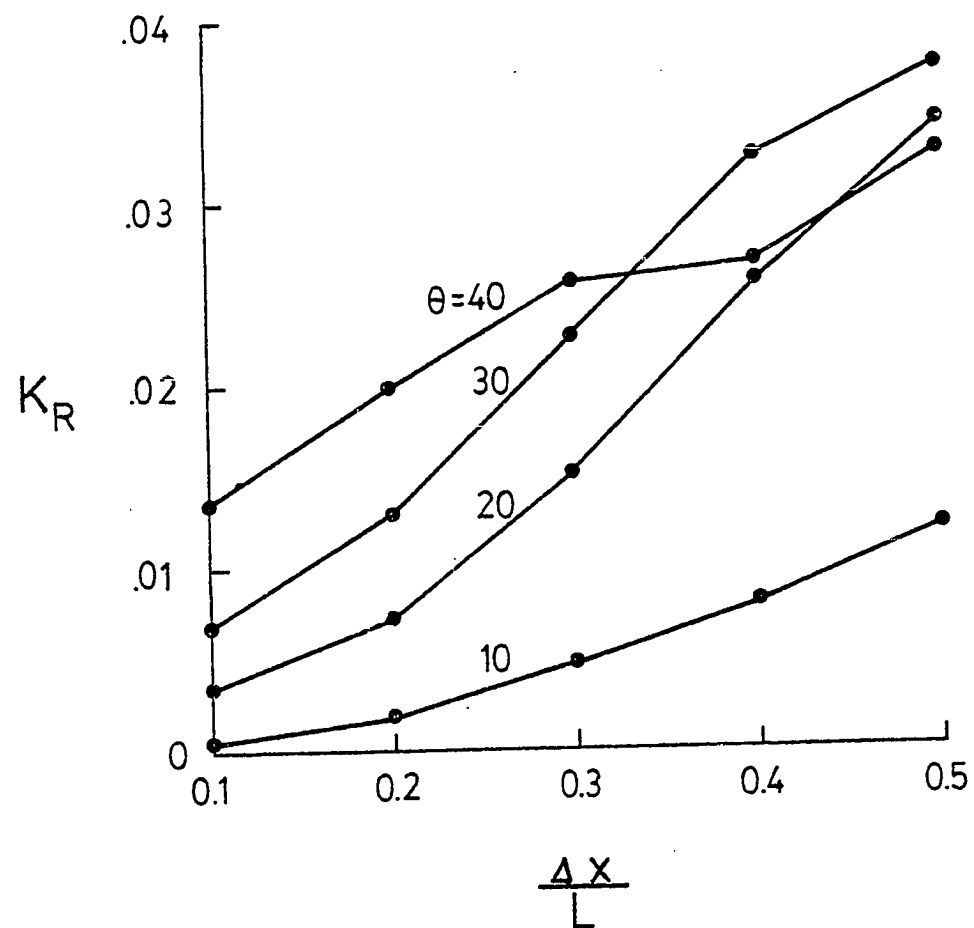


Figure 6.3 Reflection coefficient K_R at downwave boundary. Open boundary test, exact value of m .

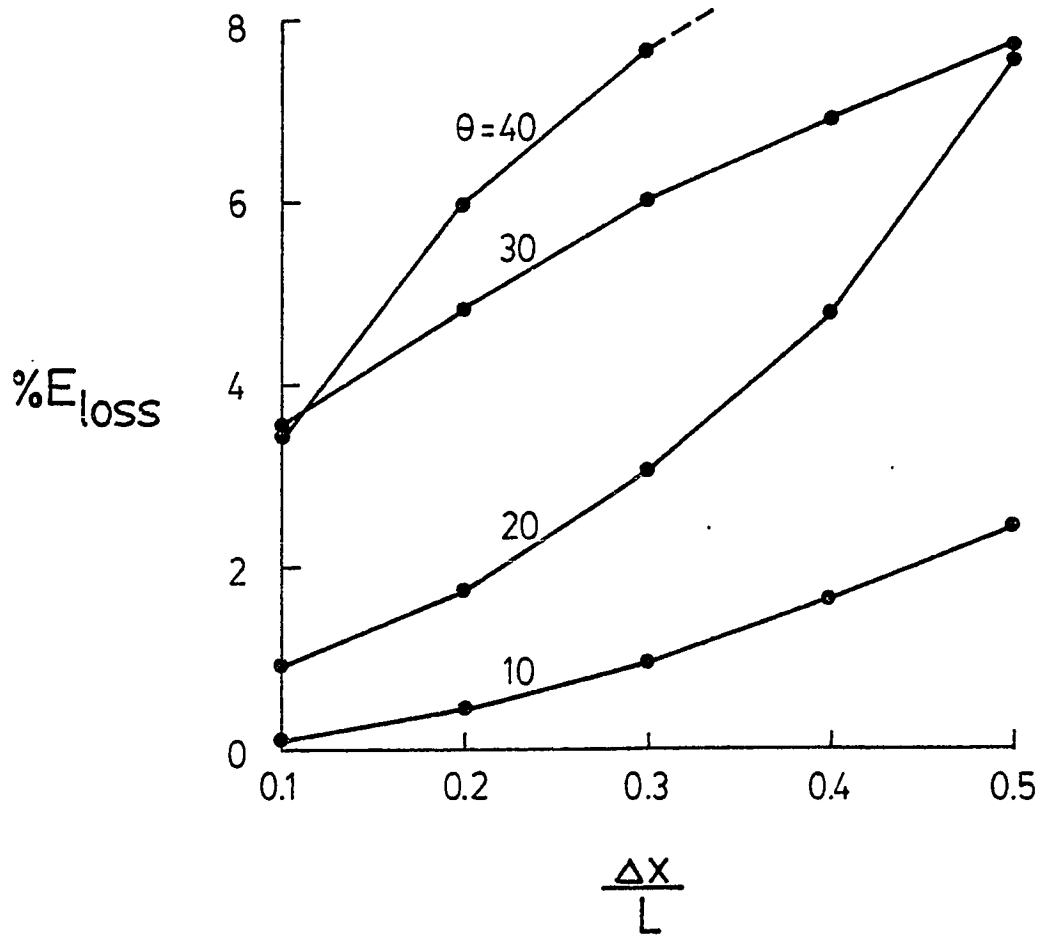


Figure 6.4 % energy loss at upwave boundary. Open boundary test, exact value of m .

for plane waves. No errors on either the upwave or downwave boundary were detected within the limits of the numerical accuracy of the calculations for any grid spacing or angle of incidence. The exactness of the numerical boundary condition coupled with energy conserving properties of the Crank-Nicolson scheme allowed the use of grid spacings in excess of a wave length with no loss in energy in the computational domain, even though the individual waves cannot be resolved at this numerical scale. A representative wavefield with $\Delta x/L=0.2$, $\theta=45^\circ$ is shown in Figure 6.5. The exactness of the boundary condition employing a numerical value m_N^i was further verified by testing the case of waves shoaling on a plane beach, where Snell's law is applicable, and again no errors associated with the open boundary conditions were detected.

As a final test of the applicability of the open boundary scheme to a general wavefield, several runs were performed for the case of two intersecting wave trains, both travelling at an angle to the grid direction x . Both waves were taken to have the same wavelength as the wave in the single wave test, and one wave was oriented at an angle of 10° for each test run, with the angle of the second wave being varied from 15° to 40° . Grid spacings were varied as in the single wave tests. A representative computed wave

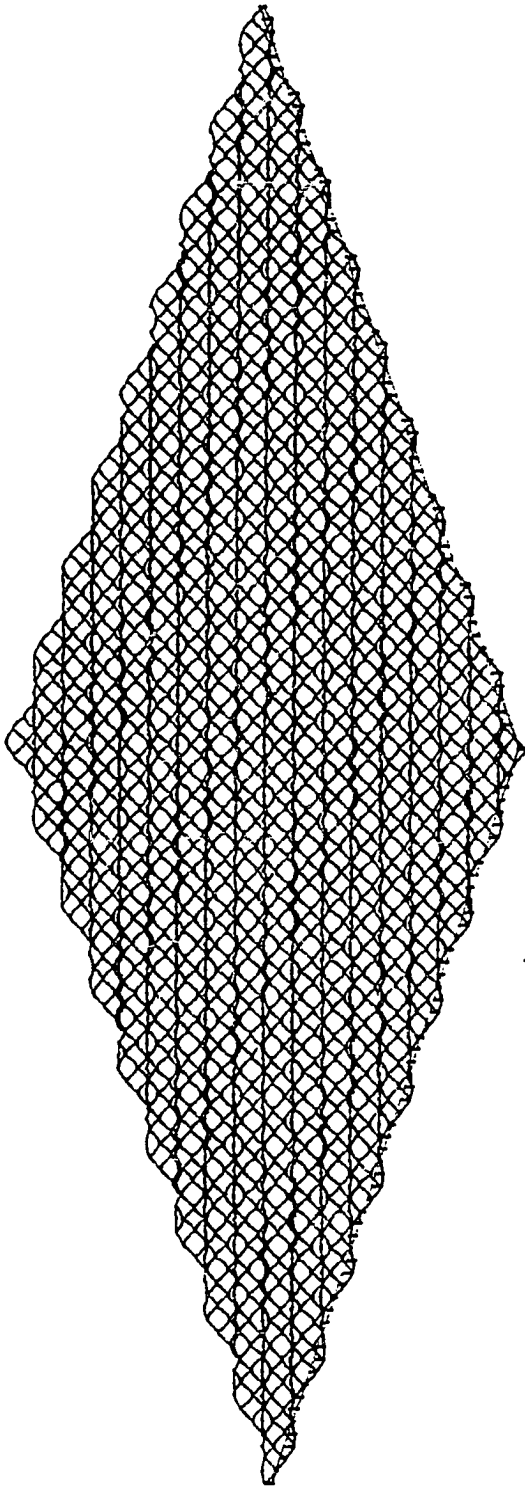


Figure 6.5 Plane wave propagating at $\theta = 45^\circ$ to x-axis.
Open boundary conditions, numerical value of m .

field is shown in Figure 6.6 for the case of $\Delta y/L = 0.1$ and $\vartheta = 20^\circ$ for wave 2.

The distortion of the wavefield adjacent to the up- and downwave boundaries (left and right boundaries, respectively, in the figure) is a result of the assumption that the wavefield could be characterised by a plane wave near the boundaries. On the upwave boundary, the boundary condition assesses the characteristics (amplitude and composite direction of propagation) of the wave at the incident ($x=0$) boundary and then lets a plane wave with these characteristics propagate into the domain, creating a plane wave in the geometric region shadowed by the starting point ($x=0$) of the side boundary. On the downwave boundary, the short-crested pattern propagates out of the domain with little difficulty until a nodal line approaches the boundary (about $1/3$ of the total boundary length from the top). At this point, the gradient of surface elevation normal to the boundary is dominated by the short crested pattern rather than by the wavenumber component normal to the boundary, and the assumptions used in deriving the boundary condition again break down. The model responds by reflecting a spurious wave back into the grid which can be seen through the disruption of the short-crested wave pattern at a considerable distance into the wavefield at the terminating

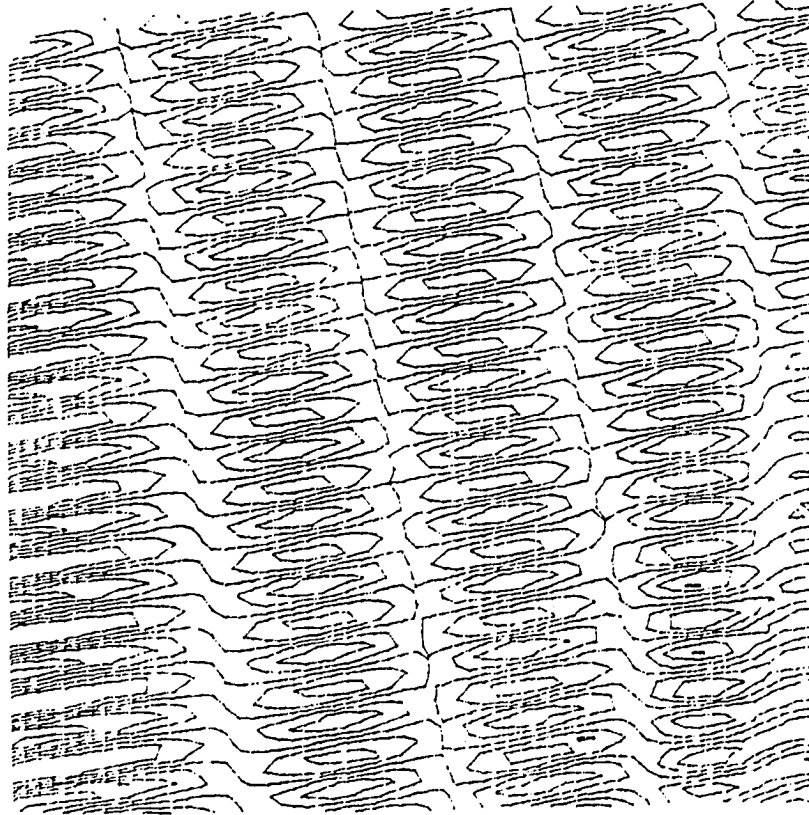


Figure 6.6 Interaction of two-component wave field and open boundary conditions; elevation contours of instantaneous surface
 $\theta_1 = 0^\circ$, $\theta_2 = 20^\circ$

boundary. This effect can become severe for large angles of incidence with respect to the x-axis.

Although the basic computational scheme developed in section 6.2 is clearly capable of modelling the propagation of a directional spectrum of waves, it is clear that more development of open boundary conditions must be pursued in order to develop a model of a fully general nature.

6.4. A Model for Breaking Waves in the Surfzone

An advantage of the parabolic method outlined above over solution techniques for elliptic and hyperbolic equations is that no downwave boundary condition is needed for the solution of the initial boundary value problem. However, in applications of wave models to coastal areas, the behavior of waves in the vicinity of a physical downwave boundary consisting of the actual coastline is of primary importance to the prediction of known physical effects such as the wave induced setup and longshore currents.

Wave breaking in the surfzone is a complex, highly nonlinear phenomenon. It is obvious that the model described in this study, which is limited to the representation of weak nonlinearities, is basically incapable of representing the underlying physics of the breaking process. However, some progress can be made by shifting our view of the model from its physical basis to its use as a predictive tool.

The forces leading to the generation and maintenance of setup and wave-induced currents depend on a physical balance between gradients of excess momentum fluxes, pressure forces due to changes in mean surface

elevation, and bottom shear stresses. The role of a wave model in determining the balance consists of predicting the local wave energy density and direction of propagation of the wave field. Thus, as a lowest approximation of the overall physics, it suffices that the wave model be able to predict the local wave amplitude in the breaking zone with some degree of reliability. The simplest model of wave decay in the surfzone is based on the assumption that the ratio of wave height to local water depth has the same value everywhere in the surfzone as at the breaker line. This assumption has been used extensively in the literature, from the earliest predictions of setup (Longuet-Higgins and Stewart (1963), Bowen, Inman and Simmons(1968)) and longshore currents (Bowen(1968), Longuet-Higgins(1970)) up to the latest applications of numerical refraction schemes to the study of wave-induced circulation over arbitrary bottoms (Ebersole and Dalrymple(1980), Wu(1983)). However, it has long been known that breaking waves, especially of the plunging type, do not follow so simple a rule. Extensive model tests of normally incident wave trains breaking on laboratory beaches have shown that the pattern of wave height decay across the surfzone is strongly a function of the beach slope. Representative measurements of Horikawa and Kuo (1966) are shown for example in Figure 6.7.

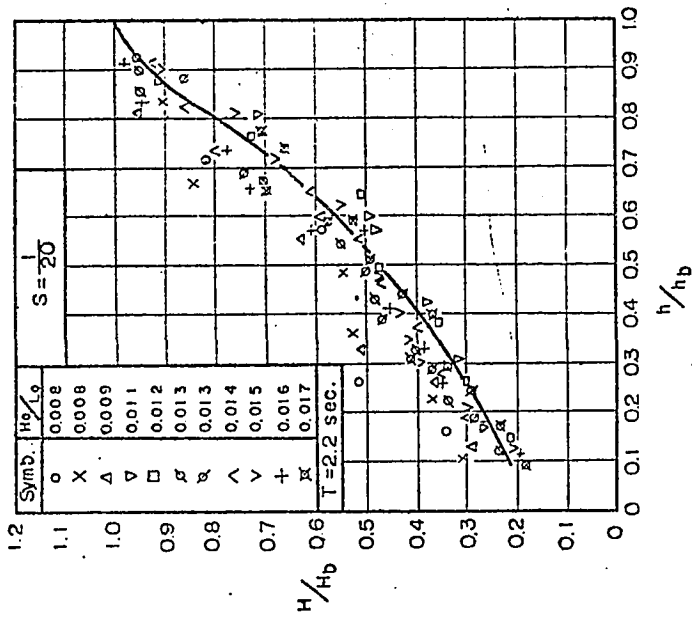
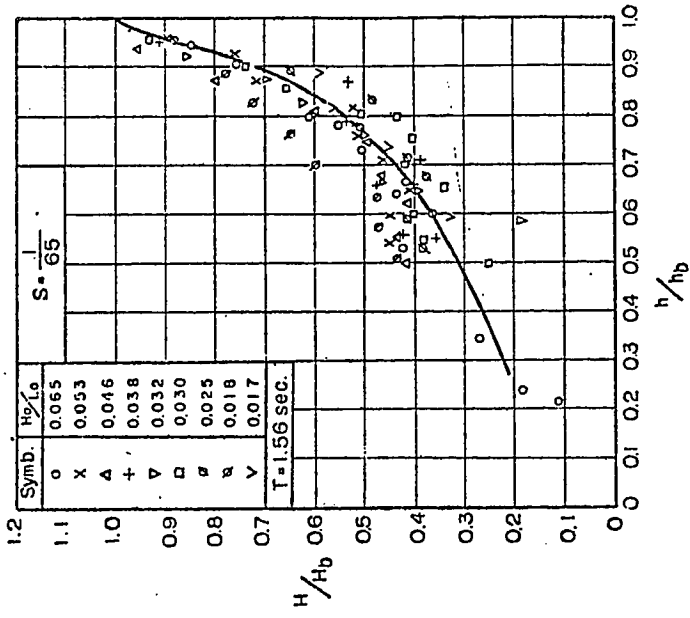


Figure 6.7 Measured waveheights in a laboratory surfzone (from Horikawa and Kuo, 1966)

The purpose of the present section is to relate an empirical model of surfzone wave energy decay to the coefficient w of the wave model, and to detail the application of the model to the prediction of wave height in the surfzone. The empirical model is taken from the work of Dally(1980).

Dally proposed that the decay of energy flux with distance in the surfzone be given by the relation

$$(EC_g)_x = -\frac{K}{h} (EC_g - (EC_g)_s) \quad (6.4.1)$$

where h is the local water depth and K is a constant to be determined, and is related to the rate of energy decay. The quantity $(EC_g)_s$ is a "stable" energy flux for a broken wave in water of depth h . The stable energy flux may be related to the height obtained by a wave propagating over a flat bottom after the cessation of breaking. Data obtained by Horikawa and Kuo (1966) suggest that waves typically reach a height of $0.4h$ at the cessation of breaking on a flat bottom, while an asymptotic value of $0.5h$ is approached for waves breaking on a plane slope. In the following derivation, we denote $(H/h)_s = \zeta$, where ζ is a free parameter.

Equation (6.4.1) may be related to the wave energy equation (E.11) after neglecting currents and assuming a time-steady wave field. For one-dimension, (E.11) becomes

$$(E C_g)_x = -wE \quad (6.4.2)$$

Noting that $C_{gs} = C_g$, w may be written as

$$w = \frac{KC_g}{h} \left(1 - \frac{E_s}{E}\right) = \frac{KC_g}{h} \left(1 - \frac{(H_s)^2}{H^2}\right) \quad (6.4.3)$$

where H is the local wave height, given by $H=2|A|$. Since H , and hence w , is not known at the location of the forward step in the implicit schemes of section 6.2, an iterative scheme must be employed to obtain an estimate of w at the forward position before the final application of the Crank-Nicolson scheme.

For a plane slope and neglecting the effect of setup (which is not calculated in the wave model), a simple analytic solution of (6.4.1) may be obtained and used for comparison with the numerical model. Letting $\mathcal{F} = EC_g$ denote the energy flux and writing $h(x)$ as $h=-s(x-x_0)$, where x_0 is the position of the shoreline, (6.4.1) may be written as

$$-\frac{\partial \bar{\zeta}}{\partial h} + \alpha \frac{\bar{\zeta}}{h} = \frac{\alpha}{h} (EC_g)_s \quad (6.4.4)$$

where $\alpha = K/s$. Assuming shallow water conditions, $(EC_g)_s$ may be written as

$$(EC_g)_s = \frac{1}{8} g^{3/2} \gamma^2 h^{5/2} \quad (6.4.5)$$

Equation (6.4.4) then has the general solution

$$\bar{\zeta} = c h^\alpha + \frac{\alpha}{\alpha - 5/2} \beta \gamma^2 h^{5/2} \quad (6.4.6)$$

where $\beta = g^{3/2}/8$. A special solution is needed for $\alpha = 5/2$. The value of c may then be determined by the value of $\bar{\zeta}_b$ at the breaker line, where

$$h = h_b ; H = H_b = K h_b ; X = X_b$$

and K is the ratio of breaking wave height to still water depth at the breaker line. $\bar{\zeta}_b$ is given by

$$\bar{\zeta}_b = \beta K^2 h_b^{5/2}$$

which leads to

$$C = \beta H^2 \left[1 - \left(\frac{\alpha}{\alpha - 5/2} \right) \left(\frac{\gamma}{H} \right)^2 \right] h_b^{(5/2 - \alpha)} \quad (6.4.7)$$

After rewriting \tilde{c} as $\tilde{c} = \beta H^2 h_b^{5/2 - \alpha}$, (6.4.6) may be rewritten in dimensionless form as

$$\left(\frac{H}{H_b} \right)^2 = \left(\frac{h}{h_b} \right)^2 \left[(1 - \Delta) \left(\frac{h}{h_b} \right)^{\alpha - 5/2} + \Delta \right]; \quad \alpha \neq \frac{5}{2} \quad (6.4.8)$$

where

$$\Delta = \left(\frac{\alpha}{\alpha - 5/2} \right) \left(\frac{\gamma}{H} \right)^2 \quad (6.4.9)$$

For the case $\alpha = 5/2$, the method of variation of parameters and application of the boundary condition at the breaker line yields the result

$$\left(\frac{H}{H_b} \right)^{5/2} = \left(\frac{h}{h_b} \right)^{5/2} \left[1 - \frac{5}{2} \left(\frac{\gamma}{H} \right)^2 \ln \left(\frac{h}{h_b} \right) \right]; \quad \alpha = \frac{5}{2} \quad (6.4.10)$$

Based on a comparison of the laboratory data of Horikawa and Kuo (1966), Dally chose the value $K=0.17$. The special case $\alpha = 5/2$ then corresponds to a beach slope $s=0.068$. Results for a range of α values of $1 < \alpha < 10$, corresponding to the range of beach slopes $0.17 > s > 0.017$, are given in Figure 6.8 for $\gamma = 0.4$, $\beta = 0.78$. The lines

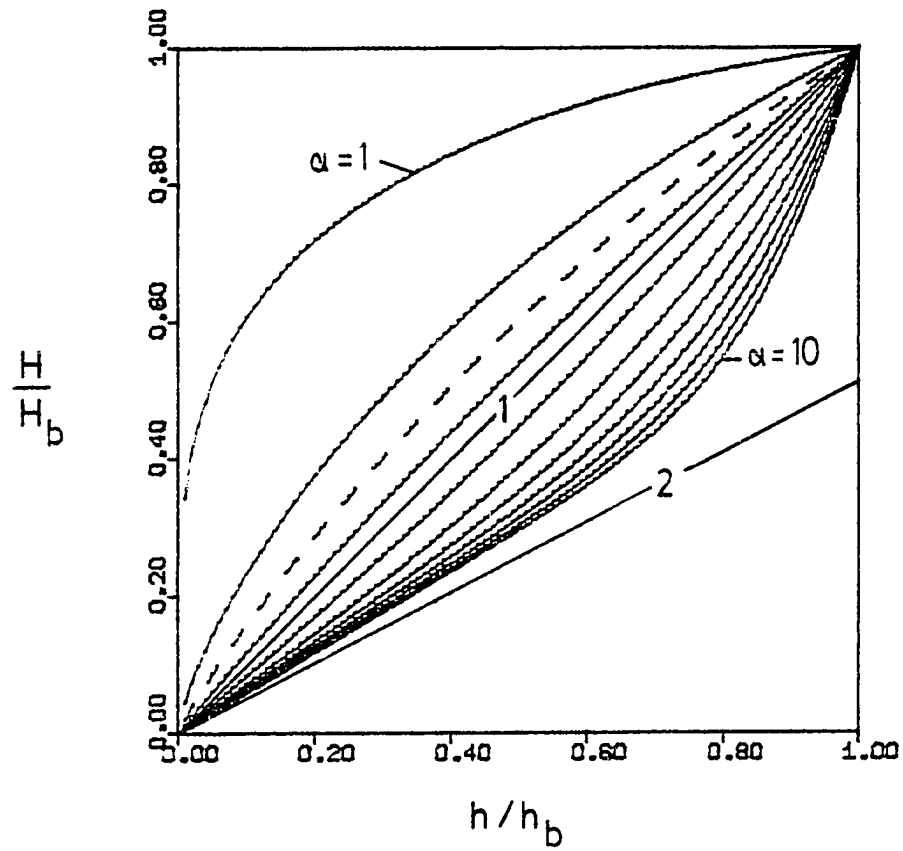


Figure 6.8 Surfzone model, plane beach.
 — $\alpha = 1, \dots, 10$; --- $\alpha = 5/2$.
 1. Constant height/depth; $H = \kappa h$
 2. $H = \gamma h$

labelled 1 and 2 correspond to the constant decay $H = \bar{h} = 0.78h$ and to the stable wave height $H_s = \gamma h = 0.4h$, respectively.

The results (6.4.8-10) provide a check for determining the accuracy of iterative schemes using the wave damping term (6.4.3). Noting that $H_s = \gamma h$ and $H = 2|A|$, (6.4.3) may be rewritten as

$$W = \frac{K C_g}{h} \left[1 - \frac{\gamma^2 h^2}{4|A|^2} \right] \quad (6.4.11)$$

We use the linearized form of the parabolic equation (4.4.4), which can be written as

$$A_x - i(k - k_0)A + \frac{1}{2C_g} C_{gx} A + \omega A = 0 \quad (6.4.12)$$

where

$$\omega = \frac{W}{2C_g} = \frac{K}{2h} \left[1 - \frac{\gamma^2 h^2}{4|A|^2} \right] \quad (6.4.13)$$

(6.4.12) is written in finite difference form as

$$\begin{aligned} & \frac{A^{i+1} - A^i}{\Delta x} - \frac{i}{2} \left[(k^{i+1} - k_0) A^{i+1} + (k^i - k_0) A^i \right] + \\ & + \frac{(C_g^{i+1} - C_g^i)}{4\Delta x} \left[\frac{A^{i+1}}{C_g^{i+1}} + \frac{A^i}{C_g^i} \right] + \frac{1}{2} (\omega^{i+1} A^{i+1} + \omega^i A^i) = 0 \end{aligned} \quad (6.4.14)$$

where

$$\omega^{i+1} = \frac{K}{2h^{i+1}} \left[1 - \frac{\gamma^2 (h^{i+1})^2}{4 |\tilde{A}^{i+1}|^2} \right] \quad (6.4.15)$$

The intermediate value \tilde{A}^{i+1} is determined by a similar step

$$\begin{aligned} \frac{\tilde{A}^{i+1} - A^i}{\Delta x} - \frac{\mu}{2} [(k^{i+1} - k_0) \tilde{A}^{i+1} + (k^i - k_0) A^i] \\ + \frac{(C_g^{i+1} - C_g^i)}{4 \Delta x} \left[\frac{\tilde{A}^{i+1}}{C_g^{i+1}} + \frac{\tilde{A}^i}{C_g^i} \right] + \frac{1}{2} [\tilde{\omega}^{i+1} \tilde{A}^{i+1} + \omega^i A^i] = 0 \end{aligned} \quad (6.4.16)$$

where

$$\tilde{\omega}^{i+1} = \frac{K}{2h^{i+1}} \left[1 - \frac{\gamma^2 (h^{i+1})^2}{4 |A^i|^2} \right] \quad (6.4.17)$$

Several cases were run for waves starting in a depth of 2m and propagating towards shore over a plane slope. The program checks at each step that the wave height has not exceeded the breaking criterion. When H becomes greater than γh , the program begins calculating values of the damping coefficient (6.4.15). Breaking continues until ω^i falls to a value of zero, which does not occur on the plane

beaches studied here but would be expected to occur readily for waves propagating over uneven topography. For each case, the wave height was assumed to be 1.0m at a depth of 2m, and wave period was assumed to be 5 seconds. Values of $\alpha = 1, 3, \text{ and } 10$ were tested using various computational grid spaces Δx . Results for $\alpha = 1$ and $\Delta x = 0.2\text{m}$ and 1.0m are shown in Figure 6.9, $\alpha = 3$ and $\Delta x = 1.0, 2.0, \text{ and } 5.0\text{m}$ in Figure 6.10, and $\alpha = 10$ and $\Delta x = 2.0, 5.0, \text{ and } 10.0\text{m}$ in Figure 6.11. The exact solution (6.4.8) is included in each figure for comparison, with h_b being taken as being the average of the depth at the last grid point before breaking and at the first grid point after breaking. In each case, the numerical results provide an adequate representation of the exact solution. In Figure 6.12, the entire process of shoaling from $h = 2\text{m}$ up to the break point and the subsequent decay in the surfzone is shown for the case $\alpha = 10$ and $\Delta x = 5\text{m}$, with the solution (6.4.8) included for comparison.

The breaking wave model has been incorporated into each of the numerical schemes discussed in section 6.2 by adapting it to the explicit-implicit iteration scheme, and is used in the remainder of the examples in Chapter 6 where applicable.

The model described in this section is empirical in

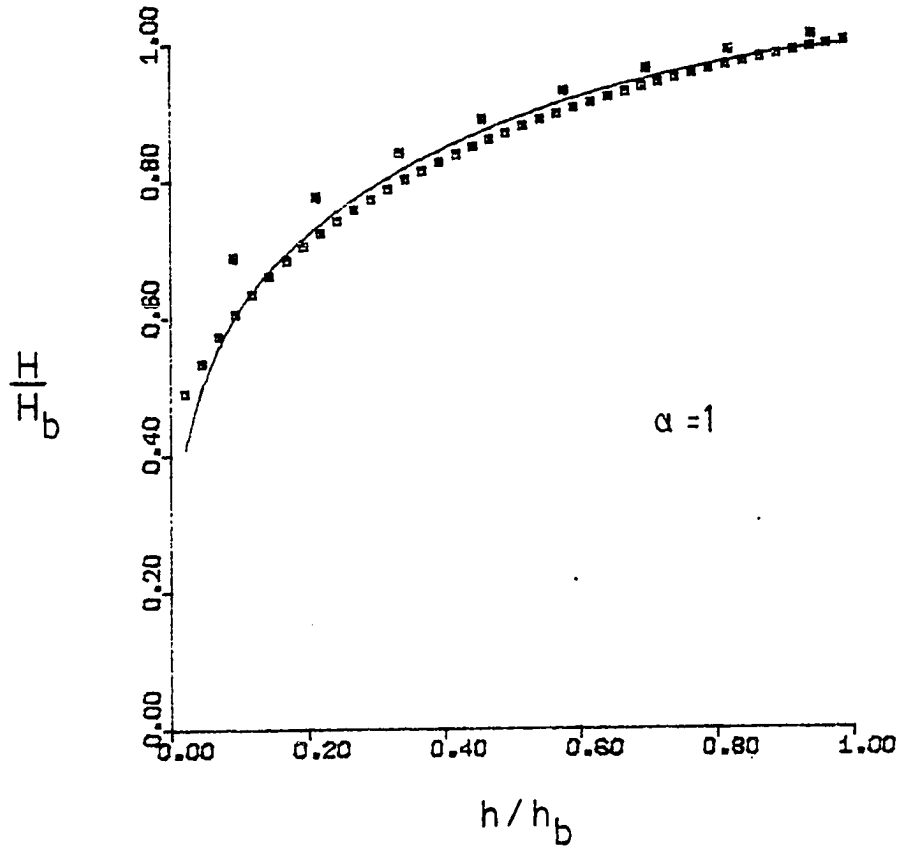


Figure 6.9 Waveheight decay in surfzone; $\alpha = 1$,
 $s = 0.17$
 — Equation (6.4.8)
 $\square \Delta x = 0.2\text{m}$
 $* \Delta x = 1.0\text{m}$

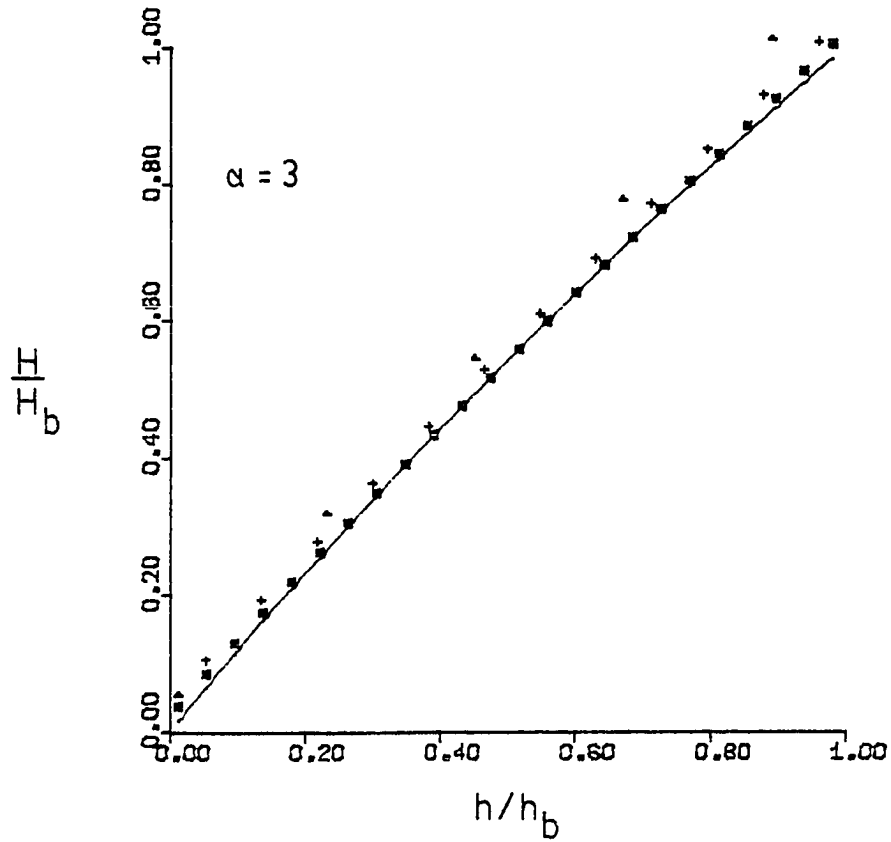


Figure 6.10 Waveheight decay in surfzone; $\alpha = 3$,
 $s = 0.0566$
 — Equation (6.4.8)
 * $\Delta x = 1.0\text{m}$
 + $\Delta x = 2.0\text{m}$
 Δ $\Delta x = 5.0\text{m}$

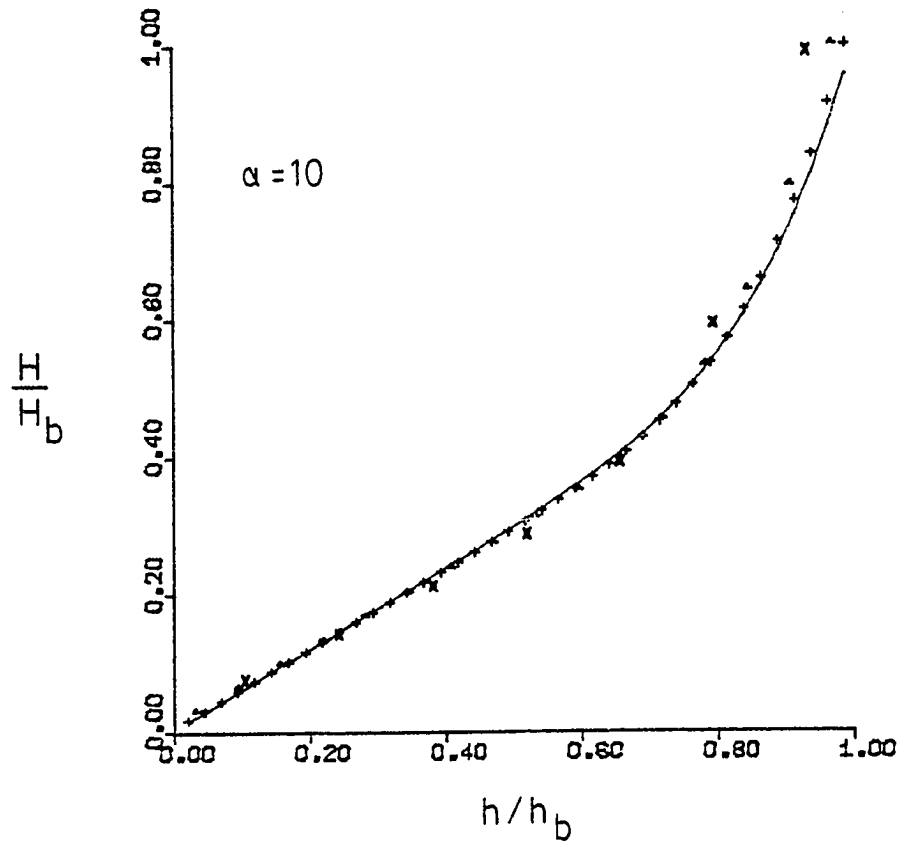


Figure 6.11 Waveheight decay in surfzone; $\alpha = 10$,
 $s = 0.017$
 — Equation (6.4.8)
 + $\Delta x = 2.0m$
 $\triangle \Delta x = 5.0m$
 $\times \Delta x = 10.0m$

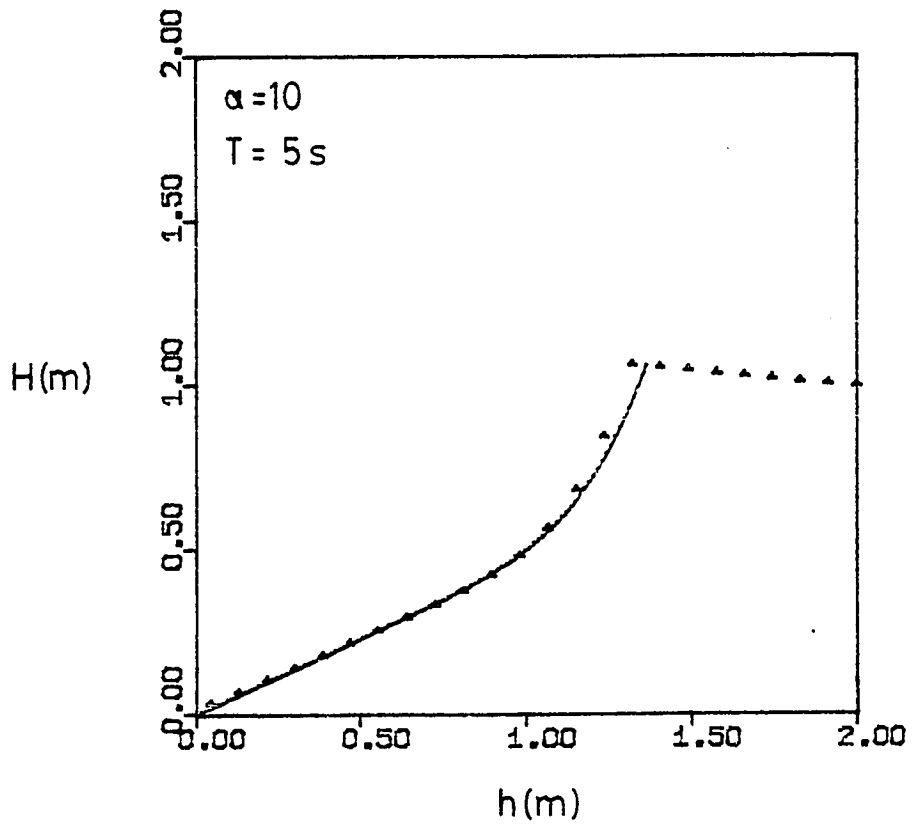


Figure 6.12 Shoaling and wave breaking.
 $T = 5$ s, $s = 0.017$, $H(h = 2\text{m}) = 1.0\text{m}$,
 $\Delta x = 5.0\text{m}$

nature and is based on a two-parameter best fit to existing laboratory data. An alternate procedure based on estimating the rate of energy decay in a turbulent bore has been suggested by Divoky, LeMehaute and Lin(1970) and has been revised to include the case of periodic waves by Battjes(1978). While these methods attempt a more thorough approach to the physics underlying the breaking process, they do not differ with the model described here in terms of results. Indeed, Divoky, LeMehaute and Lin based their conclusions on the relative validity of their model on comparison with the same set of laboratory data used to calibrate the present model.

6.5. Combined Refraction and Diffraction of Waves by a Submerged Shoal

The numerical approximations developed in sections 6.2-6.4 lead to a parabolic equation method which may be used to model wave propagation towards an open coastline up to and including the surfzone. Various sets of experimental data exist which may be used to test the predictions of the nonlinear model. Recently, Berkhoff, Booy and Radder (1982) have presented data obtained in the vicinity of a focus and cusped caustic created by an elliptic shoal resting on a plane slope, and have compared the data to the predictions of three linear wave models: a refraction scheme involving averaging over bundles of adjacent rays (Bouws and Battjes, 1982), a parabolic equation model for the scattered incident wave, and an elliptic model for the entire wave field. While the results of each computational model differ in particulars, an important conclusion may be drawn with respect to comparison between linear wave models and the data set. Linear models uniformly tend to overpredict maximum wave amplitudes in the vicinity of focussed waves, where wave steepness may become large and nonlinear effects become important. This tendency is clear in the comparison between Berkhoff, Booy and Radder's parabolic model results and data. The conclusion to be drawn from a comparison of

data and their elliptic model is less clear. The elliptic model tends to predict lower amplitudes in the region of focussed waves than the parabolic model; however, the model results are significantly contaminated with waves reflected from the downwave boundary, as evidenced by the rapid oscillations in amplitude along x-direction transects 6-8 in their results. The effect of these reflected components on the structure and development of the the focus is unknown, and it is unclear that the predictions of the elliptic model are any better than those of the parabolic model in comparison to the experimental data.

The intent of the present section is two-fold. First, we wish to verify that a parabolic equation for weakly-nonlinear wave motion is capable of predicting accurate results for waves in the vicinity of a cusped caustic, by comparing the model predictions to data. Secondly, by contrasting the difference in predictions of linear and nonlinear models, we wish to show that the difference between previous linear model results and data is largely due to the neglect of nonlinearity rather than to any inherent inaccuracy in the modelling techniques. We will concentrate on the data set of Berkhoff, Booy and Radder in performing this comparison. This data set is well suited to the present purpose due to the great detail in

which data on wave amplitude was obtained over the entire vicinity of a refractive focus, where diffractive and nonlinear effects become significant. We will use the "Radder" approximation (4.4.4) in its numerical form (6.2.9,10) in this section. Computation is halted before the breaker line is reached; consequently we neglect the effect of dissipation due to breaking.

Experimental topography and computational domain

Details of the experimental procedure and setup may be obtained from Berkhoff(1982) or Berkhoff, Booy and Radder(1982), which include a photograph of the experimental wave field and a plot of wave rays in the refraction approximation; we summarize the important points here. The experimental topography consists of an elliptic shoal resting on a plane sloping bottom with a slope of 1:50. The plane slope rises from a region of constant depth $h=0.45\text{m}$, and the entire slope is turned at an angle of 20° to a straight wave paddle.

The bottom contours and chosen computational domain are shown in Figure 6.13, where the computational domain is represented by the dashed line bounding the contours. Experimental data is given for the sections labelled 1-8.

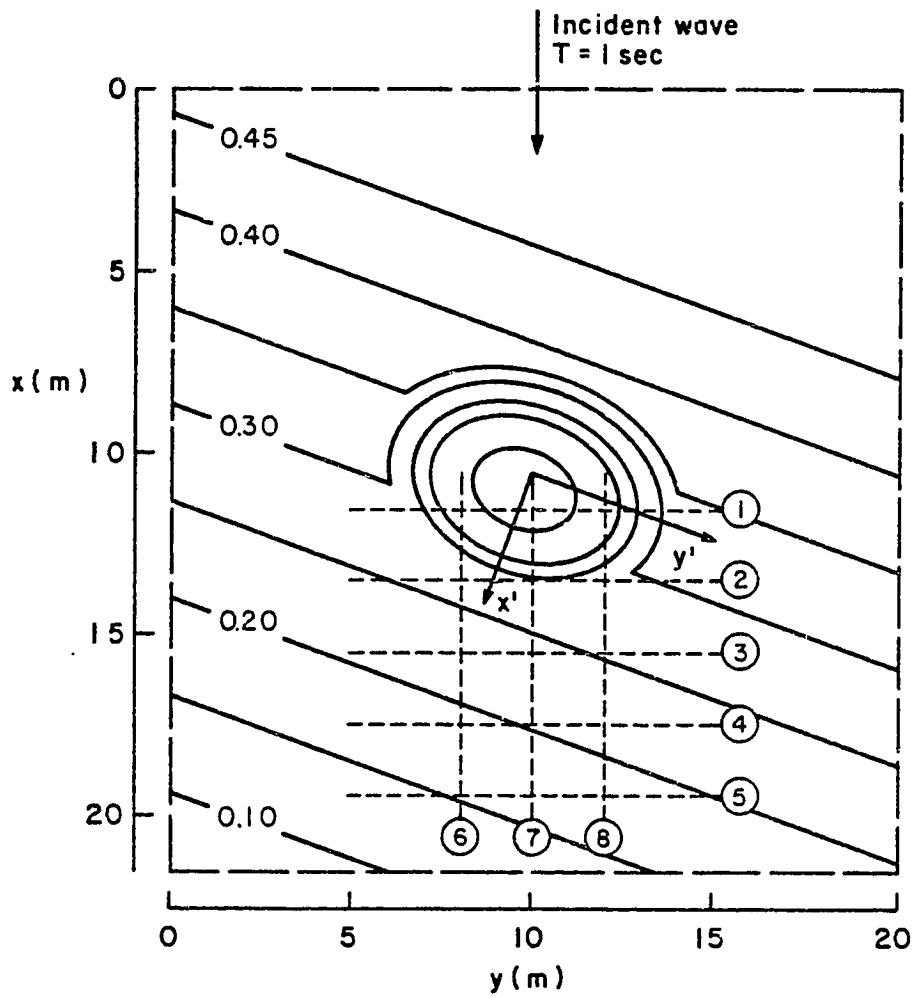


Figure 6.13 Bottom contours and computational domain for experiment of Berkhoff, Booy and Radder (1982). Experimental data given on transects 1 - 8.

Computational coordinates are established with the origin at the upper left corner of the domain, which is then given by

$$0 \leq x \leq 21.5 \text{ m} \quad ; \quad 0 \leq y \leq 20.0 \text{ m} \quad (6.5.1)$$

The offshore boundary of the domain is chosen so that water depth is constant along $x=0$. The initial condition for the wave then corresponds to the uniform wave train generated at the wave paddle; we set

$$A(x=0, y) = A_0 \quad (6.5.2)$$

where $A_0=0.0232\text{m}$ is the amplitude of the incident wave. The wave period $T=1$ sec. Slope-oriented coordinates $\{x',y'\}$ are established which are related to the computational coordinates $\{x,y\}$ according to

$$x' = (x - 10.5) \cos 20^\circ - (y - 10) \sin 20^\circ \quad (6.5.3a)$$

$$y' = (x - 10.5) \sin 20^\circ + (y - 10) \cos 20^\circ \quad (6.5.3b)$$

The origin $\{x',y'\} = \{0,0\}$ corresponds to the center of the shoal. The slope is described by

$$h = \begin{cases} 0.45 \text{ m} & ; \quad x' \leq -5.82 \text{ m} \quad (6.5.4a) \\ 0.45 \text{ m} - 0.02 (5.82 + x') \text{ m} & ; \quad x' \geq -5.82 \text{ m} \quad (6.5.4b) \end{cases}$$

The boundary of the elliptic shoal is given by

$$\left(\frac{x'}{3}\right)^2 + \left(\frac{y'}{4}\right)^2 = 1 \quad (6.5.5)$$

and the depth in the shoal region is modified according to

$$h = h_{\text{slope}} - \left\{ 0.5 \left(1 - \left(\frac{x'}{3.75} \right)^2 - \left(\frac{y'}{5} \right)^2 \right)^{1/2} - 0.3 \right\} \quad (6.5.6)$$

resulting in a depth $h(x', y'=0) = 0.1332\text{m}$.

The lateral boundaries at $y=0, 20\text{m}$ are open, and transmitting conditions are specified according to (6.3.5), where we have assumed that $|A_1|$ varies slowly in the y direction at the boundaries. The wavenumber component m at each grid row is evaluated numerically according to (6.3.9).

Comparison of Computational Results and Experimental Measurements

The nonlinear equation is valid under the same conditions as the Stokes' theory, with the principle

condition being given by

$$U_r = \left\{ \frac{|A|}{h} \right\} / (kh)^2 < O(1) \quad (6.5.7)$$

where U_r is the Ursell number. For conditions where U_r approaches $O(1)$, wave models based on the Boussinesq equations, such as that of Abbott, Petersen and Skovgaard(1978) become more appropriate. Also, the derivation of (4.4.4) technically requires that $\sqrt{h}/(k|A|)$ be $O(\epsilon)$, although this has not been found to be a necessary restriction in applications of the linear model.

Laboratory experiments designed to test the predictions of linear wave models typically satisfy the condition of small U_r in the vicinity of the wavemaker. However, as waves propagate into shallower water and are focused by bottom irregularities, U_r may increase rapidly, and care must be taken in verifying that Stokes' wave theory is valid for the problem being considered.

Preliminary studies of the relevant parameters in the wave field were performed by determining U_r at several locations in the experimental wave field. Values of U_r at the wavemaker, shoal crest, and point of maximum amplitude in the focused region are given by $U_r = .014, .290,$ and

.213, respectively. Stokes' theory should thus be valid throughout the region of principle interest.

Data from the laboratory experiment of Berkhoff, Booy and Radder (1982) is available for the labelled sections 1-8 indicated in Figure 6.13. The computational domain was discretized into square grids ($\Delta x = \Delta y =$ grid spacing), and the grid scheme was established so that grid rows coincided with the measurement transects. Grid size was decreased until the point was reached where further reduction did not affect model predictions significantly. The final numerical calculations were performed using a spacing of $\Delta x = 0.25\text{m}$, corresponding to a grid of 87×81 rows.

Contours of normalized wave amplitude are shown in relation to the bottom contours for the linear wave field in Figure 6.14 and for the nonlinear wave field in Figure 6.15. The nonlinear results indicate a broadening of the central focused region and a decrease in the maximum amplitude in the focus. The nonlinear contours are in better agreement with the experimental contours shown in Figure 2 of Berkhoff, Booy and Radder(1982).

Results of the nonlinear and linear models are shown

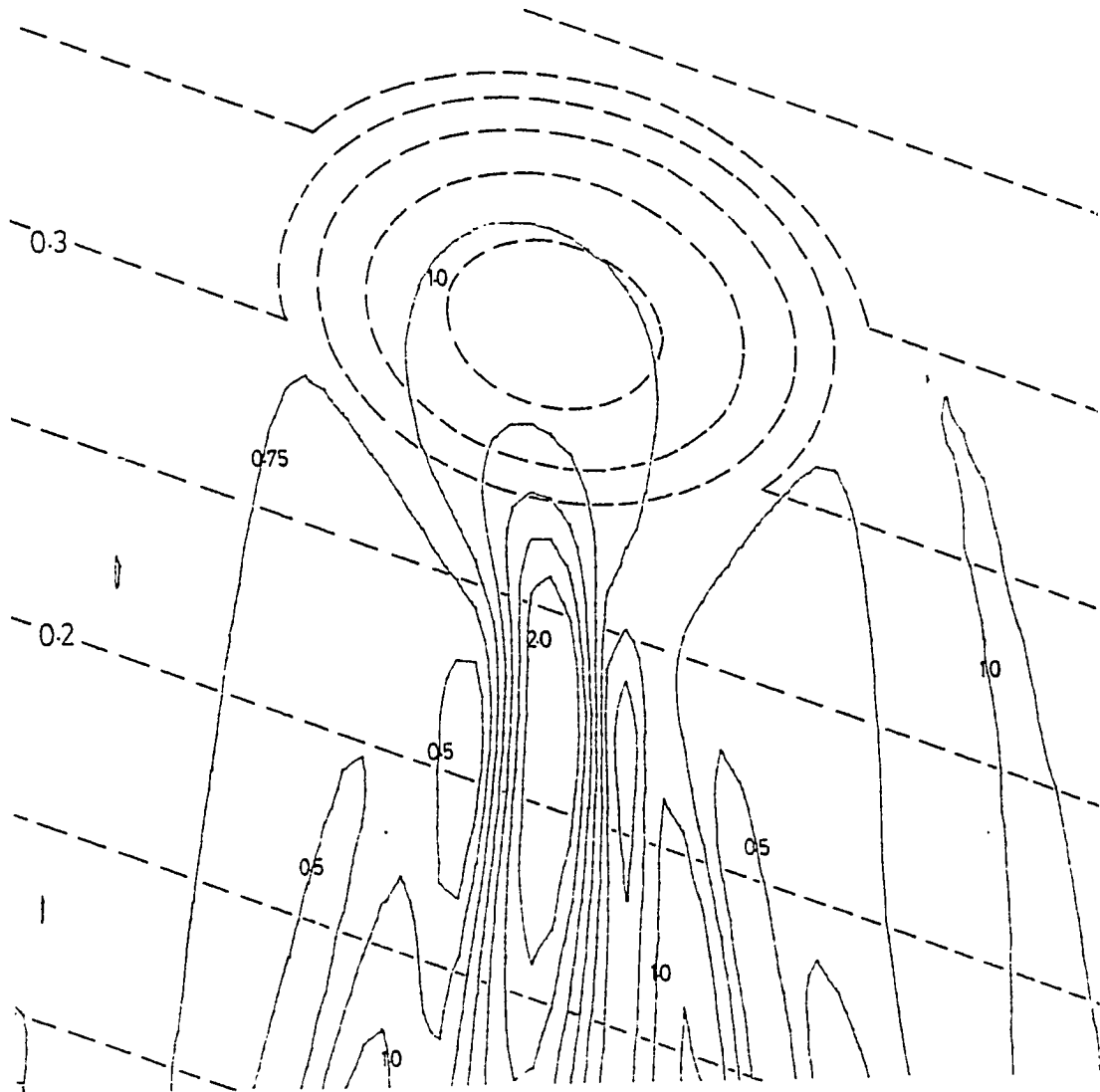


Figure 6.14 Computed amplitude contours $|A/A_0|$ for experiment of Berkhoff, Booy and Radder (1982); linear model results.

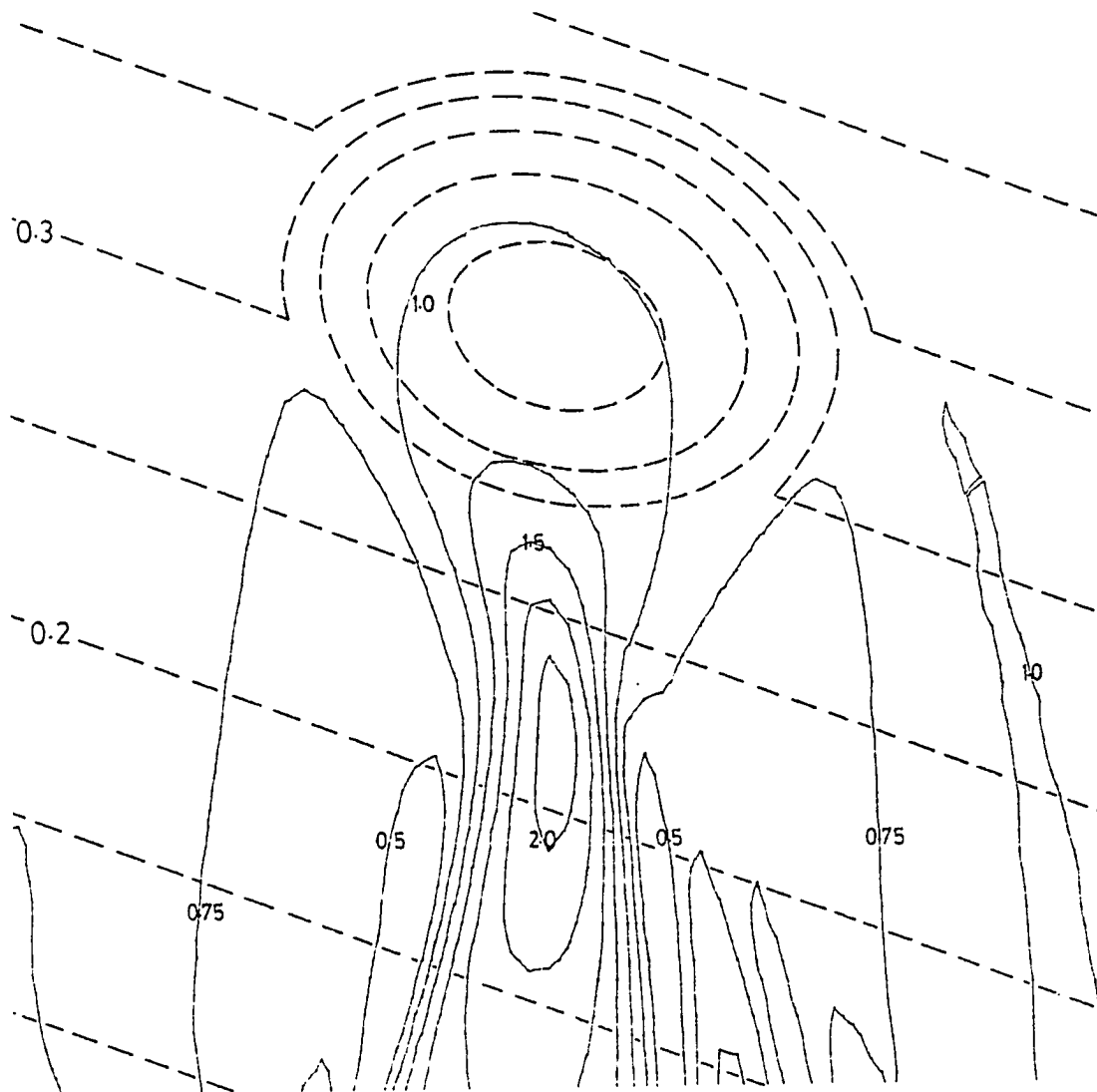


Figure 6.15 Computed amplitude contours $|A/A_0|$ or experiment of Berkhoff, Booy and Radder (1982); nonlinear model results.

in comparison to the experimental data in Figures 6.16 for the labelled sections 1-8 respectively. In each figure, nonlinear results are indicated by solid lines, linear results by dashed lines, and data points by open circles. We first consider the results on each individual section.

On section 1, focussing effects have only begun to be apparent, and only a slight difference exists between the linear and nonlinear models, which both agree well with the data. Sections 2 and 3 describe the region of the development of the cusped caustic. For both sections, data typically falls between the predictions of the two models in the region of maximum amplitude, with the nonlinear model underpredicting the maximum amplitude by about 8% on section 3. However, on sections 4 and 5, where the wave has passed through the cusped caustic, the nonlinear model predictions and the data are in striking agreement, with both the height and width of the central focussed region and the size and shape of side lobes in the diffraction pattern being very well predicted.

Agreement between the nonlinear model and the data is also very good along the longitudinal sections 6-8. On section 7, which is just off center of the axis of the focused region, the nonlinear model predicts both the drop

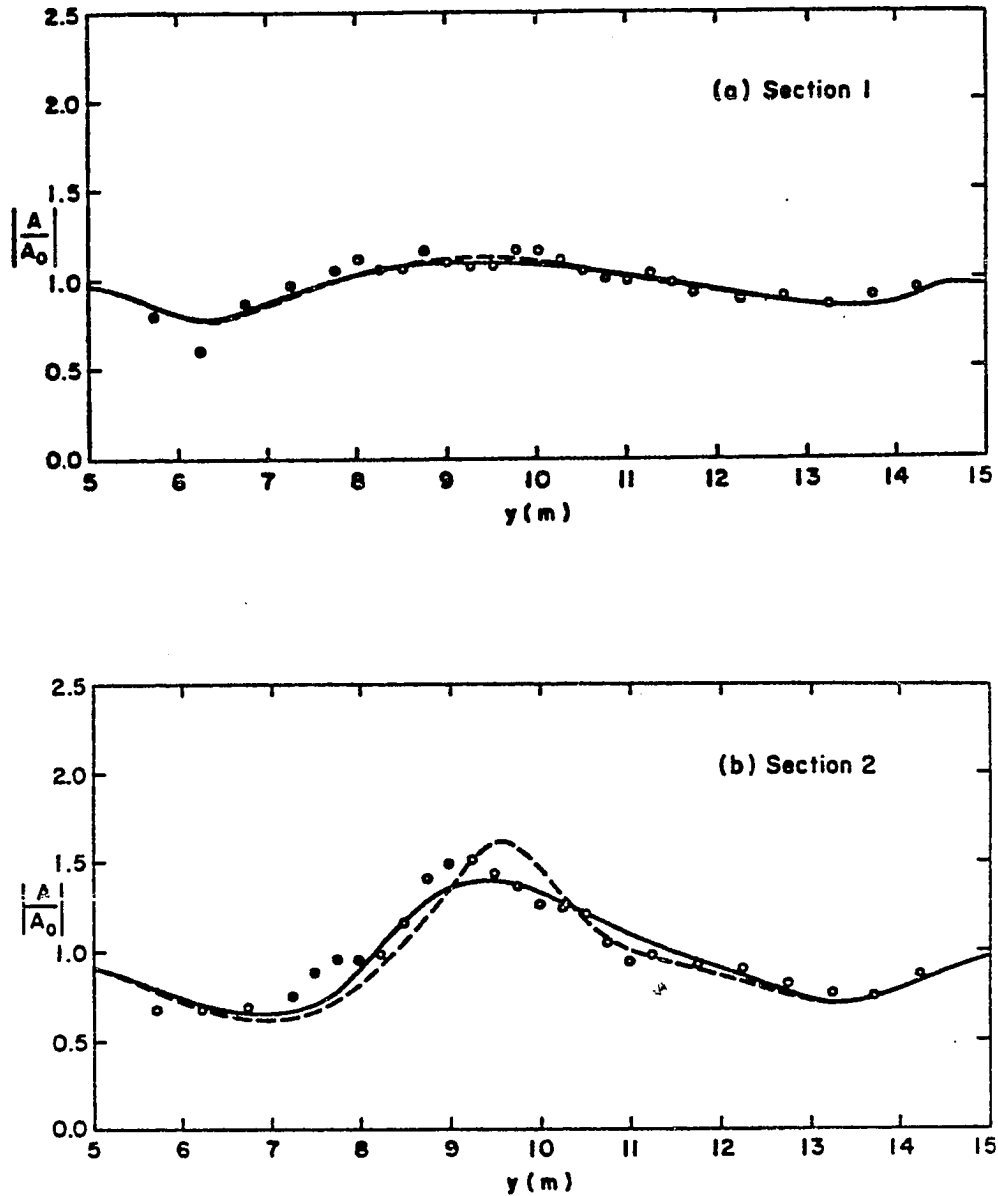


Figure 6.16 Comparison between linear and nonlinear model results and experimental data of Berkhoff, Booy and Radder (1982).
 — nonlinear model (6.2.9), $P_1 = 0$
 --- linear model (6.2.9), $P_1 = 0$
 ○ data

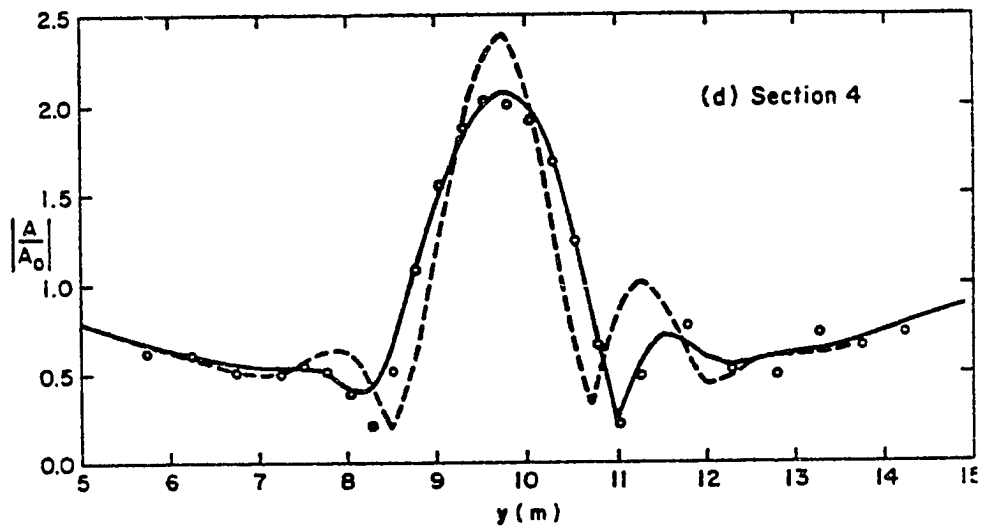
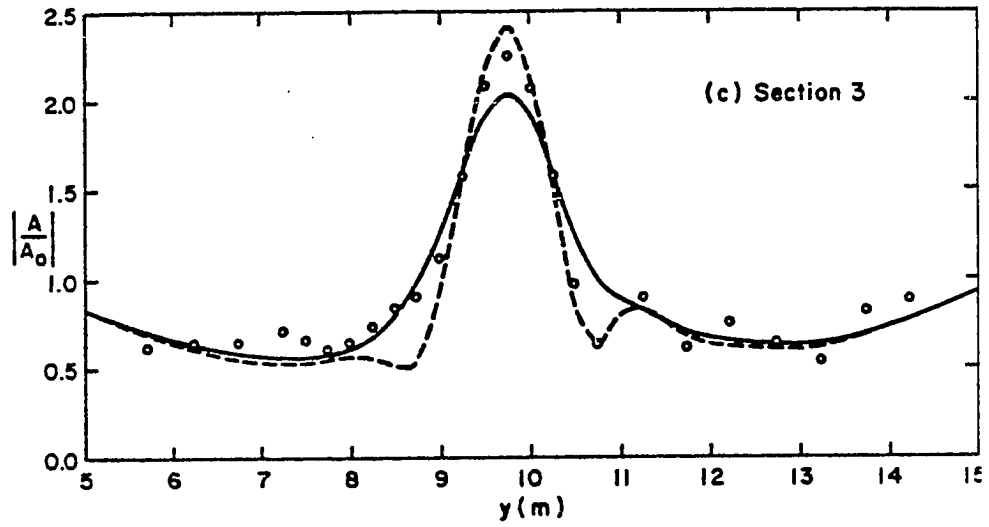


Figure 6.16 continued

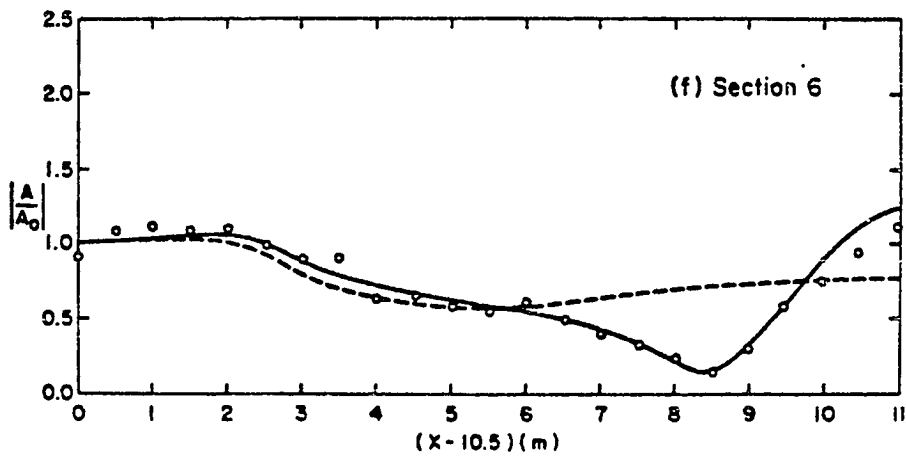
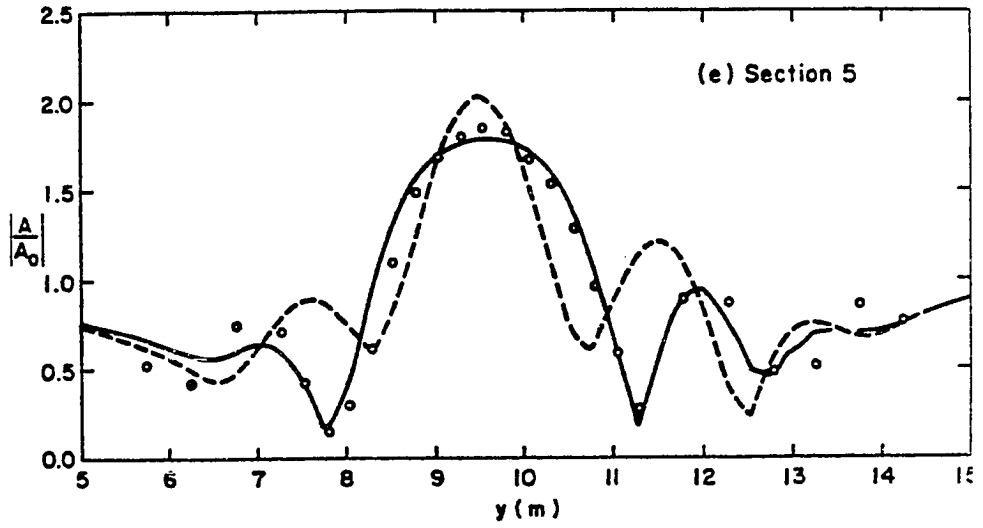


Figure 6.16 Continued

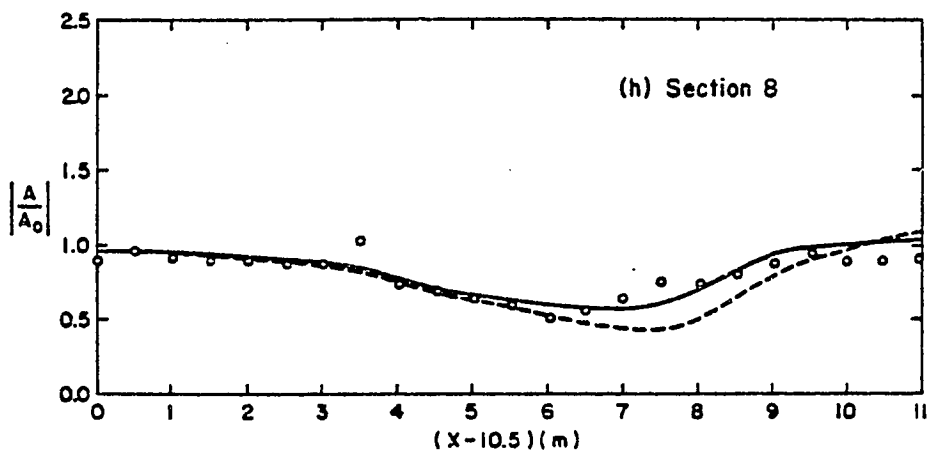
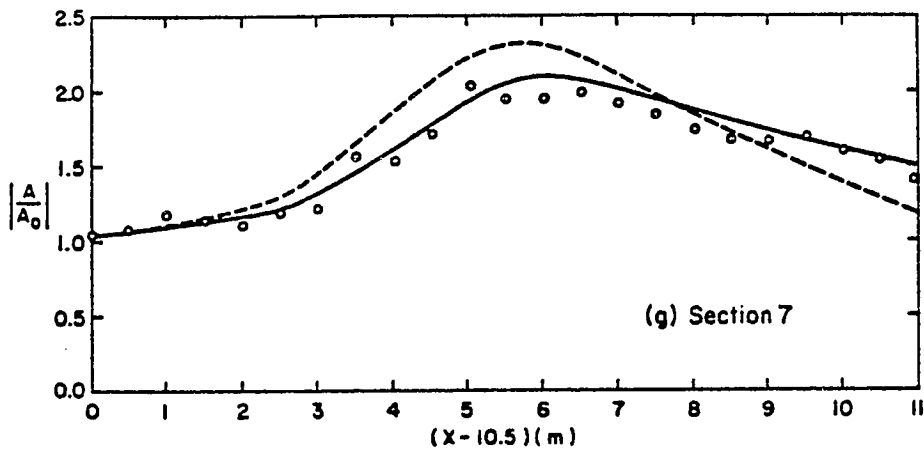


Figure 6.16 continued

in amplitude in the region of the cusp (with respect to linear model predictions) and the slower decay of amplitude towards the shoreward end of the transect (large x). On section 6, the nonlinear model quite accurately predicts a sharp drop in amplitude which is apparent in the data but totally absent in the results of the linear model. Berkhoff, Booy and Radder interpreted the discrepancy between the linear model prediction and the data in this region as being the result of the proximity of an amphidromic point in the wave phase surface and the linear model's inability to resolve this point. Here, we see that the discrepancy is entirely explained in terms of nonlinear effects and the resulting change in the geometry of the focused region.

Differences between the linear and nonlinear results are less striking along section 8; The nonlinear model does reproduce the relatively high amplitudes in the region 6 to 9 meters downwave of the shoal, in comparison to the linear model.

Taken as a whole, it is apparent that the results of the nonlinear model exhibit closer agreement with the experimental data than do the results of the linear model, with the only obvious discrepancy occurring in the region of

initial development of the wave focus. It is possible that the discrepancy in this initial region of growing amplitude, seen in sections 2 and 3, is due in part to a failure of the approximate equations to allow waves to focus rapidly enough to obtain a realistic amplitude. This discrepancy is seen to be short-lived, as evidenced by the remainder of the data set.

6.6. The Wavefield around a Shore-attached Breakwater

As a second test of the parabolic models, we next study the wavefield in the vicinity of the shore attached breakwater described in Figure 6.17. An extensive set of data for the wavefield in the shadow zone downwave of the breakwater has been given by Hales(1980) for a number of wave periods, amplitudes and angles of incidence. A less detailed set of data is available for the reflection zone on the upwave side of the breakwater in Pantazaras(1979). The given experimental arrangement has been investigated using several computational techniques for linear waves, including the finite element method for the elliptic formulation (Houston, 1981) and a parabolic equation method based on curvilinear, ray-fitted coordinates (Tsay and Liu, 1982). A closed form solution in the linear, mild-slope approximation has been provided by Liu, Lozano and Pantazaras(1979) and has been compared to the experimental data by Liu(1982), who found qualitative agreement between the linear theory and experimental results.

As a first test of the parabolic models, we restrict attention to linear wave theory and investigate the difference in predictions between the linearized "Radder" and "Booij" approximations. The computational grid is again

rectilinear, with the x-direction oriented parallel to the breakwater. Thus, waves incident on the grid may be propagating at angles of up to 30° to the x-direction. Two cases presented by Liu(1982) are studied, and results are presented for a y-direction transect 5 ft. shoreward of the breakwater tip. In case (a), the wave period $T=1$ sec. and the incident wave angle $\theta_0=20^\circ$, while for case (b), $T=1.5$ sec. and $\theta_0=30^\circ$. Results obtained using the linearized form of (6.2.9) with $P_i=0$ and $P_i=1/4$ are shown in Figures 6.18 and 6.19, respectively, for cases (a) and (b). The results of Liu, Lozano and Pantazaras(1979) are included for comparison.

Results obtained using the "Radder" approximation ($P_i=0$) indicate an inability to model the diffraction fringe on either the up- or downwave side of the breakwater. This result is particularly apparent in the region adjacent to the shadow boundary, where reflected wave activity is minimal or absent in comparison to the analytic results. Similar results have been obtained by Hasimoto(1982), who used the original model of Radder(1979). In contrast, the "Booij" approximation, with $P_i=1/4$, is seen to give a better indication of the wave field away from the shadow and reflection zone boundaries, and indeed may overestimate the size and number of fringes in comparison to the analytic

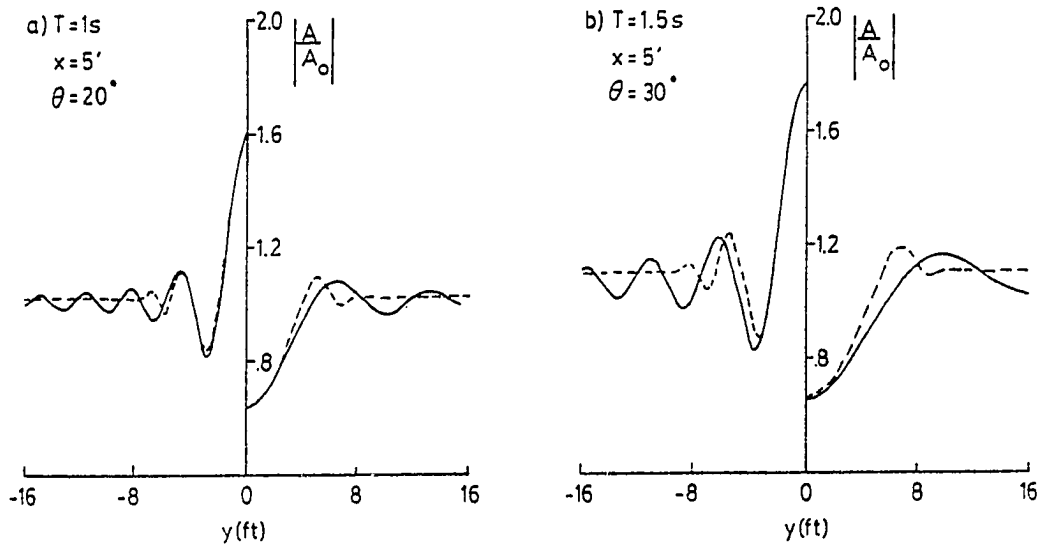


Figure 6.18 Normalized amplitude perpendicular to breakwater
 ---- linear waves, $P_1 = 0$.
 — Liu, Lozano and Pantazaras (1979)

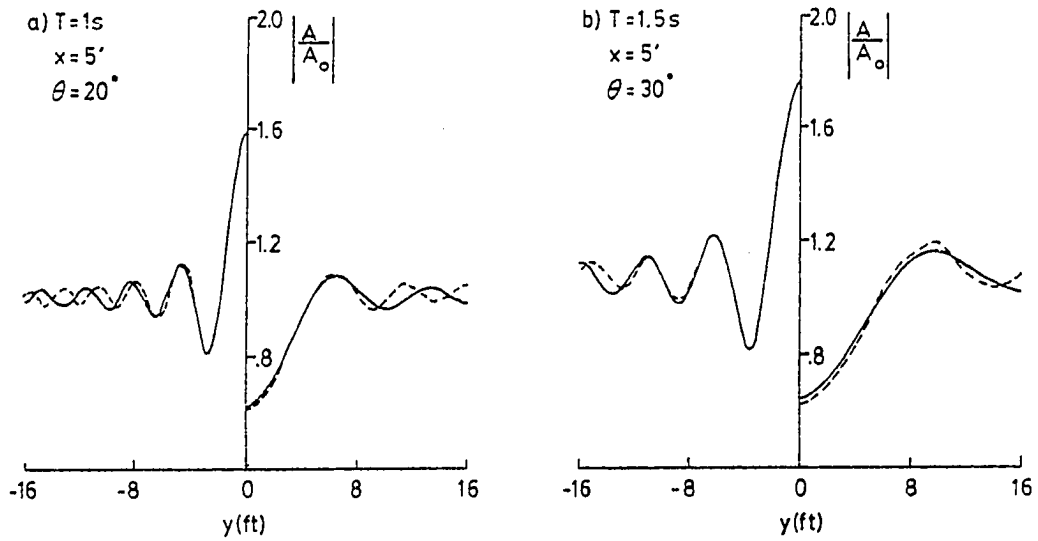


Figure 6.19 Normalized amplitude perpendicular to breakwater
 ---- linear waves, $P_1 = 1/4$.
 — Liu, Lozano and Pantazaras (1979)

results. The overall agreement of results obtained using $P_1 = 1/4$ with the analytic results is favorable in comparison to the results obtained by Tsay and Liu(1982), which tend to underestimate the diffraction fringe effects. (This underestimation may be the result of interaction with lateral boundary conditions rather than limitations of their approximation.) Both models are seen to accurately predict the characteristics of the reflection and shadow zones in the near field of the breakwater with the exception of the shift of the first amplitude maximum towards the breakwater seen in the "Radder" approximation.

The inability of the linearized form of the "Radder" approximation ($P_1 = 0$) to correctly model amplitude modulations at a distance from the obstacle disturbing the wavefield has consequences on the applicability of that model to the study of nearshore waves, where longshore amplitude modulations can be instrumental in establishing cellular circulation patterns in the surfzone and nearshore region (Dalrymple(1975), Liu and Mei(1976)).

The contours of amplitude and the breaker line are given in Figure 6.20 for the conditions of test T8 of Pantazaras(1979), assuming a breaker index of 0.78 and using the "Radder" model. We note that the breaker line would

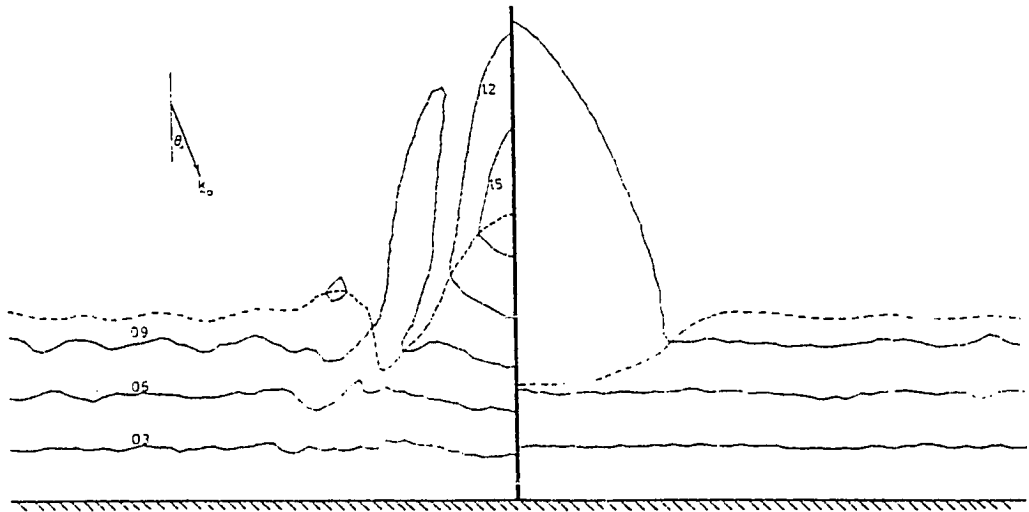


Figure 6.20 Wavefield in vicinity of shore-attached breakwater. Parameters for test T8 of Pantazaras (1979).

$T = 1 \text{ sec.}$, $\theta_0 = 20^\circ$, $A_0 = 0.0320 \text{ m}$

linear model results, $P_1 = 0$.

— amplitude contours relative to A_0

---- position of breaker line based on $H_b/h_b = 0.78$.

undergo more on-offshore displacement with distance upwave from the breakwater in the "Booij" model due to the increased amplitude modulation in the diffraction fringes predicted by that model. However, both models are adequate for predicting wave activity in the immediate vicinity of the breakwater.

We turn now to a consideration of nonlinear effects in the wavefield. In particular, we wish to determine if any Mach-stem effect is present in the reflected wavefield on the upwave side of the breakwater. Nonlinear effects on the downwave, shadow side of the breakwater would be expected to be confined to a slight increase in wave amplitude in the shadow region due to increased diffraction across the shadow boundary; see Yue(1980), section 4.3. We choose conditions corresponding to tests T5-T6 and T8 of Pantazaras(1979) in order to perform a comparison with data. The test conditions are summarized in Table 6.1. The comparison is performed using the "Radder" model ($P_r=0$), and we compare with data only in the immediate vicinity of the breakwater. Tests T5 and T6 represent identical conditions of wave period and angle of incidence and, unfortunately, Pantazaras presented results for these tests in averaged form, since he was only interested in the linear approximation. Here, we will compare each test to the

Test #	θ_o	T (sec)	A_o (m)
T5	30°	1.5	0.0229
T6	30°	1.5	0.0344
T8	20°	1.0	0.0320

Table 6.1 Test conditions for shore-attached breakwater (from Pantazaras (1979))

average of the experimental data. Results for test T8 are shown in Figure 6.21. Along the transect at $x=2.5\text{ft.}$, nonlinear effects are weak and there is no apparent difference between the two solutions. At $x=6\text{ft.}$, there is some evidence of Mach-stem formation in the nonlinear solution, and the amplitude adjacent to the breakwater is reduced by 9% in comparison to the linear solution. The experimental data is somewhat more supportive of the linear solution. For the $x=6\text{ft.}$ transect, the Ursell number for the wave adjacent to the breakwater is $U_r=0.648$.

Results for test T5 are presented in Figure 6.22. Again, there is little effect due to nonlinearity at the $x=2.5\text{ft.}$ transect. At the $x=7.5\text{ft.}$ transect, the tendency towards the formation of a Mach stem is apparent. In this case, the data of Pantazaras(1979) is more supportive of the nonlinear solution. Here, the Ursell number for the nonlinear solution at the breakwater is $U_r=1.99$, and Stokes theory is of questionable validity in this region. However, the large value of U_r and the apparent formation of a Mach-stem indicate the importance of nonlinearity in this region. Waves in this region would be expected to be of cnoidal form; waves of this class also are known to produce Mach stems during reflection at small angles of incidence.

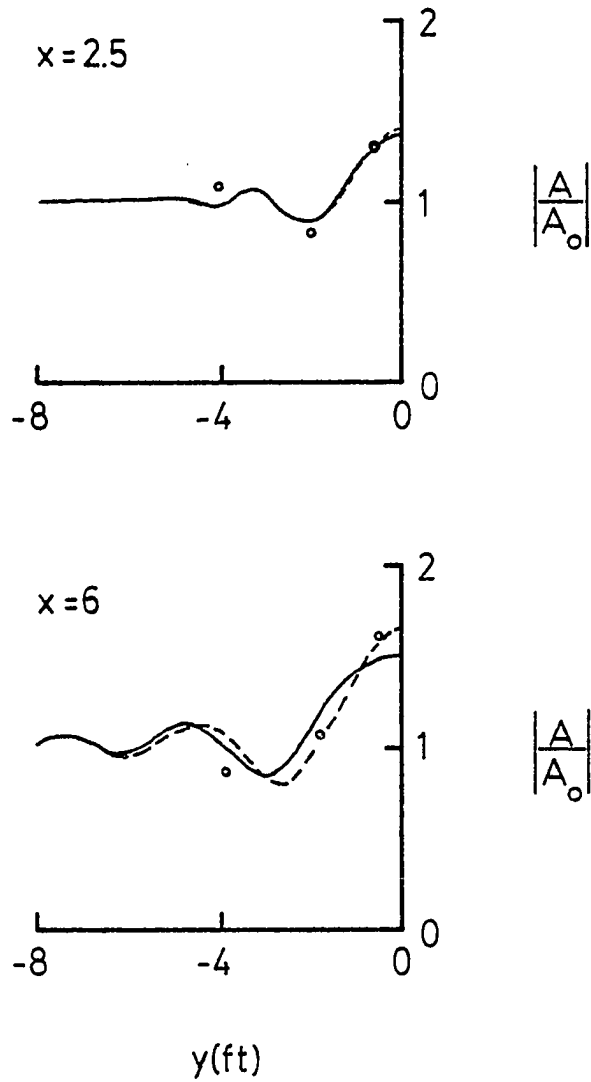


Figure 6.21 Amplitude contours perpendicular to shore-attached breakwater. Test T8; $T = 1$ sec., $\theta = 20^\circ$, $A_0 = 0.0320$ m.
 --- linear; — nonlinear;
 • Pantazaras (1979) data

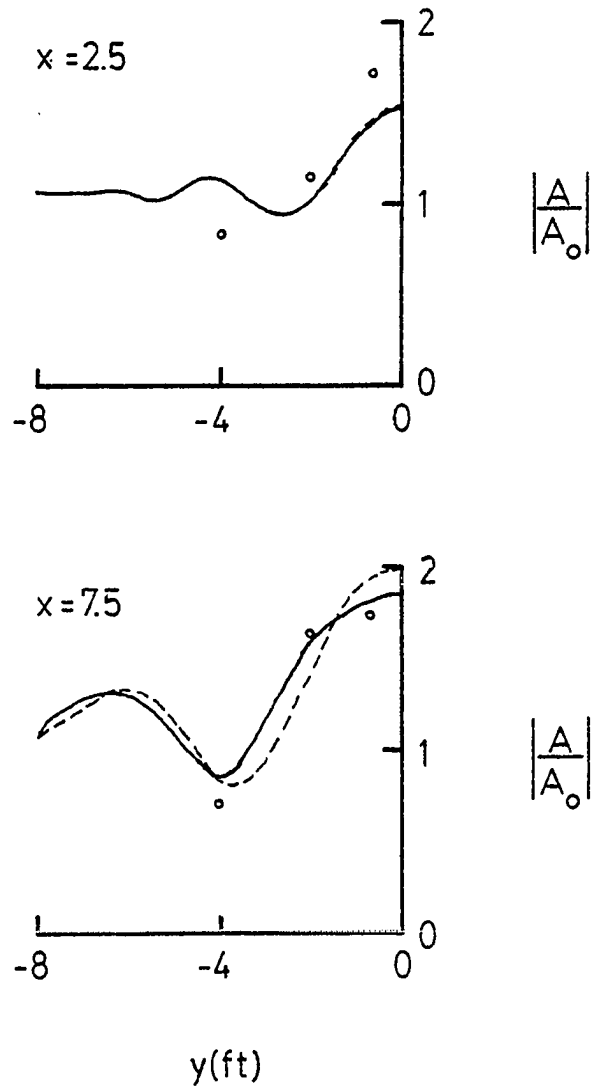


Figure 6.22 Amplitude contours perpendicular to shore-attached breakwater. Test T5; $T = 1.5$ sec., $\theta = 30^\circ$, $A_0 = 0.0229$ m.
 ---- linear; — nonlinear;
 • Pantazaras (1979) data.

For both of the tests T6 and T7, which represent larger amplitude counterparts of tests T5 and T8 respectively, results of the present study indicate that wave breaking occurs before the position of the second transect is reached, based on a breaker index of 0.78. In particular, for test T6, the value of H/h adjacent to the breakwater from the linear solution without breaking is 1.20. Values of H/h this large may occur for waves shoaling on steep beaches. The broken wave amplitude resulting from the present calculations with a breaker index of 0.78 are presented in Figure 6.23. We note that the Ursell number for this wave condition is too large for the validity of Stokes theory.

The present numerical calculations could be refined by incorporating a variable breaking index in the model. Various formulae exist for calculating H_b/h_b based on the local bottom slope and parameters of the wavefield. This body of theory and empirical results has been reviewed recently by Mallard(1978). This extension to the model is clearly warranted as indicated by the discrepancy between position of the breaker line calculated here and estimated from Pantazaras' data.

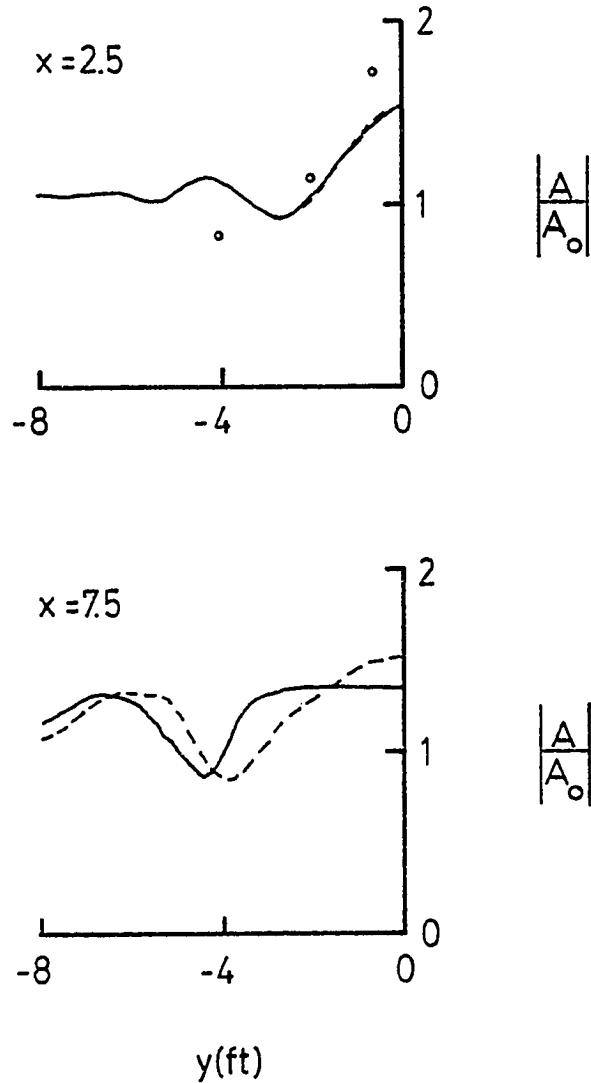


Figure 6.23 Amplitude contours perpendicular to shore-attached breakwater. Test T6; $T = 1.5$ sec., $\theta = 30^\circ$, $A_0 = 0.0344$ m. Values based on breaking index $\kappa = 0.78$.
 — nonlinear; ---- linear
 • Pantazaras (1979) data.

6.7. Reflection from a Caustic: Topographic Case.

As a final example for steady waves in the absence of a current, we study the incidence of a plane wave in constant water depth on a symmetric, wedge-shaped depression, with sides sloping down from the constant depth region. The geometry of the wedge is described in Figure 6.24. The line of symmetry is taken as $y=0$, and the boundary of the depression is given by

$$y_b = x \tan \theta \quad (6.7.1)$$

where θ is the wedge half-angle, and where the tip of the wedge is located at $x=0$. The bottom slopes down with a slope of 1:50 normal to the wedge boundary. The maximum depth of the depression is given by $2h_0$, where h_0 is the depth of the incident wave region. The incident wave is characterised by $k_0 h_0 = 1.0$ in the constant depth region outside the wedge. For the cases considered here, a caustic of the linear wave field occurs on the sloping wedge boundary, and, in the far field (x large), the wave field in the vicinity of the caustic would be described by the Airy function, with an exponentially decaying amplitude in the geometric shadow over the trench and total reflection of the incident wave. The corresponding result for weakly

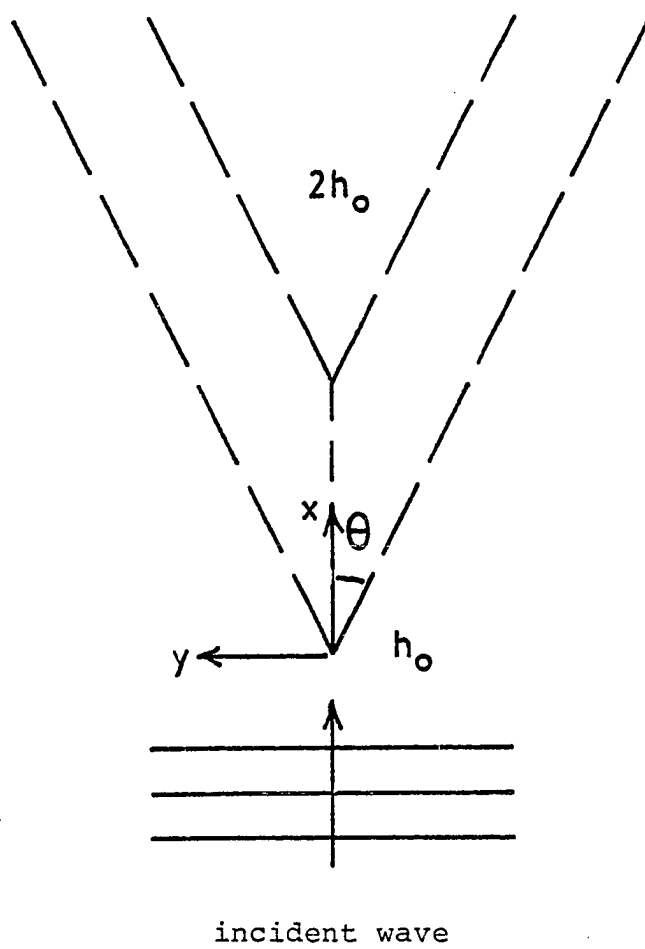
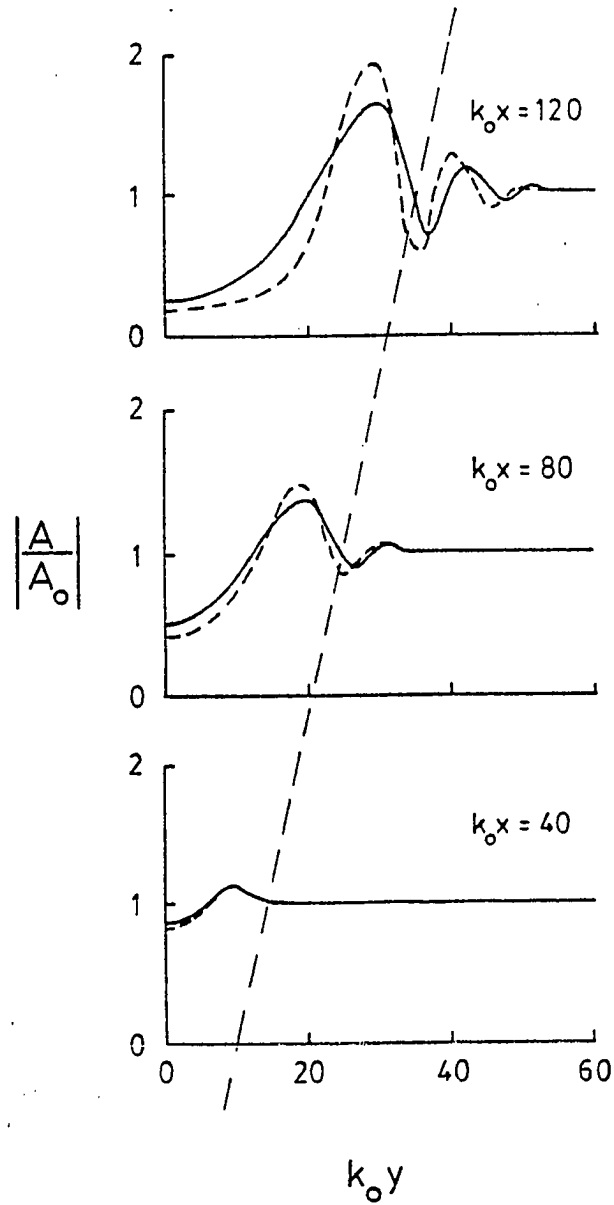


Figure 6.24 Geometry of wedge-shaped depression.

nonlinear waves would be a qualitatively similar description in terms of the second Painleve transcendent (Miles (1978)). However, as in the case of the development of a Mach stem at the leading edge of a reflective wall, the initial value problem for the wave state in the vicinity of the caustic of linear theory may be subject to the development of a wave jump condition, as described by Peregrine (1983), and the asymptotic result in qualitative similarity to the Airy function may not develop.

As a test of this hypothesis, two wedge geometries specified by $\theta = 15^\circ$ and $\theta = 25^\circ$ were tested using the parabolic model (6.2.9) with $P_1 = 0$, with incident wave steepnesses of $k_0 A_0 = 0.1$ and 0.2 . Waves are assumed to enter the grid parallel to the x-axis, and the y boundaries were assumed to be totally reflective, with one boundary located at the centerline of the wedge-shaped depression and the other located far enough away from the wedge that waves reflected at the caustic do not reflect back into the computational domain from the side boundary within the x-distance used. Results for $\theta = 15^\circ$ and $\theta = 25^\circ$ are presented in comparison to results obtained by the linearized form of (6.2.9) in Figures 6.25 and 6.26, respectively, where normalized amplitudes perpendicular to the line of symmetry $y=0$ are plotted for $k_0 x = 40, 80,$ and 120



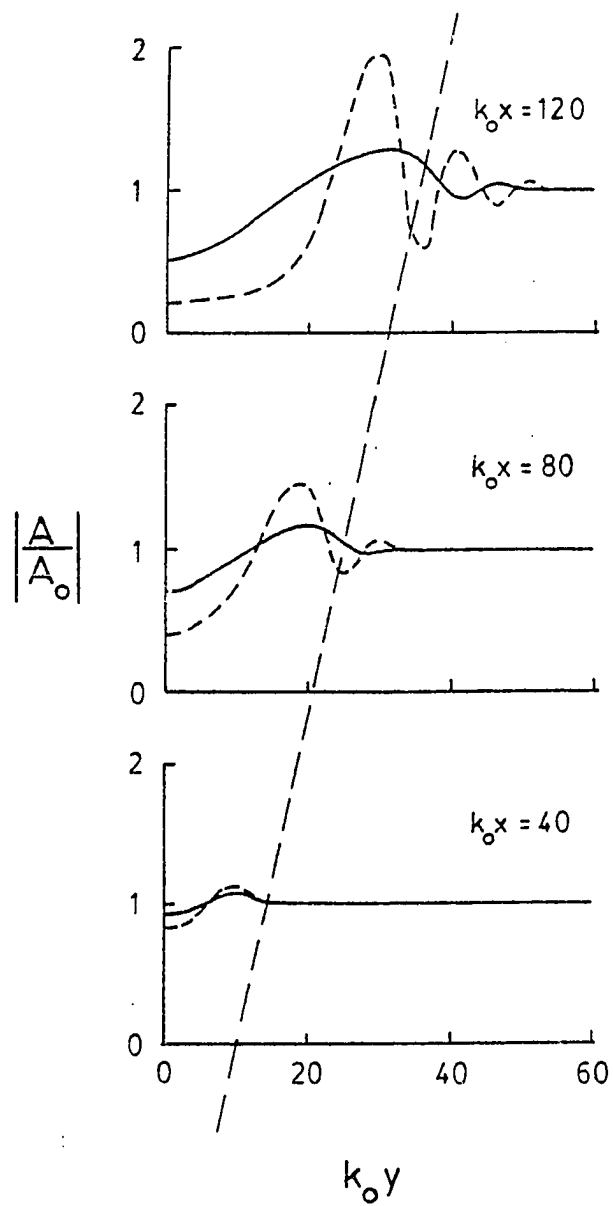
a) $k_0 A_0 = 0.1$

Figure 6.25 Submerged depression, $\theta = 15^\circ$
 Normalized amplitude vs. distance from
 centerline of depression

a) $k_0 A_0 = 0.1$; b) $k_0 A_0 = 0.2$

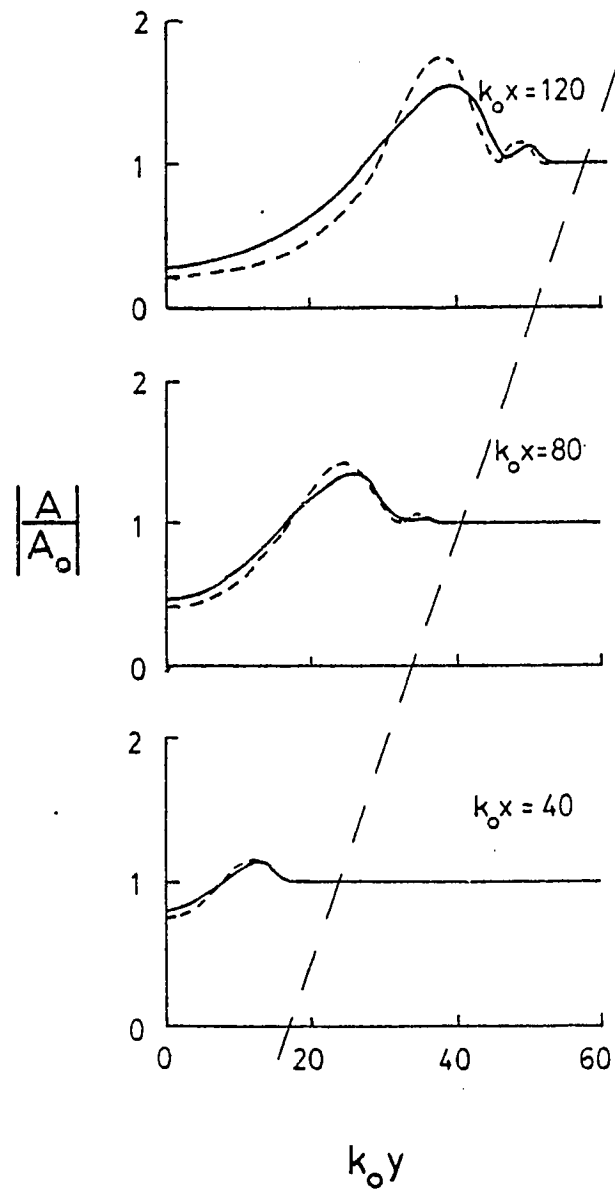
---- linear theory, $P_1 = 0$

— nonlinear theory, $P_1 = 0$



b) $k_0 A_0 = 0.2$

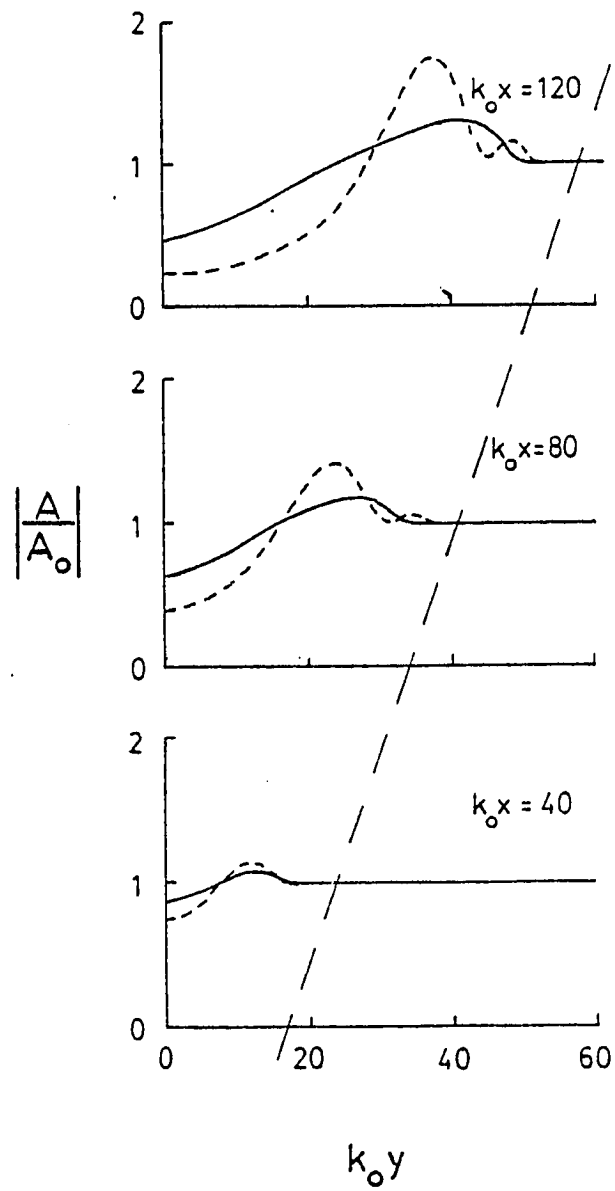
Figure 6.25 continued



a) $k_0 A_0 = 0.1$

Figure 6.26 Submerged depression, $\theta = 25^\circ$. Normalized amplitude vs. distance from centerline of depression

a) $k_0 A_0 = 0.1$; b) $k_0 A_0 = 0.2$
 ---- linear theory, $P_1 = 0$
 — nonlinear theory, $P_1 = 0$



b) $k_0 A_0 = 0.2$

Figure 6.26 continued

for each wave steepness tested. For the case of $\theta = 15^\circ$ and $k_0 A_0 = 0.1$ (Figure 6.25a), the evolution of the nonlinear wave in the vicinity of the caustic is not qualitatively dissimilar from that of the linear wave. The maximum amplitude near the caustic is seen to be decreased by the effect of nonlinearity, but the generation of a reflected wave and a large amplitude decay in the shadow zone are apparent. For $\theta = 15^\circ$ and $k_0 A_0 = 0.2$, however, the reflected wave is not as apparent, and a broad region of waves which are slightly higher than the incident wave develops in the vicinity of the caustic. Wave amplitude decays much more slowly towards the center of the wedge in the area of the linear shadow zone.

The result of nonlinearity is even more accentuated in the results for $\theta = 25^\circ$, where little reflection of the incident wave is apparent for either incident wave steepness. In order to accentuate the qualitative differences between the linear and nonlinear results, plots of the instantaneous surface for the linear wave field and for the nonlinear wave with $k_0 A_0 = 0.2$ are given in Figures 6.27 and 6.28, respectively, for a wedge angle of $\theta = 25^\circ$. It is apparent in Figure 6.28 that a broad wave crest travelling parallel to the caustic region has developed. Peregrine(1983) argues that, in the event that the jump

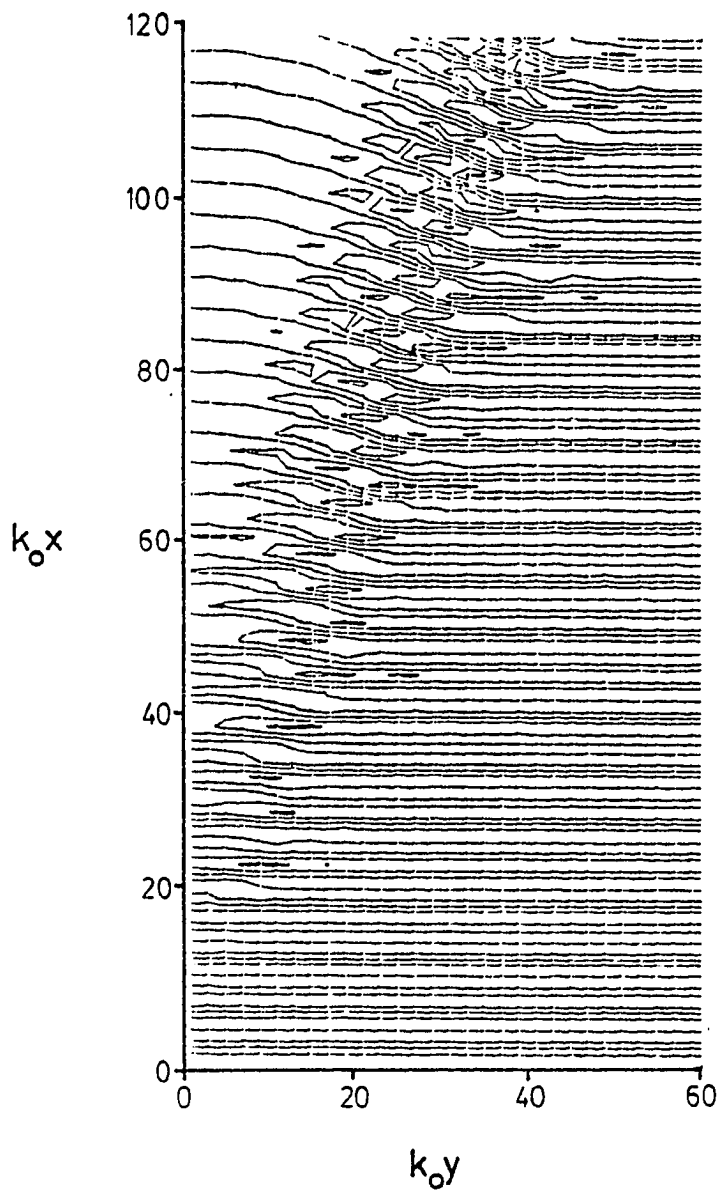


Figure 6.27 Instantaneous water surface in vicinity of wedge-shaped depression, linear result, $\theta = 25^\circ$

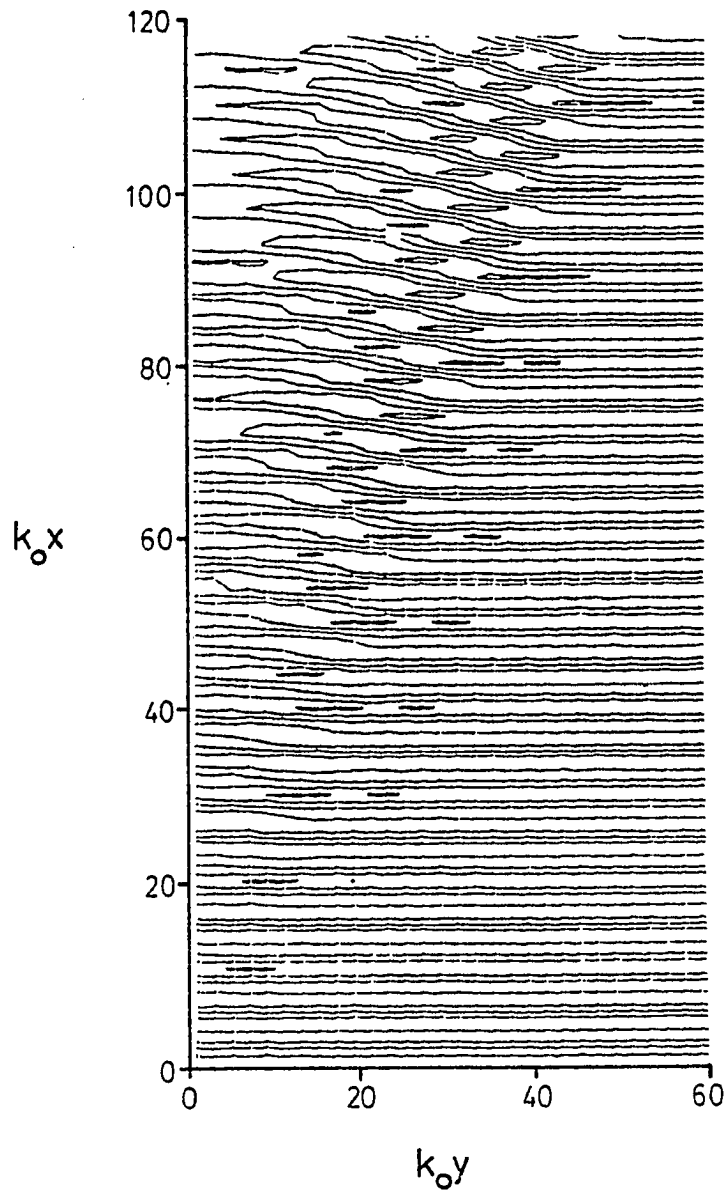


Figure 6.28 Instantaneous water surface in vicinity of wedge-shaped depression, nonlinear result, $k_0 A_0 = 0.2$, $\theta = 25^\circ$

conditions develop, this wave crest must continue to grow in width since the wave energy flux continually incident on the jump boundary cannot be balanced by the flux in a jump of constant width and height unless total reflection of the incident wave occurs. It is therefore unlikely that the wave field will evolve into its asymptotic state.

Since the principle conclusions on the evolution of the nonlinear wave field concern the absence of the development of a reflected wave, the results for the wave steepness $k_0 A_0 = 0.2$ and both $\vartheta = 15^\circ$ and $\vartheta = 25^\circ$ were recalculated using the more accurate model (6.2.9) with $P_1 = 1/4$ to insure that reflections were not being artificially suppressed. Although some increase in the magnitude of the reflected wave were noted, the results for the region of the caustic, where nonlinear effects dominate, were unaltered.

6.8. Reflection from a Caustic: Current Case

As a first example of waves in the presence of a horizontally varying current, we consider the case of a linear caustic caused by reflection by a following current. The results are then qualitatively similar to the results of section 6.7.

A stationary current distribution is established and is given by

$$U(y) = \begin{cases} 0 & ; k_0 y < 80 \\ \frac{\partial U}{\partial y} k_0 (y - 80) & ; k_0 y \geq 80 \end{cases} \quad (6.8.1)$$

$$V = 0 \quad (6.8.2)$$

Here, $\partial U / \partial y$ is taken to be a constant for each experimental case. The computational domain is given by

$$0 \leq k_0 y \leq 120 \quad (6.8.3)$$

$$0 \leq k_0 x \leq k_0 X_M$$

Waves are incident in the region $k_0 y < 80$ at an angle $\hat{\theta}$ to the x axis, and open boundary conditions are specified on the lateral boundaries. The initial wave field is given by

$$A(0, y) = \begin{cases} A_0 e^{i k_0 \sin \theta y} & ; k_0 y \leq \pi \\ 0 & ; k_0 y > \pi \end{cases} \quad (6.8.4)$$

No waves are present initially on the current. The physical situation is described in Figure 6.29, and represents a straight wave maker oriented at an angle θ to the y coordinate, with a linearly varying current distribution starting at the end of the wave maker and increasing in magnitude with distance from the wave maker. The depth is taken to be a constant, with $k_0 h = 1.0$.

Snell's law applied to this problem requires that the x -component $\hat{\lambda}$ of the wavenumber vector be constant throughout the domain, and $\hat{\lambda}$ is given by

$$\hat{\lambda} = k_0 \cos \theta = \text{constant} \quad (6.8.5)$$

The wavenumber is then uniquely determined throughout the domain according to

$$\omega = \sigma + \hat{\lambda} u \quad (6.8.6)$$

The position of the caustic in the current distribution is also simply determined, and occurs where $k(y) = \hat{\lambda}$. Since k then equals $k_0 \cos \hat{\theta}$ at the caustic, the dispersion relation

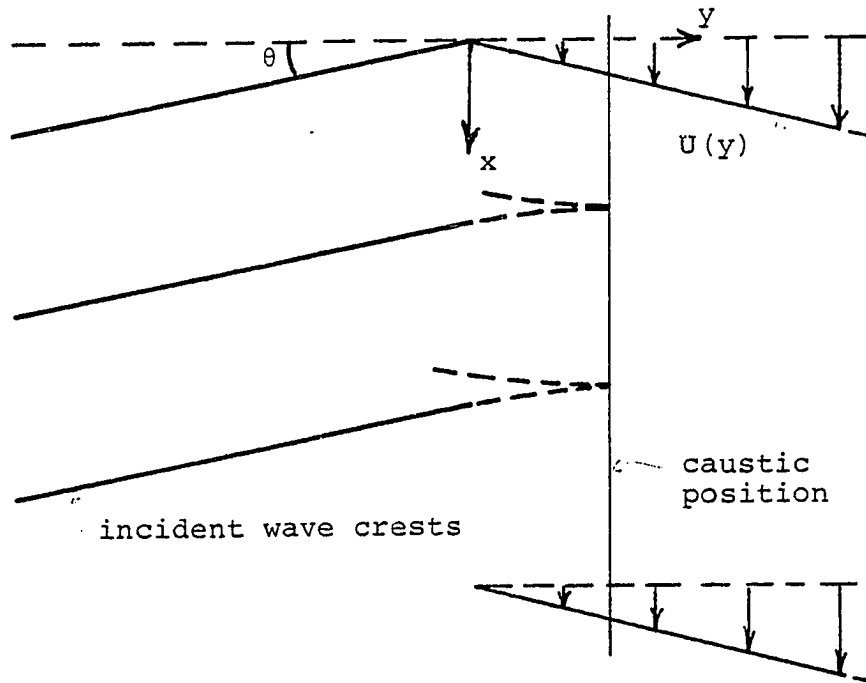


Figure 6.29 Reflection from following current

may be written as

$$\omega = \{gk_0 \cos \theta \tanh(k_0 h \cos \theta)\}^{1/2} + k_0 U \cos \theta \quad (6.8.7)$$

or, solving for U,

$$U = \frac{\omega - \{gk_0 \cos \theta \tanh(k_0 h \cos \theta)\}^{1/2}}{k_0 \cos \theta}$$

The value of U at the caustic is thus uniquely determined by the choice of ω , which gives k_0 in turn.

Two sets of computations were run with $\theta = 15^\circ$ and $T = 2.30 \text{ sec}$. for each case. The corresponding value of k_0 is 1 m^{-1} , and U at the caustic is calculated from (6.8.8) to be

$$U = 0.0755 \text{ m/sec}$$

Calculations were performed using the numerical scheme (6.2.11-12), and results were obtained for linear waves and for values $k_0 A_0 = 0.1$ and 0.2 , as in section 6.7. For the first set of calculations, $\partial U / \partial y$ was set equal to 0.05 , and the caustic occurs at $k_0 y = 81.51$. Results are presented in Figure 6.30. For $k_0 A_0 = 0.1$ (Figure 6.30a), nonlinear effects are relatively weak, and there is little qualitative difference between linear and nonlinear solutions. For

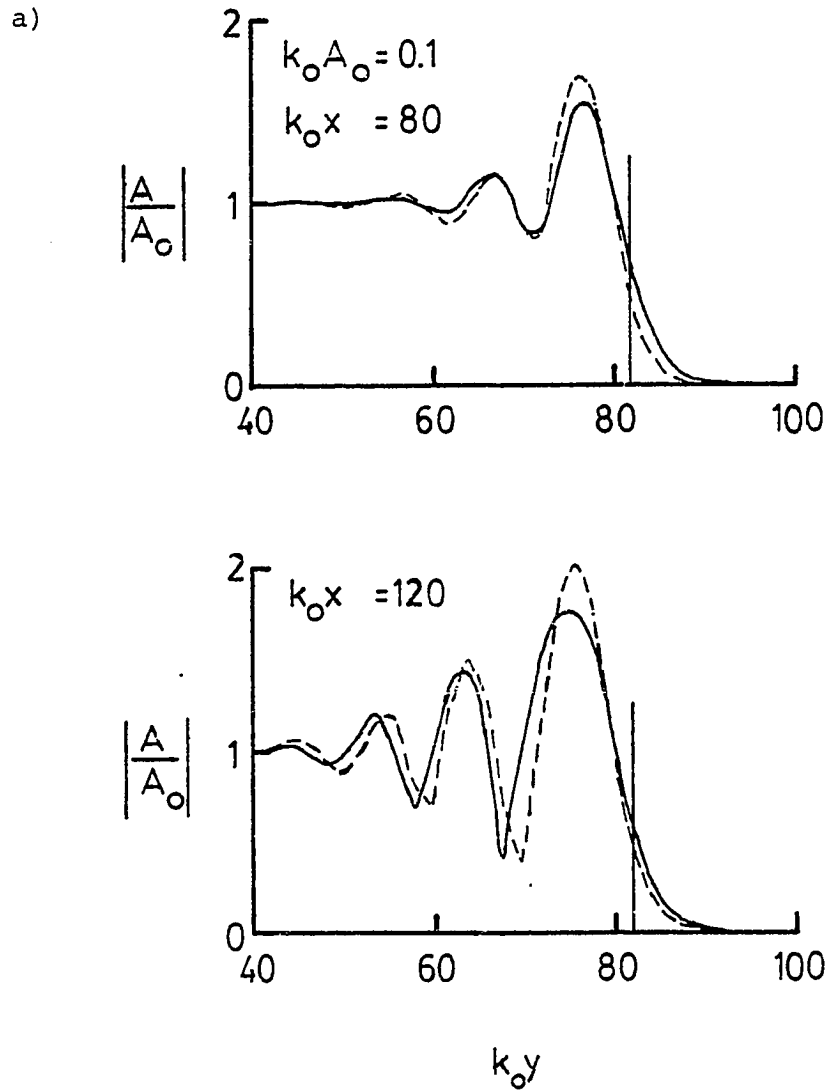


Figure 6.30 Reflection of waves from caustic caused by a following current;
 $\partial U / \partial y = 0.05$, $\theta = 15^\circ$
 — nonlinear solution;
 ---- linear solution
 a) $k_0 A_0 = 0.1$; b) $k_0 A_0 = 0.2$

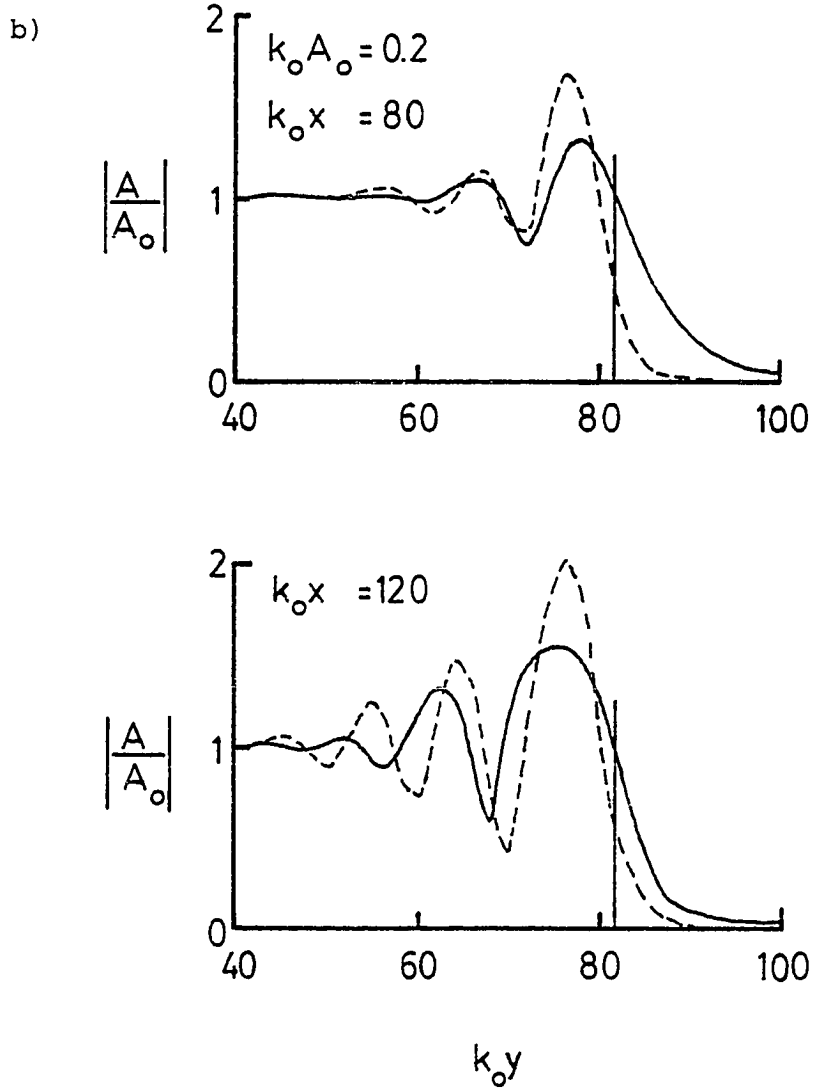


Figure 6.30 continued

$k_0 A_0 = 0.2$ (Figure 6.30b), a broadened wave crest develops in approximately the same position as the first antinode in the linear wave solution, with very little spreading of wave energy beyond the caustic being apparent. The position of the caustic is indicated by the vertical line in the figure.

A second set of calculations were performed with $\partial U / \partial y = 0.025$, representing a more slowly varying current distribution. The caustic occurs at $k_0 y = 83.02$. Results are shown in Figure 6.31. The increased effect of nonlinearity for the case $k_0 A_0 = 0.2$ (Figure 6.31b) is dramatic. A broad wave crest develops in the region of the caustic and spreads significantly beyond the caustic position. The reflection of waves from the region of the caustic has also been suppressed to a large extent. It is evident that a wave jump has occurred, and that the conjugate wave state is able to coexist with the current in the shadow region of the caustic. The wave would be expected to decay with increasing $k_0 y$ due to the continual increase in current velocity.

A possible explanation for the increase in nonlinear effects with decreasing $\partial U / \partial y$ is that, for progressively lower current gradients, waves entering the current are refracted more slowly and thus travel a greater distance

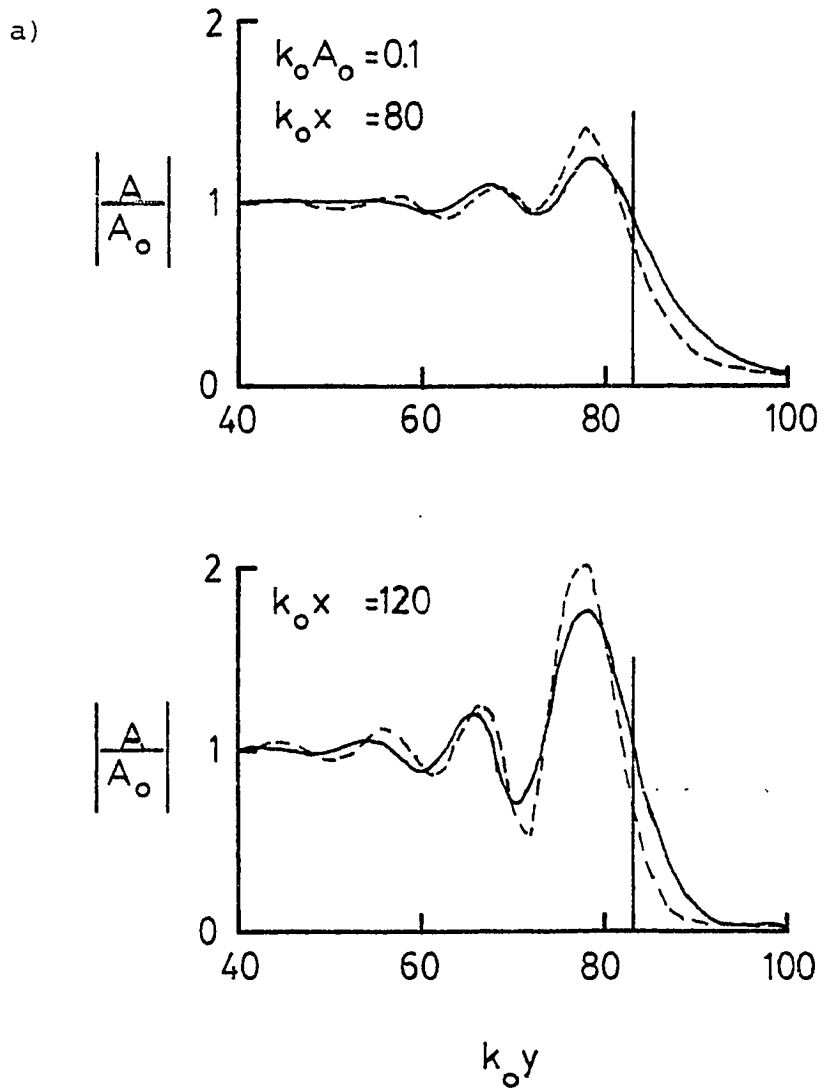


Figure 6.31 Reflection of waves from caustic caused by a following current; $\partial U/\partial y = 0.025$, $\theta = 15^\circ$

— nonlinear solution
 ---- linear solution
 a) $k_0 A_0 = 0.1$; b) $k_0 A_0 = 0.2$

b)

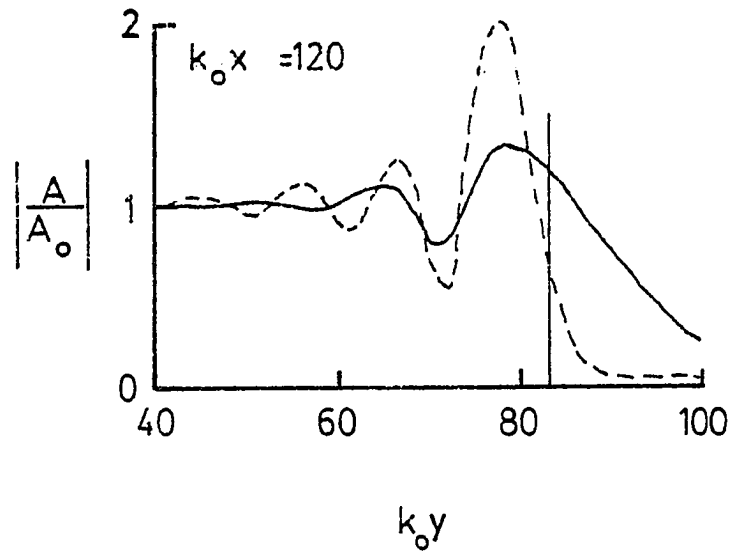
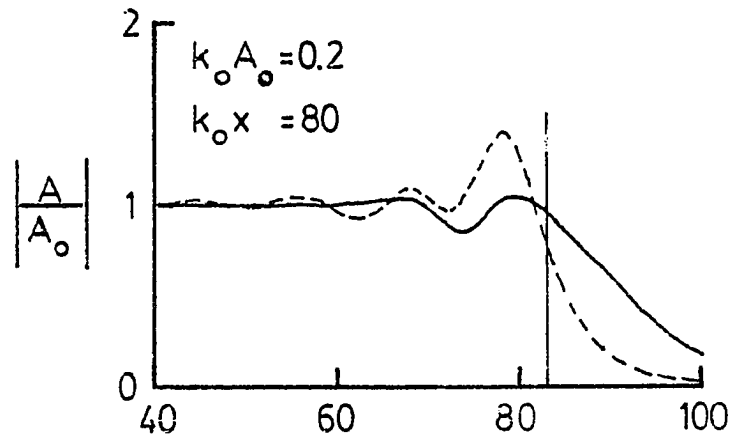


Figure 6.31 continued

before leaving the current as reflected waves. This increased distance, over which incident waves and reflected waves are nearly colinear in the vicinity of the caustic, allows for a greater span of nonlinear interaction between the individual waves and enhances the possibility for wave jump conditions to develop. An analogous behavior would be seen in the results of section 6.7 if the slope of the side walls of the wedge were decreased.

6.9. Interaction with Rip Currents

Several coastal features lead to the presence of a narrow, offshore-directed jetlike flow. On a large scale, ebb-tidal flows from inlets and river mouths may influence wave propagation over large stretches of adjacent coastline. On a smaller scale, narrow, intense seaward flows known as rip currents may occur on otherwise uniform coastlines, and lead to the presence of on-offshore channels in the beach face which may stabilize the rip current and contribute to considerable offshore sand transport. In this section, we study the interaction of an incident wave train with such a current. As in the previous section, the flow pattern of the current is assumed to be fixed.

In one of the first investigations of the influence of currents on results of the ray approximation of refraction, Arthur(1950) studied the interaction between a normally incident wavetrain on a plane beach with a flow field designed to mimic the features of a typical rip current. With the coordinate x oriented offshore and the rip centerline located along x and at $y=0$, Arthur's velocity field is given by

$$U = 0.02295 x e^{-\frac{(x/76.2)^2}{2} - \frac{(y/7.62)^2}{2}} \quad (6.9.1a)$$

$$V = -0.2188 \left(2 - (x/76.2)^2\right) e^{-\frac{(x/76.2)^2}{2}} \cdot \operatorname{erf} \left\{ \frac{y}{76.2\sqrt{2}} \right\} \cdot \operatorname{sign}(y) \quad (6.9.1b)$$

where U is positive in the offshore direction and erf denotes the error function. Current velocities are in meters/second. The bottom topography consists of a plane beach,

$$h(x) = 0.02x \quad (6.9.2)$$

Arthur calculated the ray pattern for an incident wave period of 8 seconds; his results are shown in Figure 6.32 for comparison with the refraction-diffraction results discussed below.

Arthur's solution technique involved some confusion over the relation between wave rays and wave orthogonals, as evidenced by the straight "rays" to either side of the narrow rip; the ray paths should be convected towards the centerline of the rip by the longshore current perpendicular to the wave orthogonals. Christoffersen(1982) noted this discrepancy during his development of a ray-tracing procedure for waves in the presence of a current, and Jonsson, Christoffersen and Skovgaard (1983), using

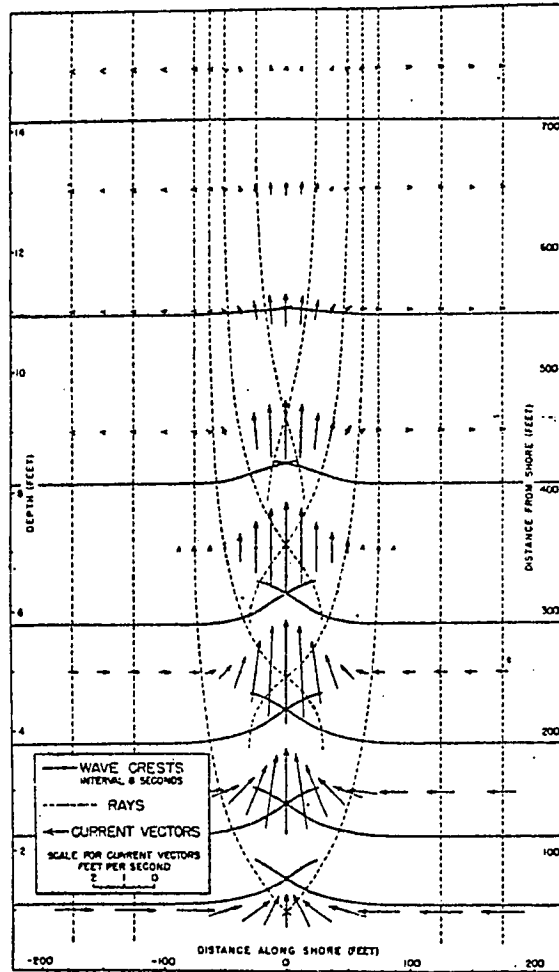


Figure 6.32 Pattern of orthogonals and wave crests for waves in presence of rip current: refraction approximation. (from Arthur, 1950).

Christoffersen's procedure, have presented a corrected version of Arthur's results which also include estimates of the local wave amplification with respect to the incident amplitude at $h=100\text{m}$. Jonsson, Christoffersen and Skovgaard's results suggest a decrease in wave height in the center of the rip; this appears to be a result of the termination of several rays and a subsequent underestimation of the local wave energy density. These results point out the difficulties of interpreting refraction patterns in regions of multiple ray crossings.

In this section, we use the parabolic model given by (6.2.11-12) to investigate the interaction between a normally incident plane wave and a fixed current pattern given by (6.9.1). The deviation of the free surface due to the $O(1)$ current is neglected.

At large distances from the centerline of the rip current, the wavefield is characterised by normally incident waves and a longshore current distribution with no on-offshore component. Consequently, the wave crests and shoaling characteristics should not be affected by the current at lateral boundaries far from the rip. In order to place the lateral boundaries close to the rip and reduce the size of the computational domain, the lateral boundary

conditions are replaced by a one-dimensional model for shoaling waves, given by

$$A_x - i(k - k_0)A + \frac{1}{2C_g} C_{gx} A + \frac{W}{2C_g} A + i\omega \frac{k^2}{2} D|A|^2 A = 0 \quad (6.9.3)$$

which is just the one-dimensional counterpart of (4.4.4). Breaking is included in all calculations in this section.

We first consider linear theory. As mentioned in section 4.4, the parabolic approximation for wave-current interaction derived by the splitting method contains errors in y -derivative terms. We first compare results obtained using the approximate equation (4.4.33), written in finite-difference form as (6.2.11), to results obtained using the correct equation (4.4.7), written in a similar finite-difference form. The computational grid is given by

$$0 \leq x' \leq 297.5 \text{ m} \quad ; \quad -89.25 \leq y \leq 89.25 \text{ m}$$

with $x'=0$ located offshore and the shoreline located at $x'=300\text{m}$. The values of Δx and Δy are 2.5m and 1.5m, respectively. A plot of the instantaneous surface elevation for an amplitude $A_0(h=6\text{m}) = 0.1\text{m}$ and a wave period $T=8\text{sec}$. is

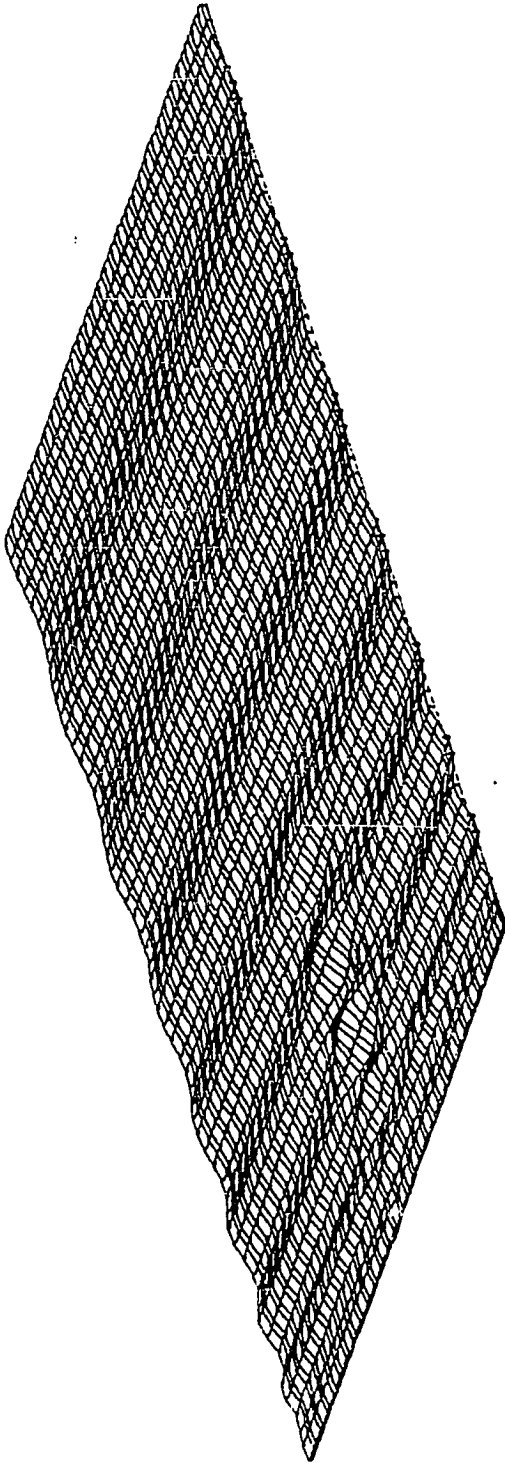


Figure 6.33 Wavefield in presence of rip current (Arthur, 1950).
Linear model results; $T = 8$ sec., $A_0 = 0.1$ m. Surf
zone included.

given in Figure 6.33. Note that the wave amplitude is strongly amplified along the centerline of the rip, and that discontinuities develop in the wave phase surface, leading to the presence of nodes in wave amplitude along the lateral boundaries of the core of the offshore directed rip. The amplification seen here is in direct contradiction to the results presented by Jonsson, Christoffersen and Skovgaard(1983). Wave breaking occurs on the rip centerline at $x'=240\text{m}$, or 60m from the shoreline.

The region of strong amplification and large currents along the centerline of the rip is likely to be a good indicator of the amount of error involved in using the approximate equation (4.4.33). Linear wave results were obtained for an initial amplitude of $A_0=0.01\text{m}$ and $T=8\text{sec}$. using both the exact (4.4.7) and approximate (4.4.33) equations. For this amplitude, breaking is confined to the last shoreward grid row. Plots of amplitude relative to the incident wave are given in Figure 6.34 for transects $y=0$ along the rip centerline and for values of $x'=197.5\text{m}$, 222.5m , 247.5m and 272.5m . The results show a decrease in maximum amplitude in the approximate solution relative to the results of the exact equation in the region of strong focussing near the shoreward end of the rip, indicating a loss in wave action density due to the errors in terms

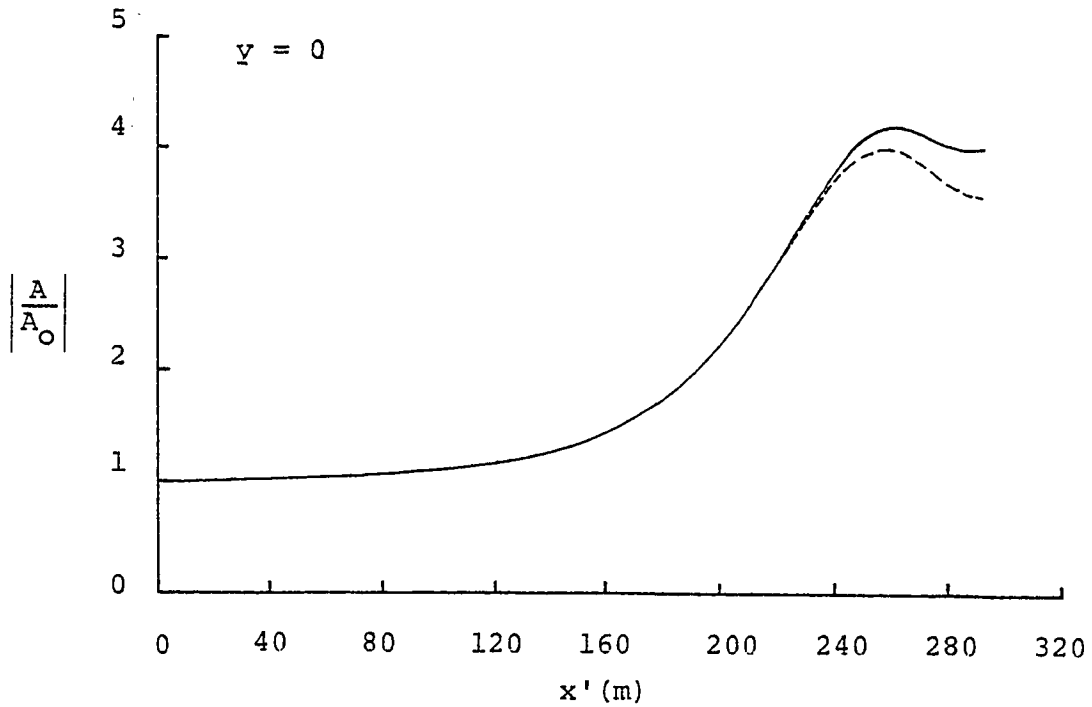


Figure 6.34 Amplitude relative to incident wave for waves interacting with rip current. Comparison of results of exact equation (4.4.4) and approximate equation (4.4.33): linear waves — (4.4.4); ---- (4.4.33).

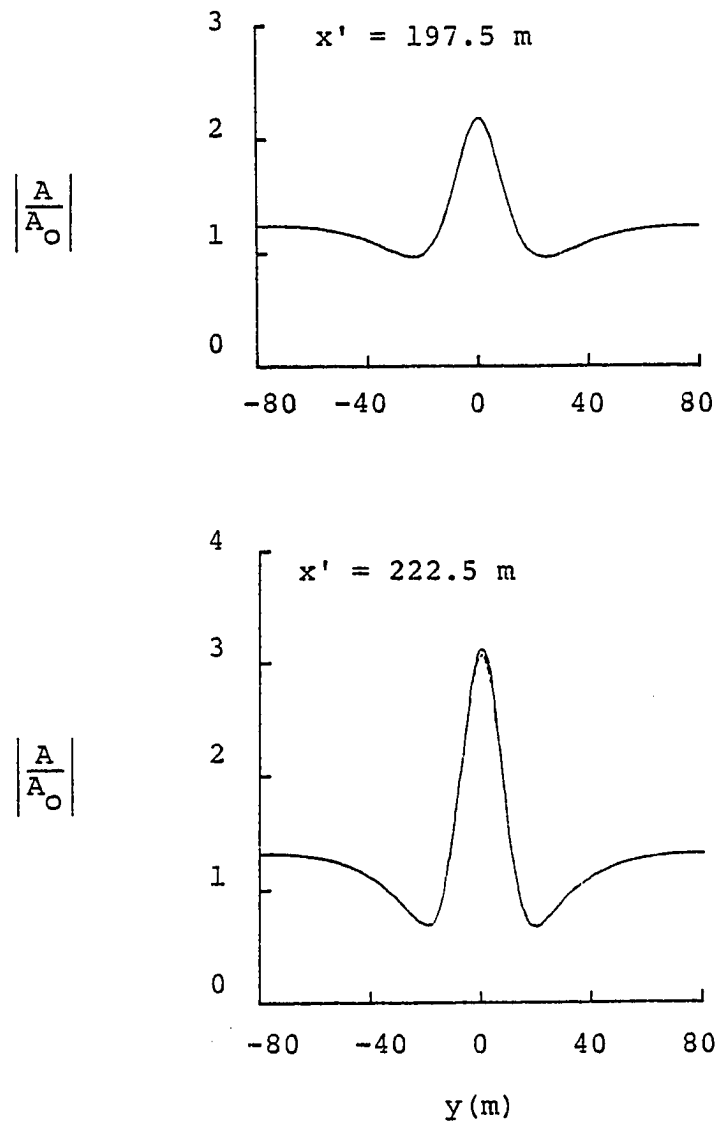


Figure 6.34 continued

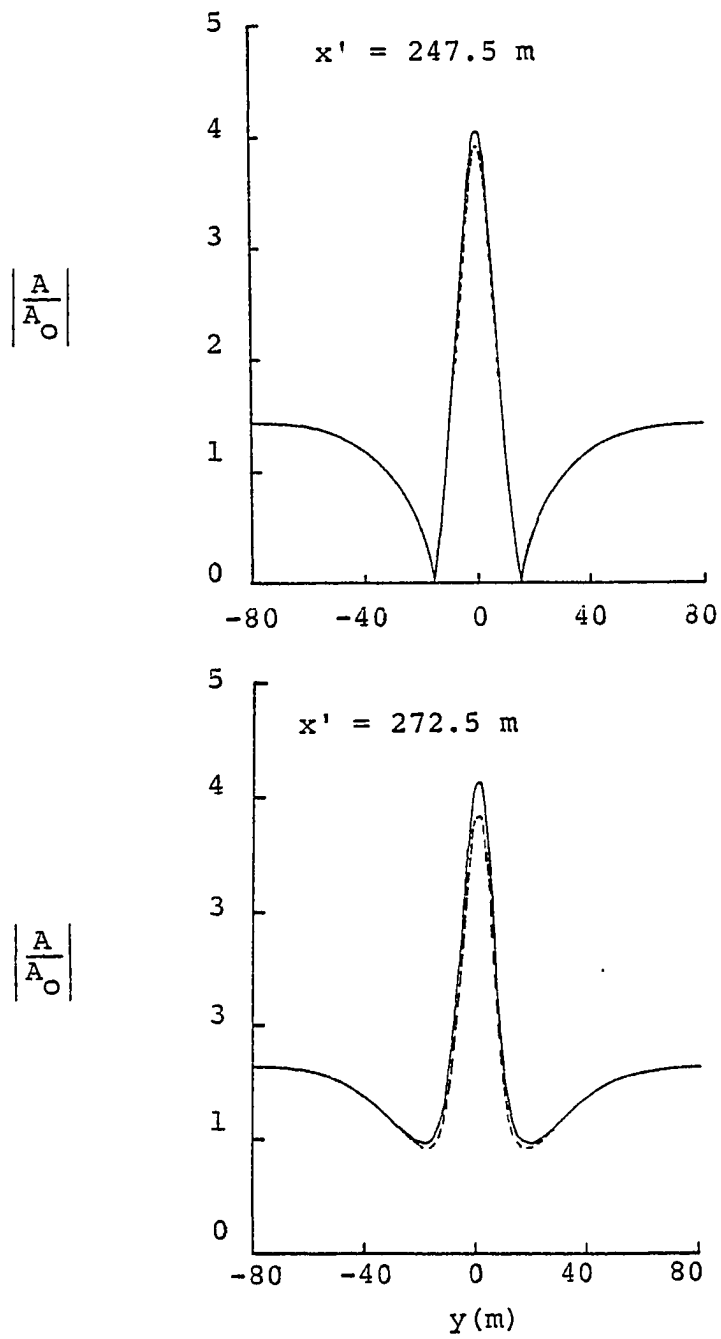


Figure 6.34 continued

involving the y velocity component V in (4.4.33). These results indicate that it is not desirable to use the approximate form (4.4.33) if detailed estimates of local wave amplitude are required. The transects for constant x' values clearly show the development of the node in the amplitude as the discontinuity in wave crests develops.

Due to the strong wave focussing in the area of the rip current, nonlinear effects are also likely to be important in this example. As in several of the cases studied in section 6.6, nonlinear effects occur in this example at Ursell numbers too large for Stokes wave theory to be valid, if reasonable values of initial wave amplitude are chosen. In order to investigate the effect of nonlinearity in this example, we incorporate the effect of amplitude dispersion in the model using the empirical dispersion relation of Walker(1976). The effect of nonlinearity is included in the model by using the linearised governing equation but calculating k based on the revised dispersion relation, as suggested in section 3.5.

The correction to linear wave theory is given by Walker as a modification to the linear phase speed. Walker's phase speed C_w is given by

$$C_w = C \left(1 + \frac{1}{2} \frac{|A|}{h} \right) \quad (6.9.4)$$

in the present notation, where C is the phase speed determined by the linear dispersion relation. Walker obtained this one parameter fit by comparison with data obtained from laboratory waves shoaling on a plane beach. A dispersion relation may be determined from (6.9.4), and is given by

$$\omega^2 = g k_w \left(1 + \frac{1}{2} \frac{|A|}{h} \right) \tanh \left\{ k_w h \left(1 + \frac{|A|}{2h} \right) \right\} \quad (6.9.5)$$

Walker's modification is purely empirical and it is desirable to gain some insight on how his results compare to theory. In order to provide this information, we compare results for Walker's phase speed prediction to values given by the stream function wave theory of Dean(1965), which is valid for all water depths. Values are compared for a range of local wave heights relative to the local breaking wave height as determined by the stream function theory, and for a range of relative depths h/L_0 , where L_0 is the linear deep water wavelength given by

$$L_0 = \frac{g T^2}{2\pi} = \frac{2\pi g}{\omega^2} \quad (6.9.6)$$

Values of $H(=2|A|)/H_b$ of 0.25, 0.5, 0.75 and 1.0 were used. Stream function values were obtained from the tables of Dean(1974). Results of Walker's modified phase speed are presented as a % error relative to stream function theory in Figure 6.35. Linear theory results are included for comparison. The range of h/L_0 values relevant to the present problem extends from 0.060 for the offshore boundary to 0.012 near $x'=240$, where breaking occurs in the linear theory for the choice $A_0=0.1m$. It is apparent from Figure 6.35 that Walker's modification provides a significant improvement over linear theory except for the region close to the offshore boundary, where wave amplitude is small. However, for small amplitudes the relative error in either Walker's or linear results are on the order of 2%. It appears that Walker's empirical formula provides an adequate estimate of the phase speed even for steep waves near breaking. We remark that it would be desirable to obtain more detailed forms of the empirical dispersion relation designed to cover the entire range of depth values, since Walker's relation is suitable mainly in shallow water and approaches linear theory asymptotically in deep water.

For the present application to wave-current interaction, we modify Walker's dispersion relation according to

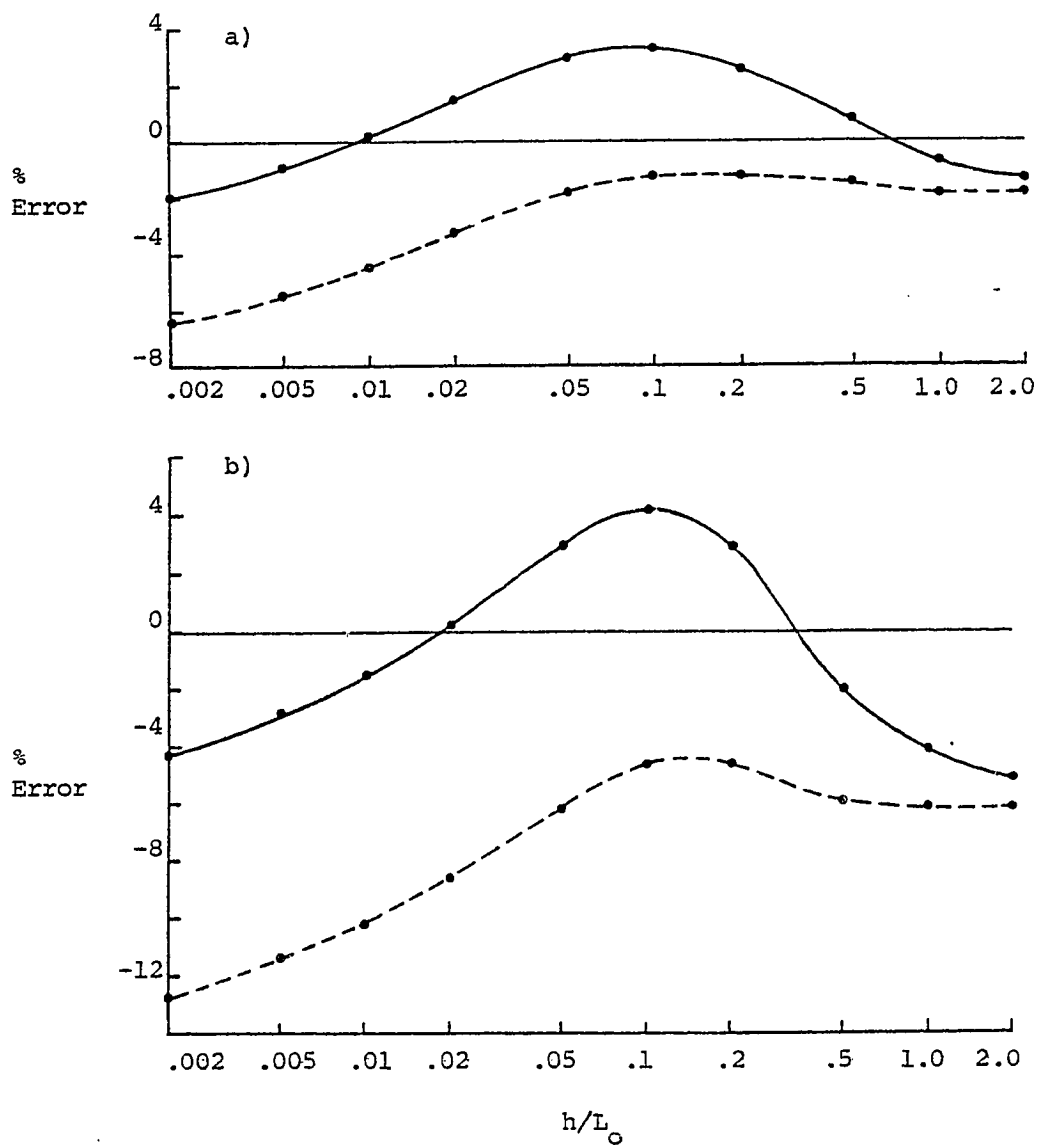


Figure 6.35 Error in predicted phase speed relative to results of stream function theory.
 a) $H/H_b = 0.25$, b) $H/H_b = 0.5$,
 c) $H/H_b = 0.75$, d) $H/H_b = 1.0$
 — Walker (1976); ---- linear theory

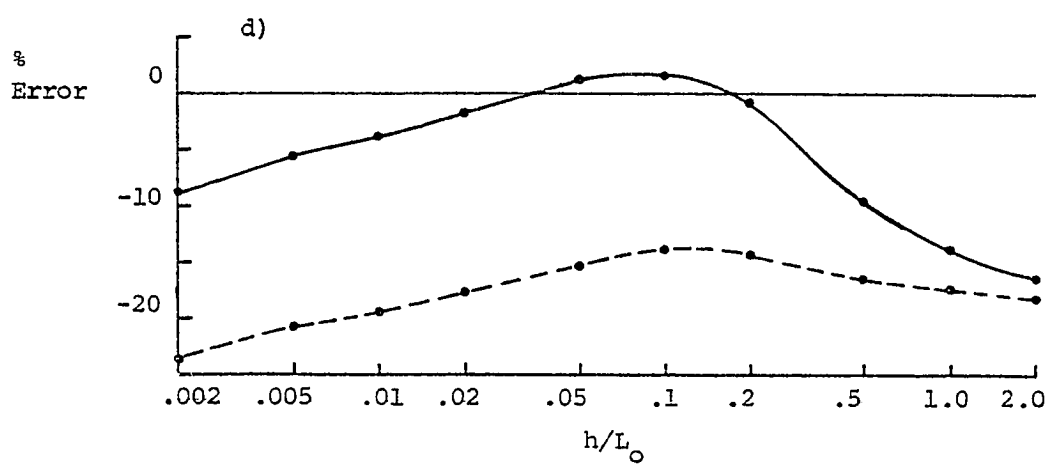
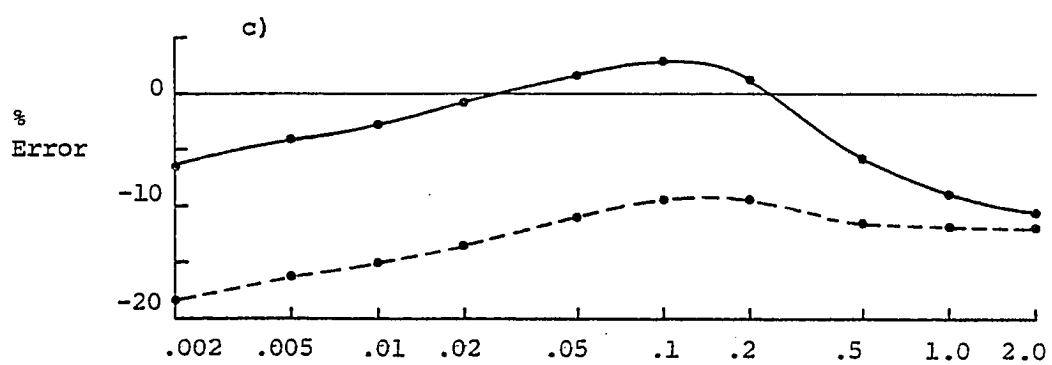


Figure 6.35 continued

$$\omega = R_w (C_w + u) = \sigma_w + R_w u \quad 6.9.7$$

where

$$\sigma_w = \left\{ g R_w \left(1 + \frac{|A|}{2h} \right) \tanh \left[R_w h \left(1 + \frac{|A|}{2h} \right) \right] \right\}^{1/2}$$

The wavefield for the case $A_0 = 0.1\text{m}$ and $T = 8\text{sec.}$ is shown in Figure 6.36. Plots of amplitude for the same transects as in Figure 6.34 are given in Figure 6.37 in comparison to linear results. The transect at $x' = 272.5\text{m}$ is inside the surfzone for both the linear and nonlinear results.

It is apparent from Figure 6.37 as well as from a comparison of Figures 6.36 and 6.33 that the effect of nonlinearity due to the empirical shallow water dispersion relation is relatively subdued in comparison to the striking examples of sections 6.7 and 6.8. An invalid application of Stokes theory to the present example leads to the prediction of strong wave jump conditions in the region of the rip; this effect is absent from the present calculations. The nonlinear effects are limited to a reduction in wave amplitude along the centerline of the rip and a slight broadening of the region of focussed waves as evidenced by the position of the partial nodes in the amplitude

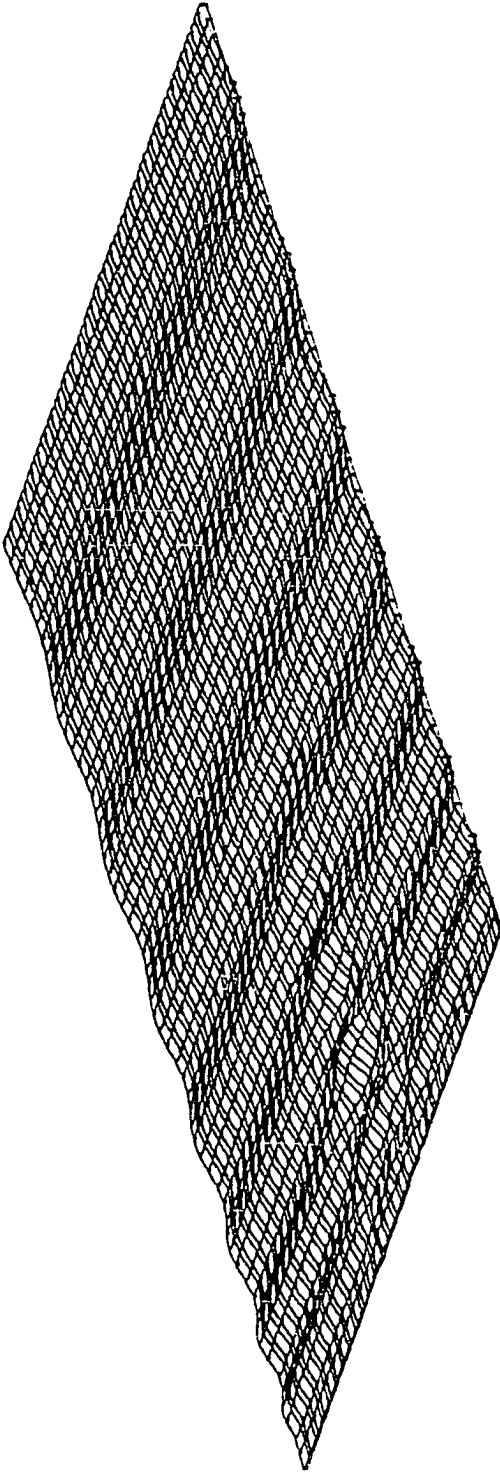


Figure 6.36 Wavefield in presence of rip current (Arthur, 1950).
Model using Walker's (1976) dispersion relation;
 $T = 8$ sec, $A_0 = 0.1$ m. Surfzone included.

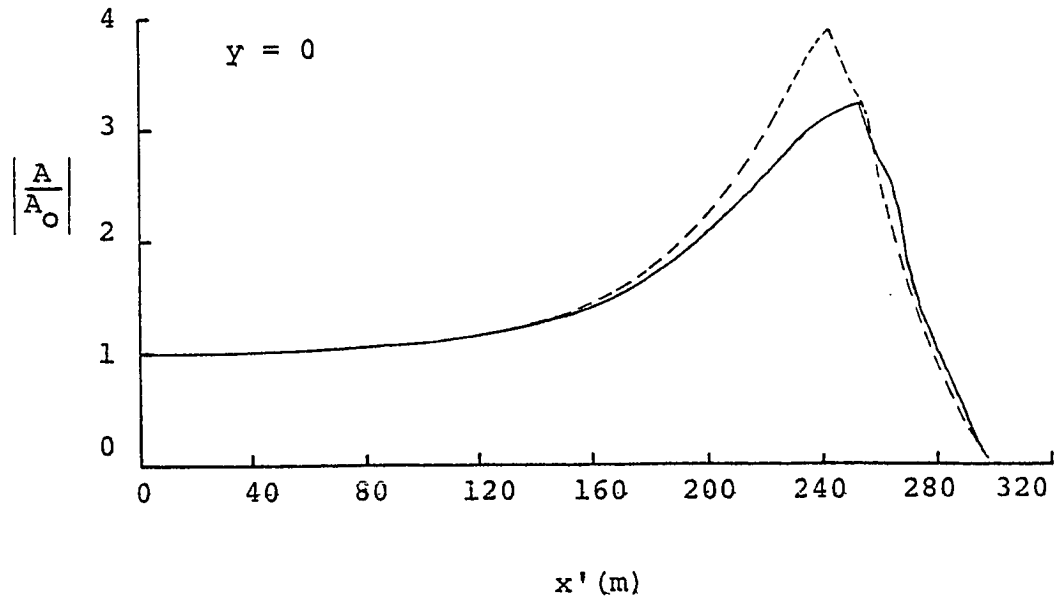


Figure 6.37 Amplitude relative to incident wave for waves interacting with rip current. Comparison of linear results to nonlinear results using Walker's dispersion relation
—— Walker; ---- linear

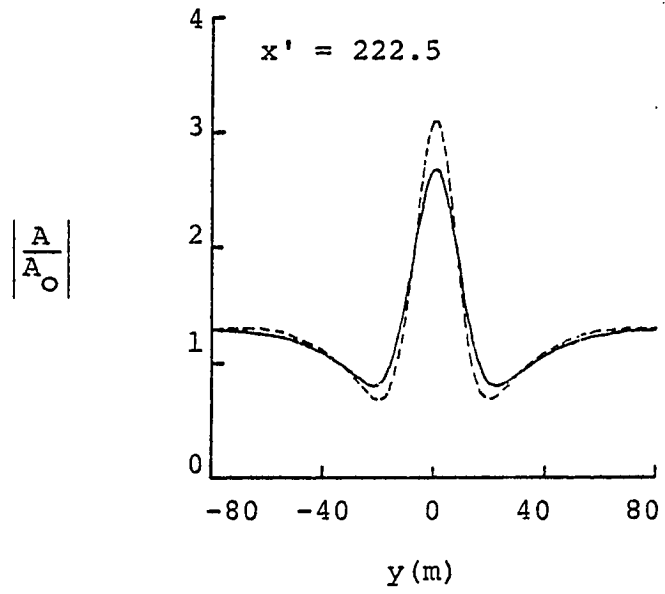
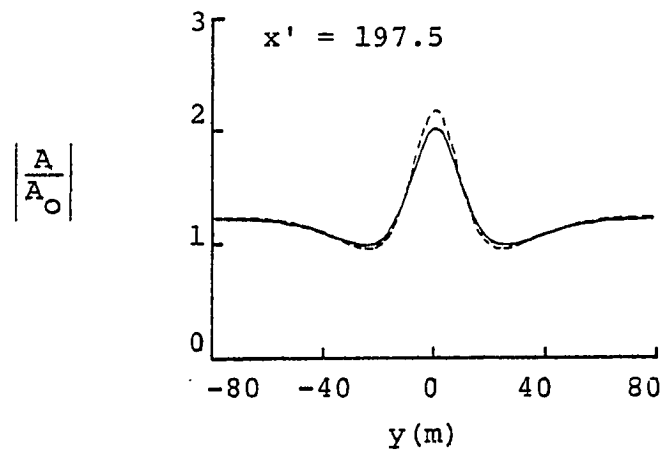


Figure 6.37 continued

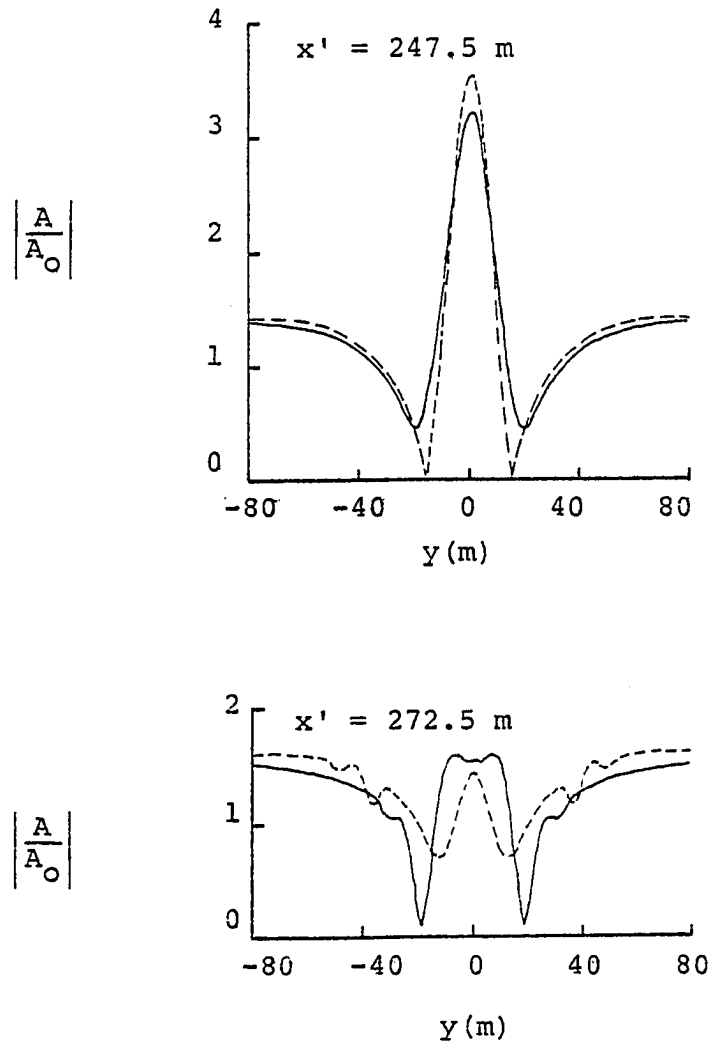


Figure 6.37 continued

transects. The results are similar to the nonlinear modification seen in the data for waves passing over the elliptic shoal in section 6.5.

The results of this section indicate that it may be possible to make use of a variety of dispersion relations within the context of the linear wave model in order to model phenomena beyond the limits of validity of Stokes theory. Before any conclusions regarding this possibility can be drawn, it will be necessary to investigate the behavior of the models in comparison to existing or future data for waves propagating and shoaling in shallow water. The benefits to be achieved in the event of the validity of this approach are clear, since existing numerical approaches depend on the use of Boussinesq or Korteweg-deVries equations, which require more involved computational procedures than the parabolic equation method used here.

CHAPTER 7. SUMMARY AND SUGGESTIONS FOR FURTHER RESEARCH

In this study, we have sought to provide a model for progressive surface waves in the presence of a large, horizontally varying current. The formulation includes the lowest order effects of nonlinearity in a manner consistent with the Stokes(1847) expansion in a small parameter based on the wave steepness. In addition, the depth is allowed to vary somewhat more rapidly than in the traditional mild slope approximation, and terms proportional to the square and derivative of the local bottom slope are retained.

In Chapter 2, we obtain a solution for the velocity potential for a plane progressive wave to $O(\epsilon^2)$ in wave steepness and $O(\bar{\epsilon})$ in bottom slope. Then, using the variational principle of Luke(1967), we obtain a Lagrangian governing the entire fluid motion in the absence of viscous effects, given in Chapter 3. Variations of the unaveraged form of the Lagrangian with respect to the unknown dependent variables, following a perturbation scheme developed here,

yields equations governing the instantaneous fluid motion.

The lowest order problem reproduces the nonlinear shallow water theory governing the $O(1)$ mean motion. This result could be further expanded for the case of small b_0/h_0 , to yield the Boussinesq equations.

For the leading order wave motion ($O(\epsilon)$), we obtain an equation including terms to $O(\epsilon^3)$ in $\tilde{\phi}_1$ and $\tilde{\phi}_2$, governing the potential $\tilde{\phi}_1$. Invoking the simplifying assumption of plane wave motion reduces the nonlinear contribution to a coefficient proportional to the square of the local amplitude multiplying the potential $\tilde{\phi}_1$. This term has the effect of modelling amplitude dispersion arising at $O(\epsilon^3)$. Interaction with the mean $O(\epsilon^2)$ wave-induced motion is also included.

At $O(\epsilon^2)$, a set of forced equations representing a free surface boundary condition and continuity equation for the entire $O(\epsilon^2)$ motion is obtained. Taking the mean over a wave period yields the continuity equation for wave induced mean flow, as found by Whitham (1962), and a forced wave equation governing the $O(\epsilon^2)$ wave-induced flow is obtained. Retaining the full equations at $O(\epsilon^2)$ yields equations which could be used to calculate the forced second

harmonic of the fundamental wave $\tilde{\phi}_1$.

The resulting formulation is a correct representation of the governing equations for plane progressive waves in the absence of strong reflection. This is demonstrated in Chapter 4, where we show the correspondence between the second order wave equation formulation and the nonlinear Schrodinger equation governing the evolution of the amplitude envelope. This correspondence points out the potential capability for modelling wavefields with narrow-banded frequency spectra and an identifiable carrier frequency. However, in the remainder of this study, we choose to limit our attention to steady, monochromatic wavefields. Parabolic approximations for waves in the mild slope formulation are derived in Chapter 4 and used to study a number of examples in Chapter 6. A detailed comparison with laboratory data for the case of waves propagating over a submerged shoal demonstrates the validity of the parabolic equation method and indicates that accurate solutions may be obtained using this computationally efficient method. This result has significant bearing on the potential for development of wave models for engineering application.

In contrast to the case for progressive waves, the

formulation contains basic ambiguities in the case of arbitrary wave motions, both in terms of the evaluation of several of the second order terms in the bottom slope as well as in the evaluation of the wavenumber for the case of waves on a current. Both evaluations require that the direction of a wavenumber vector be specified relative to the direction of the current vector or vector gradients of various quantities in the physical domain. The model does not directly calculate the local wave direction, and, in the case of partial standing waves, this quantity is not well defined. The problems associated with this ambiguity are pointed out in Chapter 5, where we study the reflection of waves by steep depth transitions.

One path along which future research could proceed is towards removing some of the limitations of the present theory. An expansion of ϕ without assuming a plane wave form of the solution a priori may alleviate the difficulties encountered in Chapter 5. Further, the limitations imposed by the assumed irrotationality of the motion should be investigated and, if possible, eliminated, since it is clear that most physical cases of interest will involve currents with rotational velocity distributions. Finally, although the effect of viscosity is neglected, we have shown that it is possible to effectively parameterize viscous effects in

the model simply through imposing the condition of a complex frequency or wavenumber. The resulting equations are able to effectively model both gradual and strong dissipative effects including wave breaking. For applications to large scale problems, it would also be desirable to include the facility to allow for wind generation of waves as well as deep water wave breaking due to excessive wave steepness.

The parabolic and Schrodinger equation wave models as formulated here are suitable for direct use in models of wave induced circulation in the nearshore region. Most currently existing models such as those by Wu(1983) and Ebersole and Dalrymple (1980, see also Kirby and Dalrymple(1982) for a recent summary) use a finite-difference refraction scheme and solution of the wave energy equation to provide the local wave amplitude and wave angle for use in the momentum equations for the mean flow. These refraction schemes do not allow directly for diffraction and do not provide detailed information in regions of strong focussing and ray crossing. The models should therefore be especially useful in applications to regions with strong currents such as rip currents and ebb tidal flows from inlets.

The limitation of the validity of Stoke's theory in

shallow water places a severe constraint on the general utility of the models formulated here. Most real waves in the nearshore zone are more appropriately modelled by the Boussinesq equations. However, it has been shown in section 6.9 that models of a more empirical nature may be developed by the direct substitution of any given dispersion relation into the linear form of the governing equations. It may be possible to develop methods by which the basic linear propagation model may be made to mimic any desired real wave process (such as the propagation of broken waves in the surfzone) by a suitable choice of dispersion relation and dissipative mechanism. It is not clear, however, that such a model would be capable of maintaining a proper balance between relevant quantities such as amplitude, energy flux and phase speed.

REFERENCES

Abbott, M. B., Petersen, H. M., and Skovgaard, O., 1978, "On the numerical modelling of short waves in shallow water", J. Hydraulic Res., 16(3), 173-204.

Abramowitz, M., and Stegun, I. A., 1972, Handbook of Mathematical Functions, Dover.

Arthur, R. S., 1950, "Refraction of shallow water waves: the combined effect of currents and underwater topography", Trans. Amer. Geophys. Union, 31(4), 549-552.

Battjes, J. A., 1978, "Energy dissipation in breaking solitary and periodic waves", unpublished manuscript.

Benjamin, T. B., 1967, "Instability of periodic wavetrains in nonlinear dispersive systems", Proc. Roy. Soc., A 299, 59-75.

Benjamin, T. B., and Feir, J. E., 1967, "The disintegration of wave trains on deep water. Part 1: Theory", J. Fluid Mech., 27(3), 417-430.

Benmoussa, C., 1983, "Evolution of surface wave packets over slowly varying depth and current", M. S. Thesis, Mass. Inst. Tech., Cambridge.

Berkhoff, J. C. W., 1972, "Computation of combined refraction-diffraction", Proc. 13th. Int. Conf. Coastal Engng., Vancouver.

Berkhoff, J. C. W., 1976, "Mathematical models for simple harmonic linear water waves: wave diffraction and refraction", Publ. no. 163, Delft Hydraulics Laboratory, Delft.

Berkhoff, J. C. W., 1982, "Refraction and diffraction of water waves: wave deformation by a shoal", Rept. W 154-VIII, Delft Hydraulics Laboratory.

Berkhoff, J. C. W., Booy, N., and Radder, A. C., 1982, "Verification of numerical wave propagation models for simple harmonic linear waves", Coastal Engrng., 6, 255-279.

Biesel, F., 1952, "Study of wave propagation in water of gradually varying depth", in Gravity Waves, Nat. Bureau of Standards, Circular 521, Washington.

Booij, N., 1981, "Gravity waves on water with non-uniform depth and current", Report no. 81-1, Dept. of Civil Engng., Delft Univ. of Technology, Delft.

Bouws, E., and Battjes, J. A., 1982, "A Monte Carlo approach to the computation of refraction of water waves", J. Geophys. Res., 87(C8), 5718-5722.

Bowen, A. J., 1969, "The generation of longshore currents on a plane beach", J. Mar. Res., 27(2), 206-215.

Bowen, A. J., Inman, D. L., and Simmons, V. P., 1968, "Wave 'set-down' and set-up", J. Geophys. Res., 73(8), 2569-2577.

Bretherton, F. P., and Garrett, C. J. R., 1968, "Wavetrains in inhomogeneous moving media", Proc. Roy. Soc., A 302, 529-554.

Carnahan, B., Luther, H. A., and Wilkes, J. O., 1969, Applied Numerical Methods, Wiley.

Christoffersen, J. B., 1982, "Current depth refraction of dissipative water waves", Series paper 30, Inst. Hydrodynamics and Hydraulic Engrng., Tech. Univ. Denmark, Lyngby.

Christoffersen, J. B., and Jonsson, I. G., 1980, "A note on wave action conservation in a dissipative current wave motion", Appl. Ocean Res., 2(4), 179-182.

Chu, V. H., and Mei, C. C., 1970a, "On slowly-varying Stokes waves", Report no. 125, Water Resources and Hydrodyn. Lab., Dept. of Civil Engrng., Mass. Inst. Tech., Cambridge.

Chu, V. H., and Mei, C. C., 1970b, "On slowly-varying Stokes waves", J. Fluid Mech., 41(4), 873-887.

Chu, V. H., and Mei, C. C., 1971, "The nonlinear evolution of Stokes waves in deep water", J. Fluid Mech., 47(2), 337-351.

Corones, J., 1975, "Bremmer series that correct parabolic approximations", J. Math. Anal. Applic., 50, 361-372.

Dally, W. R., 1980, "A numerical model for beach profile evolution", M.S. Thesis, University of Delaware, Newark.

Dalrymple, R. A., 1975, "A mechanism for rip current generation on an open coast", J. Geophys. Res., 80, 3485-3487.

Dalrymple, R. A., Kirby, J. T., and Hwang, P. A., 1983, "Wave diffraction due to areas of high energy dissipation", to appear in ASCE, J. Waterways, Port, Coast. and Ocean Div.

Dalrymple, R. A., and Liu, P. L-F., 1978, "Waves over soft muds: a two layer fluid model", J. Phys. Oceanography, 8, 1121-1131.

Davey, A. and Stewartson, K., 1974, "On three-dimensional packets of surface waves", Proc. Roy. Soc., A 338, 101-110.

Dean, R. G., 1965, "Stream function representation of nonlinear ocean waves", J. Geophys. Res., 70(18), 4561-4572.

Dean, R. G., 1974, "Evaluation and development of water wave theories for engineering application", Spec. Rept. 1, U. S. Army Corps of Engineers, Coast. Engrng. Res. Center, Fort Belvoir, Va.

Dean, R. G., and Dalrymple, R. A., 1983, Water Wave Mechanics for Scientists and Engineers, Prentice-Hall, in press.

Divoky, D., Le Mehaute, B., and Lin, A., 1970, "Breaking waves on gentle slopes", J. Geophys. Res., 75, 1681-1691.

Djordjevic, V. D., and Redekopp, L. G., 1978, "On the development of packets of surface gravity waves moving over an uneven bottom", J. App. Math. and Phys. (ZAMP), 29, 950-962.

Dysthe, K. B., 1979, "Note on a modification to the nonlinear Schrodinger equation for application to deep-water waves", Proc. Roy. Soc., A 369, 105-114.

Ebersole, B. A., and Dalrymple, R. A., 1980, "Numerical modeling of nearshore circulation", Proc. th Int. Conf. Coastal Engrng, Sydney,

Fair, J. E., 1967, "Discussion: some results from wave pulse experiments", Proc. Roy. Soc., A 299, 54-58.

Fermi, E., Pasta, J., and Ulam, S., 1955, "Studies of nonlinear problems", Doc. LA-1940, in Collected Papers of Enrico Fermi, Vol. 2.

Foda, M. A., and Mei, C. C., 1981, "Nonlinear excitation of long-trapped waves by a group of short swells", J. Fluid Mech., 111, 319-345.

Garrett, C. J. R., 1967, "Discussion: the adiabatic invariant for wave propagation in a nonuniform moving medium", Proc. Roy. Soc., A 299, 26-27.

Hales, L. Z., 1980, "Erosion control of scour during construction", TR HL-80-3, U. S. Army Corps of Engineers, Waterways Experiment Station, Vicksburg.

Hasimoto, H., 1982, "Numerical simulation of refraction and diffraction by the parabolic equation", Proc. 29th. Coastal Engineering Conf. in Japan, 115-119.

Hasimoto, H., and Ono, H., 1972, "Nonlinear modulation of gravity waves", J. Phys. Soc. Japan, 33(3), 805-811.

Hayes, W. D., 1970, "Conservation of action and modal wave action", Proc. Roy. Soc., A 320, 187-208.

Hedges, T. S., 1976, "An empirical modification to linear wave theory", Proc. Instn. Civil Engrs., 61(2), 575-579.

Hildebrand, F. B., 1976, Advanced Calculus for Applications, Prentice-Hall.

Horikawa, K., and Kuo, C-T., 1966, "A study of wave transformation inside surf zone", Proc. 10th Conf. Coastal Engng., Tokyo, 217-233.

Houston, J. R., 1981, "Combined refraction and diffraction of short waves using the finite element method", Appl. ocean Res., 3(4), 163-170.

Hui, W. H., and Hamilton, J., 1979, "Exact solutions of a three-dimensional nonlinear Schrodinger equation applied to gravity waves", J. Fluid Mech., 93(1), 117-133.

Ippen, A. T.(ed), Estuary and Coastline Hydrodynamics, McGraw- Hill.

Jeffrey, A., and Kawahara, T., 1982, Asymptotic Methods in Nonlinear Wave Theory, Pitman.

Jimenez, J., and Whitham, G. B., 1976, "An averaged Lagrangian method for dissipative wavetrains", Proc. Roy. Soc., A 349, 277-287.

Jonsson, I. G., 1981, "Booij's current-wave equation and the ray approximation", Prog. Rept. 54, pp. 7-20, Inst. Hydrodyn. and Hydraulic Engrng., Tech. Univ. Denmark.

Jonsson, I. G., Christoffersen, J. B., and Skovgaard, O., 1983, "A general computational method for current depth refraction of water waves", Proc. Int. Conf. on Coastal and Port Engrng. in Developing Countries, March 20-26, Colombo, Sri Lanka.

Keller, J. B., 1958, "Surface waves on water of non-uniform depth", J. Fluid Mech., 4, 607-614.

Kirby, J. T., and Dalrymple, R. A., 1982, "Numerical modeling of the nearshore region", ONR Tech. Rept. 11, Res. Rept. CE-82-24, Dept. of Civil Engrng., Univ. of Del., Newark.

Kirby, J. T., and Dalrymple, R. A., 1983a, "Propagation of obliquely incident water waves over a trench", J. Fluid Mech., 133, 47-63.

Kirby, J. T., and Dalrymple, R. A., 1983b, "A parabolic equation for the combined refraction-diffraction of Stokes' waves by mildly varying topography", submitted to J. Fluid Mech.

Kirby, J. T., and Dalrymple, R. A., 1983c, "Oblique envelope solutions of the Davey-Stewartson equations in intermediate water depth", to appear in Phys. Fluids.

Kirby, J. T., Dalrymple, R. A., and Liu, P. L.-F., 1981, "Modification of edge waves by barred-beach topography", Coastal Engrng., 5, 35-49.

Lassiter, J. B., 1972, "The propagation of water waves over sediment pockets", Ph.D. dissertation, Mass. Inst. Tech., Cambridge.

Lee, J.-J., 1971, "Wave-induced oscillations in harbours of arbitrary geometry", J. Fluid Mech., 45(2), 375-394.

Lighthill, M. J., 1965, "Contributions to the theory of waves in non-linear dispersive systems", J. Inst. Math. Applic., 1, 269-306.

Lighthill, M. J., 1967, "Some special cases treated by Whitham's theory", Proc. Roy. Soc., A 299, 28-53.

Liu, P. L.-F., 1973, "Damping of water waves over porous bed", ASCE J. Hydraulics Div., 99, HY12, 2263-2271.

Liu, P. L.-F., 1982, "Combined refraction and diffraction: comparison of theory and experiments", J. Geophys. Res., 87(C8), 5723-5730.

Liu, P. L.-F., and Abbaspour, M., 1982, "An integral equation method for the diffraction of oblique waves by an infinite cylinder", Int. J. Num. Meth. Engrng., 18(10), 1497-1504.

Liu, P. L.-F., Lozano, C. J., and Pantazaras, N., 1979, "An asymptotic theory of combined wave refraction and diffraction", Applied Ocean Res., 1(3), 137-146.

Liu, P. L.-F., and Mei, C. C., 1976, "Water motion on a beach in the presence of a breakwater 1. Waves", J. Geophys. Res., 81(18), 3079-3084.

Liu, P. L.-F., and Tsay, T.-K., 1983, "On weak reflection of water waves", J. Fluid Mech., to appear.

Longuet-Higgins, M. S., 1970, "Longshore currents generated by obliquely incident sea waves, 1", J. Geophys. Res., 75(33), 6778-6789.

Longuet-Higgins, M. S., and Stewart, R. W., 1962, "Radiation stress and mass transport in gravity waves, with application to 'surf beats' ", J. Fluid Mech., 13, 481-504.

Longuet-Higgins, M. S., and Stewart, R. W., 1963, "A note on wave setup", J. Mar. Res., 21(1), 4-10.

Longuet-Higgins, M. S., and Stewart, R. W., 1964, "Radiation stresses in water waves; a physical discussion, with applications", Deep-Sea Research, 11, 529-562.

Lozano, C., and Liu, P. L.-F., 1980, "Refraction-diffraction model for linear surface water waves", J. Fluid Mech., 101(4), 705-720.

Ludwig, D., 1966, "Uniform asymptotic expansions at a caustic", Comm. Pure Appl. Math., 19, 215-250.

Luke, J. C., 1967, "A variational principle for a fluid with a free surface", J. Fluid Mech., 27(2), 395-397.

Madsen, O. S., 1976, "Wave climate of the continental margin", in Marine Sediment Transport and Environment, Stanley, D. J., and Swift, J. P. (eds.), Wiley-Interscience.

Mallard, W. W., 1978, "Investigation of the effect of beach slope on the breaking height to depth ratio", M. S. thesis, Univ. of Delaware, Newark.

McDaniel, S. T., 1975, "Parabolic approximations for underwater sound propagation", J. Acoust. Soc. Am., 58(6), 1178-1185.

Mei, C. C., 1982, The Applied Dynamics of Ocean Surface Waves, Wiley-Interscience.

Miles, J. W., 1978, "On the second Painlevé transcendent", Proc. Roy. Soc., A 361, 277-291.

Newell, A. C., 1978, "Nonlinear tunneling", J. Math. Phys., 19(5), 1126-1133.

O'Brien, M. P., and Mason, "A summary of the theory of oscillatory waves", Tech. Rept. 2, Beach Erosion Board.

Ostrovskii, L. A., and Pelinovskii, E. N., 1972, "Method of averaging and the generalized variational principle for nonsinusoidal waves", J. Appl. Math. Mech., 36, 63-70.

Pantazaras, N., 1979, "Combined refraction and diffraction of water waves", M. S. Thesis, Cornell University, Ithaca.

Peregrine, D. H., 1983, "Wave jumps and caustics in the propagation of finite amplitude water waves", in preparation.

Peregrine, D. H., and Smith, R., 1979, "Nonlinear effects on waves near caustics", Phil. Trans. Roy. Soc., A 292, 341-370.

Phillips, O. M., 1960, "On the dynamics of unsteady gravity waves of finite amplitude. Part 1. The elementary interactions", J. Fluid Mech., 9, 193-217.

Phillips, O. M., 1977, The Dynamics of the Upper Ocean, 2nd ed., Cambridge Univ. Press.

Radder, A. C., 1979, "On the parabolic equation method for water-wave propagation", J. Fluid Mech., 95(1), 159-176.

Raichlen, F., and Lee, J-J., 1978, "An inclined-plate wave generator", Proc. 16th Int. Conf. Coastal Engrng., Hamburg, 388-399.

Reid, R. O., and Kajiura, K., 1957, "On the damping of gravity waves over a permeable seabed", Trans. Amer. Geophys. Union, 58, 662-666.

Saffman, P. G., and Yuen, H. C., 1978, "Stability of a plane soliton to infinitesimal two-dimensional perturbations", Phys. Fluids, 21(8), 1450-1451.

Savitsky, D., 1970, "Interaction between gravity waves and finite turbulent flow fields", Proc. 8th Symp. Naval Hydrodynamics, 389-447.

Skovgaard, O., Jonsson, I. G., and Bertelsen, J. A., "Computation of wave heights due to refraction and friction", ASCE, J. Waterways, Harbors and Coastal Engrng. Div., 101 WW1, 15-32.

Smith, R., 1976a, "Triple roots and cusped caustics for surface gravity waves", in Waves on Water of Variable Depth, (ed.) Provis, D. G., and Radok, R., Springer-Verlag.

Smith, R., 1976b, "Giant waves", J. Fluid Mech., 77(3), 417-431.

Smith, R., and Sprinks, T., 1975, "Scattering of surface waves by a conical island", J. Fluid Mech., 72(2), 373-384.

Stokes, G. G., 1847, "On the theory of oscillatory waves", Trans. Camb. Phil. Soc., 8, 441-

Thomas, G. P., 1979, "Water wave-current interactions: a review", in Shaw, T. L. (ed.), Mechanics of Wave-induced Forces on Cylinders, Pitman.

Tsay, T.-K., and Liu, P. L-F., 1982, "Numerical solution of water-wave refraction and diffraction problems in the parabolic approximation", J. Geophys. Res., 87(C10), 7932-7940.

Turpin, F.-M., 1981, "Interaction between waves and current over a variable depth", M.S. Thesis, Massachusetts Inst. Tech., Cambridge.

Turpin, F.-M., Benmoussa, C., and Mei, C. C., 1983, "Effects of slowly varying depth and current on the evolution of a Stokes wave packet", to appear in J. Fluid Mech.

Ursell, F., 1952, "Edge waves on a sloping beach", Proc. Roy. Soc., A 214, 79-97.

Walker, J. R., 1976, "Refraction of finite-height and breaking waves", Proc. 15th. Int. Conf. Coastal Engng., Honolulu.

Whitham, G. B., 1962, "Mass, momentum and energy flux in water waves", J. Fluid Mech., 12, 135-147.

Whitham, G. B., 1967, "Non-linear dispersion of water waves", J. Fluid Mech., 27(2), 399-412.

Whitham, G. B., 1970, "Two-timing, variational principles and waves", J. Fluid Mech., 44(2), 373-395.

Whitham, G. B., 1974, Linear and Nonlinear Waves, Wiley.

Wu, C-S., 1983, Ph.D. dissertation, Cornell.

Yue, D. K.-P., 1980, "Numerical study of Stokes wave diffraction at grazing incidence", Sc. D. dissertation, Dept. of Civil Engng., Mass. Inst. Tech., Cambridge.

Yue, D. K.-P., and Mei, C. C., 1980, "Forward diffraction of Stokes' waves by a thin wedge", J. Fluid Mech., 99(1), 33-52.

Yuen, H. C., and Lake, B. M., 1975, "Nonlinear deep water waves: theory and experiment", Phys. Fluids, 18(8), 956-960.

Yuen, H. C. and Lake, B. M., 1982, "Nonlinear dynamics of deepwater gravity waves", Adv. Appl. Mech., 22, 67-229.

...

APPENDIX A. THE STOKES SOLUTION TO $O(\delta)$ IN THE
PRESENCE OF A CURRENT

In this appendix, the series solution of Chu and Mei(1970a) is extended to include the case of an $O(1)$ mean current $\underline{u}(\underline{x}, t)$, given by

$$\underline{u} = \nabla_h \phi_{-10} \quad (A.1)$$

where $\phi_{-10}(\underline{x}, z, t)$ is the leading term in a Stokes expansion and is $O(\epsilon^{-1})$. The term ϕ_{-10} is assumed to be slowly varying in time. The ambient current is then of $O(\epsilon^{-1}\delta)$, or, equivalently, $O(1)$ in the present context. In this appendix, the notation of Chu and Mei(1970a) is used for convenience, with the consequence that the ordering subscripts for quasi-steady terms and $O(\delta)$ contributions are respectively one order smaller or larger than in the main body of the text.

The series solution of Chu and Mei for ϕ and η is given by (after substituting the modulation scale δ for the equivalently valued parameter ϵ where appropriate)

$$\begin{aligned} \phi &= \epsilon \phi_{11} e^{i\psi} + * + \delta^{-1} \epsilon^2 \phi_{10} + \delta \epsilon \phi_{21} e^{i\psi} + * + \\ &+ \epsilon^2 \phi_{22} e^{2i\psi} + * + \dots \end{aligned} \quad (A.2)$$

$$\begin{aligned} \eta &= \epsilon \eta_{11} e^{i\psi} + * + \epsilon^2 \eta_{20} + \delta \epsilon \eta_{21} e^{i\psi} + * \\ &+ \epsilon^2 \eta_{22} e^{2i\psi} + * + \dots \end{aligned} \quad (A.3)$$

where

$$\begin{aligned} \phi_{11} &= -\frac{ig}{2\omega} A_{11} f_{10} \quad , \quad \phi_{22} = -i \frac{3\omega}{16} A_{11}^2 f_{20} \\ \phi_{21} &= -\frac{g}{2\omega} A_{11} (\alpha_1 f_{11} + \alpha_2 f_{12} + \alpha_3 f_{13}) \end{aligned} \quad (A.4)$$

and * denotes the complex conjugate of the preceding term. The terms f_{10} - f_{20} are given in (2.3.2) and (2.3.5). Here, the α 's are given in terms of the absolute frequency ω :

$$\alpha_2 = \frac{\nabla_h \cdot \left\{ \frac{k}{R} \left(\frac{A_{11}}{\omega} \right)^2 \right\}}{2k \left(\frac{A_{11}}{\omega} \right)^2} \quad (A.5)$$

The lowest order quasisteady term in the expression for ϕ is ϕ_{10} , which is related to the second order wave-induced current. It is desired to alter the expansion to include a term of $O(\epsilon^{-1})$ which leads to an $O(1)$ current \underline{u} upon

differentiation.

For the standard, slowly modulated form of the Stokes expansion, neglecting ϕ_{21} and η_{21} , it is well known that the inclusion of a constant mean current \underline{u} leads to an expression for the relative (or intrinsic) frequency σ ,

$$\sigma = \omega - \underline{k} \cdot \underline{u} \quad (\text{A.6})$$

The terms in the expansion of ϕ are merely adjusted to account for the frequency shift by means of a Galilean transformation; see Thomas(1979). Thus ϕ_{11} and ϕ_{22} are altered to the form

$$\phi_{11} = \frac{-i\alpha}{2\sigma} A_{11} f_{10} \quad , \quad \phi_{22} = -i \frac{3\sigma}{16} A_{11}^2 f_{20} \quad (\text{A.7})$$

We must now determine the corresponding form of the fast modulation term ϕ_{21} , as well as any higher order terms due to the addition of the slowly varying term at $O(\epsilon^{-1})$. As mentioned in Chu and Mei(1970a), we may obtain this expression in the context of an expansion for linear waves; this is particularly clear if we consider ϕ_{21} as a term of $O(\epsilon, \delta)$. Correspondingly, we choose expansions of the form (see Chu and Mei(1970a))

$$\phi = \epsilon^{-1} \phi_{-10} + \phi_{00} + \sum_{n=1}^{\infty} \epsilon^n \sum_{m=-1}^1 \phi_{nm} e^{im\psi} \quad (\text{A.8a})$$

and

$$\eta = \eta_{00} + \sum_{n=1}^{\infty} \epsilon^n \sum_{m=1}^1 \eta_{nm} e^{im\psi} \quad (\text{A.8b})$$

where $|m| < 1$ since we do not need to consider the higher harmonics arising in the nonlinear problem. The governing equations are written in the form

$$\phi_{xx} + \phi_{yy} + \phi_{zz} = 0 \quad -h_0 \leq z \leq \eta \quad (\text{A.9a})$$

$$\phi_z + \nabla_h \phi \cdot \nabla_h h_0 = 0 \quad z = -h_0 \quad (\text{A.9b})$$

$$\phi_{tt} + g \phi_z + \left(\frac{\partial}{\partial t} + \frac{1}{2} \nabla \phi \cdot \nabla \right) |\nabla \phi|^2 = 0 \quad z = \eta \quad (\text{A.9c})$$

after elimination of η from the free surface boundary conditions. Equations (A.9a-b) are sufficient to obtain the results desired here. The free surface boundary condition is used to provide consistency conditions which will be obtained separately by the variational approach in Chapter 3. As an exception, we will use (A.9c) to verify the dispersion relation (2.1.6).

The expansions (A.8) are substituted into the

equations (A.9), leading to the set of equations

$$\phi_{nm} z z - m^2 k^2 \phi_{nm} = R_{nm} \quad ; \quad -h_0 \leq z \leq \eta_{00} \quad (\text{A.10a})$$

$$\phi_{nm z} = F_{nm} \quad ; \quad z = -h_0 \quad (\text{A.10b})$$

$$g \phi_{nm z} - m^2 \omega^2 \phi_{nm} = G_{nm} \quad ; \quad z = \eta_{00} \quad (\text{A.10c})$$

where, for each order n , the terms R , G , and F are determined in terms of lower order quantities or corrections to the absolute frequency ω . The Taylor series expansion of the free surface condition (A.9.c) is made with respect to the $O(1)$ free surface position $z = \eta_{00}$, since this is the total depth occupied by the current $\nabla_h \dot{\phi}_{-10}$ in the absence of waves. We define a shifted vertical coordinate $z' = z - \eta_{00}$; the free surface conditions are then applied to the position $z' = 0$, while the total depth influencing the wave motions is given by $h = h_0 + \eta_{00}$. We find that, to lowest order,

$$R_{-10} = F_{-10} = G_{-10} = 0$$

and (A.10a-b) are satisfied by $\dot{\phi}_{-10} = \dot{\phi}_{-10}(x, y, t)$. The lowest order component of the ambient current thus does not vary

over the depth, which is consistent with the neglect of friction in the formulation.

Turning now to the problem for $m=0, n=0$, it is found that

$$R_{00} = F_{00} = G_{00} = 0$$

leading to a homogeneous problem for $\dot{\phi}_{00}$. Foda and Mei (1981) have used $\dot{\phi}_{00}$ to allow for the resonant growth of a long forced wave driven by the $O(\epsilon)$ wave field. This effect is not central to our present concerns, and we neglect $\dot{\phi}_{00}$. The problem at $m=0, n=1$ is altered from Chu and Mei's problem due to forcing by the $n=-1$ current, and the coefficients R_{10}, F_{10} , and G_{10} take on the values

$$R_{10} = -\nabla_h^2 \phi_{-10}$$

$$F_{10} = -\nabla_h h_0 \cdot \nabla_h \phi_{-10}$$

and

$$G_{10} = -\phi_{-10} \epsilon \epsilon - \nabla_h (\phi_{-10} \epsilon) - \frac{1}{2} \nabla_h \phi_{-10} \cdot \nabla_h (|\nabla_h \phi_{-10}|^2) - g \eta_{00} \nabla_h^2 \phi_{-10}$$

whereas in Chu and Mei's study the corresponding problem is homogeneous. The inhomogeneous problem for $\dot{\phi}_{10}$ is given by

$$\phi_{10} \epsilon \epsilon = R_{10} \quad -h \leq z' \leq 0 \quad (\text{A.11a})$$

$$\sigma_f \dot{\phi}_{10} \epsilon = G_{10} \quad z' = 0 \quad (\text{A.11b})$$

and

$$\phi_{10z} = F_{10} \quad z' = -h \quad (\text{A.11c})$$

In previous studies where the largest current is smaller than $O(1)$, has been identifiable completely as the wave-induced current component. Here, the homogeneous solution of (A.13), denoted as ϕ_{10}' , will be identified with the wave induced current. The remaining problem for the particular solution ϕ_{10}'' can then be solved directly using (A.11 a,c), leading to the result

$$\phi_{10}'' = -\frac{(h+z')^2}{2} \nabla_h^2 \phi_{-10} - (h+z') \nabla_h h_0 \cdot \nabla_h \phi_{-10} \quad (\text{A.12})$$

The potential ϕ_{10}'' represents a higher order correction to the $O(1)$ ambient current, and could play a similar role in the overall wave-current problem as the wave-induced current ϕ_{10}' , in the sense that both may lead to small wavenumber corrections at third order through wave current interaction. It should be noted that ϕ_{10}'' is essentially an $O(\delta)$ correction to ϕ , as is ϕ_{21} , and in that sense can also be dropped from consideration in the context of a mild-slope formulation.

Turning to the problem for the wave component at

$n=1, m=1$, we find that $R_{11} = F_{11} = 0$, while

$$G_{11} = \left\{ 2\omega \underline{k} \cdot \nabla_h \phi_{-10} + (\underline{k} \cdot \nabla_h \phi_{-10})^2 \right\} \phi_{11}$$

Using (A.6) as a definition for σ , the free surface boundary condition (A.10c) can be written as

$$g \phi_{11z} - \sigma^2 \phi_{11} = 0, \quad z' = 0 \quad (A.13)$$

The solution to the homogeneous problem (A.10a-b) is given by

$$\phi_{11} = \frac{-ig}{2\sigma} A_{11} f_{10}$$

in agreement with (A.7), and the value of the coefficient has been chosen to give an amplitude A_{11} for the linear wave component. Substituting ϕ_{11} into the free surface boundary condition (A.13) gives the result

$$\sigma^2 = gk \tanh kh$$

thus verifying the dispersion relation given in section (2.1).

At $n=2, m=1$, F_{21} and R_{21} take on the values

$$F_{21} = -\nabla_h h \cdot \{ i k \phi_{11} \} \Big|_{z' = -h}$$

$$R_{21} = -i \nabla_h \cdot \{ k \phi_{11} \} - i k \cdot \nabla_h \phi_{11}$$

The solution for ϕ_{21} is then given by

$$\begin{aligned} \phi_{21} = & \cosh k(h+z') \left\{ c_1 - \frac{1}{k^2} \int_{-h}^{z'} R_{21} \sinh k(h+\xi) d\xi \right\} + \\ & + \sinh k(h+z') \left\{ c_2 + \frac{1}{k^2} \int_{-h}^{z'} R_{21} \cosh k(h+\xi) d\xi \right\} \quad (A.14) \end{aligned}$$

where c_1 and c_2 are coefficients of the homogeneous solution, and where we have used the method of variation of parameters (see, for example, Hildebrand(1976), p.24-26). Application of the bottom boundary condition (A.10b) gives the result

$$c_2 = F_{21} / k$$

while c_1 remains formally arbitrary. After performing the required integration and choosing a value for c_1 consistent with the form of ϕ_{11} , ϕ_{21} is given by

$$\begin{aligned} \phi_{21} = & -\frac{ig}{2\sigma} A_{21} f_{10} - \frac{gA_{11}}{2\sigma} \left\{ \alpha_1 k(h+z') f_{10} + \right. \\ & \left. + \alpha_2 k(h+z') \frac{\sinh k(h+z')}{\cosh kh} + \alpha_3 [k(h+z')]^2 f_{10} \right\} \end{aligned} \quad (A.15)$$

Neglecting the homogeneous term in A_{21} leads to the solution of Biesel(1951), corrected for the presence of a current. Chu and Mei(1970a) noted that ϕ_{21} becomes unbounded in the limit of deep water. Therefore A_{21} is retained and chosen so that ϕ_{21} remains formally bounded in the deep water limit, yielding the results of Chu and Mei corrected for the presence of a current:

$$\phi_{21} = -\frac{gA_{11}}{2\sigma} \left\{ \alpha_1 f_{11} + \alpha_2 f_{12} + \alpha_3 f_{13} \right\} \quad (A.16)$$

where α_2 is given by

$$\alpha_2 = \frac{\nabla_h \cdot \left\{ \frac{k}{k} \left(\frac{A_{11}}{\sigma} \right)^2 \right\}}{2k \left(\frac{A_{11}}{\sigma} \right)^2}$$

The appropriate form of the wavelike components of Chu and Mei's solution is thus obtained for our study simply by

replacing the absolute frequency ω by the relative frequency σ in each term in ϕ . It should be noted that α_2 will in general be a function of the variation of the $O(1)$ current, thus greatly complicating the expressions involving α_2 and derivatives of α_2 .

The results of the perturbation expansion give the form of ϕ and η required for the problem formulated in Chapter 2. They are given by

$$\begin{aligned} \phi = & \delta^{-1} \phi_{-10} + \epsilon \phi_{11} e^{i\psi} + * + \epsilon \delta \phi_{21} e^{i\psi} + * + \\ & + \delta^{-1} \epsilon^2 \phi'_{10} + \delta \phi''_{10} + \epsilon^2 \phi_{22} e^{2i\psi} + * + \dots \end{aligned} \quad (A.17a)$$

and

$$\begin{aligned} \eta = & \eta_{00} + \epsilon \eta_{11} e^{i\psi} + * + \epsilon \delta \eta_{21} e^{i\psi} + * + \\ & + \epsilon^2 \eta'_{20} + \delta^2 \eta''_{20} + \epsilon^2 \eta_{22} e^{2i\psi} + * + \dots \end{aligned} \quad (A.17b)$$

where the two values of η_{20} correspond to the split of ϕ_{10} .

APPENDIX B. PERTURBATION METHOD FOR THE LAGRANGIAN

The Lagrangian L for an expanded dependent variable $f = \epsilon^n f_n$, $n=0,1,2,\dots$, may be derived by substituting the assumed expansion for f into the appropriate form of L . By retaining the ordering parameter ϵ , L may then itself be expanded in the form

$$L = \epsilon^n L_n \quad ; \quad n \geq \sigma \quad (\text{B.1})$$

If L is in general nonlinear, then lowest order terms which are quadratic in f_n will appear first in L_{2n} ; subsequently, variation of L_{2n} with respect to f_n leads to a linear governing equation for f_n , containing forcing terms involving lower order terms f_m , $m < n$. The exception to this rule may occur at $O(1)$, or $n=0$, where the governing equation for an $O(1)$ quantity f_0 may not be reduced to a linear form; this will be seen in the problem for the ambient current in Chapter 3.

As an example, consider the one-dimensional Duffing equation:

$$\ddot{f} + f + \epsilon f^3 = 0 \quad (\text{B.2})$$

A Lagrangian corresponding to (B.2) may be written as

$$L = \frac{f^2}{2} - \frac{\dot{f}^2}{2} + \epsilon \frac{f^4}{4} \quad (\text{B.3})$$

Here, ($\dot{}$) denotes differentiation with respect to the independent variable. Let an expansion for f be given by

$$f = \epsilon^n f_n ; n \geq 0 . \quad (\text{B.4})$$

(B.4) is then substituted into (B.3) and ordered into the form (B.1), where

$$L_0 = \frac{f_0^2}{2} - \frac{\dot{f}_0^2}{2} \quad (\text{B.5a})$$

$$L_1 = f_0 f_1 - \dot{f}_0 \dot{f}_1 + f_0^4 / 4 \quad (\text{B.5b})$$

$$L_2 = \frac{f_1^2}{2} - \frac{\dot{f}_1^2}{2} + f_0^3 f_1 + f_0 f_2 - \dot{f}_0 \dot{f}_2 \quad (\text{B.5c})$$

etc.

Proceeding in a consistent manner, the lowest order contribution to L , given by L_0 , is varied with respect to the lowest order unknown contribution to f , given by f_0 , yielding, after partial integration

$$f_0 + \ddot{f}_0 = 0 \quad (\text{B.6a})$$

Then, regarding f_0 as known (as determined by (B.6a)), the next lowest order term L_1 is varied with respect to the lowest order unknown f_1 , yielding (B.6a) as a redundant condition. Thus L_1 , which is linear in the lowest order unknown, yields no information concerning the unknown. Then, L_2 is varied by the still unknown f_1 , yielding the governing equation

$$f_1 + \ddot{f}_1 + f_0^3 = 0 \quad (\text{B.6b})$$

This process may be continued indefinitely. (B.6a) and (B.6b) are identical to the results obtained by applying a regular perturbation scheme directly to (B.2), and (B.6b) is known to produce a secular result, which may be removed by a stretching of the independent variable. For the water wave problem to be studied, the corresponding secularity appears at $O(\epsilon^3)$, resulting from L_6 ; since it will be sufficient to carry the calculations to L_4 , the perturbation scheme will be regular in nature.

While the treatment presented here for the Duffing equation does not represent a computational advantage over the normal procedure of perturbing the governing differential equation directly, the advantage becomes apparent in the case of problems containing cross-spaces, where the form of f is known and separable. Then, use of

the Lagrangian integrated over the cross space leads directly to variational principles governing motion in the propagation space. The corresponding governing equations are obtained in the multiple scale expansions as solvability conditions related to higher order inhomogeneous problems.

APPENDIX C. DERIVATION OF L AND THE EULER EQUATION
FOR $\tilde{\phi}_1$

Due to the complexity of the calculations leading to the expression for L and the resulting Euler equations, the derivations are presented here in some detail, with L being derived in section 1. In section 2, the Euler equation for the wave component $\tilde{\phi}_1$ is derived.

C.1 The Lagrangian L

The series form for ϕ and η are given by

$$\begin{aligned} \phi = & \delta^{-1} \phi_0 + \epsilon \{ f_{10} - i \delta (\alpha_1 f_{11} + \alpha_2 f_{12} + \alpha_3 f_{13}) \} \tilde{\phi}_1 + \\ & + \delta^{-1} \epsilon^2 \phi_2' + \epsilon^2 f_{20} \tilde{\phi}_2 - (\gamma_0 + \epsilon^2 \gamma_2) t + O(\epsilon^3, \delta^2) \end{aligned} \quad (C.1.1)$$

and

$$\eta = b_0 + \epsilon \eta_1 + \epsilon^2 (\eta_2 + b_2) + O(\epsilon^3) \quad (C.1.2)$$

Also, ϕ_0 is expanded in powers of δ to give

$$\phi_0 = \phi_0' + \delta^2 \phi_0'' \quad (C.1.3)$$

where

$$\phi_0' = \phi_0'(\underline{x}, t) \quad (C.1.4)$$

and

$$\phi_0'' = -\frac{(h+z)^2}{2} \nabla_h^2 \phi_0' - (h+z) \nabla_h h \cdot \nabla_h \phi_0' \quad (C.1.5)$$

The evaluation of L requires the quantities ϕ_t and $\nabla \phi$, which are given by

$$\begin{aligned} \phi_t = & \delta^2 \phi_{0t}' + \delta^4 \phi_{0t}'' + \epsilon \left(f_{10} - i \delta \sum_{j=1}^3 \alpha_j f_{1j} \right) \tilde{\phi}_{1t} \\ & + \epsilon^2 \phi_{2t}' + \epsilon^2 f_{20} \tilde{\phi}_{2t} - \gamma_0 - \epsilon^2 \gamma_2 \end{aligned} \quad (C.1.6)$$

where we have invoked the condition that $\partial/\partial z$ of the ambient current is $O(\delta^3)$, and

$$\begin{aligned} \nabla \phi = & \nabla_h \phi + \phi_z \hat{z} \\ = & \nabla_h \phi_0' + \delta^2 \nabla_h \phi_0'' + \epsilon \delta \nabla_h \left\{ f_{10} - i \delta \sum_{j=1}^3 \alpha_j f_{1j} \right\} \tilde{\phi}_1 \\ & + \epsilon \left\{ f_{10} - i \delta \sum_{j=1}^3 \alpha_j f_{1j} \right\} \nabla_h \tilde{\phi}_1 + \end{aligned}$$

$$\begin{aligned}
& + \epsilon^2 \nabla_h \phi_2' + \epsilon^2 \delta \nabla_h f_{20} \tilde{\phi}_2 + \epsilon^2 f_{20} \nabla_h \tilde{\phi}_2 + \\
& + \left\{ \delta \phi_0'' + \epsilon \left[f_{10} - i \delta \sum_{j=1}^3 \alpha_j f_{ij} \right] \tilde{\phi}_1 + \right. \\
& \left. + \epsilon^2 f_{20} \tilde{\phi}_2 \right\} \tilde{\phi}_2 \quad (C.1.7)
\end{aligned}$$

The expression for $(\nabla\phi)^2$ only needs to retain terms to $O(\epsilon^2, \delta^2)$ and $O(\epsilon^4)$, and can then be written as (where δ 's have been dropped for convenience)

$$\begin{aligned}
\frac{(\nabla\phi)^2}{2} &= \frac{(\nabla_h \phi_0')^2}{2} + \nabla_h \phi_0' \cdot \nabla_h \phi_0'' + \epsilon^2 (\nabla_h f_{10})^2 \frac{\tilde{\phi}_1^2}{2} \\
&+ \epsilon^2 F^2 \frac{(\nabla_h \phi_1)^2}{2} + \epsilon^4 \frac{(\nabla_h \phi_2')^2}{2} + \epsilon^4 f_{20}^2 \frac{(\nabla_h \tilde{\phi}_2)^2}{2} \\
&+ \epsilon \nabla_h F \cdot \nabla_h \phi_0' \tilde{\phi}_1 + \epsilon F \nabla_h \phi_0' \cdot \nabla_h \tilde{\phi}_1 + \epsilon^2 \nabla_h \phi_0' \cdot \nabla_h \phi_2' \\
&+ \epsilon^2 \nabla_h f_{20} \cdot \nabla_h \phi_0' \tilde{\phi}_2 + \epsilon^2 f_{20} \nabla_h \phi_0' \cdot \nabla_h \tilde{\phi}_2 + \epsilon^2 \nabla_h \phi_0'' \cdot \nabla_h \phi_2' \\
&+ \epsilon^2 f_{10} \nabla_h \phi_0'' \cdot \nabla_h \tilde{\phi}_1 + \epsilon^2 f_{20} \nabla_h \phi_0'' \cdot \nabla_h \tilde{\phi}_2 \\
&+ \epsilon^2 \left\{ f_{10} \nabla_h F - i (\nabla_h f_{10}) \sum_{j=1}^3 \alpha_j f_{ij} \right\} \cdot (\nabla_h \tilde{\phi}_1) \tilde{\phi}_1 \\
&+ \epsilon^3 (\nabla_h f_{10} \cdot \nabla_h \phi_2') \tilde{\phi}_1 + \epsilon^3 f_{20} (\nabla_h f_{10} \cdot \nabla_h \tilde{\phi}_2) \tilde{\phi}_1
\end{aligned}$$

$$\begin{aligned}
& + \epsilon^3 f_{10} (\nabla_h f_{20} \cdot \nabla_h \tilde{\phi}_1) \tilde{\phi}_2 + \epsilon^3 F f_{20} (\nabla_h \tilde{\phi}_1 \cdot \nabla_h \tilde{\phi}_2) \\
& + \epsilon^4 f_{20} (\nabla_h \phi_2' \cdot \nabla_h \tilde{\phi}_2) + \frac{(\phi_{0z}''')^2}{2} + \epsilon^2 F_z^2 \frac{\tilde{\phi}_1^2}{2} \\
& + \epsilon^4 f_{20z}^2 \frac{\tilde{\phi}_2^2}{2} + \epsilon F_z \phi_{0z}'' \tilde{\phi}_1 + \epsilon^2 f_{20z} \phi_{0z}'' \tilde{\phi}_2 \\
& + \epsilon^3 F_z f_{20z} \tilde{\phi}_1 \tilde{\phi}_2
\end{aligned} \tag{C.1.8}$$

where

$$F = f_{10} - i \sum_{j=1}^3 \alpha_j f_{1j} \tag{C.1.9}$$

The expressions ϕ_t , $\frac{(\nabla\phi)^2}{2}$, and gz must now be integrated from the bottom to the instantaneous free surface η . The integrals of the known cross-space dependencies are expressed in terms of the symbolic values G and \mathcal{A} , which are defined in Appendix D and evaluated where necessary. The integration results in

$$\begin{aligned}
\mathbb{I}_1 &= \int_{-h_0}^{\eta} gz \, dz = g \frac{\eta^2}{2} - g \frac{h_0^2}{2} \\
&= g \frac{(b_0^2 - h_0^2)}{2} + \epsilon g b_0 \eta_1 + \epsilon^2 g b_0 (b_2 + \eta_2) \\
&\quad + \epsilon^2 g \frac{\eta_1^2}{2} + \epsilon^3 g \eta_1 (\eta_2 + b_2) + \epsilon^4 g \frac{(\eta_2 + b_2)^2}{2} \tag{C.1.10}
\end{aligned}$$

$$\begin{aligned}
I_2 = \int_{-h_0}^{\eta} \phi_t dz &= \phi'_{0t}(h_0 + \eta) + \epsilon \left\{ G_0 - i \sum_{j=1}^3 \alpha_j G_j \right\} \tilde{\phi}_{1t} \\
&+ \epsilon^2 (h_0 + \eta) \phi'_{2t} + \epsilon^2 \mathcal{G} \tilde{\phi}_{2t} \\
&- (h_0 + \eta) (\gamma_0 + \epsilon^2 \gamma_2) \quad (C.1.11)
\end{aligned}$$

and

$$\begin{aligned}
I_3 &= \int_{-h_0}^{\eta} \frac{(\nabla \phi)^2}{2} dz \\
&= (h_0 + \eta) \frac{(\nabla_h \phi'_0)^2}{2} + \epsilon^2 G_{\nabla_0 \nabla_0} \frac{\tilde{\phi}_1^2}{2} + \epsilon^2 \int_{-h_0}^{\eta} F^2 dz \frac{(\nabla_h \tilde{\phi}_1)^2}{2} \\
&+ \epsilon^4 (h_0 + \eta) \frac{(\nabla_h \phi'_2)^2}{2} + \epsilon^4 \mathcal{G}^2 \frac{(\nabla_h \tilde{\phi}_2)^2}{2} + \int_{-h_0}^{\eta} \nabla_h \phi'_0 \cdot \nabla_h \phi''_0 dz \\
&+ \epsilon \nabla_h \phi'_0 \cdot \int_{-h_0}^{\eta} \nabla_h F dz \tilde{\phi}_1 + \epsilon \left\{ G_0 - i \sum_{j=1}^3 \alpha_j G_j \right\} \nabla_h \phi'_0 \cdot \nabla_h \tilde{\phi}_1 \\
&+ \epsilon \int_{-h_0}^{\eta} f_{10} \nabla_h \phi''_0 dz \cdot \nabla_h \tilde{\phi}_1 + \epsilon^2 (h_0 + \eta) \nabla_h \phi'_0 \cdot \nabla_h \phi'_2 \\
&+ \epsilon^2 (\nabla_h \phi''_0 \cdot \nabla_h \phi'_2) (h_0 + \eta) + \epsilon^2 \mathcal{G} \nabla_h \phi''_0 \cdot \nabla_h \tilde{\phi}_2 \\
&+ \epsilon^2 \mathcal{G}_{\nabla} \cdot \nabla_h \phi'_0 \tilde{\phi}_2 + \epsilon^2 \mathcal{G} \nabla_h \phi'_0 \cdot \nabla_h \tilde{\phi}_2 \\
&+ \epsilon^2 \left[\left\{ G_{000} - i \sum_{j=1}^3 \alpha_j G_{0\nabla j} - i \sum_{j=1}^3 (\nabla_h \alpha_j) G_{0j} - i \sum_{j=1}^3 \alpha_j G_{\nabla 0 j} \right\} \cdot \nabla_h \tilde{\phi}_1 \right] \tilde{\phi}_1 +
\end{aligned}$$

$$\begin{aligned}
& + \epsilon^3 (G_{\nabla 0} \cdot \nabla_h \phi_2') \tilde{\phi}_1 + \epsilon^3 (G_{\nabla 0} \cdot \nabla_h \tilde{\phi}_2) \tilde{\phi}_1 + \epsilon^3 (G_{\nabla 0} \cdot \nabla_h \tilde{\phi}_1) \tilde{\phi}_2 \\
& + \epsilon^3 \left\{ G_0 - i \sum_{j=1}^3 \alpha_j G_j \right\} \nabla_h \tilde{\phi}_1 \cdot \nabla_h \tilde{\phi}_2 + \epsilon^4 G \nabla_h \phi_2' \cdot \nabla_h \tilde{\phi}_2 \\
& + \int_{-h_0}^{\eta} \frac{(\phi_{0z}''')^2}{z} dz + \epsilon^2 \int_{-h_0}^{\eta} (F_z)^2 dz \frac{\tilde{\phi}_1^2}{z} + \epsilon^4 G^{zz} \frac{\tilde{\phi}_2^2}{z} \\
& + \epsilon \int_{-h_0}^{\eta} F_z \phi_{0z}'' dz \tilde{\phi}_1 + \epsilon^2 \int_{-h_0}^{\eta} f_{2z} \phi_{0z}'' dz \tilde{\phi}_2 \\
& + \epsilon^3 \left\{ G_0^z - i \sum_{j=1}^3 \alpha_j G_j^z \right\} \tilde{\phi}_1 \tilde{\phi}_2
\end{aligned} \tag{C.1.12}$$

Here, the remaining integrals are given by

$$\int_{-h_0}^{\eta} F^2 dz = G_{00} - 2i \sum_{j=1}^3 \alpha_j G_{0j} - \sum_{k=1}^3 \sum_{j=1}^3 \alpha_j \alpha_k G_{jk} \quad j, G_{jk} = G_{kj} \tag{C.1.13}$$

$$\int_{-h_0}^{\eta} F_z^2 dz = G_{00}^z - 2i \sum_{j=1}^3 \alpha_j G_{0j}^z - \sum_{k=1}^3 \sum_{j=1}^3 \alpha_j \alpha_k G_{jk}^z \tag{C.1.14}$$

$$\int_{-h_0}^{\eta} \nabla_h F dz = G_{\nabla 0} - i \sum_{j=1}^3 (\nabla_h \alpha_j) G_j - i \sum_{j=1}^3 \alpha_j \nabla_h G_j \tag{C.1.15}$$

The integrals G and G^z can be expanded about the $O(1)$ mean

water level according to the expansion

$$G = G' + \epsilon \eta_1 G'' + \epsilon^2 \{ \eta_1^2 G''' + (\eta_2 + b_2) G'' \} + \\ + \epsilon^3 \{ \eta_1^3 G'''' + 2\eta_1 (\eta_2 + b_2) G''' \} + \dots \quad (C.1.16)$$

as shown in (D.1-3), and similarly for \mathcal{A} . The integrals containing ϕ''_0 are evaluated here.

$$\int_{-h_0}^{\eta} \left(\frac{\phi''_0}{2} \right)^2 d\bar{z} = \int_{-h}^0 \left(\frac{\phi''_0}{2} \right)^2 d\bar{z} + \eta' \left(\frac{\phi''_0}{2} \right)^2 \Big|_0 + \frac{\eta'^2}{2} \left(\frac{\phi''_0}{2} \right)^2 \Big|_0 + \dots \\ = \frac{h^3}{6} (\nabla_h^2 \phi'_0)^2 + \frac{h}{2} (\nabla_h \phi'_0 \cdot \nabla_h) (\nabla_h \cdot (h \nabla_h \phi'_0)) + \\ + \epsilon \frac{\eta_1}{2} [\nabla_h \cdot (h \nabla_h \phi'_0)]^2 + \epsilon^2 \frac{(\eta_2 + b_2)}{2} [\nabla_h \cdot (h \nabla_h \phi'_0)]^2 + \\ + \epsilon^2 \frac{\eta_1^2}{2} (\nabla_h^2 \phi'_0) \nabla_h \cdot (h \nabla_h \phi'_0) \quad (C.1.17)$$

where $\eta' = \eta - b_0$;

$$\int_{-h_0}^{\eta} F_{\bar{z}} \phi''_0 d\bar{z} = J' + (\epsilon \eta_1 + \epsilon^2 (\eta_2 + b_2)) \{ -\nabla_h \cdot (h \nabla_h \phi'_0) \} G''_0 + \\ + \text{higher order terms} \quad (C.1.18)$$

where

$$J' = \int_{-h}^0 F_z \phi_{0z}'' dz$$

$$\int_{-h_0}^{\eta} f_{20z} \phi_{0z}'' dz = \text{terms in } L \text{ of } O(\epsilon^4, \delta^2)$$

$$\begin{aligned} \int_{-h_0}^{\eta} (\nabla_h \phi_0' \cdot \nabla_h \phi_0'') dz &= -(\nabla_h \phi_0' \cdot \nabla_h) \left\{ \nabla_h \cdot \left(\frac{\hbar^3}{6} \nabla_h \phi_0' \right) \right\} \\ &\quad - \left\{ \epsilon \eta_1 + \epsilon^2 (\eta_2 + b_2) \right\} \cdot \\ &\quad \cdot (\nabla_h \phi_0' \cdot \nabla_h) \left\{ \nabla_h \cdot \left(\frac{\hbar^2}{2} \nabla_h \phi_0' \right) \right\} \\ &\quad - \epsilon^2 \eta_1^2 (\nabla_h \phi_0' \cdot \nabla_h) \left\{ \nabla_h \cdot (\hbar \nabla_h \phi_0') \right\} \\ &\quad + \text{higher order terms} \end{aligned} \quad (\text{C.1.19})$$

$$\begin{aligned} \int_{-h_0}^{\eta} f_{10} \nabla_h \phi_0'' dz &= H' - \epsilon \nabla_h \left\{ \nabla_h \cdot \left(\frac{\hbar^2}{2} \nabla_h \phi_0' \right) \right\} \eta_1 + \text{higher order terms} \\ &= H' + \epsilon \nabla_h \phi_0'' \Big|_0 \eta_1 \end{aligned} \quad (\text{C.1.20})$$

where

$$H' = \int_{-h}^0 f_{10}$$

We also note that the terms $G'_{\nabla_0 i}$ and $G'_{0 \nabla i}$ may be combined to yield

$$G'_{\nabla_0 i} + G'_{0 \nabla i} = \nabla_h G'_{0i} + f_{10} f_{1i} \Big|_{-h} \nabla_h h \quad (C.1.21)$$

The Lagrangian is constructed by adding the terms I_1 through I_3 and expanding the integrals G and \mathcal{A} . The final form of L is written in the expanded form

$$L = L_0 + \epsilon L_1 + \epsilon^2 L_2 + \epsilon^3 L_3 + \epsilon^4 L_4 + \dots$$

where

$$\begin{aligned} L_0 &= g \frac{(b_0^2 - h_0^2)}{2} + h \left\{ \phi'_{0t} - \gamma_0 + \frac{(\nabla_h \phi'_0)^2}{2} \right\} + \frac{h^3}{6} (\nabla_h^2 \phi'_0) \\ &\quad + \frac{h}{2} \nabla_h \phi'_0 \cdot \nabla_h \left\{ \nabla_h \cdot (h \nabla_h \phi'_0) \right\} - \nabla_h \phi'_0 \cdot \nabla_h \left\{ \nabla_h \cdot \left(\frac{h^3}{6} \nabla_h \phi'_0 \right) \right\} \\ L_1 &= g b_0 \eta_1 + \eta_1 \left\{ \phi'_{0t} - \gamma_0 + \frac{(\nabla_h \phi'_0)^2}{2} \right\} + \frac{\eta_1}{2} (\nabla_h \cdot (h \nabla_h \phi'_0))^2 \\ &\quad + \left\{ G'_0 - i \sum_{j=1}^3 \alpha_j G'_j \right\} \frac{D \tilde{\phi}_1}{Dt} - \eta_1 \nabla_h \phi'_0 \cdot \nabla_h \left\{ \nabla_h \cdot \left(\frac{h^2}{2} \nabla_h \phi'_0 \right) \right\} \\ &\quad + \nabla_h \phi'_0 \cdot \left\{ G'_{\nabla_0} - i \sum_{j=1}^3 \alpha_j G'_{\nabla j} - i \sum_{j=1}^3 \nabla_h \alpha_j G'_j \right\} \tilde{\phi}_1 + \mathcal{J} \tilde{\phi}_1 + H' \cdot \nabla_h \tilde{\phi}_1 \end{aligned}$$

$$\begin{aligned}
L_2 = & g \frac{\eta_1^2}{2} + g b_0 (\eta_2 + b_2) + \eta_1 \frac{D\tilde{\phi}_1}{Dt} + g' \frac{D\tilde{\phi}_2}{Dt} \\
& + h \left\{ \phi'_{2,t} + \nabla_h \phi'_0 \cdot \nabla_h \phi'_2 - \gamma_2 \right\} + G'_{\nabla_0 \nabla_0} \frac{\tilde{\phi}_1^2}{2} \\
& + (G'_{000} \cdot \nabla_h \tilde{\phi}_1) \tilde{\phi}_1 + (\eta_2 + b_2) \left\{ \phi'_{0,t} + \frac{1}{2} (\nabla_h \phi'_0)^2 - \gamma_0 \right\} \\
& + g'_{\nabla} \cdot \nabla_h \phi'_0 \tilde{\phi}_2 + (\eta_2 + b_2) \left\{ \frac{\nabla_h \cdot (h \nabla_h \phi'_0)}{2} \right\}^2 \\
& + (\nabla_h^2 \phi'_0) \nabla_h \cdot (h \nabla_h \phi'_0) \frac{\eta_1^2}{2} - G_0^{\Xi''} \nabla_h \cdot (h \nabla_h \phi'_0) \eta_1 \tilde{\phi}_1 \\
& - (\eta_2 + b_2) (\nabla_h \phi'_0 \cdot \nabla_h) \left\{ \nabla_h \cdot \left(\frac{h^2}{2} \nabla_h \phi'_0 \right) \right\} \\
& - (\nabla_h \phi'_0 \cdot \nabla_h) \left\{ \nabla_h \cdot (h \nabla_h \phi'_0) \right\} \eta_1^2 \\
& + \left\{ G'_{00} - 2i \sum_{j=1}^3 \alpha_j G'_{0j} - \sum_{k=1}^3 \sum_{j=1}^3 \alpha_j \alpha_k G'_{jk} \right\} \frac{(\nabla_h \tilde{\phi}_1)^2}{2} \\
& + \left\{ G_0^{\Xi'} - 2i \sum_{j=1}^3 \alpha_j G_0^{\Xi'j} - \sum_{k=1}^3 \sum_{j=1}^3 \alpha_j \alpha_k G_0^{\Xi'jk} \right\} \frac{\tilde{\phi}_1^2}{2} \\
& - i \nabla_h \tilde{\phi}_1 \cdot \left\{ \nabla_h \left(\sum_{j=1}^3 \alpha_j G'_{0j} \right) + \nabla_h h \sum_{j=1}^3 \alpha_j f_{10} f_{ij} \Big|_{-h} \right\} \tilde{\phi}_1
\end{aligned}$$

$$\begin{aligned}
L_3 = & g\eta_1(\eta_2 + b_2) + \eta_1 \{ \phi'_{2t} + \nabla_h \phi'_0 \cdot \nabla_h \phi'_2 - \gamma_2 \} \\
& + (\eta_2 + b_2) \frac{D\tilde{\phi}_1}{Dt} + G''' \eta_1^2 \frac{D\tilde{\phi}_1}{Dt} + G'_{\nabla_0} \cdot \nabla_h \phi'_2 \tilde{\phi}_1 \\
& + \{ G'_0 - i \sum_{j=1}^3 \alpha_j G'_j \} \nabla_h \tilde{\phi}_1 \cdot \nabla_h \phi'_2 + G'''_{\nabla_0} \cdot \nabla_h \phi'_0 \eta_1^2 \tilde{\phi}_1 \\
& + (G'_{\nabla_0} \cdot \nabla_h \tilde{\phi}_2) \tilde{\phi}_1 + (G'_{\nabla_0} \cdot \nabla_h \tilde{\phi}_1) \tilde{\phi}_2 \\
& + \{ G''_{00} - 2i \sum_{j=1}^3 \alpha_j G''_{0j} \} \eta_1 \frac{(\nabla_h \tilde{\phi}_1)^2}{2} + (G''_{000} \cdot \nabla_h \tilde{\phi}_1) \eta_1 \tilde{\phi}_1 \\
& + \{ G''_{00} - 2i \sum_{j=1}^3 \alpha_j G''_{0j} \} \eta_1 \frac{\tilde{\phi}_1^2}{2} \\
& + \{ G'_0 - i \sum_{j=1}^3 \alpha_j G'_j \} \nabla_h \tilde{\phi}_1 \cdot \nabla_h \tilde{\phi}_2 \\
& + \{ G^{\equiv\prime}_0 - i \sum_{j=1}^3 \alpha_j G^{\equiv\prime}_j \} \tilde{\phi}_1 \tilde{\phi}_2 + O(\delta^2)
\end{aligned}$$

$$\begin{aligned}
L_4 = & g \left(\frac{\eta_2 + b_2}{2} \right)^2 + (\eta_2 + b_2) \left\{ \dot{\phi}_2 + \nabla_h \phi_0' \cdot \nabla_h \phi_2' - \gamma_2 \right\} + \\
& + h \left(\frac{\nabla_h \phi_2'}{2} \right)^2 + (2\eta_1 (\eta_2 + b_2) G_0''' + \eta_1^3 G_0''') \frac{D\tilde{\phi}_2}{Dt} + \\
& + ((\eta_2 + b_2) g'' + \eta_1^2 g''') \frac{D\tilde{\phi}_2}{Dt} + \eta_1 \nabla_h \tilde{\phi}_1 \cdot \nabla_h \phi_2' \\
& + ((\eta_2 + b_2) G_{00}'' + \eta_1^2 G_{00}''') \left(\frac{\nabla_h \tilde{\phi}_1}{2} \right)^2 + \eta_1 g_0'' \nabla_h \tilde{\phi}_1 \cdot \nabla_h \tilde{\phi}_2 \\
& + ((\eta_2 + b_2) G_{00}^{z''} + \eta_1^2 G_{00}^{z'''}) \frac{\phi_1^2}{2} + \eta_1 g_0^{z''} \tilde{\phi}_1 \tilde{\phi}_2 \\
& + g' \nabla_h \tilde{\phi}_2 \cdot \nabla_h \phi_2' + g^{z'} \left(\frac{\nabla_h \tilde{\phi}_2}{2} \right)^2 + g^{zz'} \frac{\tilde{\phi}_2^2}{2}
\end{aligned}$$

These are also given as (3.2.1-5) in the main body of the text. Here, the operator D/Dt is a total derivative following the $O(1)$ mean flow $\underline{u} = \nabla_h(\phi_0' + \phi_0'')$.

C.2 The Linear Equation for $\tilde{\phi}_1$ to $O(\delta^2)$

Varying L_2 with respect to $\tilde{\phi}_1$ and performing the partial integration leads to the expression

$$\begin{aligned}
 & -\frac{D\eta_1}{Dt} - (\nabla_h \cdot \underline{u})\eta_1 + G'_{\nabla_0\nabla_0} \tilde{\phi}_1 + G'_{\delta\nabla_0} \cdot \nabla_h \tilde{\phi}_1 - \nabla_h \cdot \{G'_{\delta\nabla_0}\} \tilde{\phi}_1 \\
 & - \nabla_h \cdot \left\{ \left[G'_{\delta\nabla_0} - 2i \sum_{j=1}^3 \alpha_j G'_{\delta\nabla_j} - \sum_{k=1}^3 \sum_{j=1}^3 \alpha_j \alpha_k G'_{\delta\nabla_{jk}} \right] \nabla_h \tilde{\phi}_1 \right\} \\
 & + \left\{ G'_{\delta\nabla_0} - 2i \sum_{j=1}^3 \alpha_j G'_{\delta\nabla_j} - \sum_{k=1}^3 \sum_{j=1}^3 \alpha_j \alpha_k G'_{\delta\nabla_{jk}} \right\} \tilde{\phi}_1 \\
 & - i \left\{ \nabla_h \sum_{j=1}^3 \alpha_j G'_{\delta\nabla_j} + \nabla_h h \sum_{j=1}^3 \alpha_j f_{10} f_{ij} \Big|_{-h} \right\} \cdot \nabla_h \tilde{\phi}_1 \\
 & + i \nabla_h \cdot \left\{ \left[\nabla_h \sum_{j=1}^3 \alpha_j G'_{\delta\nabla_j} + \nabla_h h \sum_{j=1}^3 \alpha_j f_{10} f_{ij} \Big|_{-h} \right] \tilde{\phi}_1 \right\} = 0 \quad (C.2.1)
 \end{aligned}$$

Expanding slightly and performing some cancellations leads to the form

$$\begin{aligned}
 & -\frac{D\eta_1}{Dt} - (\nabla_h \cdot \underline{u})\eta_1 + G'_{\delta\nabla_0} \tilde{\phi}_1 - \nabla_h \cdot (G'_{\delta\nabla_0} \nabla_h \tilde{\phi}_1) + \{G'_{\delta\nabla_0} - \nabla_h \cdot G'_{\delta\nabla_0}\} \tilde{\phi}_1 + \\
 & + \nabla_h \cdot \left\{ 2i \sum_{j=1}^3 \alpha_j G'_{\delta\nabla_j} \right\} \cdot \nabla_h \tilde{\phi}_1 + \\
 & + \left\{ 2i \sum_{j=1}^3 \alpha_j G'_{\delta\nabla_j} + \sum_{k=1}^3 \sum_{j=1}^3 \alpha_j \alpha_k G'_{\delta\nabla_{jk}} \right\} \nabla_h^2 \tilde{\phi}_1 + \\
 & + \left\{ -2i \sum_{j=1}^3 \alpha_j G'_{\delta\nabla_j} - \sum_{k=1}^3 \sum_{j=1}^3 \alpha_j \alpha_k G'_{\delta\nabla_{jk}} \right\} \tilde{\phi}_1 = 0 \quad (C.2.2)
 \end{aligned}$$

The terms involving $\alpha_j \alpha_k$ are $O(\delta^2)$, and, in those terms, $\nabla_h^2 \tilde{\phi}_1$ may be approximated by $-k^2 \tilde{\phi}_1$. Defining the quantity

$$\tilde{z}_{jk} = k^2 G'_{jk} + G_{jk}^{\tilde{z}'}$$

we rewrite (C.2.2) as

$$\begin{aligned} & -\frac{D\eta_1}{Dt} - (\nabla_h \cdot \underline{u}) \eta_1 + G_{00}^{\tilde{z}'} \tilde{\phi}_1 - \nabla_h \cdot \{G'_{00} \nabla_h \tilde{\phi}_1\} + \\ & + \{G'_{\sigma_0 \sigma_0} - \nabla_h \cdot G'_{00}\} \tilde{\phi}_1 + 2i \nabla_h \left\{ \sum_{j=1}^3 \alpha_j G'_{0j} \right\} \cdot \nabla_h \tilde{\phi}_1 + \\ & + 2i \left\{ \sum_{j=1}^3 \alpha_j G'_{0j} \nabla_h^2 \tilde{\phi}_1 - \sum_{j=1}^3 \alpha_j G_{0j}^{\tilde{z}'} \tilde{\phi}_1 \right\} - \sum_{k=1}^3 \sum_{j=1}^3 \{ \alpha_j \alpha_k \tilde{z}_{jk} \} \tilde{\phi}_1 = 0 \end{aligned} \quad (\text{C.2.3})$$

The term $\nabla_h^2 \tilde{\phi}_1$ may be expanded according to

$$\nabla_h^2 \tilde{\phi}_1 = -k^2 \tilde{\phi}_1 + 2i \underline{k} \cdot \nabla_H \tilde{\phi}_1 + O(\delta^2) \quad (\text{C.2.4})$$

where ∇_H is defined in section (2.3) and is related to the spatial variation of the amplitude of $\tilde{\phi}_1$. Noting from Appendix D that

$$k^2 G'_{0j} + G_{0j}^{\tilde{z}'} \equiv 0 \quad ; \quad j = 1, 2, 3 \quad (\text{C.2.5})$$

it is apparent that all $O(\delta)$ contributions other than those provided by the first four terms of (C.2.3) disappear.

Also, the term

$$\nabla_h \left\{ \sum_{j=1}^3 \alpha_j G'_{0j} \right\}$$

is $O(\delta^2)$; $\nabla_h \tilde{\phi}_1$ can be approximated by $i\tilde{k} \tilde{\phi}_1$. The term

$$\left\{ G'_{\nabla_0 \nabla_0} - \nabla_h \cdot G'_{000} \right\} \tilde{\phi}_1$$

is identical to the higher order term found by Smith and Sprinks(1975), after absorbing a boundary term through Leibnitz integration. Using (C.2.4) and (C.2.5), (C.2.3) can be written in the form

$$\begin{aligned} & -\frac{D\eta_1}{Dt} - (\nabla_h \cdot \underline{u})\eta_1 - \nabla_h \cdot (G'_{00} \nabla_h \tilde{\phi}_1) + G'_{00} \tilde{\phi}_1 \\ & + \left\{ G'_{\nabla_0 \nabla_0} - \nabla_h \cdot G'_{000} \right\} \tilde{\phi}_1 - 2\tilde{k} \cdot \nabla_h \left\{ \sum_{j=1}^3 \alpha_j G'_{0j} \right\} \tilde{\phi}_1 \\ & - 4 \sum_{j=1}^3 \alpha_j G'_{0j} \tilde{k} \cdot \nabla_H \tilde{\phi}_1 - \sum_{k=1}^3 \sum_{j=1}^3 \alpha_j \alpha_k \tilde{\Gamma}_{jk} \tilde{\phi}_1 = 0 \end{aligned} \quad (C.2.6)$$

Equation (C.2.6) is the correct equation for $\tilde{\phi}_1$ to $O(\delta^2)$; however, the operator ∇_H is only symbolic and is not practically applicable. Letting $\tilde{\phi}_1$ be given by

$$\tilde{\phi}_1 = -i\frac{g}{\sigma} A e^{i\psi}$$

we can write $\nabla_H \tilde{\phi}_1$ in the form

$$\nabla_H \tilde{\phi}_1 = -\frac{ig}{\sigma} (\nabla_H A) e^{i\psi} = \left(\frac{\nabla_h A}{A} \right) \tilde{\phi}_1 \quad (\text{C.2.7})$$

where $\nabla_h A/A$ is one component of α_2 . In order to make further explicit progress, it is necessary to expand α_2 into its components, and then to take the derivatives of the products $\omega_j \zeta'_{ij}$. We define the quantities

$$\beta_1 = \frac{\underline{k} \cdot \nabla_h (\underline{k} \cdot \nabla_h h)}{k^3} \quad ; \quad \beta_2 = \frac{\underline{k} \cdot \nabla_h (\underline{k} \cdot \nabla_h k)}{2k^5} \quad ;$$

$$\beta_3 = \frac{\underline{k} \cdot \nabla_h (\underline{k} \cdot \nabla_h A)}{k^4 A} \quad ; \quad \beta_4 = \frac{\underline{k} \cdot \nabla_h (\underline{k} \cdot \nabla_h \sigma)}{k^4 \sigma} \quad ;$$

$$\beta_5 = \frac{\underline{k} \cdot \nabla_h (\nabla_h \cdot \underline{k})}{2k^4} \quad , \quad (\text{C.2.8})$$

where $\beta_1 - \beta_5$ are $O(\delta^2)$, and

$$\beta_6 = \frac{\underline{k} \cdot \nabla_h A}{k^2 A} \quad ; \quad \beta_7 = \frac{\underline{k} \cdot \nabla_h \sigma}{k^2 \sigma}$$

$$\beta_8 = \frac{\nabla_h \cdot \underline{k}}{k^2} \quad (\text{C.2.9})$$

where $\beta_6 - \beta_8$ are $O(\delta)$. Also, we let

$$\mathcal{F}_j = 2k^2 G'_{0j} \quad (\text{C.2.10})$$

The coefficient α_2 may then be expanded as

$$\alpha_2 = \frac{\beta_8}{2} + \beta_6 - \beta_7 - \alpha_3 \quad (\text{C.2.11})$$

The terms $\nabla_h \alpha_j$ may be written as

$$k \cdot \nabla_h \alpha_1 = -2k^2 \alpha_1 \alpha_3 + k^2 \beta_1$$

$$k \cdot \nabla_h \alpha_2 = -2k^2 \alpha_3 \beta_8 + k^2 (\beta_3 - \beta_4 + \beta_5 - \beta_2) - k^2 \beta_6^2 \\ - 4k^2 \alpha_3 \beta_6 + 4k^2 \alpha_3 \beta_7 + 6k^2 \alpha_3^2 + k^2 \beta_7^2$$

$$k \cdot \nabla_h \alpha_3 = -6k^2 \alpha_3^2 + k^2 \beta_2 \quad , \quad (\text{C.2.12})$$

and the terms $k \cdot \nabla_h G'_{0j}$ as

$$k \cdot \nabla_h G'_{01} = \alpha_1 \mathcal{F}_{01} + \alpha_3 \mathcal{F}_{02} \quad (\text{C.2.13})$$

where

$$\mathcal{F}_{01} = \frac{-\sigma^2}{g \sinh 2kh} \left\{ \tanh kh + kh (1 - kh \tanh kh) \right\}$$

$$\mathcal{F}_{02} = \frac{\sigma^2}{2g} \left\{ (3 - 4n) \tanh kh + 2kh \left(n - \frac{1}{2} \right) [1 - 2(1 - kh \tanh kh)] \right\}$$

$$\underline{k} \cdot \nabla_h G'_{02} = \alpha_1 \mathcal{F}_{03} + \alpha_3 \mathcal{F}_{04} \quad (C.2.14)$$

where

$$\mathcal{F}_{03} = \frac{-\sigma^2}{g \sinh 2kh} \left\{ 3kh \tanh kh (1 - kh \tanh kh) + (kh)^2 \right\}$$

$$\begin{aligned} \mathcal{F}_{04} = \frac{-\sigma^2}{g} \left\{ \frac{4(kh)^3 \tanh kh}{\sinh^2 2kh} + (\kappa - 1) \right. \\ \left. + \frac{4(kh)^2 \tanh kh (1 - kh \tanh kh)}{\sinh 2kh} \right\} \end{aligned}$$

and

$$\underline{k} \cdot \nabla_h G'_{03} = \alpha_1 \mathcal{F}_{05} + \alpha_3 \mathcal{F}_{06} \quad (C.2.15)$$

where

$$\mathcal{F}_{05} = \frac{-\sigma^2}{g} \left\{ (2\kappa - 1)kh + (2\kappa - \frac{1}{2}) \tanh kh - \frac{4}{3} \frac{(kh)^3 \tanh kh}{\sinh 2kh} \right\}$$

$$\begin{aligned} \mathcal{F}_{06} = & -\frac{\sigma^2}{g} \left\{ (1-n) + 2(kh)^2 \frac{\tanh kh}{\sinh 2kh} + \right. \\ & \left. + \frac{8(kh)^3}{3 \sinh 2kh} (1 - kh \tanh kh) \right\} \end{aligned}$$

Substituting (C.2.7-15) into (C.2.6) leads to the equation

$$\begin{aligned} \langle \text{M.S.} \rangle + \alpha \tilde{\Phi}_1 - \beta_1 \tilde{\mathcal{F}}_1 \tilde{\Phi}_1 + \beta_2 (\tilde{\mathcal{F}}_2 - \tilde{\mathcal{F}}_3) \tilde{\Phi}_1 \\ + (-\beta_3 + \beta_4 - \beta_5) \tilde{\mathcal{F}}_2 \tilde{\Phi}_1 - \gamma_1 \alpha_1^2 \tilde{\Phi}_1 + \gamma_2 \alpha_1 \alpha_3 \tilde{\Phi}_1 \\ + \gamma_3 \alpha_3^2 \tilde{\Phi}_1 + \gamma_4 (2\beta_7 - \beta_8) \alpha_1 \tilde{\Phi}_1 + (-2\tilde{\mathcal{F}}_{03} \alpha_1 + \gamma_5 \alpha_3) \beta_6 \tilde{\Phi}_1 \\ + \gamma_6 (2\beta_7 - \beta_8) \alpha_3 \tilde{\Phi}_1 + \tilde{\mathcal{F}}_{22} (\beta_7 \beta_8 - \beta_8^2/4) \tilde{\Phi}_1 = 0 \end{aligned} \quad (\text{C.2.16})$$

where

$$\langle \text{M.S.} \rangle = -\frac{D\eta_1}{Dt} - (\nabla_h \cdot \underline{u}) \eta_1 - \nabla_h \cdot (G'_{00} \nabla_h \tilde{\Phi}_1) + G''_{00} \tilde{\Phi}_1 \quad (\text{C.2.17})$$

$$\alpha = G'_{\sigma_0 \sigma_0} - \nabla_h \cdot G'_{0\sigma_0} \quad (\text{C.2.18})$$

and

$$\gamma_1 = \mathcal{F}_{11} + 2\mathcal{F}_{01}$$

$$\gamma_2 = 2(\mathcal{F}_{03} - \mathcal{F}_{02} - \mathcal{F}_{05} - \mathcal{F}_{13})$$

$$\gamma_3 = (4\mathcal{F}_3 - \mathcal{F}_2 - \mathcal{F}_{33} - 2\mathcal{F}_{06} - \gamma_5)$$

$$\gamma_4 = \mathcal{F}_{12} + \mathcal{F}_{03}$$

$$\gamma_5 = 4\mathcal{F}_2 - 2\mathcal{F}_{04}$$

$$\gamma_6 = \mathcal{F}_{23} - \mathcal{F}_2 + \mathcal{F}_{04}$$

and where we have used the results

$$\mathcal{F}_{12} + \mathcal{F}_1 = \mathcal{F}_{22} + \mathcal{F}_2 = \mathcal{F}_{23} + \mathcal{F}_3 = 0$$

Note that

$$\langle n.s. \rangle = 0 \quad (C.2.19)$$

is equivalent to Booiij's mild slope wave equation after dropping a small $O(\delta^2)$ term which appears in his equation

due to an error in the derivation. After substituting the free surface boundary condition (3.3.7) into (C.2.16), we obtain the reduced wave equation for $\tilde{\phi}_1$, correct to $O(\delta^2)$, given by (3.3.8), where an arbitrary dissipation term is included. The coefficients $\gamma_1 - \gamma_6$ are given explicitly in Appendix D.

APPENDIX D. INTEGRALS APPEARING IN L

In the derivation of the Lagrangian L, various integrals, denoted by G and \mathcal{L} , arise in the integration over the depth. The notations used are as follows.

Integrals of f_{1i} quantities:

$$G_i = \int_{-h_0}^{\eta} f_{1i} d\bar{z} \quad ; \quad G_{\nabla i} = \int_{-h_0}^{\eta} \nabla_h f_{1i} d\bar{z}$$

$$G_{ij}^{(\bar{z})} = \int_{-h_0}^{\eta} f_{1i}(\bar{z}) f_{1j}(\bar{z}) d\bar{z} \quad ; \quad G_{i\nabla j} = \int_{-h_0}^{\eta} f_{1i} \nabla_h f_{1j} d\bar{z}$$

etc.

Integrals of f_{20} :

$$\mathcal{L}^{2(\bar{z})} = \int_{-h_0}^{\eta} f_{20}^2 d\bar{z} \quad ; \quad \mathcal{L}_{(\nabla)} = \int_{-h_0}^{\eta} (\nabla_h) f_{20} d\bar{z}$$

Integrals of products of f_{20} and f_{1i} quantities:

$$G_i^{(z)} = \int_{-h_0}^{\eta} f_{z_0(z)} f_{1i}(z) dz \quad ; \quad G_{\nabla i} = \int_{-h_0}^{\eta} f_{z_0} \nabla_h f_{1i} dz$$

$$G_{i\nabla} = \int_{-h_0}^{\eta} (\nabla_h f_{z_0}) f_{1i} dz \quad ; \text{ etc.}$$

Each of the integrals G and G may be expanded about the mean water level $z=b_0$ by the following procedure:

$$\begin{aligned} I &= \int_{-h_0}^{\eta} A dz = \int_{-h_0}^{b_0} A dz + \int_{b_0}^{b_0 + \epsilon \eta_1 + \epsilon^2(\eta_2 + b_2)} A dz \\ &= \int_{-h}^0 A dz' + \int_0^{\epsilon \eta_1 + \epsilon^2(\eta_2 + b_2)} A dz' \end{aligned} \quad (D.1)$$

where A is an arbitrary function, and the wave reference level z has been shifted to the slowly varying $O(1)$ mean water level. The coefficients f_{1i} , f_{z_0} are then defined with respect to the local mean depth $h=h_0+b_0$, rather than the still water depth h_0 . The integral from $z=b_0$ ($z'=0$) up to the local water surface is further expanded to give

$$\begin{aligned} I &= \int_{-h}^0 A dz' + \left\{ \epsilon \eta_1 + \epsilon^2(\eta_2 + b_2) \right\} A \Big|_0 + \frac{\left\{ \epsilon \eta_1 + \epsilon^2(\eta_2 + b_2) \right\}^2}{2} A_{zz} \Big|_0 + \\ &\quad + \frac{\left\{ \epsilon \eta_1 + \epsilon^2(\eta_2 + b_2) \right\}^3}{6} A_{zzz} \Big|_0 + \dots \end{aligned}$$

$$\begin{aligned}
&= I' + \{ \epsilon \eta_1 + \epsilon^2 (\eta_2 + b_2) \} I'' \\
&\quad + \{ \epsilon \eta_1 + \epsilon^2 (\eta_2 + b_2) \}^2 I''' + \{ \epsilon \eta_1 + \epsilon^2 (\eta_2 + b_2) \}^3 I^{IV} + \dots
\end{aligned} \tag{D.2}$$

The contributions to I are then reordered in powers of ϵ to give

$$\begin{aligned}
I &= I' + \epsilon \eta_1 I'' + \epsilon^2 \{ (\eta_2 + b_2) I'' + \eta_1^2 I''' \} + \\
&\quad + \epsilon^3 \{ 2 \eta_1 (\eta_2 + b_2) I''' + \eta_1^3 I^{IV} \} + \dots
\end{aligned} \tag{D.3}$$

The integrals appearing explicitly in the equations follow. For the mild slope approximation (terms of $O(\delta)$ in $\tilde{\zeta}_1$ neglected), integrals of the form G_0 , G_{00} , \mathcal{L} and \mathcal{L}_0 appear in L_2 and L_4 . These are given by

$$G_0'' = 1$$

$$G_{00}' = c C_g / g \qquad G_{00}^{\prime\prime} = \sigma^2 (1 - n) / g$$

where n is the ratio C_g / C given by

$$n = \frac{1}{2} \left(1 + 2kh / \sinh 2kh \right) \quad ;$$

$$G_{00}'' = 1 \quad ; \quad G_{00}^{\prime\prime\prime} = \sigma^4 / g^2 \quad ; \quad G_{00}^{IV} = \sigma^2 / g \quad ; \quad G_{00}^{V} = k^2 \sigma^2 / g \quad ;$$

$$G_0''' = \sigma^2/2g \quad ; \quad G_0'' = k^2/6 \quad ;$$

$$G^I = \frac{\cosh kh}{k \sinh^3 kh} \quad ; \quad G'' = \frac{\cosh 2kh}{\sinh^4 kh} \quad ;$$

$$G''' = \frac{2k \cosh kh}{\sinh^3 kh} \quad ;$$

$$G_0'' = \frac{1}{2 \cosh kh \sinh^4 kh} \left\{ \cosh 3kh + \cosh kh \right\} \quad ;$$

$$G_0^{z''} = \frac{k^2}{\cosh kh \sinh^4 kh} \left\{ \cosh 3kh - \cosh kh \right\} \quad ;$$

$$G^{z'} = \frac{\sinh 2kh}{2k \sinh^3 kh} \left\{ \sinh^2 kh + n \right\} \quad ;$$

$$G^{zz'} = \frac{2k \sinh 2kh}{\sinh^3 kh} \left\{ \cosh^2 kh - n \right\} .$$

At $O(\delta)$ and $O(\delta^2)$, integrals of the form G_{λ}^i and G_{λ}^j appear in L_2 and contribute to higher order terms in the Euler equation for $\tilde{\phi}_1$. The integrals G_{λ}^i , $i=1-3$ are simply $f_{11} - f_{13}$ evaluated at $z=0$, and are equal to zero. The integrals $G_{0i}^{(z)}$ are given by:

$$G'_{01} = \frac{-(kh)^2}{4k \cosh^2 kh} - \frac{1}{4k} \tanh^2 kh$$

$$G^{z'}_{01} = \frac{k}{4} \frac{(kh)^2}{\cosh^2 kh} + \frac{k}{4} \tanh^2 kh$$

$$G'_{02} = \frac{kh}{4k} - \frac{\tanh kh}{4k} + \frac{kh}{4k} (1-4\mu) \tanh^2 kh$$

$$G^{z'}_{02} = -\frac{k}{4} (kh) + \frac{k}{4} \tanh kh - \frac{k}{4} (kh) (1-4\mu) \tanh^2 kh$$

$$G'_{03} = \frac{-(kh)^3}{3k \cosh^2 kh} + \frac{1}{4k} \tanh kh - \frac{kh}{4k} (1 + \tanh^2 kh)$$

$$G^{z'}_{03} = \frac{k(kh)^3}{3 \cosh^2 kh} - \frac{k \tanh kh}{4} + \frac{k(kh)(1 + \tanh^2 kh)}{4}$$

It is apparent that the quantities

$$k^2 G'_{0i} + G^{z'}_{0i} \quad ; \quad i = 1, 2, 3$$

are identically zero. Quantities \mathcal{F}_i , $i=1,2,3$ are defined by

$$\mathcal{F}_i = 2k^2 G'_{0i} \quad (D.4)$$

and are given by

$$\mathcal{F}_1 = -\frac{\sigma^2}{g} \left\{ \frac{(kh)^2}{\sinh 2kh} + \frac{\sigma^2}{2gk} \right\}$$

$$\mathcal{F}_2 = \frac{\sigma^2}{g} \frac{kh}{\sinh 2kh} (1 - kh \tanh kh) - \frac{\sigma^2}{g} \left(1 + \frac{(kh)^2}{\cosh^2 kh} \right)$$

$$\mathcal{F}_3 = \frac{\sigma^2}{2g} (1 - kh \tanh kh) - \frac{k(kh)}{2} - \frac{4}{3} \frac{\sigma^2}{g} \frac{(kh)^3}{\sinh 2kh}$$

where

$$\sigma^2 = gk \tanh kh$$

The remaining required integrals are the quantities $G_{ij}^{(\pm)'}$, $i, j=1, 2, 3$, and the combinations \mathcal{F}_{ij} given by

$$\mathcal{F}_{ij} = k^2 G_{ij}' + G_{ij}^{(\pm)'}$$

which are given by:

$$G_{11}' = \frac{\sigma^2}{4gk^2} (1 + kh \tanh kh) - \frac{kh}{4k} + \frac{\sigma^2}{3gk^2} \frac{(kh)^3}{\sinh 2kh}$$

$$G_{11}^{(\pm)'} = \frac{-\sigma^2}{4g} (1 + kh \tanh kh) + \frac{k}{4}(kh) - \frac{\sigma^2}{3g} \frac{(kh)^3}{\sinh 2kh} + \frac{\sigma^2 \pi}{g}$$

$$\bar{J}_{11} = \frac{\sigma^2}{g} \eta$$

$$G'_{22} = \frac{\sigma^2}{4gk^2} (1 + kh \tanh kh) - \frac{kh}{4k} + \frac{(kh)^3}{k \cosh^2 kh} \left(\frac{\tanh^2 kh}{2} - \frac{1}{6} \right)$$

$$G''_{22} = \frac{\sigma^2}{4g} (1 - kh \tanh kh) + \frac{k(kh)}{4} - \frac{k(kh)}{2 \cosh^2 kh} \\ + \frac{\sigma^2 (kh)^2}{g \cosh^2 kh} - \frac{k(kh)^3}{\cosh^2 kh} \left(\frac{\tanh^2 kh}{2} - \frac{1}{6} \right)$$

$$\bar{J}_{22} = \frac{\sigma^2}{2g} \left(1 + \frac{(kh)^2}{\cosh^2 kh} \right) - \frac{\sigma^2}{g} \frac{kh}{\sinh 2kh} (1 - kh \tanh kh)$$

$$G'_{33} = \frac{8}{15} \frac{\sigma^2}{gk^2} \frac{(kh)^5}{\sinh 2kh} + \frac{3}{4} \frac{\sigma^2}{gk^2} (1 - kh \tanh kh) \\ - \frac{3}{4k} (kh) + \frac{\sigma^2}{gk^2} (kh)^2$$

$$G''_{33} = -\frac{8}{15} \frac{\sigma^2}{g} \frac{(kh)^5}{\sinh 2kh} + \frac{1}{4} \frac{\sigma^2}{g} (1 - kh \tanh kh) \\ - \frac{k}{4} (kh) + \frac{\sigma^2}{g} (kh)^2 + \frac{4}{3} \frac{\sigma^2}{g} \frac{(kh)^3}{\sinh 2kh}$$

$$\bar{J}_{33} = \frac{\sigma^2}{g} (1 - kh \tanh kh) - k(kh) + \frac{\sigma^2}{g} \left\{ 2(kh)^2 + \frac{4}{3} \frac{(kh)^3}{\sinh 2kh} \right\}$$

$$G'_{12} = \frac{\sigma^4}{2g^2k^3} \left\{ \frac{1}{2} - \frac{(kh)[1-(kh)^2]}{\sinh 2kh} \right\}$$

$$G''_{12} = \frac{\sigma^4}{2g^2k} \left\{ \frac{1}{2} + \frac{(kh)[1-(kh)^2]}{\sinh 2kh} \right\} + \frac{\sigma^2}{g} \frac{(kh)^2}{\sinh 2kh}$$

$$J_{12} = \frac{\sigma^2}{g} \left\{ \frac{(kh)^2}{\sinh 2kh} + \frac{\sigma^2}{2gk} \right\}$$

$$G'_{13} = \frac{5}{24} \frac{(kh)^4}{k \cosh^2 kh} + \frac{\sigma^2}{2gk^2} (kh) - \frac{3}{8} \frac{\sigma^2}{gk^2} \tanh kh - \frac{1}{8k} \frac{(kh)^2}{\cosh^2 kh}$$

$$G''_{13} = -\frac{5}{24} \frac{k(kh)^4}{\cosh^2 kh} + \frac{\sigma^2}{2g} (kh) - \frac{1}{8} \frac{\sigma^2}{g} \tanh kh + \frac{5k}{8} \frac{(kh)^2}{\cosh^2 kh}$$

$$J_{13} = \frac{\sigma^2}{g} \left\{ kh - \frac{\tanh kh}{2} + \frac{(kh)^2}{\sinh 2kh} \right\}$$

$$G'_{23} = -\frac{3}{8} \frac{\sigma^2}{gk^2} (1 - kh \tanh kh) + \frac{3}{8k} (kh) - \frac{\sigma^2}{4gk^2} kh \tanh kh - \frac{\sigma^4}{g^2k^3} \frac{1}{\sinh 2kh} \left\{ \frac{(kh)^2}{2} - \frac{2}{3} (kh)^4 \right\}$$

$$G''_{23} = -\frac{1}{8} \frac{\sigma^2}{g} (1 - kh \tanh kh) + \frac{k(kh)}{8} + \frac{\sigma^2}{4g} kh \tanh kh - \frac{2}{3} \frac{\sigma^4}{g^2k} \frac{(kh)^4}{\sinh 2kh} + \frac{4}{3} \frac{\sigma^2}{g} \frac{(kh)^3}{\sinh 2kh} + \frac{\sigma^2}{4g} (kh)^2 (1 - \tanh^2 kh)$$

$$F_{23} = \frac{k}{2}(kh) + \frac{4}{3} \frac{\sigma^2}{g} \frac{(kh)^3}{\sinh 2kh} - \frac{\sigma^2}{2g} (1 - kh \tanh kh)$$

The combinations

$$F_1 + F_{12}, \quad F_2 + F_{22}, \quad F_3 + F_{23}$$

are equal to zero. Referring to the definition of F in (3.3.8), given by (3.3.10), and to (C.2.13-16), the remaining coefficients are given by

$$\gamma_1 = F_{11} + 2F_{01}$$

$$= \frac{\sigma^2}{g} \left\{ (1-n) + \frac{2 \tanh kh}{\sinh 2kh} (kh-1) \right\}$$

$$\gamma_2 = 2 \{ F_{03} - F_{02} - F_{05} - F_{13} \}$$

$$= \frac{\sigma^2}{g} \left\{ 2n \tanh kh - 2kh + \frac{2(kh)^2}{\sinh 2kh} (1 + 3 \tanh^2 kh) - \frac{20}{3} (kh)^3 \frac{\tanh kh}{\sinh 2kh} \right\}$$

$$\begin{aligned}
\gamma_3 &= 4\bar{z}_3 - \bar{z}_2 - \bar{z}_{33} - 2\bar{z}_{06} - \gamma_5 \\
&= \frac{\sigma^2}{g} \left\{ \frac{11}{2} - kh \left(\tanh kh + \frac{1}{\tanh kh} + \frac{9}{\sinh 2kh} \right) - 2(kh)^2 \right. \\
&\quad + 6(kh)^2 \frac{\tanh kh}{\sinh 2kh} - \frac{16}{3} (kh)^4 \frac{\tanh kh}{\sinh 2kh} \\
&\quad \left. - 4 \frac{(kh)^3}{\sinh 2kh} \left[\frac{1}{3} - 2 \tanh kh \left(\frac{1}{\sinh 2kh} - 1 \right) \right] \right\}
\end{aligned}$$

$$\begin{aligned}
\gamma_4 &= \bar{z}_{12} + \bar{z}_{03} \\
&= \frac{\sigma^2}{g} \left\{ \frac{\sigma^2}{2gk} - \frac{3kh \tanh kh}{\sinh 2kh} (1 - kh \tanh kh) \right\}
\end{aligned}$$

$$\begin{aligned}
\gamma_5 &= 4\bar{z}_2 - 2\bar{z}_{04} \\
&= \frac{2\sigma^2}{g} \left\{ \pi - 2 - \frac{(kh)^2}{\cosh^2 kh} + \frac{4(kh)^3 \tanh kh}{\sinh^2 2kh} + \right. \\
&\quad \left. + \frac{2kh}{\sinh 2kh} (1 + 2kh \tanh kh)(1 - kh \tanh kh) \right\}
\end{aligned}$$

$$\begin{aligned}
\gamma_6 &= \bar{z}_{23} - \bar{z}_2 + \bar{z}_{04} \\
&= \frac{\sigma^2}{g} \left\{ \left[\frac{1}{2} - 2\pi - \frac{4(kh)^2}{\sinh 2kh} \right] (1 - kh \tanh kh) + 1 \right. \\
&\quad \left. + \frac{gk(kh)}{2\sigma^2} + \frac{4(kh)^3}{\sinh 2kh} \left(\frac{1}{3} - \frac{1}{\sinh 2kh} \right) \right\}
\end{aligned}$$

The coefficient α , expanded in (3.3.13), has the terms $\delta_1 - \delta_5$, which are given by

$$\delta_1 = \frac{\sigma^2}{2g \cosh^2 kh} - \frac{k(kh)}{2 \cosh^4 kh}$$

$$\delta_2 = \frac{h}{2} \frac{\tanh kh}{\cosh^2 kh} + \frac{(kh)^2}{k \cosh^2 kh} \left(\tanh^2 kh - \frac{1}{2} \right)$$

$$\delta_3 = \frac{h^3}{\cosh^2 kh} \left(\frac{\tanh^2 kh}{2} - \frac{1}{6} \right) + \frac{\tanh kh}{4k^3} - \frac{h}{4k^2 \cosh^2 kh}$$

$$\delta_4 = -kh \frac{\tanh^2 kh}{\sinh 2kh}$$

$$\delta_5 = \frac{1}{4k^2} \left\{ kh - \tanh kh + kh(1-4\pi) \tanh^2 kh \right\}$$

APPENDIX E. CONSERVATION EQUATION FOR WAVE ACTION

In order to derive several of the results in Chapter 4, an equation governing the flux of an energy related quantity is required in addition to the Euler equations found in Chapter 3. It has been shown that, for propagation in a moving medium, the appropriate conserved quantity is the wave action, given by

$$\text{WAVE ACTION} = E/\sigma \quad (E.1)$$

(Garrett(1967), Bretherton and Garrett(1968)), where E is given by $E=g|A|^2/2$. Note that the expressions for conserved quantities are formulated here with respect to unit masses, which is possible since the density has been assumed to be constant throughout the fluid domain. The lowest order conservation equation for E/σ may be obtained directly from the linear wave equation (3.4.1), using the definition of W given by (4.2.1):

$$\begin{aligned} \frac{D^2 \tilde{\phi}_1}{Dt^2} + (\nabla_h \cdot \underline{u}) \frac{D \tilde{\phi}_1}{Dt} - \nabla_h \cdot (c c_g \nabla_h \tilde{\phi}_1) + \sigma^2 (1-n) \tilde{\phi}_1 = \\ = i \sigma W \tilde{\phi}_1 \end{aligned} \quad (E.2)$$

where w in the last term is a coefficient related to the rate of energy dissipation (Booij(1981), Dalrymple, Kirby and Hwang (1983)). Following the approach of Jonsson(1981), we assume that $\tilde{\phi}_1$ may be represented by the ansatz

$$i\tilde{\phi}_1 = R e^{i\theta} \quad (E.3)$$

where R and θ are real quantities. Comparing (E.3) to (A.4), it is apparent that

$$R = g\sigma^{-1} |A| \quad (E.4)$$

while θ absorbs the higher order phase effects neglected in the definition of ψ . Since we are looking for the lowest order results, we may approximate θ and its derivatives according to

$$\theta = \psi + O(\epsilon^2) \quad (E.5a)$$

$$\theta_t = \psi_t + O(\epsilon^2) \cong -\omega \quad (E.5b)$$

$$\nabla_h \theta = \nabla_h \psi + O(\epsilon^2) \cong \underline{k} \quad (E.5c)$$

Substituting (E.4) and (E.5) into (E.2) leads to the complex equation

$$\begin{aligned} & \frac{D^2 R}{Dt^2} + (\nabla_h \cdot \underline{u}) \frac{DR}{Dt} - \nabla_h \cdot (CC_g \nabla_h R) - i(\sigma_\epsilon R + 2\sigma R_t) \\ & - i\left\{ \nabla_h \cdot (\underline{u}\sigma) R + 2(\sigma \underline{u}) \cdot \nabla_h R + \nabla_h \cdot (\underline{k} CC_g) R + 2\underline{k} CC_g \cdot \nabla_h R \right\} \\ & - i\sigma_w R = 0 \end{aligned} \quad (E.6)$$

Since R and θ are real by definition, the real and imaginary parts of (E.6) must individually equal zero. Gathering the imaginary terms and multiplying by R , we obtain the equation

$$\begin{aligned}
 & -(\sigma R^2)_t - \sigma \underline{u} \cdot \nabla_h R^2 - \nabla_h \cdot (\sigma \underline{u}) R^2 - c c_g \underline{k} \cdot \nabla_h R^2 \\
 & - \nabla_h \cdot (\underline{k} c c_g) R^2 - \sigma w R^2 = 0
 \end{aligned} \tag{E.7}$$

Then, noting that we can write

$$c c_g \underline{k} = k c (c_g \underline{k} / k) = \sigma \underline{\zeta}_g \tag{E.8}$$

we rearrange (E.7) to the form

$$(\sigma R^2)_t + \nabla_h \cdot (\sigma R^2 (\underline{u} + \underline{\zeta}_g)) = -\sigma w R^2 \tag{E.9}$$

Now, R^2 may be replaced by

$$R^2 = g^2 |A|^2 / \sigma^2 = \frac{2g}{\sigma} \left(\frac{E}{\sigma} \right) \tag{E.10}$$

which yields the relation

$$\left(\frac{E}{\sigma} \right)_t + \nabla_h \cdot \left\{ \left(\frac{E}{\sigma} \right) (\underline{u} + \underline{\zeta}_g) \right\} = -w \left(\frac{E}{\sigma} \right) \tag{E.11}$$

It is apparent that $w > 0$ for a dissipative motion. Neglecting the right hand side of (E.11) gives the standard equation for conservation of wave action in a conservative, inhomogeneous, moving system, given originally by Garrett(1967). The result with dissipation has been shown to be somewhat incomplete by Christoffersen and Jonsson(1980), who show that the right hand side should

contain a term involving the bottom shear stress resulting from the $O(1)$ mean current. In this study, we regard the ambient current as an imposed flow and neglect frictional effects related to the current, thus yielding the version of the conservation equation given by (E.11)

Jonsson(1981) shows how the equations governing the geometric optics approximation of (3.4.1) may be obtained by using the real part of (E.6). In this case, it is necessary to retain the expressions $\nabla_h \psi$ and ψ_t in order to obtain the desired results.

APPENDIX F. BOUNDARY INTEGRAL METHOD FOR THE
ONE-DIMENSIONAL PROBLEM

The one-dimensional problem (topographic variation in the x-direction only) treated in Chapter 5 admits an "exact" solution by means of the boundary integral method (BIM). The method is exact in terms of its basic formulation, whereas the theory of the main body of the text relies on series expansion representations for the propagating components of the wave field alone. However, solution by BIM still requires discretization of the domain and numerical evaluation of the results.

The method used in this study was described originally by Lee(1971) and was applied by Raichlen and Lee(1978) to the study of linear waves radiated in one direction from an infinite inclined plate wave generator. Here, we extent the method to waves travelling at an oblique angle to the direction x. Let the total velocity potential ϕ be represented by

$$\phi(x, y, z, t) = \Phi(x, z) e^{i(my - \omega t)} \quad (\text{F.1})$$

where $m=0$ for normal incidence and $0 < m < k_A$ for oblique incidence, where k_A is the wavenumber for a constant depth region A on the upwave ($x \rightarrow -\infty$) side of the topographic obstacle. The incident wave ϕ_I is then given by

$$\phi_I = \Phi_I e^{i(my - \omega t)} \quad (\text{F.2})$$

with unit amplitude, where

$$\Phi_I = -ig (\omega \cosh kh_A)^{-1} \cosh k(h+z)_A e^{i l_A x} \quad (\text{F.3a})$$

and

$$l_A = (k_A^2 - m^2)^{1/2} \quad (\text{F.3b})$$

Substituting ϕ into Laplace's equation (2.1.1) leads to a modified Helmholtz equation

$$L(\Phi) = \Phi_{xx} + \Phi_{zz} - m^2 \Phi = 0 \quad (\text{F.4})$$

with the associated free space Green's functions

$$G(r) = -\frac{K_0(mr)}{2\pi} \quad m > 0 \quad (\text{F.5a})$$

$$G(r) = \frac{\ln r}{2\pi} \quad m = 0 \quad (\text{F.5b})$$

where K_0 is the modified Bessel function of the second kind and zeroth order and r is the radial distance from the singularity to the field point in question

$$r = \left\{ (x - x_0)^2 + (z - z_0)^2 \right\}^{1/2} \quad (\text{F.6})$$

A fluid domain $\Omega(x, z)$, shown in Figure F.1, is constructed by separating the constant depth regions from the region containing the variable topography, but including enough of the constant depth region to either side of the variation to allow for the decay of nonpropagating modes. The solutions in the exterior regions A and C may then be given by

$$\Phi_A = \Phi_I - ig R (\omega \cosh kh_A)^{-1} \cosh k_A(h_A + z) e^{-il_A x} \quad (\text{F.7a})$$

$$\Phi_C = -ig T (\omega \cosh kh_C)^{-1} \cosh k_C(h_C + z) e^{il_C x} \quad (\text{F.7b})$$

where R and T represent reflection and transmission coefficients, and are in general complex to allow for phase shifts in x and y . Conservation of energy in the diffracted

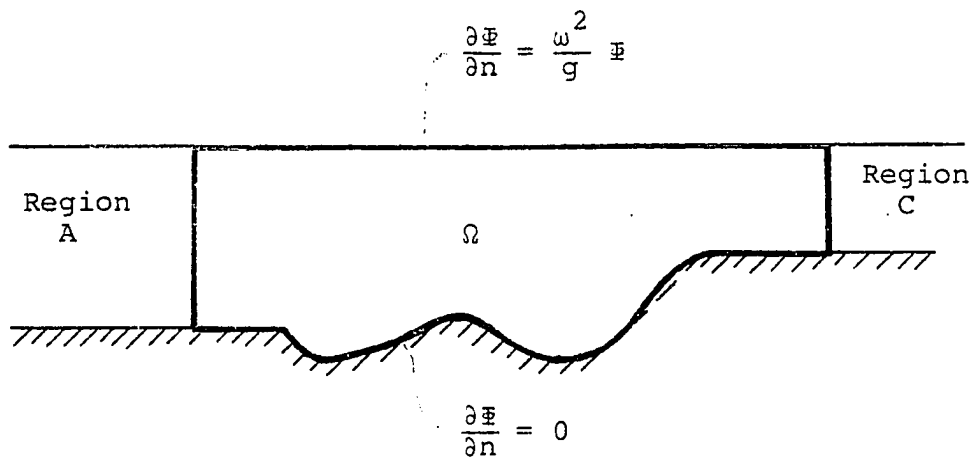


Figure F.1 Boundary integral method domain in relation to extent of variable topography

wave field requires that

$$|R|^2 + |T|^2 \left\{ \frac{n_c k_A^2 l_c}{n_A k_c^2 l_A} \right\} = 1 \quad (F.8)$$

Also, the boundary of Ω is denoted by $\partial\Omega$. Following the standard procedure for constructing solutions by means of Green's functions, we take the inner product to be given by

$$(L(\Phi), G) = \int_{\Omega} G (\nabla_V^2 - m^2) \Phi \, d\Omega \quad (F.9)$$

$$\nabla_V^2 = \frac{\partial^2}{\partial x^2} + \frac{\partial^2}{\partial z^2}$$

Then, using Green's Second Identity, a formula for the value of $\Phi(x_0, z_0)$ for an interior point of the domain Ω is obtained:

$$\Phi(x_0, z_0) = \int_{\partial\Omega} \left\{ \Phi(\underline{x}) \frac{\partial G(\underline{x} - \underline{x}_0)}{\partial n} - G(\underline{x} - \underline{x}_0) \frac{\partial \Phi(\underline{x})}{\partial n} \right\} dS(\underline{x}) \quad (F.10)$$

where n denotes the outward normal to $\partial\Omega$. Values of Φ in the interior of Ω are thus completely determined by Φ on $\partial\Omega$, and the problem is reduced to finding $\Phi(\partial\Omega)$. Values

of $\bar{\Phi}$ on $\partial\Omega$ are determined by moving the point (x_0, z_0) to the boundary and determining the principle value of the integral in (F.10) (see Figure F.2). Including the point (x_0, z_0) within the contour and retaining the residue leads to the formula

$$\bar{\Phi}(x_0) = 2 \oint_{\partial\Omega} \left\{ \bar{\Phi}(x) \frac{\partial G}{\partial n}(x) - G(x) \frac{\partial \bar{\Phi}}{\partial n}(x) \right\} dS(x)$$

for points (x_0, z_0) on $\partial\Omega$. Substituting for G from (F.5) leads to the formulas

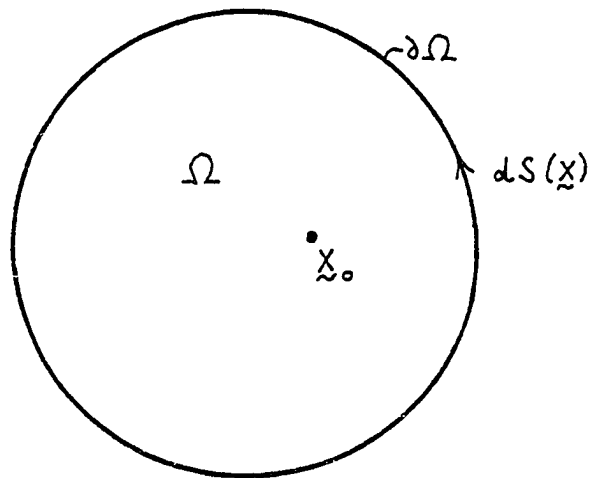
$$\bar{\Phi}(x_0) = \frac{1}{\pi} \oint_{\partial\Omega} \left\{ K_0(mr) \frac{\partial \bar{\Phi}}{\partial n}(x) - \bar{\Phi}(x) \frac{\partial}{\partial n} (K_0(mr)) \right\} dS(x) \quad (\text{F.11a})$$

for oblique incidence, and

$$\bar{\Phi}(x_0) = \frac{-1}{\pi} \oint_{\partial\Omega} \left\{ \ln r \frac{\partial \bar{\Phi}}{\partial n}(x) - \bar{\Phi}(x) \frac{\partial}{\partial n} (\ln r) \right\} dS(x) \quad (\text{F.11b})$$

for normal incidence.

The details for the numerical approximation of (F.11a) follow; the corresponding details for (F.11b) may be derived in analogous fashion or obtained from Raichlen and Lee(1978). First, the boundary $\partial\Omega$ is discretised into N boundary segments which are presumed to be straight line segments (thus leading to discretization errors in the case



a) interior point

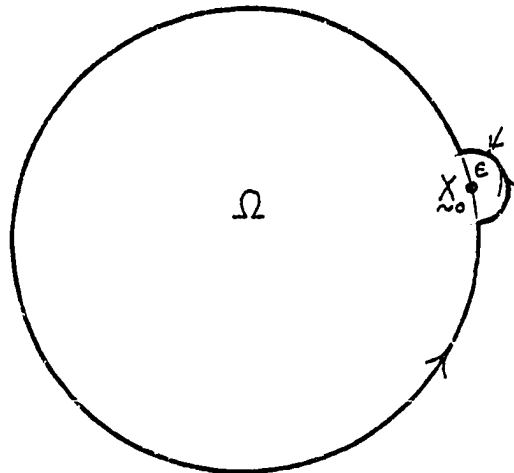
b) point on boundary $\partial\Omega$

Figure F.2 Integration paths for interior points and points on boundary

of locally curved boundaries). Taking $\underline{x}_i = \{x_o, z_o\}$ to be the boundary point for which $\bar{\Phi}$ is being determined and \underline{x}_j to vary over all boundary points, (F.11a) is approximated by

$$\bar{\Phi}(\underline{x}_i) = \frac{1}{\pi} \sum_{j=1}^N \left\{ K_o(m r_{ij}) \frac{\partial \bar{\Phi}}{\partial n}(\underline{x}_j) - \bar{\Phi}(\underline{x}_j) \frac{\partial}{\partial n} (K_o(m r_{ij})) \right\} \Delta S_j \quad (\text{F.12})$$

where Δs_j is the length of the j th boundary segment and $\bar{\Phi}$ is assumed to be uniform over each boundary segment. Special treatment is needed for $i=j$, where $r_{ij}=0$. Writing (F.12) out in matrix form, we get:

$$\begin{Bmatrix} \bar{\Phi}(\underline{x}_1) \\ \vdots \\ \bar{\Phi}(\underline{x}_N) \end{Bmatrix} = \frac{1}{\pi} \left\{ K_o(m r_{ij}) \Delta S_j \right\} \begin{Bmatrix} \frac{\partial \bar{\Phi}}{\partial n}(\underline{x}_1) \\ \vdots \\ \frac{\partial \bar{\Phi}}{\partial n}(\underline{x}_N) \end{Bmatrix} - \frac{1}{\pi} \left\{ \frac{\partial}{\partial n} [K_o(m r_{ij}) \Delta S_j] \right\} \begin{Bmatrix} \bar{\Phi}(\underline{x}_1) \\ \vdots \\ \bar{\Phi}(\underline{x}_N) \end{Bmatrix} \quad (\text{F.13})$$

Let

$$G_{ij} = K_o(m r_{ij}) \Delta S_j \quad (\text{F.14a})$$

$$G_{nij} = \frac{\partial}{\partial n} [K_o(m r_{ij})] \Delta S_j = -m K_1(m r_{ij}) \frac{\partial r_{ij}}{\partial n} \Delta S_j \quad (\text{F.14b})$$

The normal derivative $\partial r_{ij} / \partial n$ is given by (for $i \neq j$)

$$\frac{\partial r_{ij}}{\partial n} = - \frac{(x_i - x_j) \Delta z_j}{r_{ij} \Delta S_j} + \frac{(z_i - z_j) \Delta x_j}{r_{ij} \Delta S_j}$$

and the evaluation of (F.14) for $i \neq j$ is straightforward. For $i=j$, G_{ii} in a small neighborhood of x_i can be approximated by (Abromowitz and Stegun (1972) , p.375)

$$dG_{ii} \cong - \ln(m r_{ii}) dS_i \quad (F.15)$$

Integrating over the boundary segment Δs_i leads to

$$G_{ii} = - \left\{ \ln \left(\frac{m \Delta S_i}{2} \right) - 1 \right\} \Delta S_i \quad (F.16)$$

Following Lee(1971) and Raichlen and Lee(1978), $G_{\kappa ii}$ is given by

$$G_{\kappa ii} = 0 \quad (F.17)$$

due to the neglect of the local curvature of the boundary. Finally, $\partial \bar{\Phi} / \partial n$ can be specified in terms of boundary and radiation conditions:

$$\frac{\partial \Phi}{\partial n} = \begin{cases} il_A \Phi - 2il_A \Phi_I & \text{upwave boundary} \\ 0 & \text{solid boundaries} \\ il_c \Phi & \text{downwave boundary} \\ \frac{\omega^2}{g} \Phi & \text{free surface} \end{cases} \quad (\text{F.18})$$

leading to the final matrix equation

$$\left\{ \mathbf{I} + \frac{G_{\kappa \lambda j}}{\pi} - \frac{G_{\lambda j}}{\pi} \begin{pmatrix} il_A \\ 0 \\ \dots \\ il_c \\ \dots \\ \omega^2/g \end{pmatrix} \right\} \frac{\Phi}{\omega} = \frac{1}{\pi} G_{\lambda j} \begin{pmatrix} \frac{\partial \Phi}{\partial n_I} \\ 0 \\ \dots \\ 0 \end{pmatrix} \quad (\text{F.19})$$

where \mathbf{I} is the diagonal identity matrix $\delta_{\lambda j}$. Kirby and Dalrymple (1983a) have compared the results of the present approximation to results obtained using integral equations based on eigenfunction expansions of Φ in regions of constant depth separated by vertical boundaries, as shown in

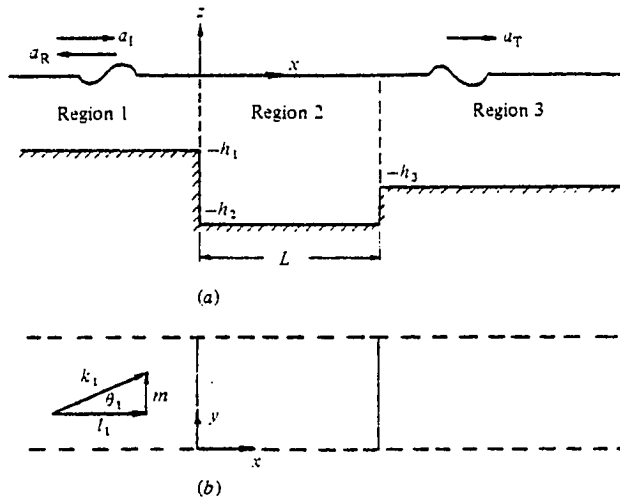


Figure F.3 Geometry for test of BIM
 $a_R = R$, $a_I = l$, $a_T = T$
 a) elevation b) plan
 (from Kirby and Dalrymple,
 1983a)

Figure F.3. Two such comparisons are shown in Figures F.4 and F.5. In Figure F.4, results are for the case of an asymmetric trench, with the trench being twice as deep as the incident wave region, and the transmitted wave region being half as deep as the incident wave region. The ratio of trench width to incident region water depth is 5:1, and only normally incident waves ($m=0$) are studied. Generally good agreement is found between the BIM and eigenfunction solutions. The results of Lassiter(1972), included for comparison, are seen to deviate significantly from the solutions of Kirby and Dalrymple(1983a). In Figure F.5, BIM results are shown for a symmetric trench and an oblique angle of incidence of 45° . Here, $h_2/h_1=3$ and $L/h_1=10$, using the notation of Figure F.3. For values of $kh_1 < 0.792$ for the incident waves, the value of the x-component of the wavenumber vector in the trench is imaginary; this result is seen to present no difficulties to the analysis technique.

The method used in the present study represents a relatively crude approach to the boundary discretization. For a more satisfactory approach, where $\bar{\phi}$ is assumed to vary linearly over each segment, see Liu and Abbaspour (1982).

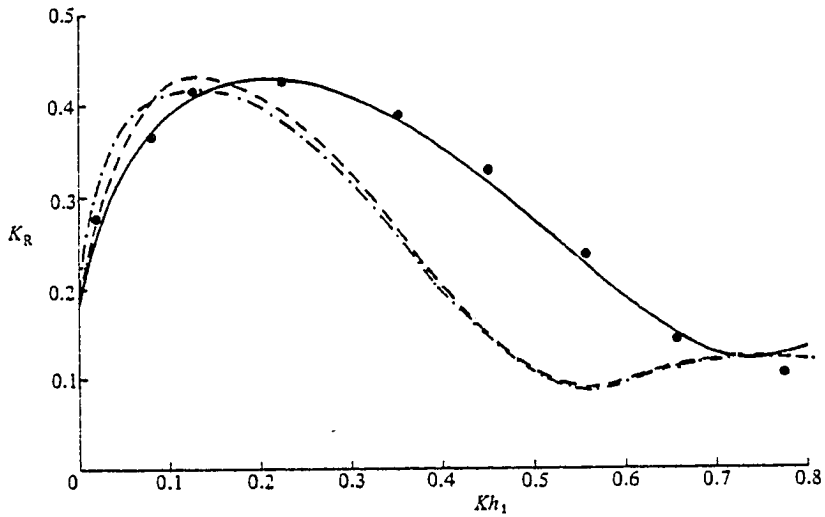


Figure F-4. Reflection coefficient: asymmetric trench
 $h_2/h_1 = 2$, $L/h_1 = 5$, $h_3/h_1 = 0.5$
 $\theta_1 = 0$.
 $K_R = |R|$, $K = \omega^2/g$
 — Kirby & Dalrymple (1983a);
 ---, --- Lassiter (1972);
 • BIM solution
 (from Kirby and Dalrymple, 1983a)

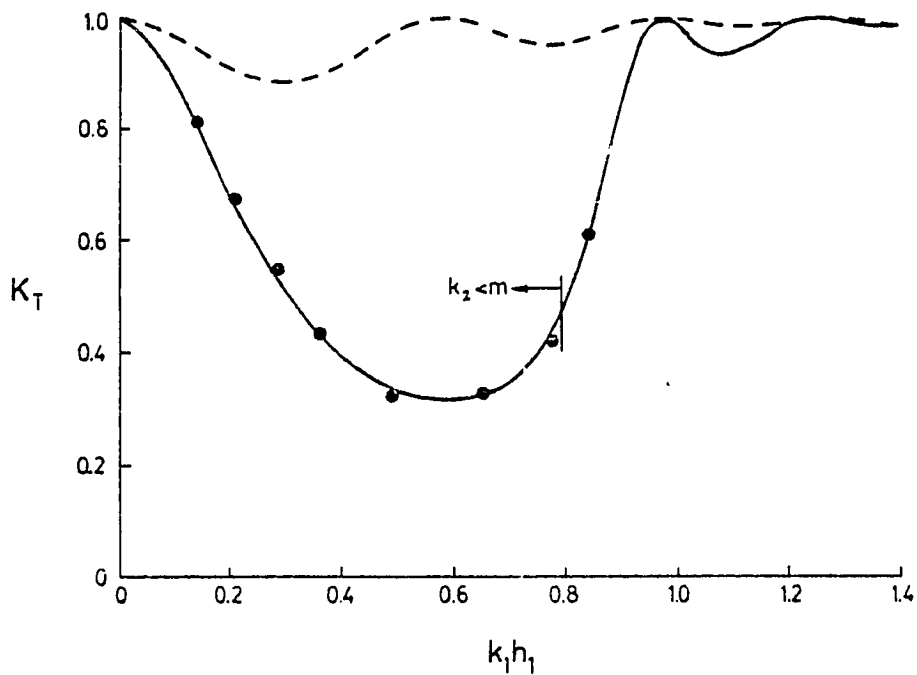


Figure F.5 Transmission coefficient: symmetric trench
 $h_2/h_1 = 3, L/h_1 = 10$
 $K_T = T$
 --- $\theta_1 = 0^\circ$; — $\theta_1 = 45^\circ$, Kirby and Dalrymple (1983a)
 • BIM solution
 (after Kirby and Dalrymple, 1983a)

APPENDIX G. RELATIONS FOR THE DISSIPATION COEFFICIENT
w BASED ON VARIOUS DISSIPATION MECHANISMS.

In this appendix, the role of the dissipation coefficient w in the governing equation for wave motion is investigated, and its value is related to physical quantities based on various mechanisms for wave energy dissipation.

The role of w in determining the wave amplitude can be investigated by using the current-free form of the elliptic model (4.2.4), which reduces to

$$\nabla_h \cdot (CC_g \nabla_h \tilde{\phi}_1) + (n\omega^2 + i\omega w) \tilde{\phi}_1 = 0 \quad (G.1)$$

Considering the simple case of waves propagating in the x -direction over a flat bottom reduces (G.1) to

$$\tilde{\phi}_1_{xx} + k_c^2 \tilde{\phi}_1 = 0 \quad (G.2).$$

where

$$k_c^2 = k^2 \left(1 + \frac{iW}{\pi\omega} \right) \quad (G.3)$$

The solution of (G.2) for waves travelling in the positive x direction is given by

$$\tilde{\phi}_1(x) = A e^{i k_c x} \quad (G.4)$$

where A is real and arbitrary or can be related to an initial condition. If k_c is expressed in real and imaginary parts, $k_c = k_r + ik_i$, the exponentially decaying solution for $\tilde{\phi}_1$ is given by

$$\tilde{\phi}_1(x) = A e^{-k_i x} e^{i k_r x} \quad (G.5)$$

From (G.3), we find

$$k_r = k \left\{ \frac{\left[1 + \left(\frac{W}{\pi\omega} \right)^2 \right] + 1}{2} \right\}^{1/2} \quad (G.6a)$$

$$k_c = k \left\{ \frac{\left[1 + \left(\frac{W}{\pi\omega} \right)^2 \right] - 1}{2} \right\}^{1/2} \quad (G.6b)$$

Solving (G.6b) for w yields

$$W = 2\pi\omega \left(\frac{k_i}{k} \right) \left(1 + \left(\frac{k_i}{k} \right)^2 \right)^{1/2} \quad (G.7)$$

Depending on the nature of the localized energy dissipation, w takes on different values. For a number of dissipative mechanisms, the wave height decay is exponential, in agreement with (G.5), and k_i is known. Several examples are:

1. Porous bottom (Reid and Kajiura, 1957).

$$k_i = \left(\frac{k\omega}{\nu h} \right) \left(\frac{2kh}{2kh + \sinh 2kh} \right) \quad (G.8)$$

2. Viscous mud bottom of thickness d , viscosity ν_m , and density ρ_m (Dalrymple and Liu, 1978).

$$k_i = \frac{(gk/\omega^2)(\nu/\omega)^{1/2}}{(2d)^2 \left[1 + \left(\frac{\rho}{\rho_m} \right) \left(\frac{\nu}{\nu_m} \right)^{1/2} \right]}$$

$$\cdot \frac{\left\{ \left[k(d+h) - (\omega^2/gk) \right]^2 + \left[1 + \left(\frac{\rho_m}{\rho} \right) \left(\frac{\nu_m}{\nu} \right)^{1/2} \right] \left[\frac{\omega^2}{gk} - kh \right]^2 \right\}}{\left\{ 1 + \left[\frac{\rho_m}{\rho} - 1 \right] \left[1 - \frac{gk}{\omega^2} (kh) \right]^2 \right\}} \quad (G.9)$$

where k_i is for shallow water (for simplicity).

3. Laminar bottom boundary layer (Ippen, 1966).

$$k_i = \frac{k^2}{n} \frac{(\nu/2\omega)^{1/2}}{\sinh 2kh} \quad (G.10)$$

4. Densely packed surface film (Phillips, 1977).

$$k_i = \frac{k^2}{n} \frac{(\nu/2\omega)^{1/2}}{2 \tanh kh} \quad (G.11)$$

For case 1, a more complete expression has been obtained, including the effect of boundary layers, by Liu(1973).

For other types of damping, the wave amplitude is not exponential but varies as

$$A(x) = \frac{A_0}{1 + \alpha x} \quad (G.12)$$

where A_0 is the initial wave amplitude and α is a damping coefficient. For a rough bottom with a turbulent boundary layer, Madsen(1976) showed that

$$\alpha = \frac{2f_w}{3\pi} \frac{k^2 A_0}{\sinh kh (2kh + \sinh 2kh)} \quad (G.13)$$

where f_w is a wave friction factor. Dalrymple, Kirby, and

Hwang(1983) derived a dissipation formula for waves propagating through an array of vertical cylinders occupying an arbitrary fraction of the total water depth, based on drag-dominated dissipation for each cylinder times the density of cylinders per unit area. The resulting value of α is given by

$$\alpha = \frac{8k}{3\pi} C_D \left(\frac{A_0}{b}\right) \left(\frac{D}{b}\right) \left(\frac{\sinh^3 ks + 3 \sinh ks}{3 \sinh kh (2kh + \sinh 2kh)} \right) \quad (G.14)$$

where s is the position of the top of the cylinder relative to the bottom, b is the spacing between cylinders, D is the cylinder diameter, and C_D is a representative drag coefficient for each cylinder acting alone.

In order to relate α to w it is convenient to first relate α to $k_i x$ by comparing the following expansions

$$(1 + \alpha x)^{-1} = 1 - \alpha x + (\alpha x)^2 - (\alpha x)^3 + \dots \quad (G.15a)$$

$$e^{-k_i x} = 1 - k_i x + \frac{(k_i x)^2}{2} - \frac{(k_i x)^3}{3} + \dots \quad (G.15b)$$

Therefore, for small values of $k_i x$ or αx , we may take $\alpha = k_i$. We can thus use (G.7) in either case with C' .

replacing k_{μ} , as long as $\alpha \Delta x$ is relatively small. For subsequent numerical modeling it is sufficient to approximate (G.7) by

$$W = 2\pi\omega\left(\frac{k_{\mu}}{R}\right) \quad \text{or} \quad 2\pi\omega\left(\frac{\alpha}{R}\right) \quad (\text{G.16})$$

for $\{k_{\mu}, \alpha\} \ll k$.